The Dissertation Committee for Kalyan Vikram Vasudevan certifies that this is the approved version of the following dissertation:

Synthesis of Novel Bis(alkylimino)acenaphthene (BIAN) and Tetrakis(imino)pyracene (TIP) Ligands and Studies of Their Redox Chemistry

Committee:

Alan H. Cowley, Supervisor

Richard A. Jones

Bradley J. Holliday

Christopher W. Bielawski

John C. Gordon

Synthesis of Novel Bis(alkylimino)acenaphthene (BIAN) and Tetrakis(imino)pyracene (TIP) Ligands and Studies of Their Redox Chemistry

by

Kalyan Vikram Vasudevan, B.S., B.A.

Dissertation

Presented to the Faculty of the Graduate School of

The University of Texas at Austin

in Partial Fulfillment

of the Requirements

for the Degree of

Doctor of Philosophy

The University of Texas at Austin

August 2009

Acknowledgements

While countless individuals have played a role in my development as a student, I must give paramount credit for everything I have ever achieved to my family. My parents have been a lifelong source of support throughout my academic career and have instilled in me a work ethic that is responsible for any success I have attained or will ever see. While I will never verbally affirm so out of respect to fraternal rivalry, I would be remiss without mentioning that Bharath has been my role model from my earliest memories. While I could allude to any of his many academic and personal achievements, it should suffice to say that his profound impact during my youth is perhaps only equaled by his presence over the past five years. To my family I would like to simply say, thank you, and I love you.

Family aside, no single individual has shared with me more of their knowledge than Professor Alan Cowley. Over the last few years he has shared countless stories of his worldly experiences and has served admirably as a teacher of history, literature and linguistics. He even managed to teach me a little chemistry here and there. I would like to thank you for my tenure in your research group and the opportunity to be your friend.

I would also like to offer my sincere thanks to my friends in the Cowley group, both former and current. You have all been for me a daily source of wisdom and comfort and I value my experiences, most notably those of the Friday evening variety, with each and every one of you. I would also like to thank my colleagues in the department, particularly those in the Jones and Holliday groups, for their friendship and advice during my time in Austin.

"Synthesis of Novel Bis(alkylimino)acenaphthene (BIAN) and Tetrakis(imino)pyracene (TIP) Ligands and Studies of Their Redox Chemistry"

Publication No._____

Kalyan Vikram Vasudevan, Ph.D

The University of Texas at Austin, 2009

Supervisor: Alan H. Cowley

The evolution of the present work began with the syntheses of novel bis(alkylimino)acenaphthene (BIAN) ligands. At the outset of this research, despite the presence of dozens of aryl-BIAN ligands in the literature, there were as of yet no reported BIAN ligands bearing alkyl substituents. Given the nearly ubiquitous use of transition metal complexes of alkyl diazabutadiene (DAB) ligands for *e.g.* catalysis and as ligands for carbene chemistry, interest was generated in developing this emerging field of synthetic chemistry. Initial studies focused on the synthesis of alkyl-BIAN ligands since the traditional synthetic approaches that had been developed for aryl-BIAN ligands were unsuccessful for the alkyl analogues. As an alternate synthetic route, it was decided to employ amino- and imino-alane transfer reagents which had previously proved successful for the conversion of C=O into C=N-R functionalities. While this transfer route had proved successful to synthesize moderate yields of highly fluorinated DAB ligands, it

was unknown how or whether this methodology would apply in the case of alkylated BIAN systems.

Over the past decade, there has been a surge of interest regarding lanthanide complexes that are capable of undergoing spontaneous electron transfer processes. There are several reports in the literature that describe the ability of Ln(II) ions to undergo spontaneous oxidation, thereby causing one-electron reduction of the coordinated ligand and generally resulting in the corresponding Ln(III) complex. The present work focused on an enhanced understanding of the electronic communication between the lanthanide and the attached ligand. Particular emphasis was placed on defining the resulting oxidation states and the manner in which delocalized electrons of the radical anion species travel over a conjugated system. This fundamental information was gleaned from single-crystal X-ray diffraction studies and magnetic moment measurements that were obtained using the Evans method. Additional insights stemmed from the use of more classical techniques such as IR and NMR spectroscopy. In favorable cases, the presence or absence of spectral peaks can permit assignment of the lanthanide oxidation state. Accordingly, the research plan was to synthesize a series of BIAN-supported decamethyllanthanocene complexes with the goal of learning how to control the spontaneous charge transfer that had been reported in the literature.

A longer term goal was to develop a bifunctional ligand of the BIAN type that was capable of accommodating two lanthanide or main group element moieties. Systems with tunable electronic interactions between lanthanide or main group elements are of interest because they offer the prospect of extended delocalization of electron density. Systems of this type have potential applications as *e.g.* molecular wires and single-

molecule magnets. Indeed, such systems have been investigated by using bis(bipyridyl) and bis(terpyridyl) ligands to support two redox-active moieties. However, in the present work, it was recognized that a bifunctional BIAN-type ligand might be of considerable interest as the supporting structure for studying the communication between lanthanide or main group element moieties. A synthesis of variously substituted tetrakis(imino)pyracene (TIP) ligands was therefore undertaken. The flat, rigid nature of the TIP ligands rendered them ideal scaffolds for studying the redox behavior and electronic communication between lanthanide or main group element centers. The new TIP ligand class also proved to be useful for the assembly of the first example of a metallopolymer based on a BIAN-type ligand.

Table of Contents

Chapter 1

"The Synthesis of Novel Nitrogen Donor Ligands Based on the BIAN Architecture"

Chapter 1 Introduction

Over the past few decades, the chemistry of nitrogen-donor ligands based on α-diimine frameworks has been explored at great length. From ligand development to coordination chemistry, the availability of this ligand class has had far reaching implications in the fields of catalysis and fundamental redox chemistry. For example, late transition metal complexes of the diazabutadiene (DAB) ligand class have found widespread utility as alkene polymerization catalysts[1]. While the excellent activity of such catalysts is evident from the literature, it became apparent that the diimine-supported catalysts had limited lifetimes. Detailed investigation revealed that the catalyst lifetimes were shortened by cleavage of the diimine C-C bond. As a consequence, a ligand design was sought that addressed these issues without compromising catalytic activity. The key to solving this problem lay in the use of the bis(imino)acenaphthene (BIAN) ligand which was first reported in the 1960's[2, 3]. The robust BIAN ligand can be

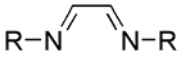

DAB

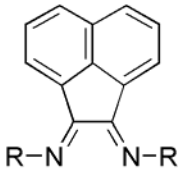

BIAN

regarded as the product of fusion of a diazabutadiene fragment with a naphthalene moiety. The metal-BIAN complexes indeed proved to be as catalytically active as their

DAB counterparts with the added advantage of having significantly increased lifetimes. The naphthalene backbone imparts conformational rigidity and safeguards against ligand decomposition. However, it is only in the past twenty years that the coordination chemistry of this ligand been widely explored[4-6]. A significant number of R-DAB (R = aryl or alkyl) ligands can be readily synthesized by the condensation reaction of glyoxal with an excess of the appropriate amine, generally in the presence of a Lewis acid. The ease of synthesis and ability to tune the electronics of the ligand undoubtedly contributes to the now widespread use of R-DAB ligands in coordination chemistry. A similar synthetic approach is viable for the synthesis of aryl-BIAN ligands (Scheme 1.01).

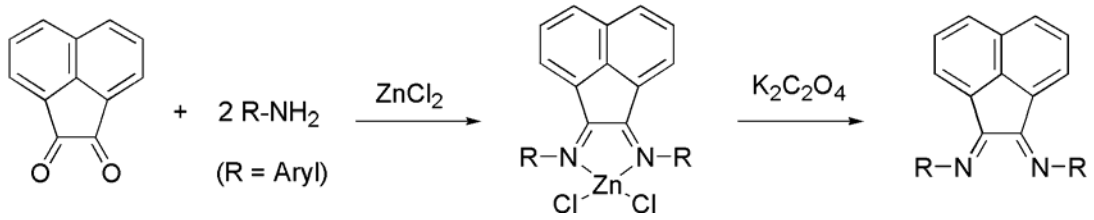

Scheme 1.01. Synthesis of Aryl-BIAN ligands via condensation.

Interestingly, until 2005, all attempts to synthesize the corresponding alkyl-BIAN ligands by the analogous route of treating with alkyl amine and Lewis acid met with failure. At first glance, the reason for this lack of reactivity is unclear. However, in 2005, Ragaini *et al*. reported the synthesis of a cyclopropyl-substituted BIAN ligand[7]. These authors selected the highly strained cyclopropyl ring system in order to avoid the previously observed isomerization shown in Scheme 1.02. In the case of the cyclopropyl-substituted BIAN ligand this would result in a more energetically unfavorable product. While unique, this synthetic route is limited to R substituents that feature highly strained ring systems. The challenge was therefore to devise a method for

the synthesis of non-strained, acyclic alkyl groups as BIAN substituents. The response to this challenge involved the use of organometallic amine and imine transfer agents.

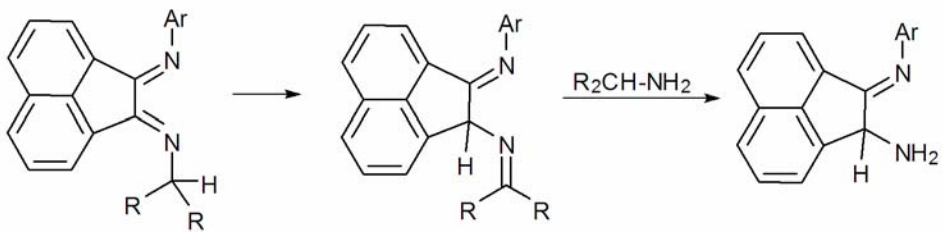

Scheme 1.02. Observed isomerization pathway in attempted alkyl-BIAN syntheses via transimination.

The iminoalane cubane $[MeAl(\mu_3\text{-}NMes)]_4$ has been shown to transfer an imido functionality to $(\eta^5\text{-}C_5H_4Me)_2TiF_2$ to yield $[\eta^5\text{-}C_5H_4Me)TiF(NMes)]_2$[8]. Furthermore, it has been shown recently that the aminoalane dimer $[Me_2Al\text{-}\mu\text{-}N(H)R]_2$ (R = fluoroaryl) is capable of effecting the conversion of C=O groups to C=N-R moieties[9]. This aminoalane reagent has been employed for the preparation of DAB ligands featuring highly electron-withdrawing N-substituents. Such ligands were previously accessible in only very low yields. Given the paucity of alkyl-BIAN ligands, it was of interest to develop a synthetic strategy based on the use of imino- and aminoalane transfer reagents. The specific synthetic targets were the *tert*-butyl-BIAN (^{t}Bu-BIAN) and 1-adamantyl-BIAN (Ad-BIAN) ligands.

A further goal in the context of new BIAN ligands was the synthesis of the elusive 2,3,4,5,6-pentafluorophenyl substituted derivative (C_6F_5-BIAN). A convenient synthetic route to novel BIAN-type ketoimine ligands bearing fluorinated or alkyl substituents has also been devised. Furthermore, by combining these synthetic approaches it was also possible to synthesize a BIAN ligand bearing mixed R

substituents. Accordingly, the syntheses of these ketoimine and mixed BIAN ligands will also be addressed in the present chapter.

As stated in the Introduction, the overall goal of this research program was to develop the field of alkyl-BIAN ligands, probe the charge transfer processes that occur in lanthanide-BIAN complexes and to use the pertinent information to enable the synthesis of a bifunctional BIAN-type ligand capable of supporting two redox-active metals or main group moieties. The synthesis and characterization of the so called tetrakis(imino)pyracene (TIP) ligand will also be discussed in the present chapter.

Results and Discussion

Section 1.1 Introduction

The initial attempts at synthesizing new BIAN ligands focused on the alkyl and fluorinated derivatives, ^{t}Bu-BIAN, Ad-BIAN and C_6F_5-BIAN. Traditional condensation and transimination routes described in the literature failed in all attempts that were made to prepare BIAN ligands bearing alkyl or heavily fluorinated substituents. Accordingly, a series of aluminum transfer reagents were employed in attempts to synthesize the desired compounds. A significant degree of difficulty was encountered in doubly substituting the starting diketone precursor, acenaphthenequinone. Nevertheless, the failed attempts resulted in the synthesis and characterization of singly-substituted ketoimine ligands based on a BIAN-type framework. By varying the amine transfer reagent and optimizing stoichiometry, a viable method was developed for accessing this class of ligand. Only a handful of such ligands have been reported in the literature[10] and, as in the case of BIAN ligands, examples bearing alkyl or heavily fluorinated substituents were unknown.

Synthesis and Characterization of $[(C_6F_5)N\text{-}Al(H)(THF)]_2$ (1)

The aluminum transfer reagent dimer $[(C_6F_5)N\text{-}Al(H)(THF)]_2$ (**1**) was synthesized via the reaction of equimolar quantities of $(CH_3)_3N\text{-}AlH_3$ and 2,3,4,5,6-pentafluoroaniline in THF solution. Following workup of the reaction mixture, a colorless powder was obtained in high yield (87%). Recrystallization of **1** from a saturated THF solution at -15°C for one week afforded colorless crystals suitable for X-ray diffraction experiments. A single-crystal X-ray diffraction study confirmed the identity of the product as the title compound shown in Figure 1.01. Details of the data

collection, structure solution and refinement are compiled in Table 1.01 and selected metrical parameters are listed in Tables 1.02 and 1.03.

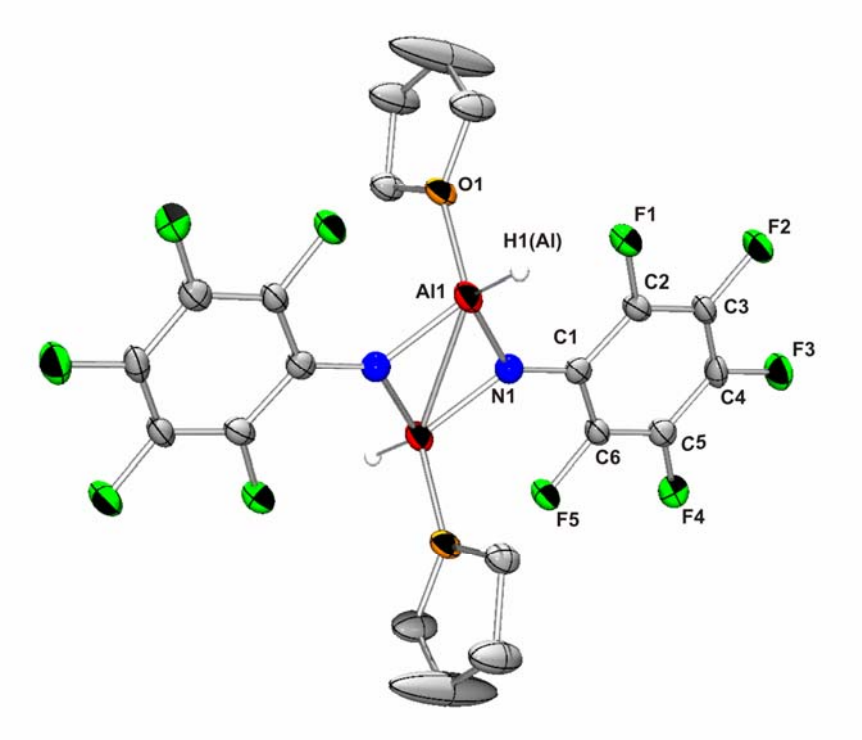

Figure 1.01. Molecular structure of 1 showing a partial numbering scheme. The thermal ellipsoids are shown at the 40% probability level. With the exception of H1(Al), all hydrogen atoms have been omitted for clarity.

A single-crystal X-ray diffraction study revealed that **1** crystallizes in the monoclinic space group $P2_1/n$. The asymmetric unit consists of the monomeric form of the transfer reagent while the dimeric structure is evident upon growing of the lattice. The most notable metrical parameter is the Al(1)-N(1) bond distance of 1.844(3) Å which falls in the range of known amine-based aluminum transfer reagents[9]. Additionally, the crystal structure reveals the presence of one THF molecule and one hydride atom bound to each aluminum atom thus completing the aluminum coordination sphere.

Synthesis and Characterization of 2-pentafluorophenylimino-2H-acenaphthylen-1-one (2)

2-pentafluorophenylimino-2H-acenaphthylen-1-one (**2**) was synthesized from the reaction of three equivalents of **1** with one equivalent of acenaphthenequinone. Following workup of the reaction mixture and removal of solvent, an amorphous orange solid was isolated. Slow evaporation under ambient conditions from a saturated toluene solution over four weeks resulted in the formation of large orange blocks of **2** suitable for X-ray diffraction experiments (24%). A single-crystal X-ray diffraction study confirmed the identity of the product as the title compound shown in Figure 1.02. Details of the data collection, structure solution and refinement are compiled in Table 1.04 and selected metrical parameters are listed in Tables 1.05 and 1.06.

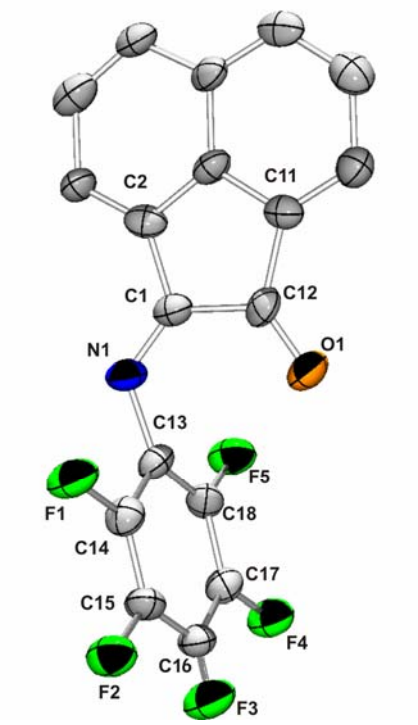

Figure 1.02. Molecular structure of 2 showing a partial numbering scheme. The thermal ellipsoids are shown at the 40% probability level. All hydrogen atoms have been omitted for clarity.

X-ray analysis reveals that **2** crystallizes in the triclinic space group *P-1*. The C(1)-C(12) bond distance of 1.591(6) Å and the C(1)-N(1) bond distance of 1.252(5) Å imply bond orders of two and one, respectively. Analysis of the ^{1}H NMR spectrum reveals multiple aromatic signals indicative of a lower order symmetry compared to the spectra of known BIAN ligands. Crystallization of the crude product was necessary as residual pentafluoroaniline was evident upon workup of the reaction mixture. The amorphous orange product was purified by slow evaporation from a saturated toluene solution, affording orange blocks of **2**. Variation of reaction stoichiometry or reaction conditions invariably led to the isolation of **2**, with no measurable quantity of the doubly-substituted pentafluorophenyl-substituted BIAN ligand being formed.

Synthesis and Characterization of 2-(2,3,5,6-tetrafluoro-phenylimino)-2H-acenaphthylen-1-one (3)

2-(2,3,5,6-tetrafluoro-phenylimino)-2H-acenaphthylen-1-one (**3**) was synthesized by reaction of 0.33 equivalents of acenaphthenequinone with a stirred solution comprised of equimolar quantities of 2,3,5,6-tetrafluoroaniline and $(CH_3)_3N$-AlH_3. Following workup of the reaction mixture and removal of solvent, an orange solid was isolated. This crude solid was dissolved in acetonitrile and the temperature was reduced to -15°C for 3 days, after which small orange rods of **3** suitable for X-ray diffraction experiments were obtained (21%). A single-crystal X-ray diffraction study confirmed the identity of the product as the title compound shown in Figure 1.03. Details of the data collection, structure solution and refinement are compiled in Table 1.07 and selected metrical parameters are listed in Tables 1.08 and 1.09.

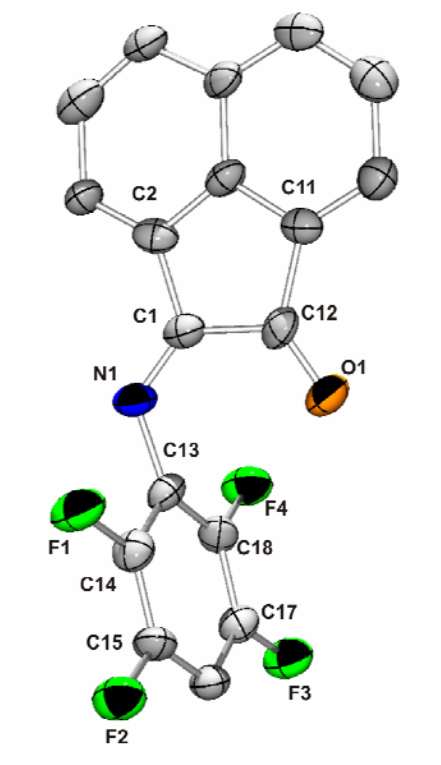

Figure 1.03. Molecular structure of 3 showing a partial numbering scheme. The thermal ellipsoids are shown at the 40% probability level. All hydrogen atoms have been omitted for clarity.

Compound **3** crystallizes in the triclinic space group *P-1*. The C(1)-C(12) bond distance of 1.543(14) Å is indicative of a bond order of one. The C(12)-N(1) bond distance of 1.275(11) Å is in accord with the presence of a C-N double bond. Both bond distances are similar to those found in BIAN ligands. Lastly, the C(1)-O(1) bond distance of 1.215(11) Å is in accord with that expected for a C-O double bond. The foregoing metrical parameters are consistent with a structure for **3** that features both ketone and imine functionalities.

The ^{1}H NMR spectrum of **3** was not indicative of formation of the doubly-substituted BIAN ligand. Despite variations in the reaction stoichiometry, reaction conditions or solvent, **3** was always the exclusively isolated product.

Synthesis and Characterization of 2-*tert*-butylimino-2H-acenaphthylen-1-one (4)

2-*tert*-butylimino-2H-acenaphthylen-1-one (**4**) was synthesized by treatment of 0.33 equivalents of acenaphthenequinone with a stirred solution consisting of equimolar quantities of *tert*-butyl-amine and $(CH_3)_3N$-AlH_3. Following workup of the reaction mixture and removal of the solvent, a yellow solid was isolated in moderate yield (75%). The crude solid was dissolved in a THF/hexanes mixture and the resulting solution was cooled to -15°C for 3 days, after which yellow crystals of **4** suitable for X-ray diffraction experiments were obtained (8%). A single-crystal X-ray diffraction study confirmed the identity of the product as the title compound shown in Figure 1.04. Details of the data collection, structure solution and refinement are compiled in Table 1.10 and selected metrical parameters are listed in Tables 1.11 and 1.12.

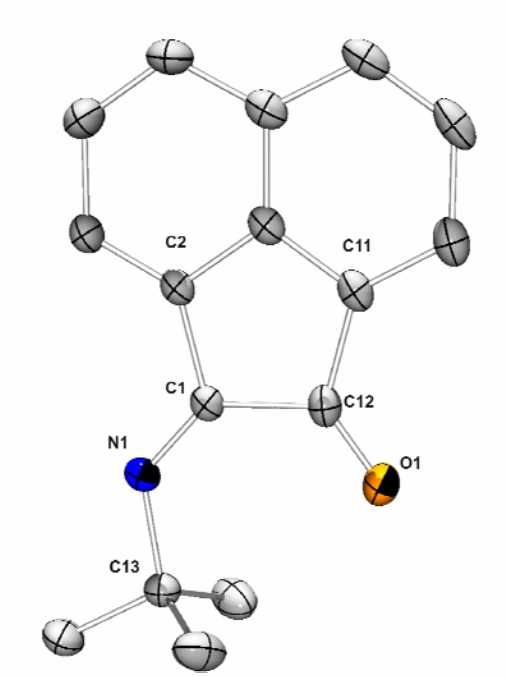

Figure 1.04. Molecular structure of 4 showing a partial numbering scheme. The thermal ellipsoids are shown at the 40% probability level. All hydrogen atoms have been omitted for clarity.

Compound **4** crystallizes in the orthorhombic space group *Pnma*. The C(1)-C(12) bond distance of 1.564(3) Å is indicative of a C-C single bond and the C(1)-N(1) bond distance of 1.272(3) Å is in accord with a C-N double bond. Both bond distances are similar to those of the BIAN ligand class. Finally, the C(12)-O(1) bond distance of 1.208(3) Å is consistent with a C-O bond order of two. Taken collectively, the foregoing metrical parameters are consistent with the presence of both ketone and imine functionalities. ^{1}H NMR and mass spectral data did not provide any evidence for the formation of the desired ^{t}Bu-BIAN ligand. The 1:1 reaction stoichiometry was necessary for isolation of **4**.

Section 1.1 Conclusions

The aluminum transfer reagent $[(C_6F_5)N\text{-}Al(H)(THF)]_2$ (**1**) was synthesized in high yield by treatment of $(C_6F_5)\text{-}NH_2$ with $(CH_3)_3N\text{-}AlH_3$. The reactions of aminoalane transfer reagents with acenaphthenequinone furnished a series of ketoimine ligands based on a BIAN framework. The specific compounds synthesized are 2-pentafluorophenylimino-2H-acenaphthylen-1-one (**2**), 2-(2,3,5,6-tetrafluoro-phenylimino)-2H-acenaphthylen-1-one (**3**) , and 2-*tert*-butylimino-2H-acenaphthylen-1-one (**4**). While a few examples of such ligands are described in the literature, there are no examples of such ligands bearing fluorinated or alkyl substituents. Given the failure of condensation reactions to produce ligands bearing these potentially useful substituents, it is anticipated that this synthetic approach will provide a route to previously inaccessible ketoimine ligands featuring a wide variety of aryl or alkyl substituents.

Section 1.2 Introduction

As discussed in Section 1.1, with the use of a number of aluminum transfer reagents, it was only possible to effect mono-substitution of acenaphthenequinone. However, by modification of the transfer reagents and variation of the reaction stoichiometries, BIAN ligands were found to be accessible in moderate yield. Section 1.2 includes a discussion of the synthesis of several new, structurally authenticated BIAN ligands. Although the synthesis of a C_6F_5-substituted BIAN ligand proved to be impossible using this synthetic approach, the attempted synthesis of this compound sheds some light on the degree of difficulty encountered in the synthesis of this particular ligand.

Synthesis and Characterization of (1-methyl-2-pentafluorophenylimino-acenaphthen-1-yl)-pentafluorophenylamine (5)

The synthesis of (1-methyl-2-pentafluorophenylimino-acenaphthen-1-yl)-pentafluorophenylamine (**5**) was achieved by adding a stirred solution of equimolar quantities of $AlMe_3$ and C_6F_5-NH_2 to 0.33 equivalents of acenaphthenequinone. Following workup of the reaction mixture and solvent removal, a pale yellow solid was isolated. The crude solid was dissolved in a THF/hexanes mixture and the resulting solution was stored at -15°C for 3 days, during which time pale yellow crystals of **5** suitable for X-ray diffraction experiments were obtained (19%). A single-crystal X-ray diffraction study confirmed the identity of the product as the title compound shown in Figure 1.05. Details of the data collection, structure solution and refinement are compiled in Table 1.13 and a selection of metrical parameters is presented in Tables 1.14 and 1.15.

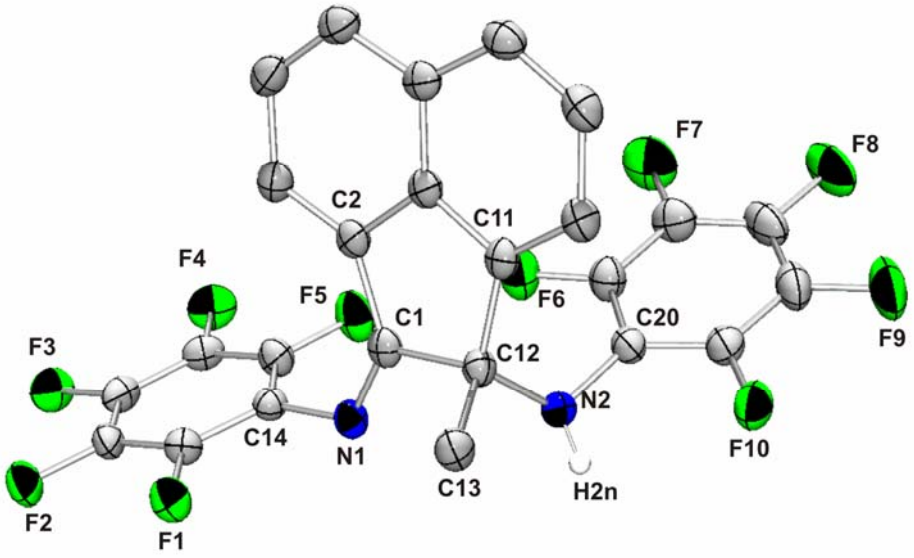

Figure 1.05. Molecular structure of 5 showing a partial numbering scheme. The thermal ellipsoids are shown at the 40% probability level. With the exception of H2n, all hydrogen atoms have been omitted for clarity.

Compound **5** crystallizes in the triclinic space group *P-1*. Several of the metrical parameters provide insight into the molecular structure of **5**. Thus, the C(1)-C(12) and C(1)-N(1) bond distances of 1.566(3) Å and 1.277(3) Å are indicative of C-C single and C-N double bonds, respectively. However, the C(12)-N(2) and C(12)-C(13) bond distances of 1.474(3) Å and 1.523(3) Å, respectively, are both consistent with the presence of single bonds. The presence of C(13) further confirms the saturated nature of the bonds. The ^{1}H NMR spectrum of **5** revealed the presence of a singlet at δ 1.53 corresponding to the methyl protons on C(13). Additionally, a low-intensity singlet at δ 4.50 integrating to one proton can be assigned to the amine proton H(2n). As a consequence of the low molecular symmetry of **5**, all six individual aromatic naphthalene-based protons were clearly discernable. The ^{19}F spectrum of **5** is also consistent with the broken symmetry. Specifically, seven ^{19}F resonances were detected in the range δ -152 to -172 and integrate to a total of ten fluorine atoms. Perhaps the most

intriguing aspect of the structure of **5** is the presence of a methyl group on C(12). By analogy with work reported by Ragaini *et al.*[7], it is suggested that the presence of this methyl group is a consequence of the excessive ring strain that exists in the transiently formed C_6F_5-BIAN ligand. The sp^2 hybridization of the resultant five-membered ring causes severe ring strain. Subsequent methylation results in an sp^3 hybridized C(12) atom which offers partial relief of the aforementioned strain. It is clear from this result that the use of an aluminum transfer reagent possessing a methyl group is unlikely to result in formation of the desired C_6F_5-BIAN ligand.

Synthesis and Characterization of bis(4-fluorophenylimino)acenaphthene (6)

Bis(4-fluorophenylimino)acenaphthene (p-F-BIAN) (**6**) was synthesized by means of a two-step process. The initially formed $ZnCl_2$ complex was prepared by stirring acenaphthenequinone with three equivalents of 4-fluoroaniline and three equivalents of $ZnCl_2$ in acetic acid under reflux conditions. The resulting $ZnCl_2$ complex precipitated as an orange solid which was isolated by filtration and overnight drying. This complex was treated with $K_2C_2O_4$ to afford compound **6** in moderate yield (59%). A single-crystal X-ray diffraction study of a crystal grown from a toluene solution at -15°C confirmed the identity of the product as the title compound shown in Figure 1.06. Details of the data collection, structure solution and refinement are compiled in Table 1.16 and selected metrical parameters are compiled in Tables 1.17 and 1.18.

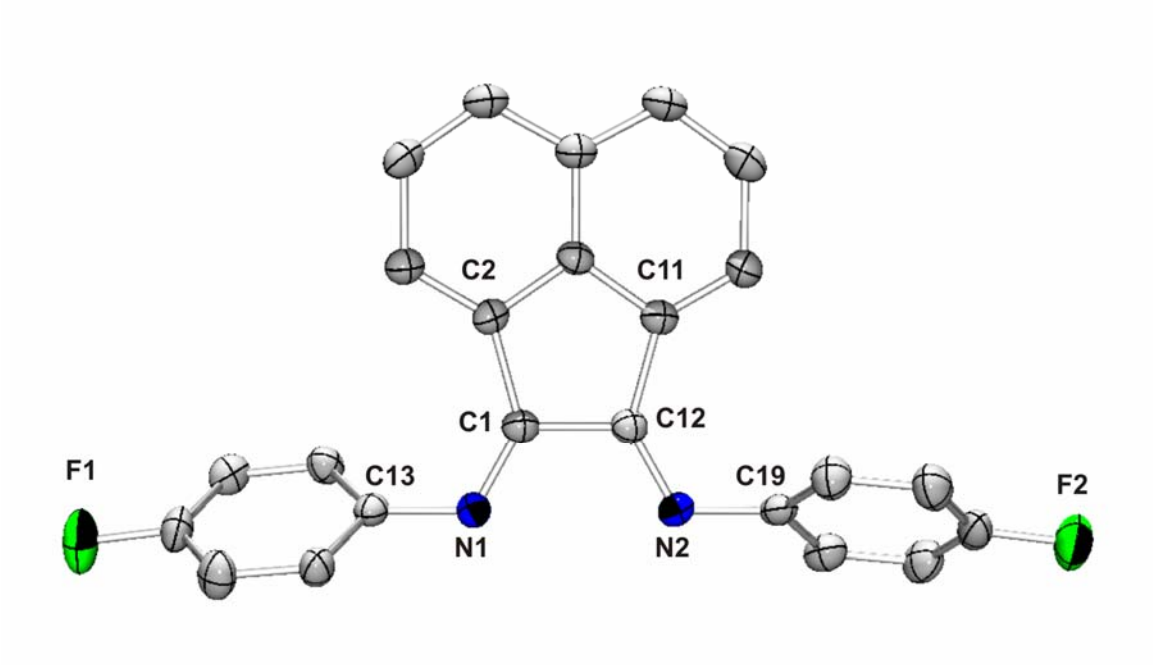

Figure 1.06. Molecular structure of 6 showing a partial numbering scheme. The thermal ellipsoids are shown at the 40% probability level. All hydrogen atoms have been omitted for clarity.

Although the p-F-BIAN ligand has been synthesized previously[11], no single-crystal X-ray data were available. Accordingly, a crystalline sample of **6** was prepared using the literature procedure. Compound **6** crystallizes in the monoclinic space group $P2_1/n$. Several of the metrical parameters provide insight into the structure of **6**. Thus, the C(1)-C(12) bond distance of 1.518(5) Å is consistent with a bond order of one while the average C-N bond distance of 1.277(4) Å is indicative of the presence of C-N double bonds. Overall, the foregoing metrical parameters are similar to those reported for other structurally authenticated BIAN ligands.

Synthesis and Characterization of bis(1-adamantylimino)acenaphthene (7)

Bis(1-adamantylimino)acenaphthene (Ad-BIAN) (**7**) was synthesized by the addition of a stirred solution consisting of equimolar quantities of 1-adamantylamine and

$Al(CH_3)_3$ in THF to 0.33 equivalents of acenaphthenequinone. A viscous, brown oil was isolated following work up of the reaction mixture and the removal of solvent. The addition of hexanes to this initially oily product resulted in the formation of a yellow solid. This solid was filtered off and recrystallized from toluene solution at -15°C to afford yellow crystals of **7** in 60% yield. A single-crystal X-ray diffraction study confirmed the identity of the product as the title compound shown in Figure 1.07. Details of the data collection, structure solution and refinement are compiled in Table 1.19 and selected metrical parameters are listed in Tables 1.20 and 1.21.

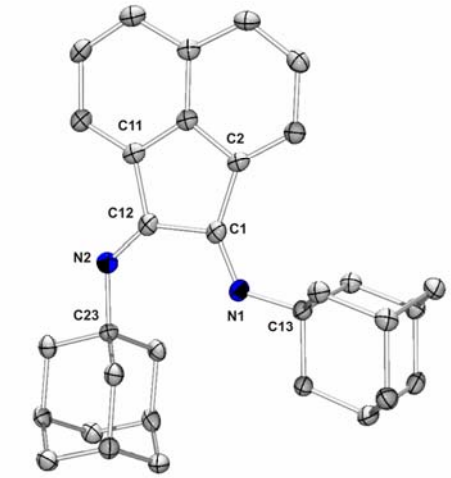

Figure 1.07. Molecular structure of 7 showing a partial numbering scheme. The thermal ellipsoids are shown at the 40% probability level. All hydrogen atoms have been omitted for clarity.

Compound **7** crystallizes in the triclinic space group *P-1*. Some of the metrical parameters provide insight into the structure of **7.** Thus, the C(1)-C(12) distance of 1.563(4) Å is indicative of a C-C single bond, while the average C-N bond distance of 1.271(3) Å is consistent with a bond order of two. Overall, the skeletal structure is similar to those of reported BIAN ligands. It should be noted that, with only one exception[12], all BIAN ligands crystallize in the *E,E* conformation. The Ad-BIAN ligand

therefore represents only the second example of this ligand class to exhibit an *E,Z* conformation in the crystalline state.

Synthesis and Characterization of bis(*tert*-butylimino)acenaphthene (8)

Bis(*tert*-butylimino)acenaphthene (^{t}Bu-BIAN) (**8**) was synthesized by adding one equivalent of $[HAlN(tBu)]_4$ to 0.20 equivalents of acenaphthenequinone at room temperature. A viscous, brown oil was isolated following work up of the reaction mixture and solvent removal. The addition of hexanes to the initial oily product resulted in the formation of the yellow solid **8.** The solid was filtered off and recrystallized from toluene at -15°C to afford a large crop of yellow crystals in 48% yield. A single-crystal X-ray diffraction study confirmed the identity of the product as the title compound shown in Figure 1.08. Details of the data collection, structure solution and refinement are compiled in Table 1.22 and a selection of metrical parameters for **8** is presented in Tables 1.23 and 1.24.

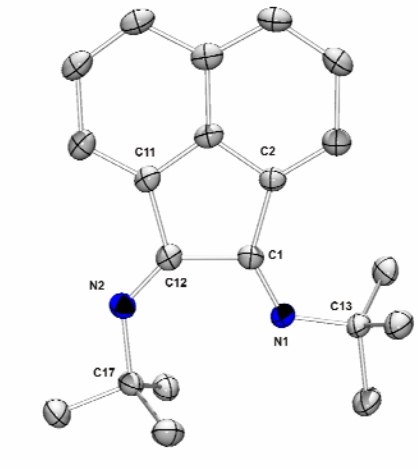

Figure 1.08. Molecular structure of 8 showing a partial numbering scheme. The thermal ellipsoids are shown at the 40% probability level. All hydrogen atoms have been omitted for clarity.

Compound **8** crystallizes in the tetragonal space group *P43*. Metrical parameters which are pertinent to the description of the structure of **8** include the C(1)-C(12) bond distance of 1.552(3) Å, which is indicative of a C-C single bond, and the average C-N bond distance of 1.277(3) Å which implies a bond order of two. As expected, these metrical parameters are similar to those of unligated BIAN ligands. Akin to **7**, compound **8** also exists in the *E,Z* conformation in the crystalline state.

Synthesis and Characterization of 2-tert-butylimino-2H-acenaphthylen-1-ylidene-pentafluorophenyl-amine (9)

2-tert-butylimino-2H-acenaphthylen-1-ylidene-pentafluorophenyl-amine (^{t}Bu/C_6F_5-BIAN) (**9**) was prepared by the addition of one equivalent of **2** to three equivalents of $[HAl(N\text{-}^t Bu)]_4$. A viscous, orange oil was obtained following work up of the reaction mixture and stripping of the solvent. The orange oil was crystallized by the addition of hexanes. The resulting yellow solid was filtered off and recrystallized from toluene at -15°C, thereby affording a small crop of yellow crystals in 21% yield. The molecular structure of **9** was confirmed on the basis of a single-crystal X-ray diffraction study. The structure of **9** is illustrated in Figure 1.09. Details of the data collection, structure solution and refinement are compiled in Table 1.25 and salient metrical parameters are listed in Tables 1.26 and 1.27.

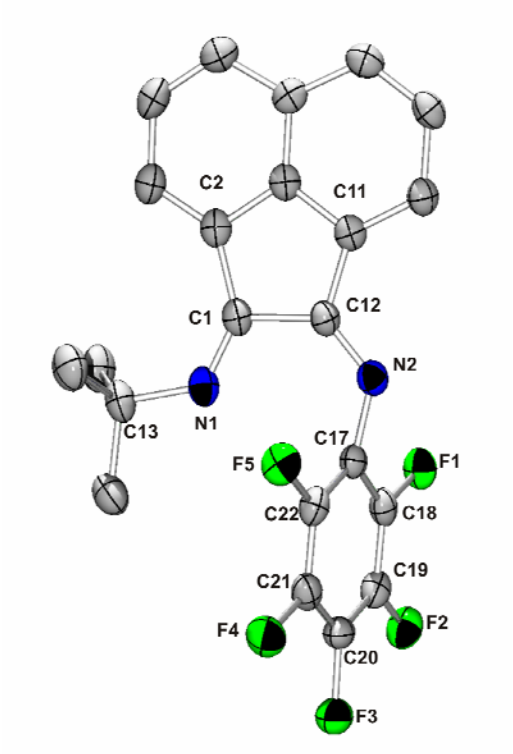

Figure 1.09. Molecular structure of 9 showing a partial numbering scheme. The thermal ellipsoids are shown at the 40% probability level. All hydrogen atoms have been omitted for clarity.

Compound **9** crystallizes in the monoclinic space group $P2_1/n$. The C(1)-C(12) distance of 1.541(4) Å and the average C-N bond distance of 1.276(3) Å are similar to those for other uncoordinated BIAN ligands.

The ^{1}H spectrum of **9** comprises a singlet at δ 1.33 corresponding to the nine ^{t}Bu protons. The six naphthalene protons are distributed over three overlapping resonances in the aromatic region of the spectrum and the ^{19}F spectrum consists of five discreet resonances ranging from δ -153 to -167.

The synthesis of ligand **9** represents an alternative synthetic scheme to the transimination reactions employed by Ragaini *et al.*[13] for the synthesis of BIAN ligands bearing mixed R substituents. The advantage of this synthetic methodology lies in the

ability to employ alkyl or heavily fluorinated groups for the synthesis of BIAN ligands with unique electronic properties.

Synthesis and Characterization of bis(*tert*-butylimino)acenaphthene zinc chloride complex (10)

The zinc chloride complex of bis(*tert*-butylimino)acenaphthene (**10**) was synthesized by stirring equimolar quantities of **8** and $ZnCl_2$ in THF solution. Removal of the reaction solvent afforded a yellow-green solid which was dissolved in acetonitrile and stored for three days at -15°C. During this time, a crop of lime green crystals was formed in moderate yield (51%). The molecular structure (Figure 1.10) was confirmed on the basis of a single-crystal X-ray diffraction study. Details of the data collection, structure solution and refinement are compiled in Table 1.28 and a selection of relevant metrical parameters is assembled in Tables 1.29 and 1.30.

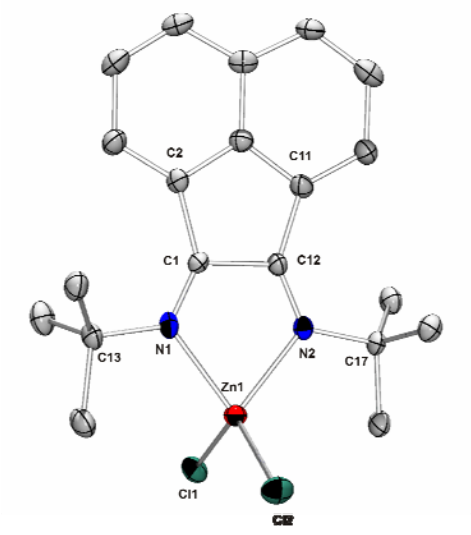

Figure 1.10. Molecular structure of 10 showing a partial numbering scheme. The thermal ellipsoids are shown at the 40% probability level. All hydrogen atoms and one molecule of acetonitrile have been omitted for clarity.

Compound **10** crystallizes in the monoclinic space group $P2_1/n$. Overall, the molecular structure of **10** is very similar to those of unligated BIAN ligands thus implying that coordination of the BIAN nitrogen atoms to zinc has very little impact on the rest of the structure. Thus, the C(1)-C(12) bond distance of 1.552(8) Å and average C-N bond distance of 1.274(8) Å are virtually identical to the analogous bond distances of 1.552(3) Å and 1.277(3) Å observed in the free ^{t}Bu-BIAN ligand[14].

Section 1.2 Conclusions

The Ad-BIAN (**7**) and ^{t}Bu-BIAN (**8**) ligands have been synthesized in moderate yields by treatment of acenaphthenequinone with imino- and aminoalane transfer reagents. These ligands had previously been inaccessible by traditional routes including condensation and transimination methods. A $ZnCl_2$ coordination complex of ^{t}Bu-BIAN (**10**) has also been synthesized, thereby demonstrating the donor ability of this diimine. Moreover, by controlling the reaction stoichiometry and by careful selection of the transfer reagent, it has also been possible to prepare the mixed BIAN ligand ^{t}Bu/C_6F_5-BIAN (**9**).

The product (1-methyl-2-pentafluorophenylimino-acenaphthen-1-yl)-pentafluorophenylamine (**5**) was isolated from an attempt to synthesize the hitherto unknown C_6F_5-BIAN ligand by treatment of acenaphthenequinone with a mixture of $AlMe_3$ and C_6F_5-NH_2. It is conceivable that the desired C_6F_5-BIAN ligand exists as an unstable intermediate on the reaction pathway to **5**.

Finally, the 4-fluoro-substituted BIAN ligand (p-F-BIAN) (**6**) was synthesized according to the literature method. As discussed later, this structural information was

pertinent to an understanding of the electron transfer processes in p-F-BIAN charge transfer complexes.

Section 1.3 Introduction

The final section of this chapter is concerned with a discussion of the synthesis and structures of the compounds that were isolated during the synthesis of the tetrakis(imino)pyracene (TIP) ligand. The synthetic approach to this ligand began with the oxidation of acenaphthylene with oxalyl bromide in the presence of aluminum(III) bromide to form 1,2-diketopyracene. Subsequent oxidation of the ethylene bridge with benzene selenic anhydride (BSA) resulted, after work up of the reaction mixture, in the isolation of the TIP ligand precursor, 1,2,7,8-tetraketopyracene. The keto groups of tetraketopyracene were converted into imino functionalities using the synthetic protocol that is employed for the synthesis of various aryl-BIAN ligands.

Synthesis and Characterization of bis(2,6-diisopropylphenylimino)pyracene zinc chloride complex (11)

The bis(2,6-diisopropylphenylimino)pyracene zinc chloride complex (**11**) was synthesized by treatment of 1,2-diketopyracene with four equivalents of 2,6-diisopropylaniline and two equivalents of $ZnCl_2$ in acetic acid at reflux. Following work up of the reaction mixture, **11** was isolated in an overall yield of 76%. Crystals suitable for X-ray diffraction studies were grown from a saturated CH_2Cl_2 solution stored at -15°C for four days. Single-crystal X-ray analysis verified the proposed structure, a

depiction of which is shown in Figure 1.11. Details of the data collection, structure solution and refinement are presented in Table 1.31 and some pertinent metrical parameters are listed in Tables 1.32 and 1.33.

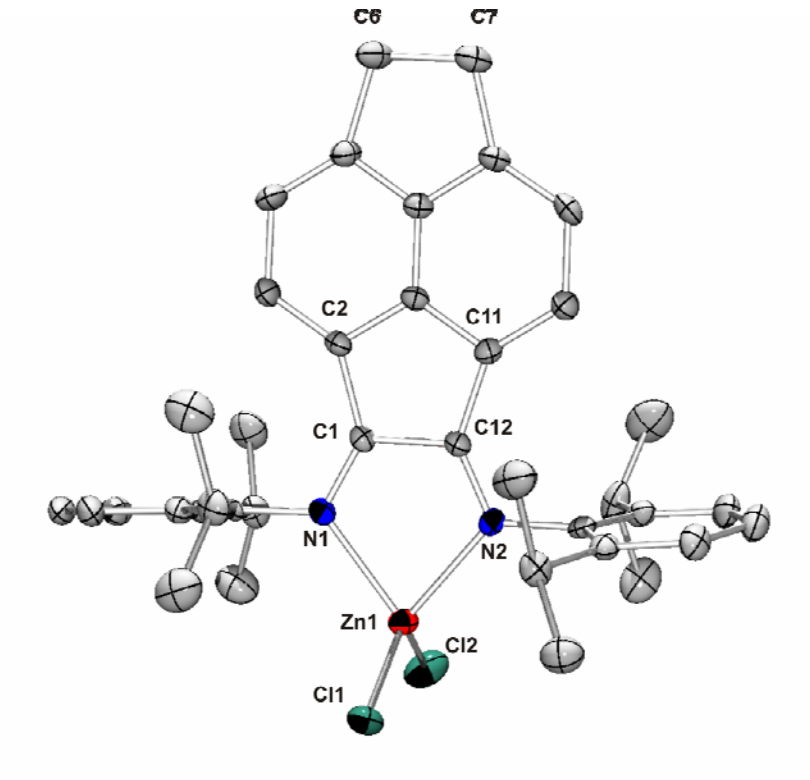

Figure 1.11. Molecular structure of 11 showing a partial numbering scheme. The thermal ellipsoids are shown at the 40% probability level and all hydrogen atoms have been omitted for clarity.

Compound **11** crystallizes in the orthorhombic space group $P2_12_12_1$. The 2,6-(diisopropylphenyl)imino ligand is bonded to zinc by N→Zn donor-acceptor bonds and no redox reaction has taken place as evidenced by the C(1)-C(12) bond distance of 1.534(6) Å which corresponds to a single bond and the average C-N bond distance of 1.283(5) Å which falls in the region anticipated for C-N double bonds.

The ^{1}H NMR spectrum of **11** features a single resonance associated with the C(6)-C(7) bridging atoms and appears at δ 3.54. Since this resonance integrates to four protons and the C(6)-C(7) bond distance is 1.564(7) Å, the presence of a saturated ethylene bridge is confirmed.

Synthesis and Characterization of bis(2,6-diisopropylphenylimino)pyracene (12)

The bis(2,6-diisopropylphenylimino)pyracene (**12**) ligand was synthesized by decomplexation of **11** with an aqueous solution of $K_2C_2O_4$. Workup of the reaction mixture and removal of solvent afforded an analytically pure yellow-orange powder. The solid was dissolved in CH_2Cl_2 and stored at -15°C for two days, after which yellow crystals were obtained in moderate yield (71%). A single-crystal X-ray diffraction study confirmed the identity of this product and a depiction of the structure is presented in Figure 1.12. Details of the data collection, structure solution and refinement are compiled in Table 1.34 and a compilation of relevant metrical parameters appears in Tables 1.35 and 1.36.

An alternate synthetic route to **12** was found and involved reaction of 1,2-diketopyracene with four equivalents of 2,6-diisopropylaniline in acetic acid. Interestingly, the yield of **12** obtained via this route (90%) exceeded that obtained using the $ZnCl_2$ coordination/decomplexation method described above.

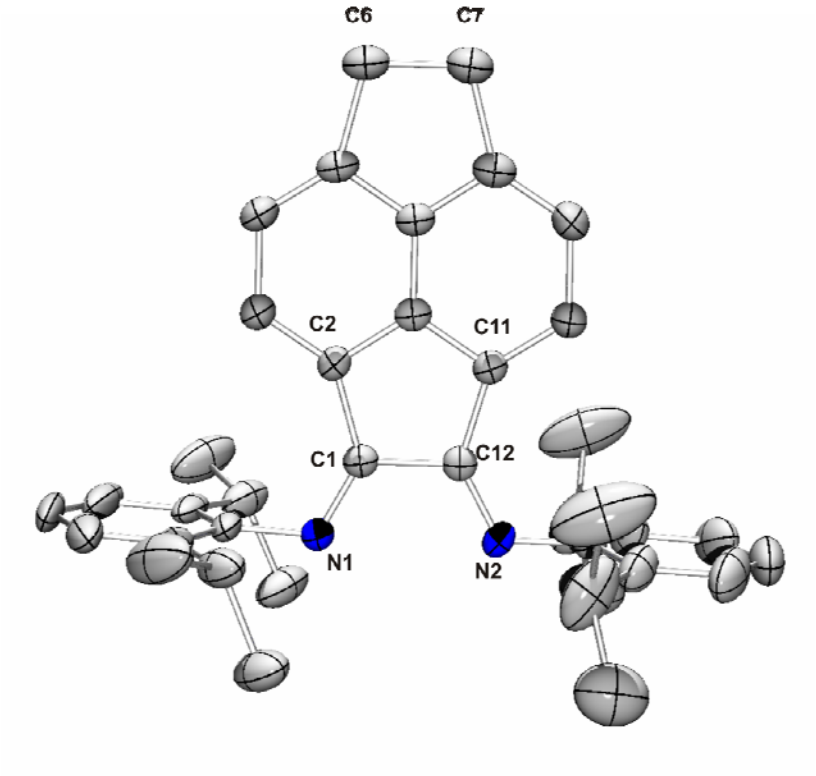

Figure 1.12. Molecular structure of 12 showing a partial numbering scheme. The thermal ellipsoids are shown at the 40% probability level. All hydrogen atoms have been omitted for clarity.

Compound **12** crystallizes in the orthorhombic space group *Pnma*. The bond order for the C(1)-C(12) bond (1.527(4) Å) is one while the average C-N separation of 1.277(4) Å corresponds to the assignment of double bonds. As expected, these bond distances fall in the same range as those found for the BIAN ligands that were discussed earlier.

Analysis of the ^{1}H NMR spectrum reveals a singlet resonance at δ 3.44 which is attributable to the four hydrogen atoms located on the C(6)-C(7) bridging atoms. Along with the fact that the C(6)-C(7) bond distance of 1.569(5) Å corresponds to a single bond, it is evident that, as in the case of **11**, this bridge is saturated.

Synthesis and Characterization of tetrakis(2,6-diisopropylphenylimino)pyracene bis(zinc chloride) complex (13)

The tetrakis(2,6-diisopropylphenylimino)pyracene bis(zinc chloride) complex [$(ZnCl_2)_2$Dipp-TIP] (**13**) was synthesized by reaction of one equivalent of 1,2,7,8-tetraketopyracene, six equivalents of 2,6-diisopropylaniline and four equivalents zinc chloride in acetic acid at reflux. Filtration and washing of the resultant orange precipitate, followed by recrystallization from chloroform at -15°C for two days resulted in a moderate yield (47%) of orange crystals. A single-crystal X-ray diffraction study confirmed the identity of the product as the title compound as shown in Figure 1.13. Details of the data collection, structure solution and refinement are compiled in Table 1.37 with selected metrical parameters listed in Tables 1.38 and 1.39.

An alternate synthetic route involved the reaction of **14** with four equivalents of zinc chloride in THF solution. Workup of the reaction mixture resulted in an orange powder. While a crystal of **13** suitable for X-ray diffraction studies was obtained from chloroform at -15°C, the crude orange powder was found to be predominantly **14** as determined by ^{1}H NMR spectroscopy.

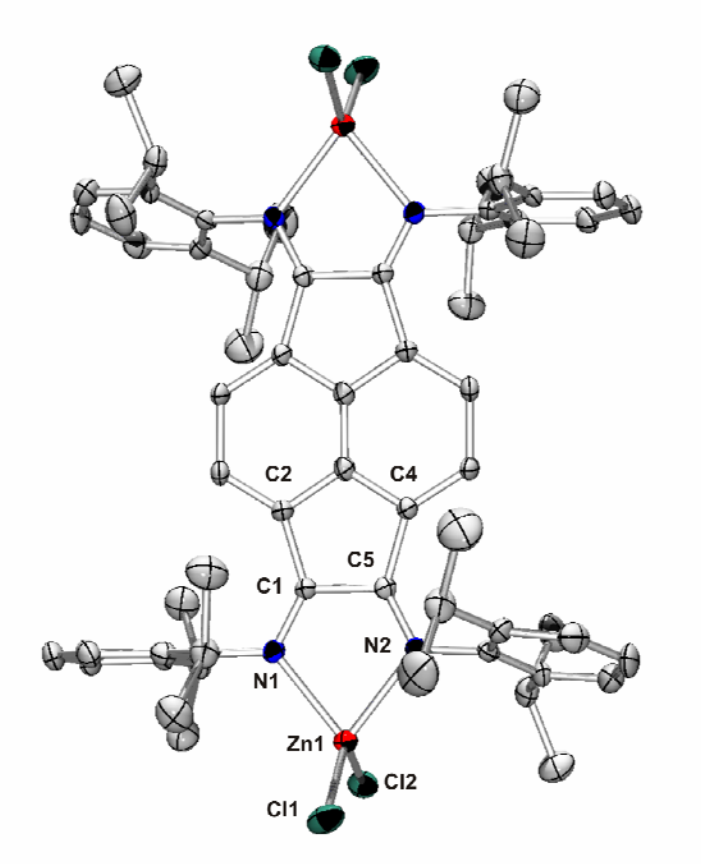

Figure 1.13. Molecular structure of 13 showing a partial numbering scheme. The thermal ellipsoids are shown at the 40% probability level. All hydrogen atoms and six chloroform molecules have been omitted for clarity.

Compound **13** crystallizes in the triclinic space group *P-1* with a crowded asymmetric unit consisting of two independent half molecules of **13** with six chloroform molecules. Metrical parameters providing insight into the structure of **13** include the C(1)-C(5) distance of 1.532(7) Å, indicative of a C-C single bond, and the average C-N bond distance of 1.268(6) Å, indicative of C-N double bonds. These distances are indicative of the same bonding mode present in zinc chloride complexes of BIAN ligands. It is evident that the $ZnCl_2$ moieties are coordinated in a donor-acceptor fashion.

Analysis of the ^1H NMR spectrum reveals high symmetry associated with the molecule. Further, the purity of the spectrum attests to the high reactivity of the ligand in that no mononuclear complexes were obtained in any measurable amount.

Synthesis and Characterization of tetrakis(2,6-diisopropylphenylimino)pyracene (14)

Tetrakis(2,6-diisopropylphenylimino)pyracene (Dipp-TIP) (**14**) was synthesized by reaction of 1,2,7,8-tetraketopyracene with six equivalents of 2,6-diisopropylaniline in an acetic acid/acetonitrile mixture at reflux. Cooling of the solution with subsequent filtration resulted in an orange precipitate. Washing and drying afforded an analytically pure orange solid in high yield (85%). Recrystallization from chloroform at -15°C for three days yielded large orange blocks. A single-crystal X-ray diffraction study confirmed the identity of the title compound as shown in Figure 1.14. Details of the data collection, structure solution and refinement are compiled in Table 1.40 with selected metrical parameters listed in Tables 1.41 and 1.42.

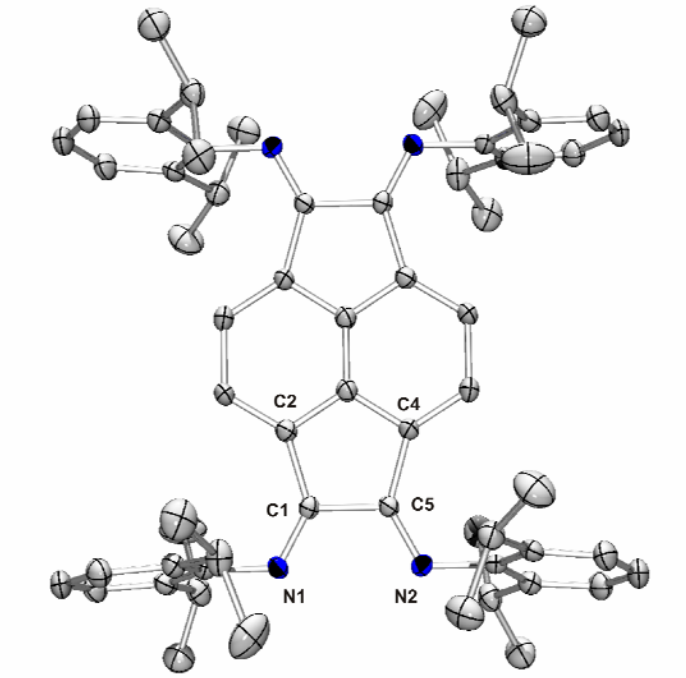

Figure 1.14. Molecular structure of 14 showing a partial numbering scheme. The thermal ellipsoids are shown at the 40% probability level. All hydrogen atoms and two chloroform molecules have been omitted for clarity.

Compound **14** crystallizes in the monoclinic space group $P2_1/n$ with two molecules of chloroform. Metrical parameters providing insight into the structure of **14** include the C(1)-C(5) distance of 1.549(4) Å, indicative of a C-C single bond, and the average C-N bond distance of 1.266(3), indicative of C-N double bonds. These metrical parameters fall in the same range of bond distances present in BIAN ligands.

The 8 isopropyl methine peaks give rise to a single septet at δ 2.89. The analogous Dipp-BIAN peak is found at nearly the same value and its shift is often used as a diagnostic to determine whether metal coordination has successfully occurred.

Synthesis and Characterization of tetrakis(2,4,6-trimethylphenylimino)pyracene (15)

Tetrakis(2,4,6-trimethylphenylimino)pyracene (Mes-TIP) (**15**) was synthesized by reaction of 1,2,7,8-tetraketopyracene with six equivalents of 2,4,6-trimethylaniline and four equivalents of zinc chloride in acetic acid at reflux. Cooling of the solution and subsequent filtration resulted in a red precipitate. Washing and drying afforded the analytically pure zinc chloride ligand complex. Decomplexation was accomplished with an aqueous solution of $K_2C_2O_4$. Workup of the reaction mixture and removal of solvent resulted in the isolation of an analytically pure red solid (54%). Recrystallization from dichloromethane at -15°C for three days resulted in a crop of large red blocks. A single-crystal X-ray diffraction study confirmed the identity of the title compound as shown in Figure 1.15. Details of the data collection, structure solution and refinement are compiled in Table 1.43 with selected metrical parameters listed in Tables 1.44 and 1.45.

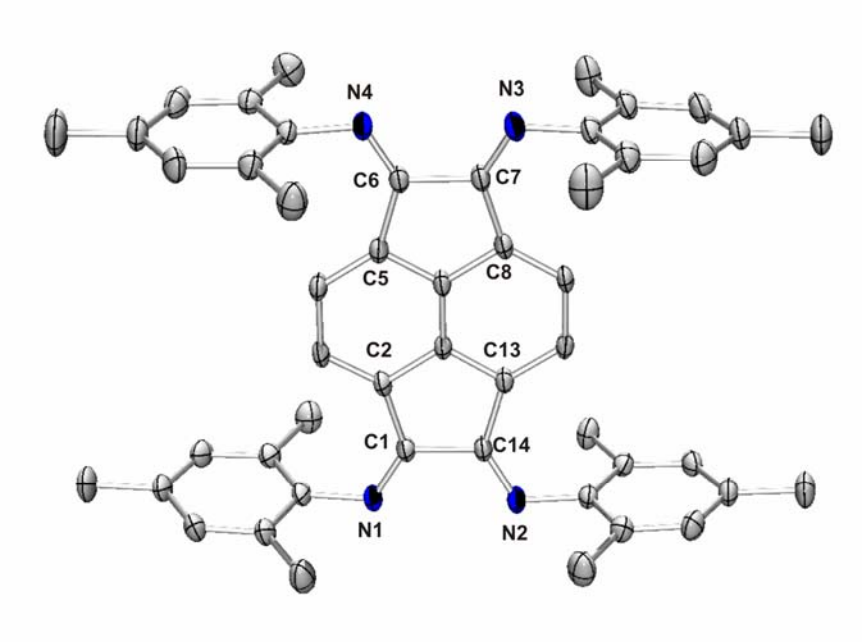

Figure 1.15. Molecular structure of 15 showing a partial numbering scheme. The thermal ellipsoids are shown at the 40% probability level. All hydrogen atoms and one molecule of chloroform have been omitted for clarity.

Compound **15** crystallizes in the monoclinic space group $P2_1/n$. Metrical parameters providing insight into the structure of **15** include the C(1)-C(14) distance of 1.543(3) Å, indicative of a C-C single bond, and the average C-N bond distance of 1.270(2) Å, indicative of C-N double bonds. These metrical parameters fall in the same range of bond distances present in BIAN ligands.

Synthesis and Characterization of tetrakis(4-fluorophenylimino)pyracene (16)

The tetrakis(4-fluorophenylimino)pyracene (p-F-TIP) ligand (**16**) was synthesized by reaction of 1,2,7,8-tetraketopyracene with six equivalents of 4-fluoroaniline and four equivalents of zinc chloride in acetic acid at reflux. Cooling of the solution and subsequent filtration resulted in an orange-red precipitate. Washing and drying afforded

the analytically pure zinc chloride ligand complex. Decomplexation was accomplished with an aqueous solution of $K_2C_2O_4$. Workup of the reaction mixture and removal of solvent resulted in an analytically pure red-orange solid (43%). Recrystallization from dichloromethane at -15°C for three days resulted in the formation of large orange blocks. A single-crystal X-ray diffraction study confirmed the identity of the title compound as shown in Figure 1.16. Details of the data collection, structure solution and refinement are compiled in Table 1.46 with selected metrical parameters listed in Tables 1.47 and 1.48.

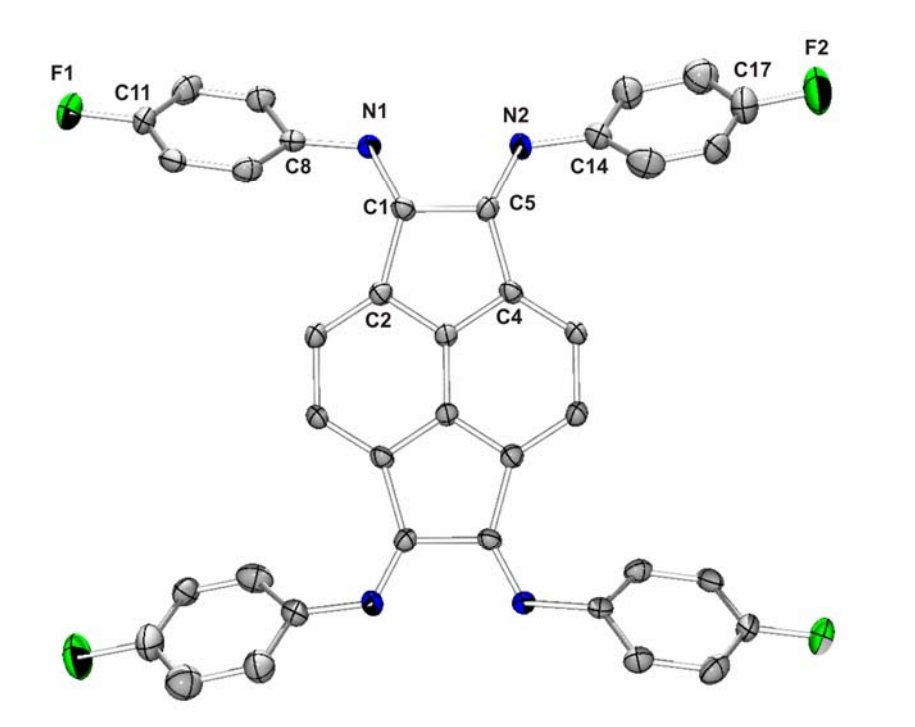

Figure 1.16. Molecular structure of 16 showing a partial numbering scheme. The thermal ellipsoids are shown at the 40% probability level. All hydrogen atoms have been omitted for clarity.

Compound **16** crystallizes in the monoclinic space group $P2_1/c$. Metrical parameters providing insight into the structure of **16** include the C(1)-C(5) distance of 1.547(6) Å, indicative of a C-C single bond, and the average C-N bond distance of

1.260(5) Å, indicative of C-N double bonds. These metrical parameters fall in the same range of bond distances present in BIAN ligands.

The highly symmetric nature of the ligand is demonstrated by the presence of a minimal number of ^{1}H NMR signals and by the single ^{19}F resonance at δ -73.9.

Section 1.3 Conclusions

The zinc chloride complex of 1,2-bis(2,6-diisopropylphenyl)pyracene (**11**) was synthesized via the reaction of 1,2-diketopyracene with 2,6-diisopropylaniline and zinc chloride. The free 1,2-bis(2,6-diisopropylphenyl)pyracene ligand (**12**) was synthesized subsequently by decomplexation of the zinc chloride complex. This new ligand class can be considered to be a BIAN ligand framework possessing an ethyl bridge above the naphthalene backbone. This particular framework may be of structural and synthetic interest in that the ethyl bridge may serve as a site for oxidation. The resulting diketone/diimine species could allow the synthesis of a TIP ligand bearing mixed R substituents. By varying the substituents on either end of the molecule, the ligand could then serve as a platform for mixed valence systems bearing two identical metal fragments.

The Dipp-TIP ligand (**14**) was synthesized in high yield from 1,2,7,8-tetraketopyracene and an excess of 2,6-diisopropylaniline. The p-F-TIP (**16**) and Mes-TIP (**15**) ligands were obtained in good yield from their zinc chloride complexes, synthesized from 1,2,7,8-tetraketopyracene, an excess of the appropriate aniline and zinc chloride. The $(ZnCl_2)_2$ coordination complex of Dipp-TIP (**13**) has also been synthesized from the

free ligand to demonstrate basic reactivity. While the reported TIP ligand structures are limited to the above examples, a variety of TIP ligands bearing aryl substituents should be accessible through this synthetic methodology.

It is noted that the metrical parameters observed for the TIP ligands are markedly similar to those of free BIAN ligands. The average C-N and C-C distances of the TIP diazabutadiene fragments are ~1.27 Å and 1.54 Å, respectively, while the analogous BIAN ligand distances fall in the range of 1.25-1.29 Å and 1.50-1.57 Å, respectively. These two bond distances serve as two primary diagnostic tools for oxidation state determination in metal-BIAN complexes from single crystal X-ray diffraction studies. Given the similarity of these distances in both ligand sets, it is expected that the metrical parameters obtained from X-ray studies of TIP complexes will be an essential tool in analyses of redox products.

Experimental Section

General Procedures

The solvents toluene, THF and hexanes were distilled over sodium with sodium benzophenone ketyl indicator and degassed prior to use. Dichloromethane was distilled over calcium hydride and degassed prior to use. Concentrated acetic acid and acetonitrile were used without purification. An M-Braun argon-filled drybox was employed for the manipulation of all air-sensitive solid reagents. All reactions requiring anaerobic conditions were performed using standard Schlenk or drybox techniques. All glassware was dried at least 24 h in a 120°C oven prior to use.

The compounds $[HAl(N\text{-}^{t}Bu)]_4$[15] and 1,2,7,8-tetraketopyracene[16] were synthesized according to literature procedures. *Tert*-butylamine, 2,6-diisopropylaniline, 2,4,6-trimethylaniline and 4-fluoroaniline were distilled and degassed prior to use. 2,3,4,5,6-pentafluoroaniline and 1-adamantylamine were used as purchased from Aldrich without any purification. Zinc chloride was dried rigorously prior to use. Acenaphthenequinone (technical grade) was purchased from Aldrich and recrystallized from hot acetonitrile prior to use.

Physical Measurements

Low resolution CI mass spectra were collected on a Finnigan MAT TSQ-700 mass spectrometer. High resolution mass spectra were collected on a VG Analytical ZAB-VE sector instrument. All ^{1}H, ^{13}C and ^{19}F NMR spectra were recorded at 295K on

a Varian 300 MHz NMR spectrometer (^{1}H, 300 MHz; ^{13}C, 75 MHz; ^{19}F, 470 MHz). Deuterated solvents were obtained from Cambridge Isotopes and stored over molecular sieves prior to use. ^{1}H and ^{13}C spectra are reported relative to tetramethylsilane and referenced to solvent. Melting points were obtained on a Fisher-Johns apparatus and are reported uncorrected.

X-Ray Crystallography

The X-ray data were collected on a Nonius Kappa CCD diffractometer equipped with an Oxford Cryostream liquid nitrogen cooling stream. All structure determinations and refinements were performed at the University of Texas at Austin. Samples were covered in mineral oil and mounted on a nylon thread loop prior to data collection. All data collection were performed at 153(2) K using graphite monochromated Mo Kα radiation (λ = 0.71073). A correction was applied for Lorentz-polarization in each case. All structures were solved by direct methods and refined by full-matrix least squares on F^2 using the Siemens SHELXL PLUS 5.0 (PC) software package. All hydrogen atoms were either placed in calculated positions (C-H = 0.96 Å) and refined using a riding model and a general isotropic thermal parameter or manually assigned. The total number of reflections, collection ranges and final R-values for each molecule are listed in the appropriate crystallographic data tables.

Preparation of $[(C_6F_5)N\text{-}Al(H)(THF)]_2$ (1)

To a stirred solution of $(CH_3)_3N\text{-}AlH_3$ (3.00 g, 34.70 mmol) in diethyl ether (50 mL) was added dropwise a solution of 2,3,4,5,6-pentafluoroaniline (6.17 g, 33.70 mmol) in diethyl ether (50 mL) at room temperature. Gas evolution occurred immediately upon addition. The solution was allowed to stir under an argon atmosphere for 20 minutes after diethyl ether (25 mL) was added to the solution. The reaction vessel was then closed and stirred for 1 hour after which a white precipitate was evident. The reaction mixture was allowed to stir for 2 days. The solvent was then reduced in volume and the reaction vessel was placed in a dry ice/IPA bath for 20 minutes. The reaction mixture was then filtered with a glass frit and the solid white precipitate was washed with cold diethyl ether (50 mL). Yield 8.30 g (87%). Final purification was carried out by allowing a concentrated THF solution of **1** to stand for one week at -15°C.

Peparation of 2-pentafluorophenylimino-2H-acenaphthylen-1-one (2)

To a stirred suspension of acenaphthenequinone (0.43 g, 2.36 mmol) in THF (100 mL) was added a suspension of **1** (2.0 g, 3.56 mmol) in THF (100 mL). The brown-orange reaction mixture was stirred for 24 h at room temperature. The resultant mixture was then cooled to 0°C and IPA (15 mL) was added slowly over 1 minute. Deionized water (350 mL) and diethyl ether (200 mL) were then added and the solution transferred to a separatory funnel. The organic phase was isolated and the aqueous phase back-extracted with diethyl ether (3 x 25 mL). The combined organic layers were washed with deionized water, dried with $MgSO_4$ and filtered. All solvents were removed affording a viscous, orange oil. The crude oil was dissolved in toluene (200 mL) and was allowed to

slowly evaporate over 1 month. During this time, a crop of large orange crystals was obtained. Yield 0.21 g (24%).

MS (CI^+, CH_4): *m/z* 348 $[M+H]^+$; HRMS (CI^+, CH_4): calcd for $C_{18}H_6NF_5O$ *m/z* 348.0448; found, 348.0451; ^1H NMR ($CDCl_3$): δ 6.91 (d, 1H, NapC-H), 7.01-7.20 (b, 3H, NapC-H), 7.39 (t, 1H, NapC-H), 7.90 (d, 1H, NapC-H); mp: 120°C(d).

Preparation of 2-(2,3,5,6-tetrafluoro-phenylimino)-2H-acenaphthylen-1-one (3)

To a solution of $(CH_3)_3N$-AlH_3 (1.34 g, 15.05 mmol) in diethyl ether (150 mL) was added dropwise a solution of 2,3,5,6-tetrafluoroaniline (2.50 g, 15.15 mmol) in diethyl ether (15 mL). The solution was stirred under an atmosphere of argon for 2 hours, during which time a white precipitate was formed in solution. The solid was filtered and washed with cold diethyl ether (25 mL). The obtained white solid (2.30 g) was dissolved in THF (75 mL) and added to a suspension of acenaphthenequinone (0.20 g, 1.10 mmol) in THF (75 mL). The reaction was stirred under reflux conditions for 2 days as a purple mixture. The resultant mixture was then cooled to 0°C and IPA (5 mL) was added slowly over 1 minute. Deionized water (75 mL) was then added to the mixture resulting in an orange organic phase. Diethyl ether (125 mL) was added and the solution transferred to a separatory funnel. The organic phase was isolated and the aqueous phase back-extracted with diethyl ether (3 x 25 mL). The combined organic layers were washed with deionized water, dried with $MgSO_4$ and filtered. All solvents were removed affording a viscous, orange oil. Hexanes (5 mL) were added to this oil resulting in the formation of a fine orange precipitate which was filtered and dried overnight. The orange solid was recrystallized from a saturated dichloromethane solution stored at -15°C for two days. Yield 0.10 g (20.7%).

MS (CI^+, CH_4): *m/z* 330; ^1H NMR ($CDCl_3$): δ 7.80-7.88 (b, 2H, NapC-H), 8.00-8.13 (b, 2H, NapC-H), 8.22-8.33 (b, 2H, NapC-H), 8.61 (s, 1H, Ar-H); ^{19}F NMR (CD_2Cl_2): δ -139.7 (m, 1F, Ar-F), -141.9 (m, 1F, Ar-F), -151.6 (m, 1F, Ar-F), -153.0 (m, 1F, Ar-F).

Preparation of 2-*tert*-butylimino-2H-acenaphthylen-1-one (4)

To a suspension of acenaphthenequinone (0.46 g, 2.53 mmol) in toluene (50 mL) was added a solution of $[(HAl(N\text{-}^tBu)]_4$ (1.00 g, 2.53 mmol) in toluene (50 mL). The solution was stirred for two days at room temperature. IPA (5 mL), deionized water (50 mL) and diethyl ether (75 mL) were added sequentially and the resulting solution transferred to a separatory funnel. The organic phase was isolated and the aqueous phase back-extracted with diethyl ether (3 x 10 mL). The combined organic layers were washed with deionized water, dried with $MgSO_4$ and filtered. All solvents were removed affording a viscous, brown oil, to which hexanes (5 mL) were added causing precipitation of yellow and orange solids. The precipitate was filtered and dried overnight and subsequently recrystallized from a saturated dichloromethane solution stored at -15°C for two days. Small yellow needles were isolated in very low yield. Yield 0.05 g (8.3%).

MS (CI^+, CH_4): *m/z* 238; ^1H NMR ($CDCl_3$): δ 1.47 (s, 9H, ^{t}Bu), 7.50-7.58 (b, 4H, NapC-H), 7.76 (d, 2H, NapC-H).

Preparation of (1-methyl-2-pentafluorophenylimino-acenaphthen-1-yl)-pentafluorophenylamine (5)

A solution of $AlMe_3$ (30 mL, 2M in toluene, 0.06 mol) was added dropwise to a flask containing a solution of 2,3,4,5,6-pentafluoroaniline (10.98 g, 0.06 mol) in toluene (50 mL). The formation of a colorless precipitate was observed upon addition. The mixture

was stirred at room temperature for 24 h. At this point, the solvent volume was decreased to a volume of 50 mL. To this mixture was added a suspension of acenaphthenequinone (1.82 g, 0.01 mol) in toluene (75 mL). The total solution volume was reduced to 75 mL and the resulting brown mixture was stirred at ambient temperature for 4 days. After this period, the mixture was exposed to air and ethanol was added dropwise until gas evolution ceased. Deionized water (75 mL) and diethyl ether (125 mL) were then added and the mixture transferred to a separatory funnel. The ether phase was separated and the aqueous phase was back-extracted with diethyl ether (3 x 25 mL). The combined organic phases were then washed with deionized water, dried over $MgSO_4$ and filtered. The solvents were removed affording a viscous, brown oil which was dissolved in a minimal amount of diethyl ether, filtered, and stored at -15°C for 4 days affording light brown crystals suitable for X-ray diffraction studies. Yield 0.98 g, (18.6%).

MS (CI^+, CH_4): *m/z* 529; ^{1}H NMR ($CDCl_3$): δ 1.93 (s, 3H,CH_3), 4.50 (s, 1H, N-H), 7.06 (d, 1H, NapC-H), 7.50 (b, 2H, NapC-H), 7.63 (t, 1H, NapC-H), 7.82 (d, 1H, NapC-H), 8.00 (d, 1H, NapC-H); ^{19}F NMR ($CDCl_3$): δ -152.5 (d, 1F, Ar-F), -153.2 (d, 1F, Ar-F), -154.0 (d of d, 2F, Ar-F), -162.5 (t, 1F, Ar-F), -162.8 (t, 2F, Ar-F), -164.6 (t, 2F, Ar-F), -168.2 (t, 1F, Ar-F); mp: 135°C.

Preparation of bis(4-fluorophenylimino)acenaphthene (6)

Acenaphthenequinone (1.0 g, 5.49 mmol) and $ZnCl_2$ (2.0 g, 14.67 mmol) were suspended in acetic acid (20 mL) and heated to 60°C. 4-fluoroaniline (1.52 g, 13.69 mmol) was added by means of a syringe to the suspension and the solution allowed to stir at reflux for 45 min. The resulting mixture was cooled to room temperature and filtered, affording the red zinc chloride complex of **6**. This solid was thoroughly washed with deionized water to remove residual acetic acid. The dried red precipitate was then suspended in

dichloromethane and shaken with a saturated aqueous solution of $K_2C_2O_4$ (50 mL) for 5 min. The organic layer was isolated, washed with deionized water, dried with $MgSO_4$ and filtered. The solvent was then removed affording **6** as a flaky, red solid. Yield 1.20 g (59.4%).

^{1}H NMR ($CDCl_3$): δ 6.85 (d, 2H, NapC-H), 6.99-7.05 (m, 4H, Ar-H), 7.06-7.15 (m, 4H, Ar-H), 7.33 (t, 2H, NapC-H), 7.84 (d, 2H, NapC-H); IR (cm^{-1}): 1652s, 1090s, 804s.

Preparation of bis(1-adamantylimino)acenaphthene (7)

To a solution of $AlMe_3$ (16.5 mL, 2M in toluene, 33.00 mmol) in toluene (100 mL) was added dropwise a solution of 1-adamantlyamine (5.00 g, 33.00 mmol) in toluene (75 mL). The solution was stirred at 100°C overnight. The solvent volume was then reduced to 50 mL and the solution filtered, affording 2.80 g of white solid. This solid was then dissolved in toluene (50 mL) and added slowly to a solution of acenaphthenequinone (0.30 g, 1.65 mmol) in toluene (50 mL). The resulting mixture was stirred for 5 days as a cloudy orange solution. IPA (20 mL), deionized water (100 mL) and diethyl ether (100 mL) were added sequentially and the resulting mixture transferred to a separatory funnel. The organic layer was collected and the aqueous phase back extracted with diethyl ether (3 x 15 mL). The combined organic phases were washed with deionized water, dried with $MgSO_4$ and filtered. Removal of all volatiles resulted in a viscous, brown oil. Addition of ethanol (5 mL) resulted in the formation of a fine yellow precipitate. Filtration of this solid with subsequent drying resulted in isolation of 0.55 g of a crude yellow powder. This solid was dissolved in a minimal amount of dichloromethane and stored at -15°C for three days, affording yellow crystals of **7** suitable for X-ray diffraction studies. Yield 0.45 g (60.1%).

MS (CI^+, CH_4): *m/z* 449 $[M+H]^+$; HRMS (CI^+, CH_4): calcd for $C_{32}H_{36}N_2$ *m/z* 449.2957; found, 449.2955; ^1H NMR (THF-d_8): δ 1.11-1.55 (CH_2, Ad), 2.30-2.50 (CH, Ad), 7.88 (d of d, 1H, NapC-H), 7.93 (d of d, 1H, NapC-H), 8.05 (d, 1H, NapC-H), 8.16 (d, 1H, NapC-H), 8.22 (d, 1H, NapC-H), 8.44 (d, 1H, NapC-H); mp: 195°C(d).

Preparation of bis(*tert*-butylimino)acenaphthene (8)

To a solution of acenaphthenequinone (0.30 g, 1.65 mmol) in toluene (30 mL) was added a solution of $[HAl(N\text{-}^tBu)]_4$ (2.0 g, 5.00 mmol) in toluene (50 mL). The resulting deep red-brown solution was stirred for 5 minutes, after which time the solvent was reduced to a total volume of 50 mL. The mixture was stirred at room temperature for 3 days. IPA (5 mL), deionized water (150 mL) and diethyl ether (100 mL) were added sequentially and the mixture transferred to a separatory funnel. The organic layer was isolated and the aqueous phase back-extracted with diethyl ether (3 x 10 mL). The combined organic layers were washed with deionized water, dried over $MgSO_4$ and filtered. All volatiles were removed resulting in a viscous, brown oil. Diethyl ether (2 mL) and hexanes (10 mL) were added resulting in precipitation of a fine yellow powder which was collected by filtration and dried. The crude solid was dissolved in a minimal volume of dichloromethane and stored at -15°C for 3 days, after which time yellow crystals suitable for X-ray diffraction were isolated. Yield 0.36 g (48.0%).

MS (CI^+, CH_4): *m/z* 293 $[M+H]^+$; HRMS (CI^+, CH_4): calcd for $C_{20}H_{25}N_2$ *m/z* 293.2018; found, 293.2023; ^1H NMR (C_6D_6): δ 1.49 (s, 9H, ^{t}Bu), 1.91 (s, 9H, ^{t}Bu), 7.19 (d of d, 1H, NapC-H), 7.32 (d of d, 1H, NapC-H), 7.51 (d, 2H, NapC-H), 7.69 (d, 1H, NapC-H), 8.11 (d, 1H, NapC-H), 8.44 (d, 1H, NapC-H), 8.44 (d, 1H, NapC-H); IR (cm^{-1}): 1633s, 1261w, 1227w, 1008w, 777s; mp: 104°C.

Preparation of 2-tert-butylimino-2H-acenaphthylen-1-ylidene-pentafluorophenyl-amine (9)

To a solution of **2** (0.175 g, 0.50 mmol) in toluene (20 mL) was added a solution of $[HAlN\text{-}^tBu]_4$ (0.60 g, 1.52 mmol) in toluene (25 mL). The solution was stirred under reflux conditions for 2 days. IPA (5 mL), deionized water (75 mL) and diethyl ether (75 mL) were added sequentially and the mixture transferred to a separatory funnel. The organic phase was separated and the aqueous phase back-extracted with diethyl ether (3 x 10 mL). The combined organic phases were washed with deionized water, dried with $MgSO_4$ and filtered. All volatiles were removed affording a viscous, orange-brown oil. Addition of hexanes (5 mL) resulted in formation of yellow and orange solids. The crude solid was dissolved in a 1:1 saturated toluene/hexanes solution and stored at -15°C for 3 days, after which time a crop of yellow needles suitable for X-ray diffraction studies was obtained. Yield 0.04 g (19.9%).

^1H NMR ($CDCl_3$): δ 1.33 (s, 9H, ^{t}Bu), 7.42-7.48 (t, 1H, NapC-H), 7.51-7.61 (b, 3H, NapC-H), 7.74-7.82 (b, 2H, NapC-H); ^{19}F NMR ($CDCl_3$): δ -153.1 (d, 1F, Ar-F), -157.8 (d, 1F, Ar-F), -158.8 (t, 1F, Ar-F), -164.1 (b, 1F, Ar-F), -166.9 (t, 1F, Ar-F).

Preparation of bis(*tert*-butylimino)acenaphthene zinc chloride complex (10)

To a solution of **8** (0.200 g, 0.68 mmol) in THF (20 mL) was added $ZnCl_2$ (0.093 g, 0.68 mmol). The solution was stirred for 24 h at room temperature after which time the solvent was removed affording a yellow solid. Acetonitrile (20 mL) was added to the flask and the suspension heated to 70°C to dissolve the solid. The solution was filtered through a pre-heated pipette fitted with a cotton plug. The resulting clear, yellow solution was stored at -15°C for 3 days, after which time a crop of pale yellow-green needles suitable for X-ray diffraction were isolated. Yield 0.15 g (51.2%).

MS (CI^+, CH_4): *m/z* 428 $[M+H]^+$; HRMS (CI^+, CH_4): calcd for $C_{20}H_{24}Cl_2N_2Zn$, *m/z* 426.0608; found, 426.0607; ^1H NMR (CD_2Cl_2): δ 1.90 (s, 18H, ^{t}Bu), 7.91 (d of d, 2H, NapC-H), 8.25 (d, 2H, NapC-H), 8.44 (d, 1H, NapC-H).

Preparation of bis(2,6-diisopropylphenyl)iminopyracene zinc chloride complex (11)

1,2-diketopyracene (0.087 g, 0.42 mmol) and $ZnCl_2$ (0.114 g, 0.84 mmol) were suspended in acetic acid (30 mL). After heating the suspension to 80°C, 2,6-diisopropylaniline (0.298 g, 1.68 mmol) was added via syringe. The solution was then stirred at reflux for 1 h. After cooling to room temperature, the orange precipitate was filtered, washed with deionized water and dried overnight. The crude solid was recrystallized from a saturated chloroform solution stored at -15°C for 3 days. Yield 0.209 g (75.6%).

MS (CI^+, CH_4): *m/z* 664 $[M+H]^+$; HRMS (CI^+, CH_4): calcd for $C_{38}H_{43}Cl_2N_2Zn$, *m/z* 663.2681; found, 663.2687; ^1H NMR (CD_2Cl_2): δ 0.87 (d, 12H, ^{i}Pr), 1.34 (d, 12H, ^{i}Pr), 3.27 (sept, 4H, CH), 3.54 (s, 4H, CH_2), 6.65 (d, 2H, NapC-H), 7.32 (d, 2H, NapC-H), 7.39-7.55 (b, 6H, Ar-H); mp: 283°C(d).

Preparation of bis(2,6-diisopropylphenyl)iminopyracene (12)

1,2-diketopyracene (0.100 g, 0.48 mmol) was suspended in a 9:1 acetic acid/acetonitrile solution (30 mL). After heating the suspension to 80°C, 2,6-diisopropylaniline (0.34 g, 1.92 mmol) was added via syringe. The solution was then stirred at reflux for 1 h. After cooling to room temperature, the yellow-orange precipitate was filtered, washed with deionized water and dried overnight. The analytically pure solid was recrystallized from a saturated chloroform solution stored at -15°C for 3 days. Yield 0.228 g (90.0%).

MS (CI^+, CH_4): *m/z* 527 $[M+H]^+$; HRMS (CI^+, CH_4): calcd for $C_{38}H_{43}N_2$, *m/z* 527.3426; found, 527.3428; ^1H NMR (CD_2Cl_2): δ 0.99 (d, 12H, ^{i}Pr), 1.21 (d, 12H, ^{i}Pr), 3.00 (sept, 4H, CH), 3.44 (s, 4H, CH_2), 6.52 (d, 2H, NapC-H), 7.13 (d, 2H, NapC-H), 7.20-7.38 (b, 6H, Ar-H); mp: 222°C(d).

Preparation of tetrakis(2,6-diisopropylphenyl)iminopyracene bis(zinc chloride) complex (13)

1,2,7,8-tetraketopyracene (0.050 g, 0.212 mmol) and $ZnCl_2$ (0.115 g, 0.847 mmol) were suspended in acetic acid (20 mL) and the suspension heated to 80°C. To this stirred mixture was added 2,6-diisopropylaniline (0.225 g, 1.27 mmol) and the resulting mixture was stirred at reflux for 1 h. After cooling to room temperature, an orange precipitate was filtered and washed with copious amounts of deionized water. Recrystallization of **13** was performed by dissolving the crude solid in chloroform and storing the resulting solution at -15°C for 3 days. Yield 0.113 g (46.8%).

MS (CI^+, CH_4): *m/z* 1140 $[M+H]^+$; HRMS (CI^+, CH_4): calcd for $C_{62}H_{72}Cl_4N_4Zn_2$ *m/z* 1140.3094; found, 1140.3109; ^1H NMR (CD_2Cl_2): δ 0.78 (d, 24H, ^{i}Pr), 1.32 (d, 24H, ^{i}Pr), 3.17 (sept, 8H, CH), 6.59 (d, 4H, NapC-H), 7.39 (br, m, 12H, Ar-H).

Preparation of tetrakis(2,6-diisopropylphenyl)iminopyracene (14)

1,2,7,8-tetraketopyracene (0.10 g, 0.42 mmol) was heated to 70°C as a suspension in a 9:1 acetic acid/acetonitrile (30 mL) solution. 2,6-diisopropylaniline (0.45 g, 2.54 mmol) was then added by means of a syringe and the solution stirred at 110°C for 1 h. The solution was cooled to room temperature and the orange precipitate filtered, washed with deionized water and allowed to dry overnight. The resulting analytically pure orange

powder was recrystallized from a saturated dichloromethane solution stored at -15°C for 3 days. Yield 0.31 g (84.5%).

MS (CI^+, CH_4): *m/z* 873 $[M+H]^+$; HRMS (CI^+, CH_4): calcd for $C_{62}H_{72}N_4$, *m/z* 873.5835; found, 873.5833; ^1H NMR ($CDCl_3$): δ 0.89 (d, 24H, ^{i}Pr), 1.17 (d, 24H, ^{i}Pr), 2.89 (sept, 8H, CH), 6.44 (d, 4H, NapC-H), 7.22 (br, m, 12H, Ar-H); IR (cm^{-1}): 1634s, 1461w, 1431w, 1383w, 1362w, 1326w, 1274w, 1192w, 1110w, 1060w, 968w, 936w, 852w; mp: 264°C.

Preparation of tetrakis(2,4,6-trimethylphenyl)iminopyracene (15)

1,2,7,8-tetraketopyracene (0.10 g, 0.42 mmol) and $ZnCl_2$ (0.29 g, 2.13 mmol) were heated to 70°C as a suspension in acetic acid (30 mL). 2,4,6-trimethylaniline (0.34 g, 2.54 mmol) was added by means of a syringe and the solution stirred at 110°C for 1 h. The solution was then cooled to ambient temperature and the red precipitate filtered, washed with deionized water and permitted to dry overnight. The resulting $ZnCl_2$ complex was suspended in dichloromethane and shaken for 5 minutes with a saturated aqueous $K_2C_2O_4$ (1.00 g, 6.02 mmol) solution. The organic layer was separated, washed with deionized water, dried with $MgSO_4$ and filtered. All volatiles were removed affording an analytically pure red solid. Crystals suitable for X-ray diffraction studies were grown from a saturated chloroform solution stored at -15°C for 3 days. Yield 0.16 g, (54.0%).

MS (CI^+, CH_4): *m/z* 705 $[M+H]^+$; HRMS (CI^+, CH_4): calcd for $C_{50}H_{48}N_4$, *m/z* 704.3957; found, 704.3953; ^1H NMR ($CDCl_3$): δ 2.02 (s, 24H, Ar-CH_3), 2.33 (s, 12H, Ar-CH_3), 6.62 (d, 4H, NapC-H), 6.93 (s, 8H, Ar-H); mp: 300°C(d).

Preparation of tetrakis(4-fluorophenyl)iminopyracene (16)

1,2,7,8-tetraketopyracene (0.10 g, 0.42 mmol) and $ZnCl_2$ (0.29 g, 2.13 mmol) were heated to 70°C as a suspension in acetic acid (30 mL). 4-fluoroaniline (0.28 g, 2.52 mmol) was added via syringe and the solution stirred at 110°C for 1 h. The solution was then cooled to room temperature and the red precipitate filtered, washed with deionized water and left to dry overnight. The $ZnCl_2$ complex was suspended in dichloromethane and shaken for 5 minutes with a saturated aqueous $K_2C_2O_4$ (1.00 g, 6.02 mmol) solution. The organic layer was separated, washed with deionized water, dried with $MgSO_4$ and filtered. All volatiles were removed affording an analytically pure red-orange solid. Crystals suitable for X-ray diffraction studies were obtained from a saturated chloroform solution stored at -15°C for 3 days. Yield 0.11 g, (43.1%).

MS (CI^+, CH_4): *m/z* 608 $[M+H]^+$; HRMS (CI^+, CH_4): calcd for $C_{38}H_{20}F_4N_4$, *m/z* 609.1708; found, 609.1697; ^1H NMR (CD_2Cl_2): δ 6.82 (s, 4H, NapC-H), 7.06 (b, 8H, Ar-H), 7.18 (b, 8H, Ar-H); ^{19}F NMR (CD_2Cl_2): δ -73.9 (s, Ar-F); mp: 221°C.

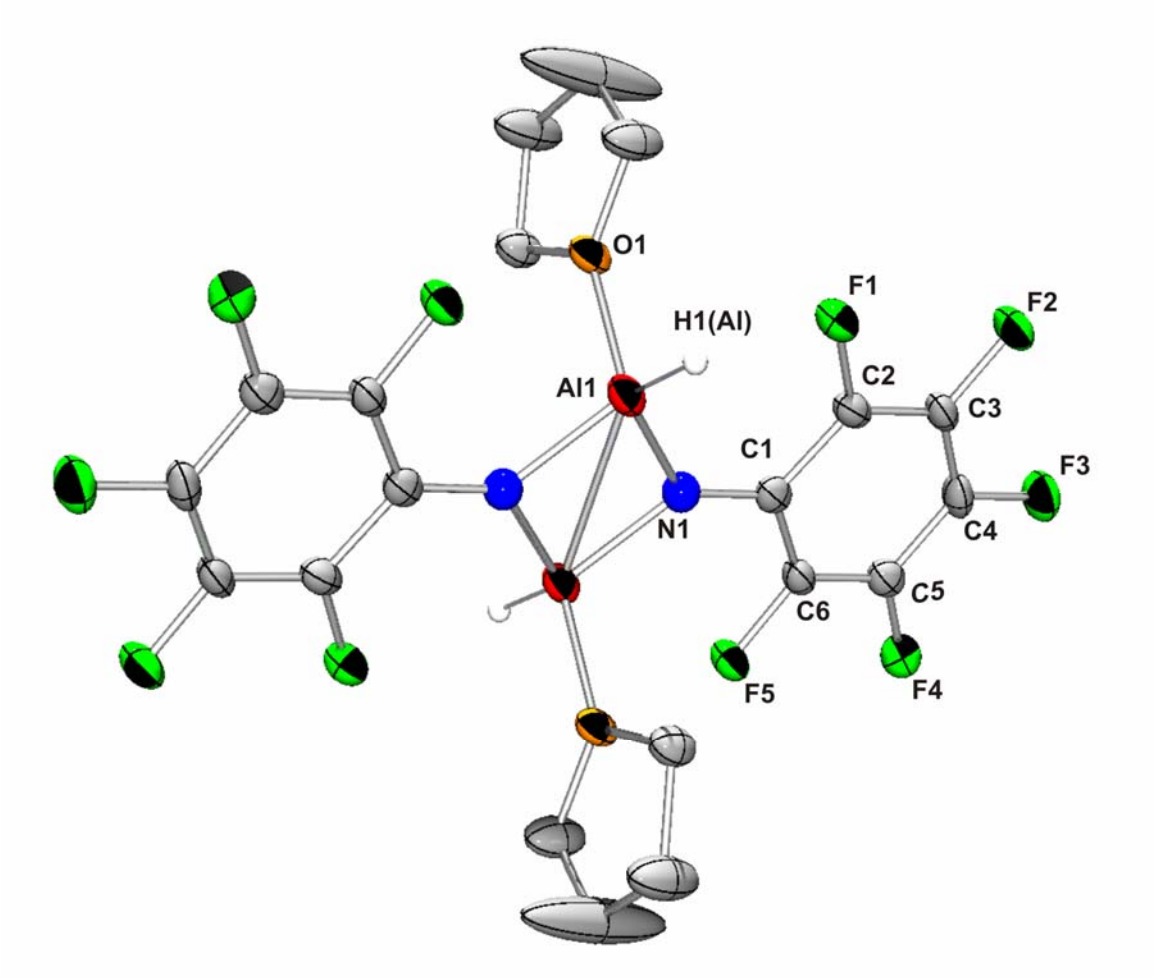

Figure 1.01. Molecular structure of 1 showing a partial numbering scheme. The thermal ellipsoids are shown at the 40% probability level. With the exception of H1(Al), all hydrogen atoms have been omitted for clarity.

Table 1.01. Crystal data and structure refinement for 1.

Identification code	kvgr057	
Empirical formula	C20 H18 Al2 F10 N2 O2	
Formula weight	562.32	
Temperature	153(2) K	
Wavelength	0.71073 Å	
Crystal system	Monoclinic	
Space group	P21/n	
Unit cell dimensions	a = 10.972(2) Å	α= 90°.
	b = 15.540(3) Å	β= 103.38(3)°.
	c = 7.0557(14) Å	γ = 90°.
Volume	1170.4(4) $Å^3$	
Z	2	
Density (calculated)	1.596 Mg/m^3	
Absorption coefficient	0.225 mm^{-1}	
F(000)	568	
Crystal size	0.12 x 0.11 x 0.05 mm^3	
Theta range for data collection	2.31 to 27.49°.	
Index ranges	-14<=h<=13, -20<=k<=15, -9<=l<=9	
Reflections collected	7573	
Independent reflections	2671 [R(int) = 0.0764]	
Completeness to theta = 27.49°	99.4 %	
Absorption correction	None	
Refinement method	Full-matrix least-squares on F^2	
Data / restraints / parameters	2671 / 0 / 162	
Goodness-of-fit on F^2	1.019	
Final R indices [I>2sigma(I)]	R1 = 0.0590, wR2 = 0.1447	
R indices (all data)	R1 = 0.1536, wR2 = 0.1802	
Largest diff. peak and hole	0.529 and -0.464 $e.Å^{-3}$	

Table 1.02. Selected Bond Lengths (Å) for $[(C_6F_5)N\text{-}Al(H)(THF)]_2$ (1)

C1-C2	1.392(5)
C1-C6	1.412(5)
C1-N1	1.365(4)
C2-C3	1.370(5)
C2-F1	1.365(4)
C3-C4	1.377(5)
C3-F2	1.346(4)
C4-C5	1.367(5)
C4-F3	1.348(4)
C5-C6	1.369(5)
C5-F4	1.356(4)
C6-F5	1.363(4)
N1-Al1	1.844(3)
Al1-H1(Al)	1.51(3)
Al1-O1	1.872(2)

Table 1.03. Selected Bond Angles (°) for $[(C_6F_5)N\text{-}Al(H)(THF)]_2$ (1)

C1-N1-Al1	133.7(2)
C2-C1-N1	124.5(3)
C6-C1-N1	123.1(3)
N1-Al1-H1al	120.5(12)
N1-Al1-O1	108.97(12)
O1-Al1-H1al	104.9(12)

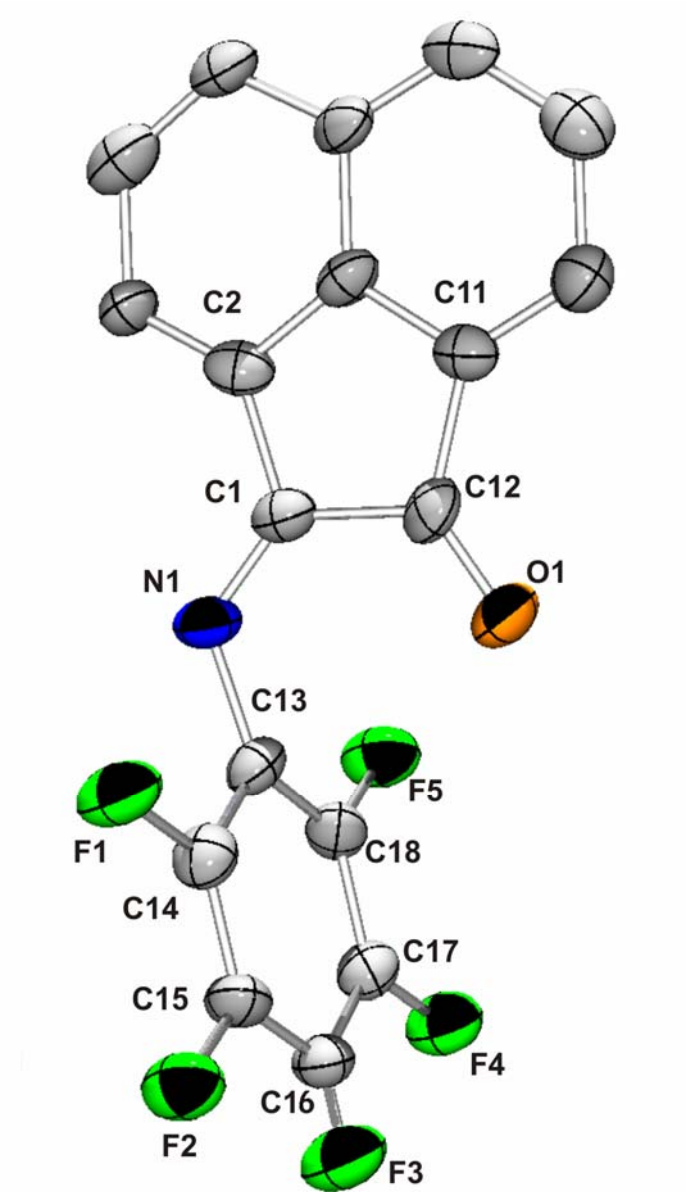

Figure 1.02. Molecular structure of 2 showing a partial numbering scheme. The thermal ellipsoids are shown at the 40% probability level. All hydrogen atoms have been omitted for clarity.

Table 1.04. Crystal data and structure refinement for 2.

Identification code	kvgr088	
Empirical formula	C18 H6 F5 N O	
Formula weight	347.24	
Temperature	153(2) K	
Wavelength	0.71073 Å	
Crystal system	Monoclinic	
Space group	P21/n	
Unit cell dimensions	a = 11.324(2) Å	α= 90.000(5)°.
	b = 10.366(2) Å	β= 98.390(3)°.
	c = 11.915(2) Å	γ = 90.000(5)°.
Volume	1383.5(4) $Å^3$	
Z	4	
Density (calculated)	1.667 Mg/m^3	
Absorption coefficient	0.150 mm^{-1}	
F(000)	696	
Crystal size	0.11 x 0.10 x 0.10 mm^3	
Theta range for data collection	2.32 to 27.39°.	
Index ranges	-14<=h<=14, -11<=k<=13, -15<=l<=15	
Reflections collected	5529	
Independent reflections	3136 [R(int) = 0.0383]	
Completeness to theta = 27.47°	99.6 %	
Absorption correction	Semi-empirical from equivalents	
Refinement method	Full-matrix least-squares on F^2	
Data / restraints / parameters	3135 / 0 / 226	
Goodness-of-fit on F^2	1.044	
Final R indices [I>2sigma(I)]	R1 = 0.0789, wR2 = 0.2050	
R indices (all data)	R1 = 0.1425, wR2 = 0.2434	
Largest diff. peak and hole	0.911 and -0.359 $e.Å^{-3}$	

Table 1.05. Selected Bond Lengths (Å) for 2-pentafluorophenylimino-2H-acenaphthylen-1-one (2)

C1-C12	1.591(6)
C1-N1	1.252(5)
C12-O1	1.204(5)
C13-N1	1.438(5)

Table 1.06. Selected Bond Angles (°) for 2-pentafluorophenylimino-2H-acenaphthylen-1-one (2)

C1-C12-C11	104.9(3)
C1-C12-O1	120.6(4)
C2-C1-N1	124.4(4)
C2-C1-C12	105.4(3)
C12-C1-N1	130.1(4)

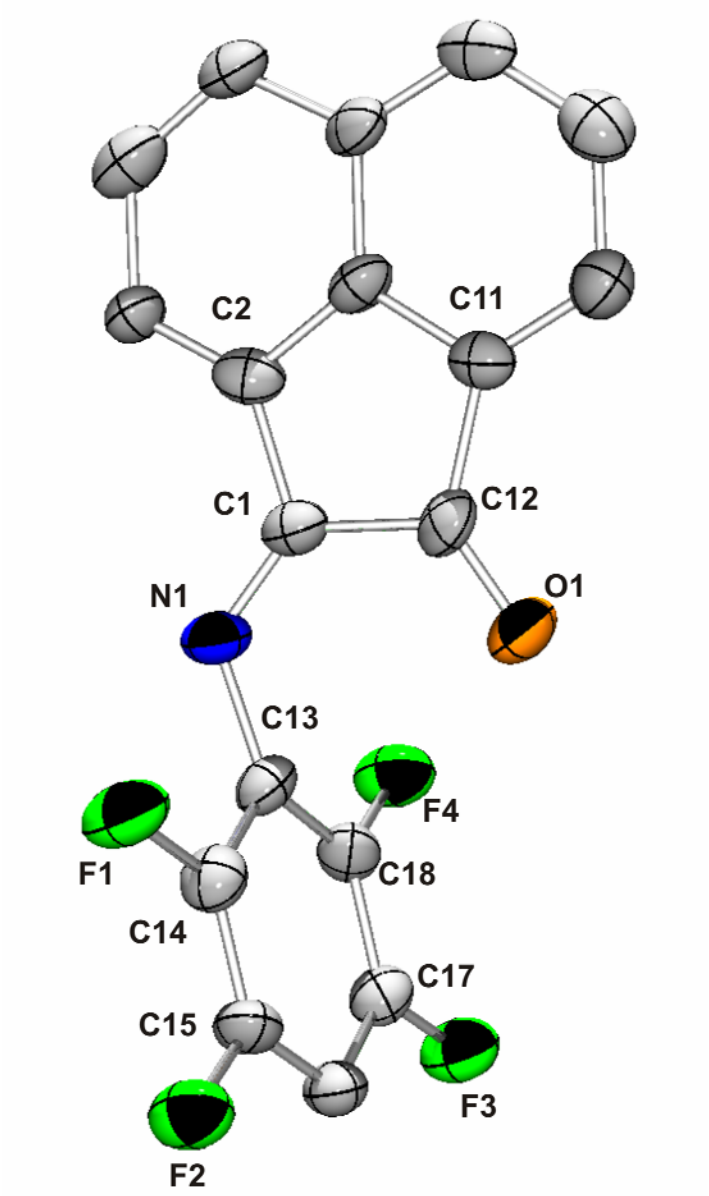

Figure 1.03. Molecular structure of 3 showing a partial numbering scheme. The thermal ellipsoids are shown at the 40% probability level. All hydrogen atoms have been omitted for clarity.

Table 1.07. Crystal data and structure refinement for 3.

Identification code	kvkv041a	
Empirical formula	C20 H10 F4 N2 O	
Formula weight	370.30	
Temperature	153(2) K	
Wavelength	0.71073 Å	
Crystal system	Triclinic	
Space group	P-1	
Unit cell dimensions	a = 7.419(5) Å	α= 78.964(5)°.
	b = 9.146(5) Å	β= 89.497(5)°.
	c = 13.246(5) Å	γ = 68.047(5)°.
Volume	816.3(8) $Å^3$	
Z	2	
Density (calculated)	1.507 Mg/m^3	
Absorption coefficient	0.126 mm^{-1}	
F(000)	376	
Crystal size	0.10 x 0.05 x 0.05 mm^3	
Theta range for data collection	1.57 to 27.51°.	
Index ranges	-9<=h<=9, -11<=k<=11, -14<=l<=16	
Reflections collected	5270	
Independent reflections	3461 [R(int) = 0.0878]	
Completeness to theta = 27.51°	92.2 %	
Absorption correction	None	
Refinement method	Full-matrix least-squares on F^2	
Data / restraints / parameters	3461 / 0 / 245	
Goodness-of-fit on F^2	1.063	
Final R indices [I>2sigma(I)]	R1 = 0.1251, wR2 = 0.3681	
R indices (all data)	R1 = 0.3436, wR2 = 0.4449	
Largest diff. peak and hole	0.541 and -0.386 e.$Å^{-3}$	

Table 1.08. Selected Bond Lengths (Å) for 2-(2,3,5,6-tetrafluoro-phenylimino)-2H-acenaphthylen-1-one (3)

C1-O1	1.215(11)
C1-C12	1.543(14)
C12-N1	1.275(11)
C18-F1	1.353(11)
C17-F2	1.362(10)
C15-F3	1.347(11)
C14-F4	1.360(9)

Table 1.09. Selected Bond Angles (°) for 2-(2,3,5,6-tetrafluoro-phenylimino)-2H-acenaphthylen-1-one (3)

O1-C1-C12	125.5(9)
N1-C12-C1	129.8(9)
C1-C12-C11	107.9(8)
C12-C1-C2	105.3(8)
C12-N1-C13	120.2(9)

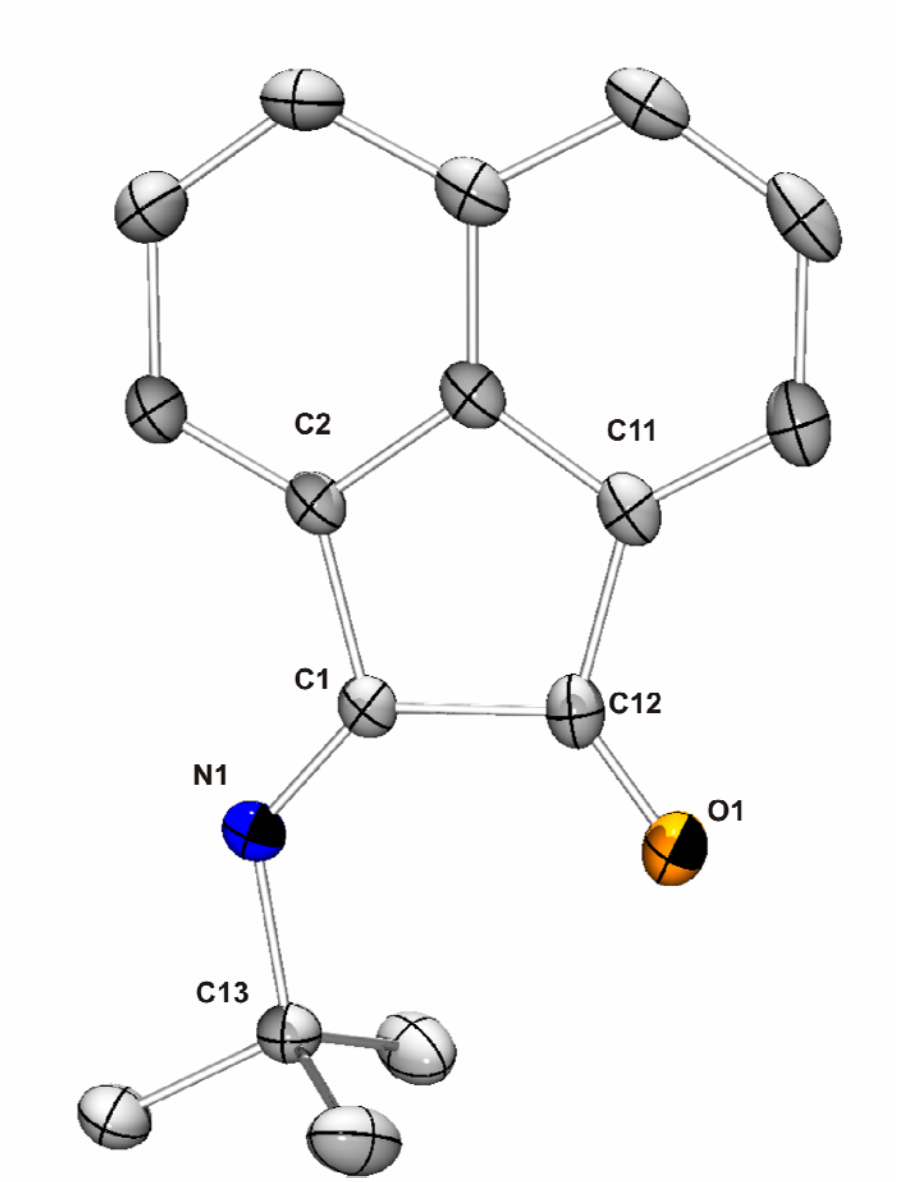

Figure 1.04. Molecular structure of 4 showing a partial numbering scheme. The thermal ellipsoids are shown at the 40% probability level. All hydrogen atoms have been omitted for clarity.

Table 1.10. Crystal data and structure refinement for 4.

Identification code	kvjm002	
Empirical formula	C16 H15 N O	
Formula weight	237.29	
Temperature	153(2) K	
Wavelength	0.71069 Å	
Crystal system	Orthorhombic	
Space group	Pnma	
Unit cell dimensions	a = 20.606(5) Å	α= 90.000(5)°.
	b = 6.802(5) Å	β= 90.000(5)°.
	c = 9.025(5) Å	γ = 90.000(5)°.
Volume	1265.0(12) $Å^3$	
Z	4	
Density (calculated)	1.246 Mg/m^3	
Absorption coefficient	0.078 mm^{-1}	
F(000)	504	
Crystal size	0.09 x 0.09 x 0.05 mm^3	
Theta range for data collection	3.00 to 27.47°.	
Index ranges	-26<=h<=26, -8<=k<=8, -11<=l<=11	
Reflections collected	2722	
Independent reflections	1571 [R(int) = 0.0399]	
Completeness to theta = 27.47°	99.7 %	
Absorption correction	None	
Refinement method	Full-matrix least-squares on F^2	
Data / restraints / parameters	1571 / 0 / 108	
Goodness-of-fit on F^2	0.994	
Final R indices [I>2sigma(I)]	R1 = 0.0481, wR2 = 0.1150	
R indices (all data)	R1 = 0.0951, wR2 = 0.1366	
Largest diff. peak and hole	0.260 and -0.217 $e.Å^{-3}$	

Table 1.11. Selected Bond Lengths (Å) for 2-*tert*-butylimino-2H-acenaphthylen-1-one (4)

C12-O1	1.208(3)
C1-C12	1.564(3)
C1-N1	1.272(3)
N1-C13	1.483(3)

Table 1.12. Selected Bond Angles (°) for 2-*tert*-butylimino-2H-acenaphthylen-1-one (4)

C11-C12-O1	126.41(19)
C1-C12-O1	127.64(19)
C2-C1-N1	121.40(18)
C12-C1-N1	134.02(18)

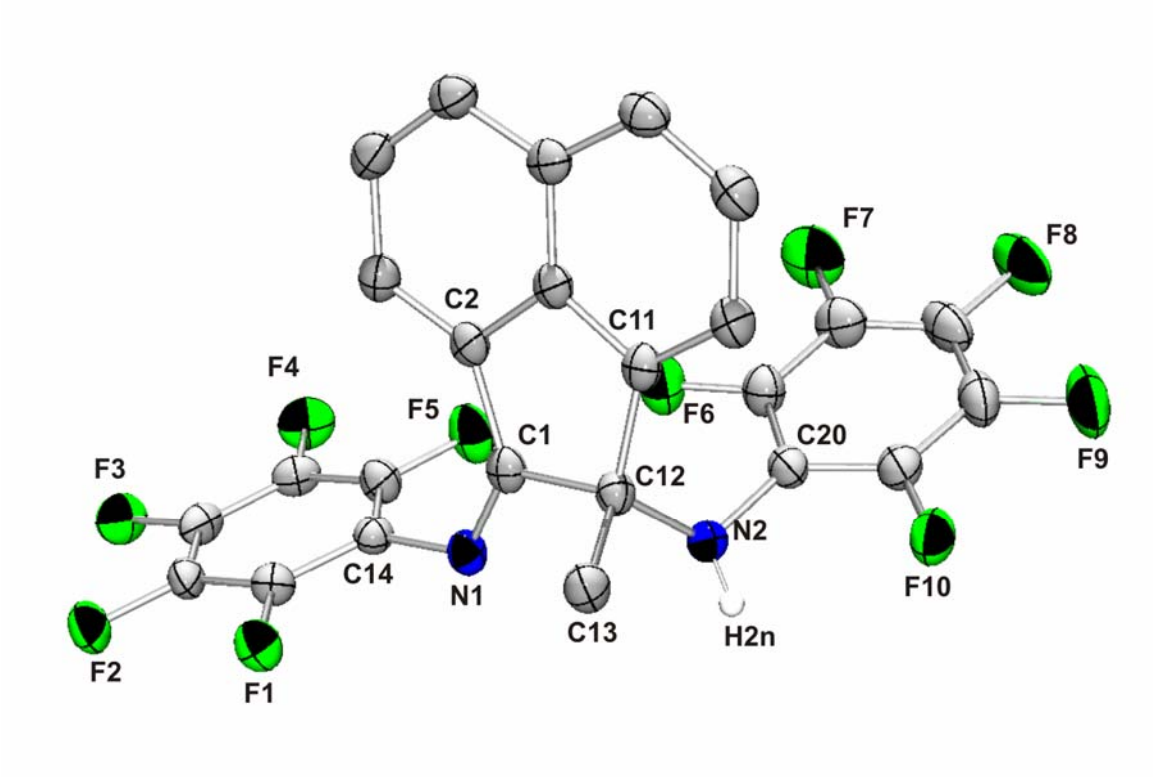

Figure 1.05. Molecular structure of 5 showing a partial numbering scheme. The thermal ellipsoids are shown at the 40% probability level. With the exception of H2n, all hydrogen atoms have been omitted for clarity.

Table 1.13. Crystal data and structure refinement for 5.

Identification code	kvnh018	
Empirical formula	C25 H10 F10 N2	
Formula weight	528.35	
Temperature	153(2) K	
Wavelength	0.71073 Å	
Crystal system	Triclinic	
Space group	P-1	
Unit cell dimensions	a = 8.080 Å	α= 117.12°.
	b = 11.938 Å	β= 95.72°.
	c = 12.573 Å	γ = 94.54°.
Volume	1063.4 $Å^3$	
Z	2	
Density (calculated)	1.650 Mg/m^3	
Absorption coefficient	0.159 mm^{-1}	
F(000)	528	
Crystal size	0.20 x 0.20 x 0.20 mm^3	
Theta range for data collection	1.94 to 27.50°.	
Index ranges	-10<=h<=10, -14<=k<=15, -16<=l<=14	
Reflections collected	7496	
Independent reflections	4785 [R(int) = 0.0339]	
Completeness to theta = 27.50°	97.9 %	
Absorption correction	None	
Max. and min. transmission	0.9688 and 0.9688	
Refinement method	Full-matrix least-squares on F^2	
Data / restraints / parameters	4785 / 0 / 334	
Goodness-of-fit on F^2	1.005	
Final R indices [I>2sigma(I)]	R1 = 0.0537, wR2 = 0.1209	
R indices (all data)	R1 = 0.1277, wR2 = 0.1483	
Largest diff. peak and hole	0.257 and -0.296 $e.Å^{-3}$	

Table 1.14. Selected Bond Lengths (Å) for (1-methyl-2-pentafluorophenylimino-acenaphthen-1-yl)-pentafluorophenylamine (5)

C1-C12	1.566(3)
C1-N1	1.277(3)
C14-N1	1.412(3)
C12-N2	1.474(3)
C20-N2	1.396(3)
C12-C13	1.523(3)

Table 1.15. Selected Bond Angles (°) for (1-methyl-2-pentafluorophenylimino-acenaphthen-1-yl)-pentafluorophenylamine (5)

C1-N1-C14	120.5(2)
C1-C12-C13	108.58(18)
C1-C12-N2	111.96(19)
C2-C1-C12	108.21(19)
C2-C1-N1	133.0(2)
C10-C12-N2	113.59(18)
C12-C1-N1	118.8(2)
C12-N2-C20	120.7(2)
C13-C12-C10	112.03(19)
C13-C12-N2	108.4(2)

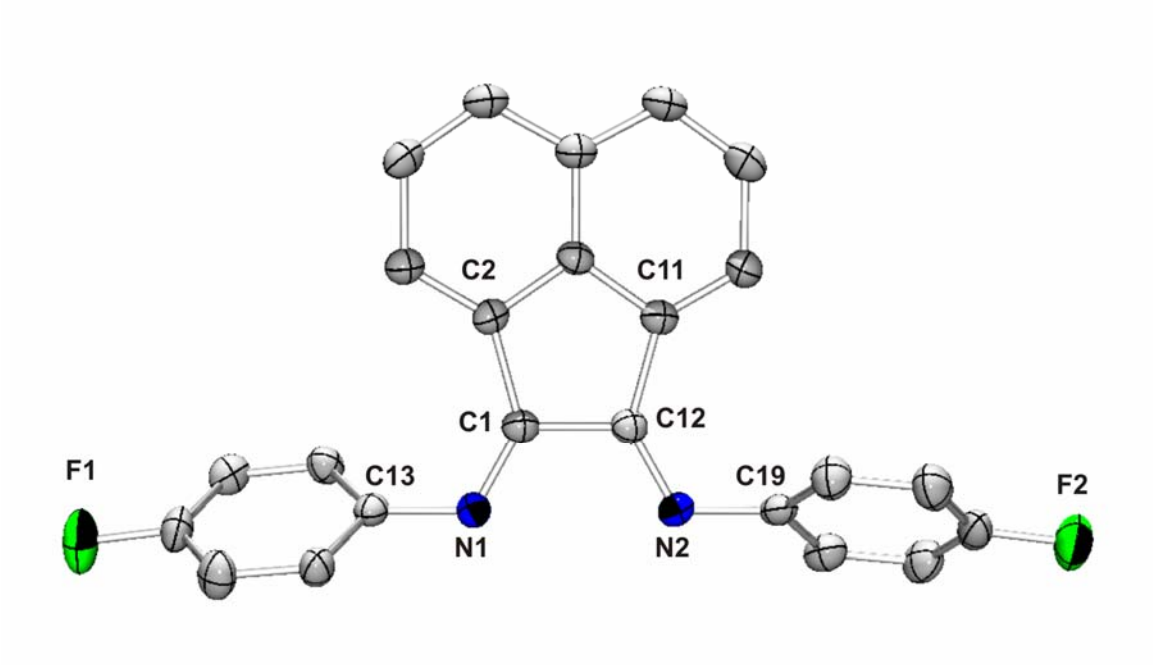

Figure 1.06. Molecular structure of 6 showing a partial numbering scheme. The thermal ellipsoids are shown at the 40% probability level. All hydrogen atoms have been omitted for clarity.

Table 1.16. Crystal data and structure refinement for 6.

Identification code	kvkv007	
Empirical formula	C24 H14 F2 N2	
Formula weight	368.37	
Temperature	153(2) K	
Wavelength	0.71073 Å	
Crystal system	Monoclinic	
Space group	P21/n	
Unit cell dimensions	a = 8.8788(18) Å	α= 90°.
	b = 9.6220(19) Å	β= 95.90(3)°.
	c = 21.147(4) Å	γ = 90°.
Volume	1797.0(6) $Å^3$	
Z	4	
Density (calculated)	1.362 Mg/m^3	
Absorption coefficient	0.095 mm^{-1}	
F(000)	760	
Crystal size	0.1 x 0.15 x 0.15 mm^3	
Theta range for data collection	2.41 to 27.39°.	
Index ranges	-11<=h<=11, -12<=k<=11, -27<=l<=27	
Reflections collected	6513	
Independent reflections	4044 [R(int) = 0.0535]	
Completeness to theta = 27.39°	99.0 %	
Absorption correction	None	
Refinement method	Full-matrix least-squares on F^2	
Data / restraints / parameters	4044 / 0 / 253	
Goodness-of-fit on F^2	1.090	
Final R indices [I>2sigma(I)]	R1 = 0.0790, wR2 = 0.2165	
R indices (all data)	R1 = 0.1563, wR2 = 0.2479	
Largest diff. peak and hole	0.435 and -0.297 $e.Å^{-3}$	

Table 1.17. Selected Bond Lengths (Å) for bis(4-fluorophenylimino)acenaphthylene (6)

C1-C12	1.518(5)
C1-N1	1.276(4)
C12-N2	1.278(4)
C13-N1	1.424(4)
C19-N2	1.420(4)

Table 1.18. Selected Bond Angles (°) for bis(4-fluorophenylimino)acenaphthylene (6)

C1-C12-C11	106.5(3)
C1-C12-N2	120.3(3)
C1-N1-C13	121.0(3)
C2-C1-C12	106.6(3)
C2-C1-N1	132.6(3)
C11-C12-N2	133.2(3)
C12-C1-N1	120.8(3)
C12-N2-C19	120.4(3)

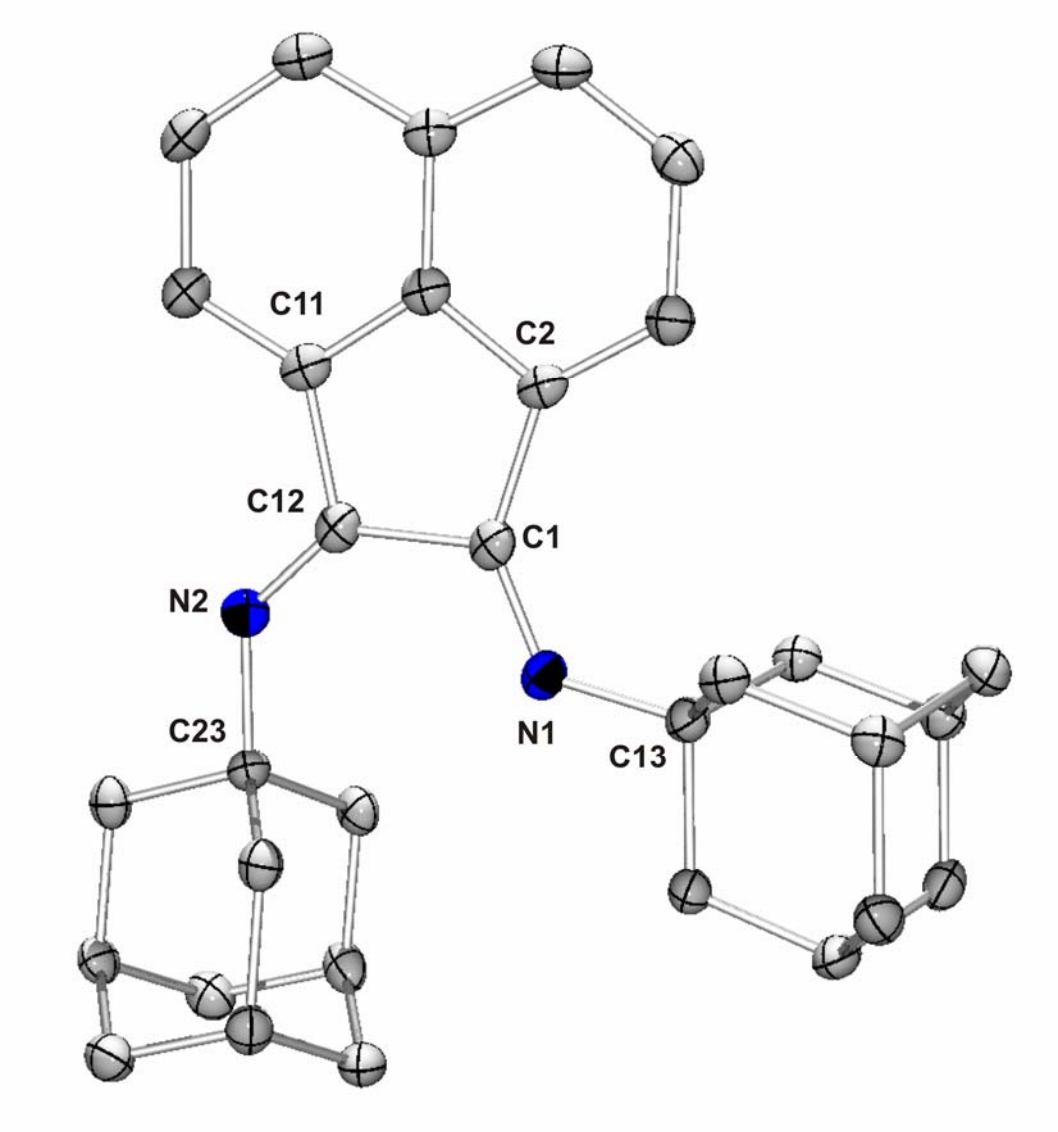

Figure 1.07. Molecular structure of 7 showing a partial numbering scheme. The thermal ellipsoids are shown at the 40% probability level. All hydrogen atoms have been omitted for clarity.

Table 1.19. Crystal data and structure refinement for 7.

Identification code	jmkv006	
Empirical formula	C32 H36 N2	
Formula weight	448.63	
Temperature	153(2) K	
Wavelength	0.71069 Å	
Crystal system	Triclinic	
Space group	P-1	
Unit cell dimensions	a = 9.965(5) Å	α= 92.589(5)°.
	b = 11.003(5) Å	β= 105.670(5)°.
	c = 11.964(5) Å	γ = 108.860(5)°.
Volume	1182.5(9) $Å^3$	
Z	2	
Density (calculated)	1.260 Mg/m^3	
Absorption coefficient	0.073 mm^{-1}	
F(000)	484	
Crystal size	0.20 x 0.12 x 0.03 mm^3	
Theta range for data collection	2.26 to 27.46°.	
Index ranges	-9<=h<=12, -14<=k<=14, -15<=l<=15	
Reflections collected	8920	
Independent reflections	5357 [R(int) = 0.0746]	
Completeness to theta = 27.46°	98.9 %	
Absorption correction	None	
Max. and min. transmission	0.9978 and 0.9856	
Refinement method	Full-matrix least-squares on F^2	
Data / restraints / parameters	5357 / 0 / 307	
Goodness-of-fit on F^2	0.825	
Final R indices [I>2sigma(I)]	R1 = 0.0580, wR2 = 0.1171	
R indices (all data)	R1 = 0.1970, wR2 = 0.1734	
Largest diff. peak and hole	0.228 and -0.263 $e.Å^{-3}$	

Table 1.20. Selected Bond Lengths (Å) for bis(1-adamantylimino)acenaphthylene (7)

C1-C12	1.563(4)
C1-N1	1.269(3)
C12-N2	1.272(3)
C13-N1	1.478(3)
C23-N2	1.475(3)

Table 1.21. Selected Bond Angles (°) for bis(1-adamantylimino)acenaphthylene (7)

C1-C12-C10	105.0(2)
C1-C12-N2	136.2(3)
C1-N1-C13	127.9(2)
C2-C1-C12	105.2(2)
C2-C1-N1	136.4(3)
C10-C12-N2	118.8(3)
C12-C1-N1	118.4(2)
C12-N2-C23	130.4(2)

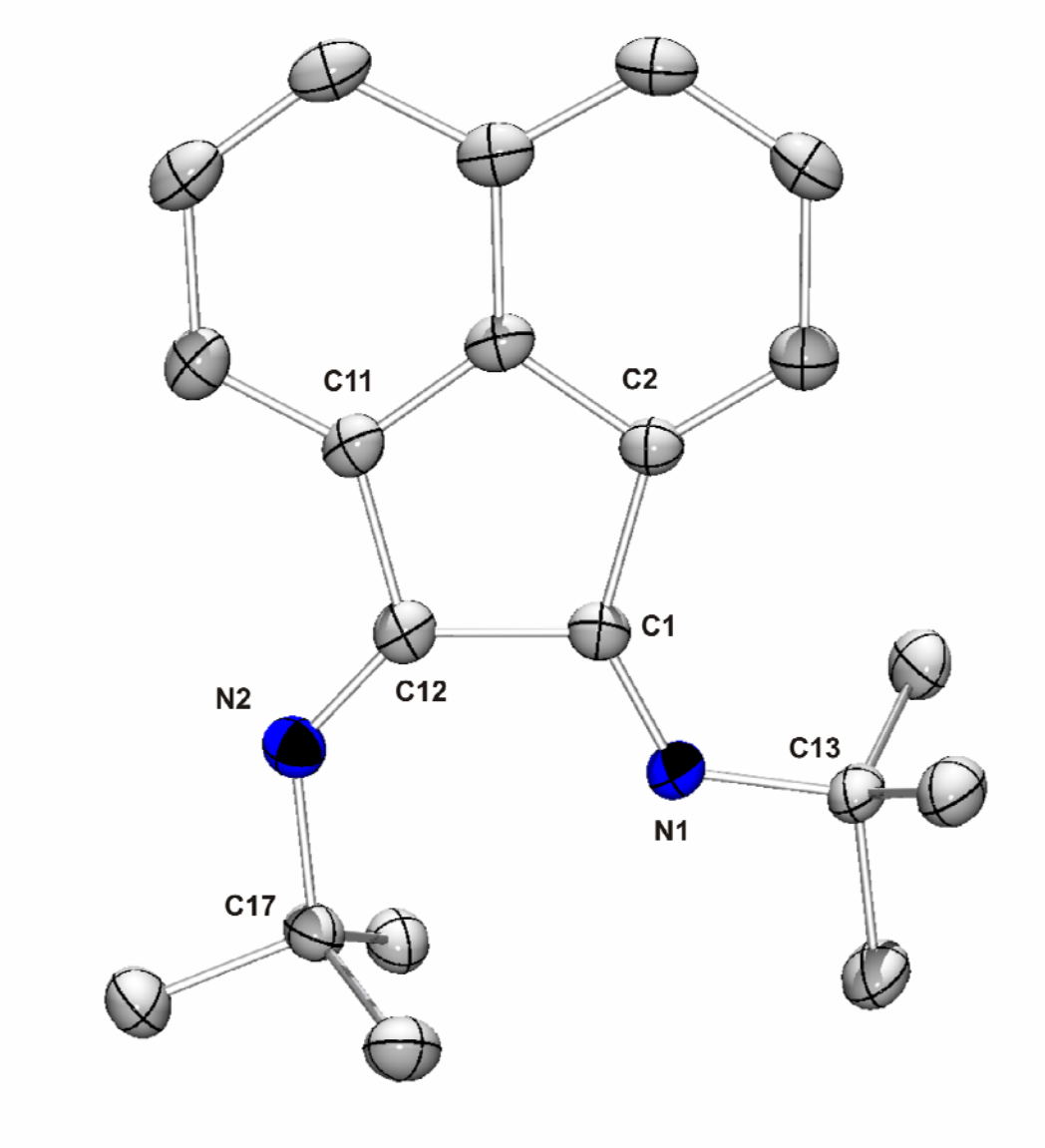

Figure 1.08. Molecular structure of 8 showing a partial numbering scheme. The thermal ellipsoids are shown at the 40% probability level. All hydrogen atoms have been omitted for clarity.

Table 1.22. Crystal data and structure refinement for 8.

Identification code	kvgr022	
Empirical formula	C20 H24 N2	
Formula weight	292.41	
Temperature	153(2) K	
Wavelength	0.71073 Å	
Crystal system	Tetragonal	
Space group	P43	
Unit cell dimensions	a = 10.9856(16) Å	α= 90°.
	b = 10.9856(16) Å	β= 90°.
	c = 13.853(3) Å	γ = 90°.
Volume	1671.8(5) $Å^3$	
Z	4	
Density (calculated)	1.162 Mg/m^3	
Absorption coefficient	0.068 mm^{-1}	
F(000)	632	
Crystal size	0.10 x 0.10 x 0.05 mm^3	
Theta range for data collection	2.37 to 27.47°.	
Index ranges	-14<=h<=14, -10<=k<=10, -14<=l<=17	
Reflections collected	3288	
Independent reflections	3288 [R(int) = 0.0000]	
Completeness to theta = 27.47°	99.7 %	
Absorption correction	None	
Refinement method	Full-matrix least-squares on F^2	
Data / restraints / parameters	3288 / 1 / 205	
Goodness-of-fit on F^2	1.112	
Final R indices [I>2sigma(I)]	R1 = 0.0498, wR2 = 0.1094	
R indices (all data)	R1 = 0.0810, wR2 = 0.1343	
Absolute structure parameter	1(4)	
Largest diff. peak and hole	0.286 and -0.280 $e.Å^{-3}$	

Table 1.23. Selected Bond Lengths (Å) for bis(*tert*-butylimino)acenaphthylene (8)

C1-C12	1.552(3)
C1-N1	1.280(3)
C12-N2	1.274(3)
C13-N1	1.478(3)
C17-N2	1.472(3)

Table 1.24. Selected Bond Angles (°) for bis(*tert*-butylimino)acenaphthylene (8)

C1-C12-C11	105.24(18)
C1-C12-N2	135.2(2)
C1-N1-C13	126.88(19)
C2-C1-C12	106.16(18)
C2-C1-N1	135.0(2)
C11-C12-N2	119.6(2)
C12-C1-N1	118.84(19)
C12-N2-C17	129.5(2)

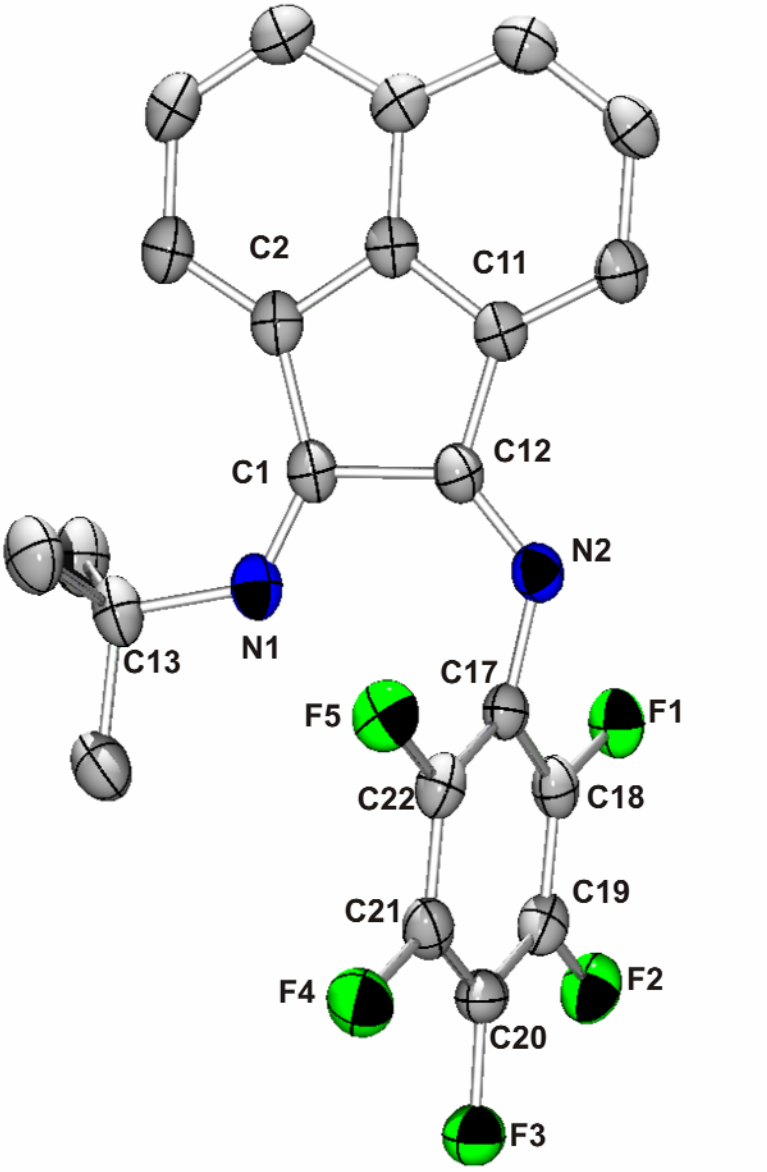

Figure 1.09. Molecular structure of 9 showing a partial numbering scheme. The thermal ellipsoids are shown at the 40% probability level. All hydrogen atoms have been omitted for clarity.

Table 1.25. Crystal data and structure refinement for 9.

Identification code	kvmf015	
Empirical formula	C22 H15 F5 N2	
Formula weight	402.36	
Temperature	153(2) K	
Wavelength	0.71073 Å	
Crystal system	Monoclinic	
Space group	P21/n	
Unit cell dimensions	a = 12.078(2) Å	α= 90°.
	b = 7.9445(16) Å	β= 96.26(3)°.
	c = 19.011(4) Å	γ = 90°.
Volume	1813.4(6) $Å^3$	
Z	4	
Density (calculated)	1.474 Mg/m^3	
Absorption coefficient	0.123 mm^{-1}	
F(000)	824	
Crystal size	0.20 x 0.20 x 0.10 mm^3	
Theta range for data collection	3.07 to 27.48°.	
Index ranges	-15<=h<=15, -10<=k<=9, -24<=l<=24	
Reflections collected	7144	
Independent reflections	4153 [R(int) = 0.0472]	
Completeness to theta = 27.48°	99.8 %	
Absorption correction	None	
Max. and min. transmission	0.9878 and 0.9758	
Refinement method	Full-matrix least-squares on F^2	
Data / restraints / parameters	4153 / 0 / 263	
Goodness-of-fit on F^2	1.016	
Final R indices [I>2sigma(I)]	R1 = 0.0612, wR2 = 0.1419	
R indices (all data)	R1 = 0.1463, wR2 = 0.1805	
Extinction coefficient	0.0039(17)	
Largest diff. peak and hole	0.465 and -0.230 $e.Å^{-3}$	

Table 1.26. Selected Bond Lengths (Å) for 2-tert-butylimino-2H-acenaphthylen-1-

ylidene-pentafluorophenyl-amine (9)

C1-C2	1.503(4)
C1-C12	1.541(4)
C1-N1	1.281(3)
C12-C11	1.445(4)
C12-N2	1.270(3)
C13-N1	1.492(3)
C17-N2	1.396(3)
C18-F1	1.354(3)
C19-F2	1.350(3)
C20-F3	1.356(3)
C21-F4	1.348(3)
C22-F5	1.349(3)

Table 1.27. Selected Bond Angles (°) for 2-tert-butylimino-2H-acenaphthylen-1-ylidene-pentafluorophenyl-amine (9)

C1-C12-N2	131.0(2)
C1-C12-C11	106.9(2)
C1-N1-C13	127.1(2)
C2-C1-C12	105.1(2)
C2-C1-N1	138.1(3)
C11-C12-N2	122.1(2)
C12-C1-N1	116.8(2)
C12-N2-C17	126.0(2)

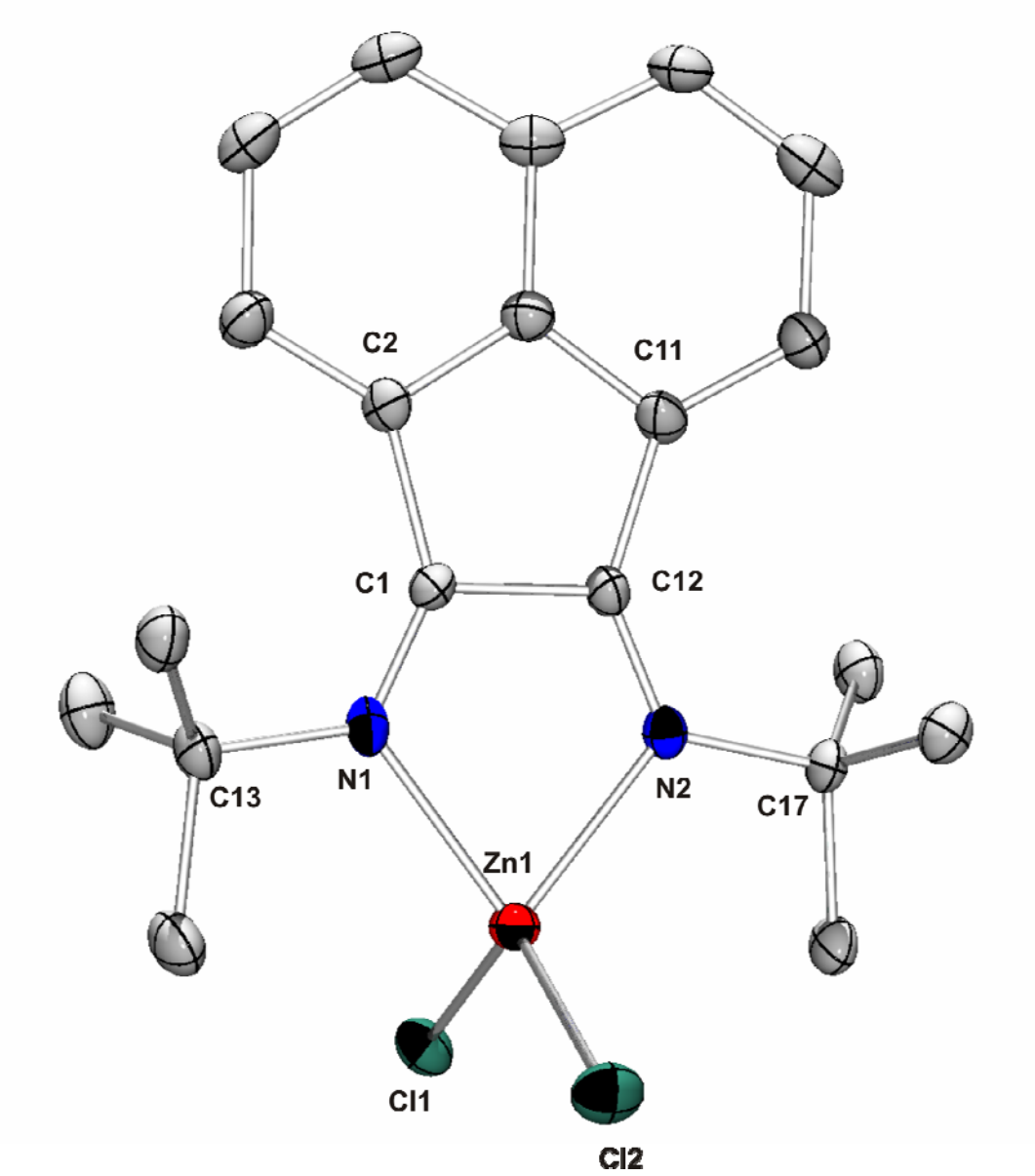

Figure 1.10. Molecular structure of 10 showing a partial numbering scheme. The thermal ellipsoids are shown at the 40% probability level. All hydrogen atoms and one molecule of acetronitrile have been omitted for clarity.

Table 1.28. Crystal data and structure refinement for 10.

Identification code	kvgr021b	
Empirical formula	C22 H27 Cl2 N3 Zn	
Formula weight	469.74	
Temperature	153(2) K	
Wavelength	0.71073 Å	
Crystal system	Monoclinic	
Space group	Cc	
Unit cell dimensions	a = 11.276(2) Å	α= 90°.
	b = 20.656(4) Å	β= 93.97(3)°.
	c = 9.4297(19) Å	γ = 90°.
Volume	2191.0(8) $Å^3$	
Z	4	
Density (calculated)	1.424 Mg/m^3	
Absorption coefficient	1.377 mm^{-1}	
F(000)	976	
Crystal size	0.10 x 0.06 x 0.04 mm^3	
Theta range for data collection	1.97 to 27.48°.	
Index ranges	-14<=h<=14, -26<=k<=25, -12<=l<=12	
Reflections collected	4365	
Independent reflections	4358 [R(int) = 0.0106]	
Completeness to theta = 27.48°	99.4 %	
Absorption correction	None	
Refinement method	Full-matrix least-squares on F^2	
Data / restraints / parameters	4358 / 2 / 260	
Goodness-of-fit on F^2	1.141	
Final R indices [I>2sigma(I)]	R1 = 0.0482, wR2 = 0.1328	
R indices (all data)	R1 = 0.0718, wR2 = 0.1647	
Absolute structure parameter	0.487(19)	
Largest diff. peak and hole	0.642 and -1.222 $e.Å^{-3}$	

Table 1.29. Selected Bond Lengths (Å) for bis(*tert*-butylimino)acenaphthene zinc chloride complex (10)

C1-C2	1.503(8)
C1-C12	1.552(8)
C1-N1	1.274(8)
C11-C12	1.474(9)
C12-N2	1.273(8)
C13-N1	1.503(7)
C17-N2	1.517(7)
N1-Zn1	2.088(5)
N2-Zn1	2.078(5)
Cl1-Zn1	2.2215(18)
Cl2-Zn1	1.2242(16)

Table 1.30. Selected Bond Angles (°) for bis(*tert*-butylimino)acenaphthene zinc chloride complex (10)

C1-C12-C11	106.2(5)
C1-C12-N2	116.5(2)
C1-N1-C13	125.8(5)
C1-N1-Zn1	111.3(4)
C2-C1-C12	105.4(5)
C2-C1-N1	137.2(5)
C11-C12-N2	137.3(5)
C12-C1-N1	117.2(5)
C12-N2-C17	126.4(5)
C12-N2-Zn1	112.3(4)
N1-Zn1-N2	81.4(2)
N1-Zn1-Cl1	111.04(15)
N1-Zn1-Cl2	114.43(16)
N2-Zn1-Cl1	114.74(15)
N2-Zn1-Cl2	111.10(14)
Cl1-Zn1-Cl2	118.49(6)

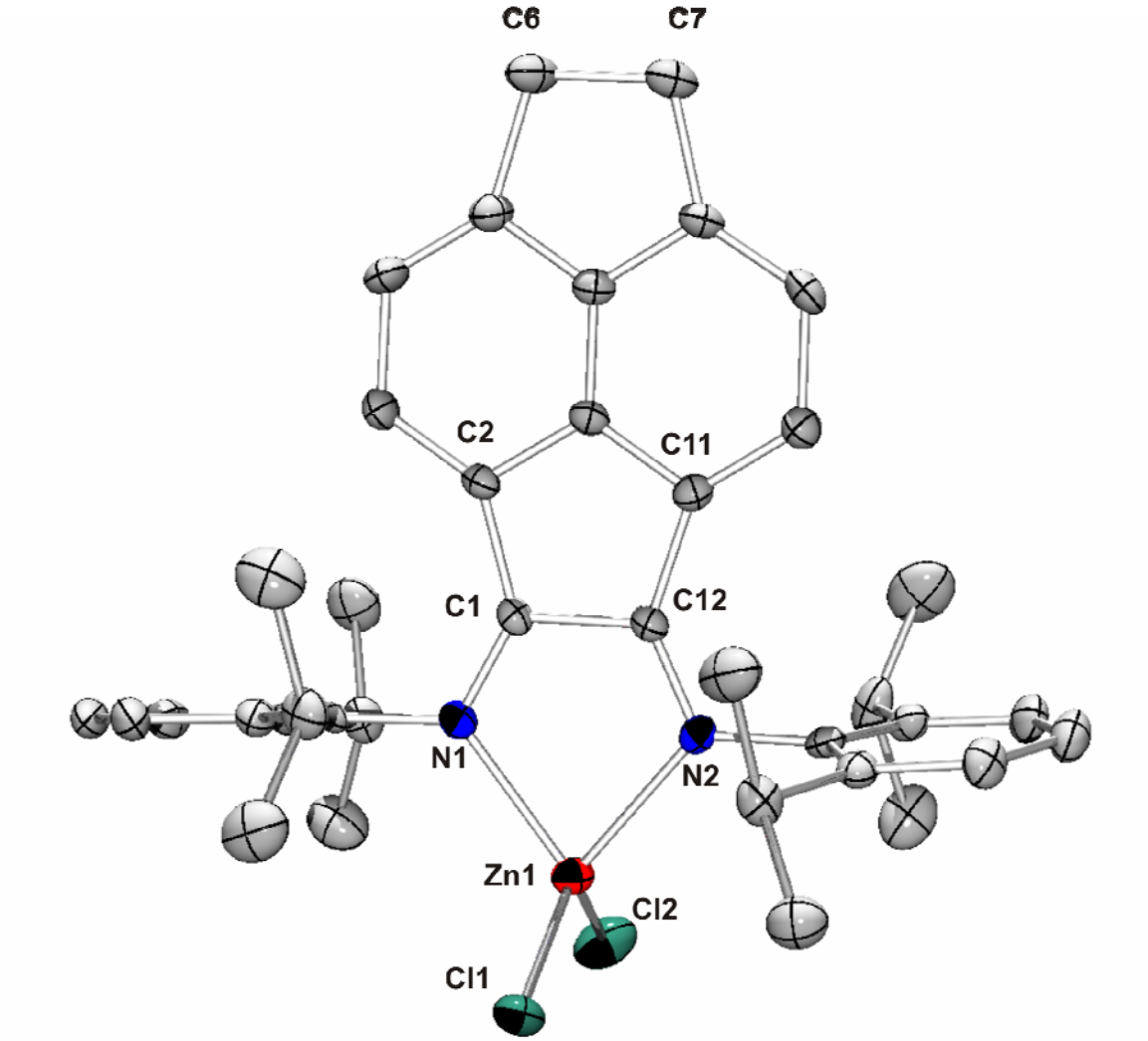

Figure 1.11. Molecular structure of 11 showing a partial numbering scheme. The thermal ellipsoids are shown at the 40% probability level. All hydrogen atoms have been omitted for clarity.

Table 1.31. Crystal data and structure refinement for 11.

Identification code	kvkv065a	
Empirical formula	C39 H44 Cl4 N2 Zn	
Formula weight	747.93	
Temperature	153(2) K	
Wavelength	0.71073 Å	
Crystal system	Orthorhombic	
Space group	P212121	
Unit cell dimensions	a = 11.473(2) Å	α= 90°.
	b = 14.018(3) Å	β= 90°.
	c = 23.295(5) Å	γ = 90°.
Volume	3746.8(13) $Å^3$	
Z	4	
Density (calculated)	1.326 Mg/m^3	
Absorption coefficient	0.970 mm^{-1}	
F(000)	1560	
Crystal size	0.15 x 0.20 x 0.30 mm^3	
Theta range for data collection	1.75 to 27.48°.	
Index ranges	-14<=h<=14, -18<=k<=18, -30<=l<=30	
Reflections collected	8537	
Independent reflections	8537 [R(int) = 0.0000]	
Completeness to theta = 27.48°	99.7 %	
Absorption correction	None	
Refinement method	Full-matrix least-squares on F^2	
Data / restraints / parameters	8537 / 0 / 423	
Goodness-of-fit on F^2	1.023	
Final R indices [I>2sigma(I)]	R1 = 0.0480, wR2 = 0.1088	
R indices (all data)	R1 = 0.0992, wR2 = 0.1463	
Absolute structure parameter	-0.014(14)	
Largest diff. peak and hole	0.606 and -0.977 $e.Å^{-3}$	

Table 1.32. Selected Bond Lengths (Å) for bis(2,6-diisopropylphenylimino)pyracene zinc chloride complex (11)

C1-C2	1.473(6)
C1-C12	1.534(6)
C1-N1	1.286(5)
C11-C12	1.471(6)
C12-N2	1.279(5)
N1-Zn1	2.102(3)
N2-Zn1	2.120(4)
Cl1-Zn1	2.1987(13)
Cl2-Zn1	2.2057(12)

Table 1.33. Selected Bond Angles (°) for bis(2,6-diisopropylphenylimino)pyracene zinc chloride complex (11)

C1-C12-C11	107.1(3)
C1-C12-N2	118.2(4)
C1-N1-Zn1	111.3(3)
C2-C1-C12	107.7(4)
C2-C1-N1	134.2(4)
C11-C12-N2	134.6(4)
C12-C1-N1	118.1(4)
C12-N2-Zn1	110.9(3)
N1-Zn1-N2	81.05(13)
N1-Zn1-Cl1	113.50(10)
N1-Zn1-Cl2	108.73(10)
N2-Zn1-Cl1	112.22(10)
N2-Zn1-Cl2	115.25(9)
Cl1-Zn1-Cl2	119.67(6)

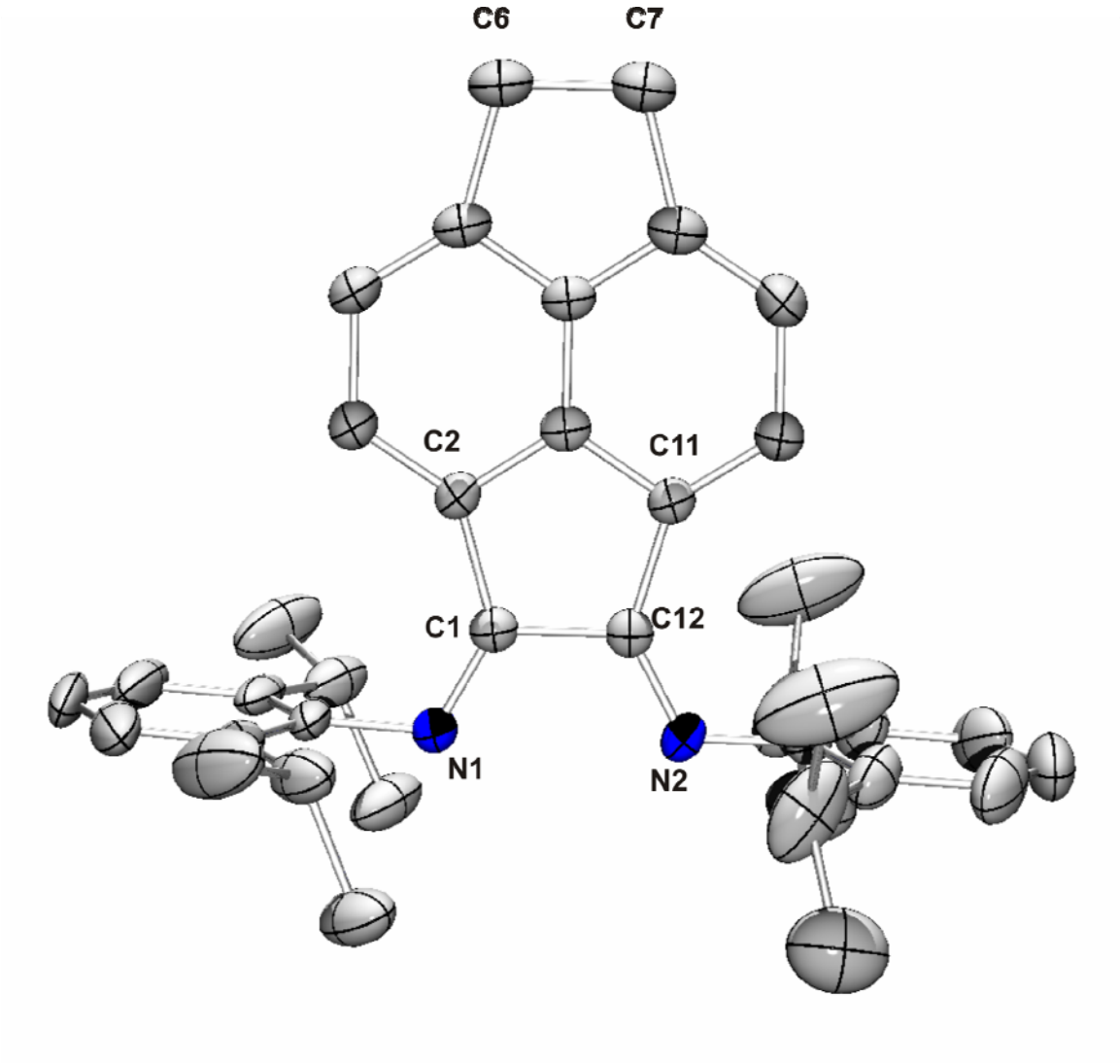

Figure 1.12. Molecular structure of 12 showing partial numbering scheme. The thermal ellipsoids are shown at the 40% probability level. All hydrogen atoms have been omitted for clarity.

Table 1.34. Crystal data and structure refinement for 12.

Identification code	kvkv064a	
Empirical formula	C38 H42 N2	
Formula weight	526.74	
Temperature	153(2) K	
Wavelength	0.71073 Å	
Crystal system	Orthorhombic	
Space group	Pnma	
Unit cell dimensions	a = 12.070(2) Å	α= 90°.
	b = 13.894(3) Å	β= 90°.
	c = 18.947(4) Å	γ = 90°.
Volume	3177.2(11) $Å^3$	
Z	4	
Density (calculated)	1.101 Mg/m^3	
Absorption coefficient	0.063 mm^{-1}	
F(000)	1136	
Crystal size	0.15 x 0.20 x 0.30 mm^3	
Theta range for data collection	1.82 to 27.48°.	
Index ranges	-15<=h<=15, -17<=k<=18, -24<=l<=24	
Reflections collected	6949	
Independent reflections	3782 [R(int) = 0.0949]	
Completeness to theta = 27.48°	99.8 %	
Absorption correction	None	
Refinement method	Full-matrix least-squares on F^2	
Data / restraints / parameters	3782 / 0 / 215	
Goodness-of-fit on F^2	0.978	
Final R indices [I>2sigma(I)]	R1 = 0.0689, wR2 = 0.1755	
R indices (all data)	R1 = 0.1786, wR2 = 0.2273	
Largest diff. peak and hole	0.264 and -0.267 $e.Å^{-3}$	

Table 1.35. Selected Bond Lengths (Å) for bis(2,6-diisopropylphenylimino)pyracene (12)

C1-C2	1.487(4)
C1-C12	1.527(4)
C1-N1	1.276(4)
C11-C12	1.486(4)
C12-N2	1.378(4)

Table 1.36. Selected Bond Angles (°) for bis(2,6-diisopropylphenylimino)pyracene (12)

C1-C12-C11	107.1(2)
C1-C12-N2	120.5(3)
C2-C1-C12	106.9(2)
C2-C1-N1	133.1(3)
C11-C12-N2	132.4(3)
C12-C1-N1	120.0(3)

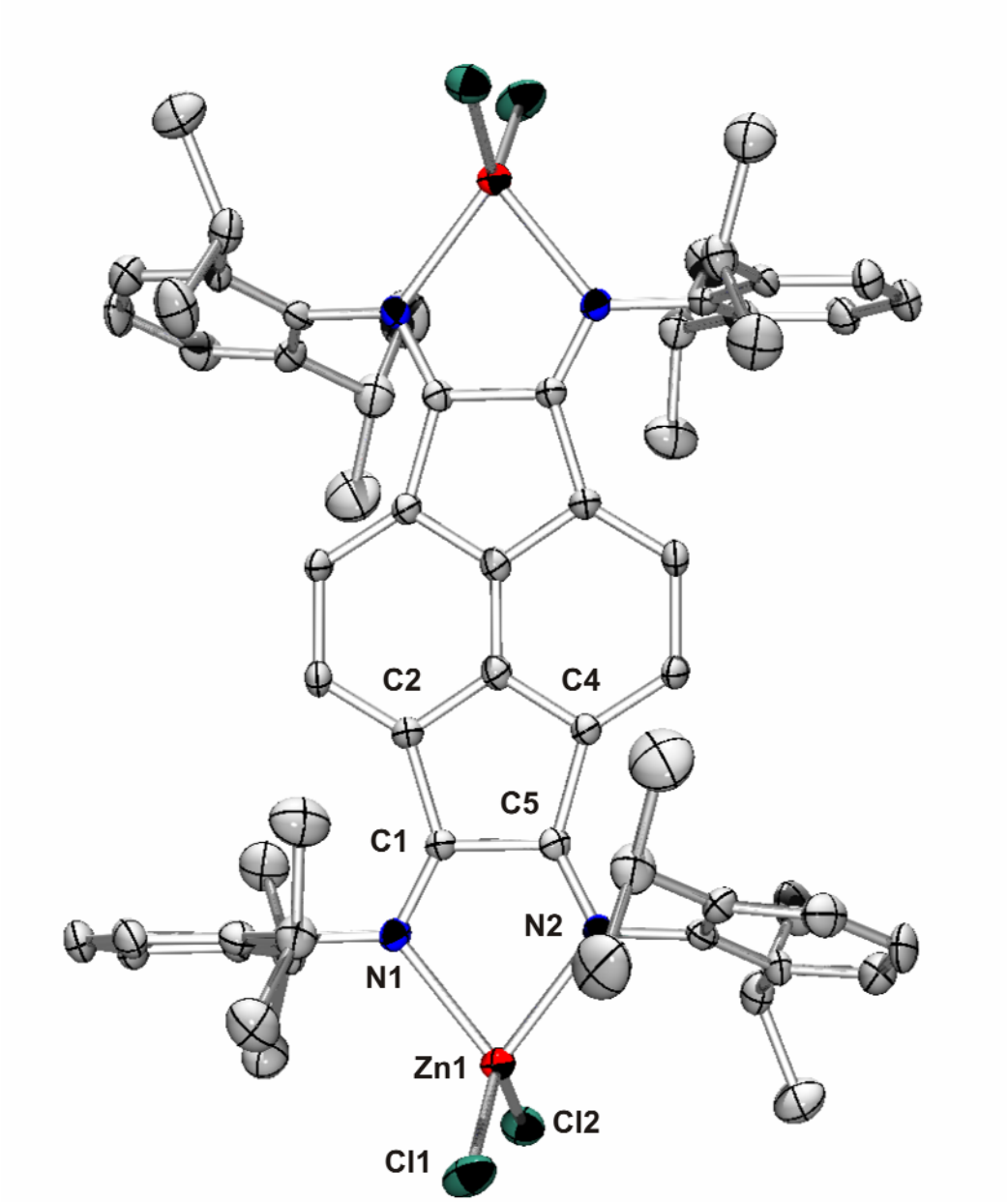

Figure 1.13. Molecular structure of 13 showing a partial numbering scheme. The thermal ellipsoids are shown at the 40% probability level. All hydrogen atoms and six molecules of chloroform have been omitted for clarity.

Table 1.37. Crystal data and structure refinement for 13.

Identification code	kvkv036a	
Empirical formula	C68 H78 Cl22 N4 Zn2	
Formula weight	1861.98	
Temperature	153(2) K	
Wavelength	0.71073 Å	
Crystal system	Triclinic	
Space group	P-1	
Unit cell dimensions	a = 13.151(5) Å	α= 81.542(5)°.
	b = 15.312(5) Å	β= 77.600(5)°.
	c = 23.978(5) Å	γ = 64.858(5)°.
Volume	4260(2) $Å^3$	
Z	2	
Density (calculated)	1.451 Mg/m^3	
Absorption coefficient	1.293 mm^{-1}	
F(000)	1896	
Crystal size	0.10 x 0.20 x 0.20 mm^3	
Theta range for data collection	1.76 to 27.46°.	
Index ranges	-17<=h<=17, -17<=k<=19, -27<=l<=31	
Reflections collected	28557	
Independent reflections	19305 [R(int) = 0.0398]	
Completeness to theta = 27.46°	99.1 %	
Absorption correction	None	
Refinement method	Full-matrix least-squares on F^2	
Data / restraints / parameters	19305 / 0 / 881	
Goodness-of-fit on F^2	1.048	
Final R indices [I>2sigma(I)]	R1 = 0.0732, wR2 = 0.1824	
R indices (all data)	R1 = 0.1621, wR2 = 0.2233	
Largest diff. peak and hole	2.033 and -1.817 $e.Å^{-3}$	

Table 1.38. Selected Bond Lengths (Å) for tetrakis(2,6-

diisopropylphenylimino)pyracene zinc chloride complex (13)

C1-C2	1.479(6)
C1-C5	1.532(7)
C1-N1	1.277(6)
C4-C5	1.489(6)
C5-N2	1.259(6)
N1-Zn1	2.109(4)
N2-Zn1	2.147(4)
Cl1-Zn1	2.1950(15)
Cl2-Zn1	2.1734(17)

Table 1.39. Selected Bond Angles (°) for tetrakis(2,6-diisopropylphenylimino)pyracene zinc chloride complex (13)

C1-C5-C4	106.7(4)
C1-C5-N2	118.5(4)
C1-N1-Zn1	111.2(3)
C2-C1-C5	107.7(4)
C2-C1-N1	133.8(5)
C4-C5-N2	134.4(5)
C4-C5-C1	106.7(4)
C5-C1-N1	118.1(4)
C5-N2-Zn1	110.4(3)
N1-Zn1-Cl1	111.33(11)
N1-Zn1-Cl2	115.63(12)
N2-Zn1-Cl1	110.66(11)
N2-Zn1-Cl2	112.02(12)

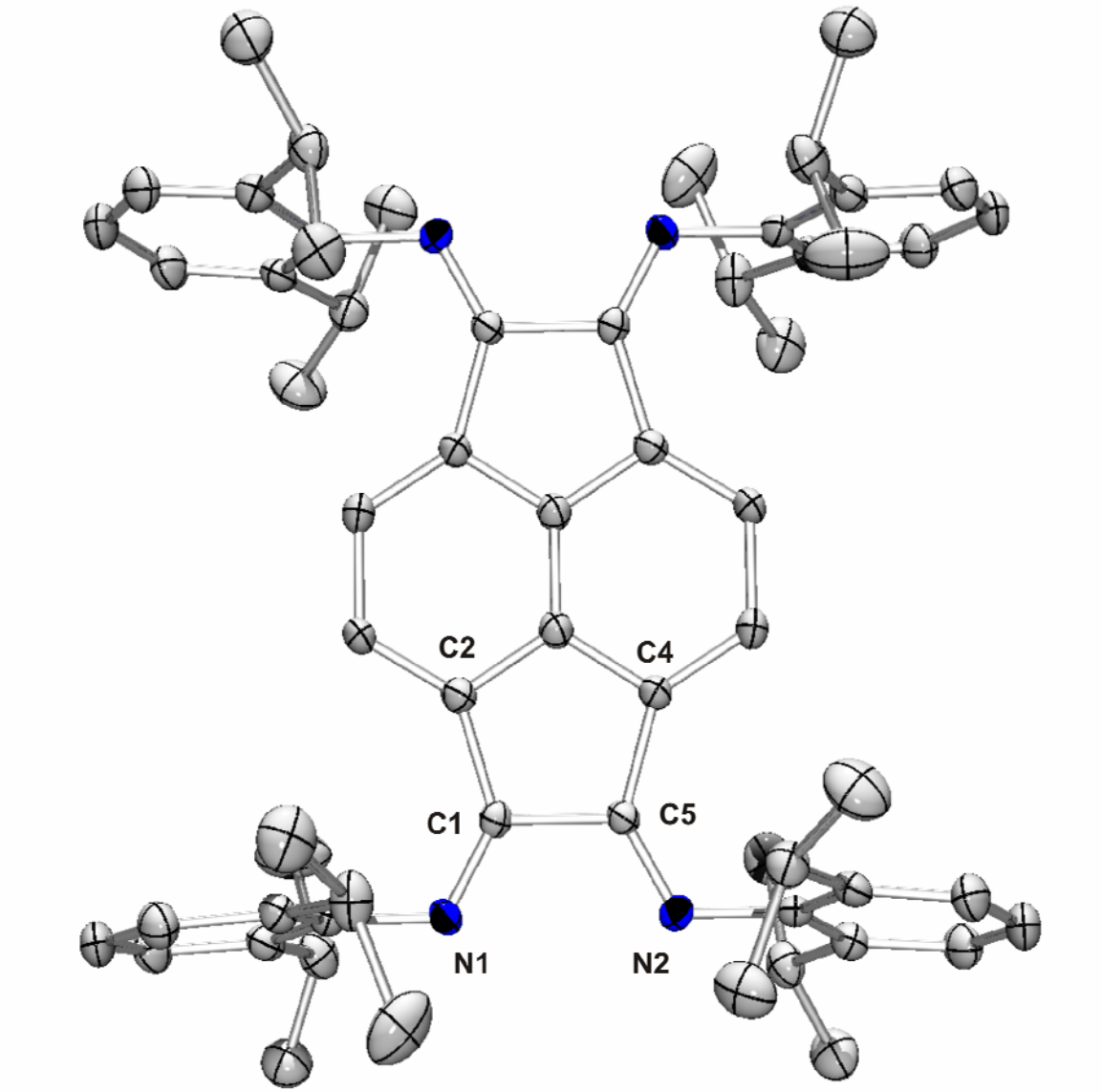

Figure 1.14. Molecular structure of 14 showing a partial numbering scheme. The thermal ellipsoids are shown at the 40% probability level. All hydrogen atoms and two molecules of chloroform have been omitted for clarity.

Table 1.40. Crystal data and structure refinement for 14.

Identification code	kvkv025	
Empirical formula	C64 H74 Cl6 N4	
Formula weight	1112.04	
Temperature	153(2) K	
Wavelength	0.71073 Å	
Crystal system	Monoclinic	
Space group	P21/n	
Unit cell dimensions	a = 12.673(3) Å	α= 90°.
	b = 15.048(3) Å	β= 97.68(3)°.
	c = 18.514(4) Å	γ = 90°.
Volume	3499.1(12) $Å^3$	
Z	2	
Density (calculated)	1.055 Mg/m^3	
Absorption coefficient	0.282 mm^{-1}	
F(000)	1176	
Crystal size	0.20 x 0.15 x 0.11 mm^3	
Theta range for data collection	1.75 to 27.44°.	
Index ranges	-16<=h<=16, -18<=k<=19, -24<=l<=23	
Reflections collected	13531	
Independent reflections	7965 [R(int) = 0.0419]	
Completeness to theta = 27.44°	99.6 %	
Absorption correction	None	
Refinement method	Full-matrix least-squares on F^2	
Data / restraints / parameters	7965 / 0 / 342	
Goodness-of-fit on F^2	1.003	
Final R indices [I>2sigma(I)]	R1 = 0.0692, wR2 = 0.2071	
R indices (all data)	R1 = 0.1169, wR2 = 0.2333	
Largest diff. peak and hole	0.528 and -0.320 $e.Å^{-3}$	

Table 1.41. Selected Bond Lengths (Å) for tetrakis(2,6-diisopropylphenylimino)pyracene (14)

C1-C2	1.486(4)
C1-C5	1.549(4)
C1-N1	1.267(3)
C4-C5	1.501(4)
C5-N2	1.264(3)

Table 1.42. Selected Bond Angles (°) for tetrakis(2,6-diisopropylphenylimino)pyracene (14)

C1-C5-C4	106.6(2)
C1-C5-N2	119.7(2)
C2-C1-C5	106.5(2)
C2-C1-N1	133.8(2)
C4-C5-N2	133.7(2)
C5-C1-N1	119.6(2)

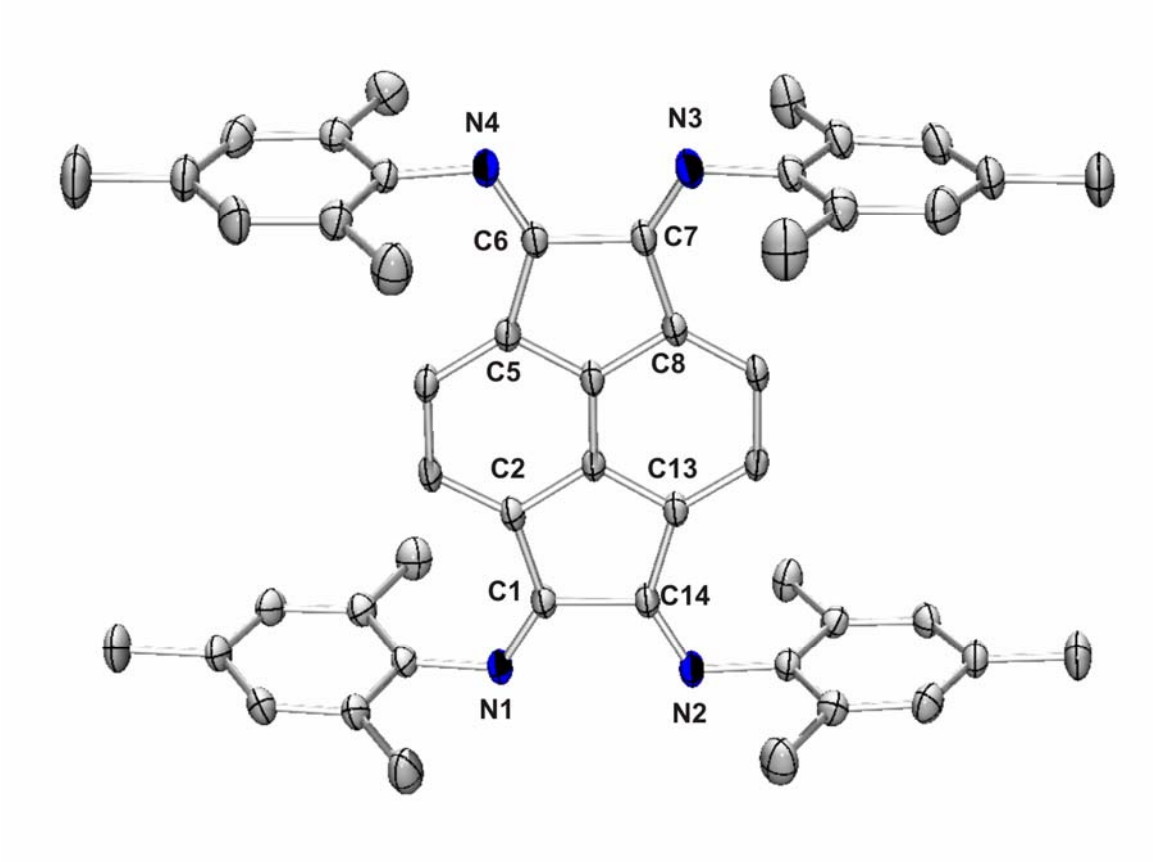

Figure 1.15. Molecular structure of 15 showing a partial numbering scheme. The thermal ellipsoids are shown at the 40% probability level. All hydrogen atoms and one molecule of dichloromethane have been omitted for clarity.

Table 1.43. Crystal data and structure refinement for 15.

Identification code	kvkv016a	
Empirical formula	C51 H50 Cl2 N4	
Formula weight	789.85	
Temperature	153(2) K	
Wavelength	0.71073 Å	
Crystal system	Monoclinic	
Space group	P21/n	
Unit cell dimensions	a = 13.568(3) Å	α= 90°.
	b = 24.864(5) Å	β= 111.16(3)°.
	c = 13.852(3) Å	γ = 90°.
Volume	4357.6(15) $Å^3$	
Z	4	
Density (calculated)	1.204 Mg/m^3	
Absorption coefficient	0.188 mm^{-1}	
F(000)	1672	
Crystal size	0.20 x 0.15 x 0.10 mm^3	
Theta range for data collection	1.61 to 27.46°.	
Index ranges	-16<=h<=17, -28<=k<=32, -16<=l<=17	
Reflections collected	28050	
Independent reflections	9946 [R(int) = 0.0552]	
Completeness to theta = 27.46°	99.8 %	
Absorption correction	None	
Refinement method	Full-matrix least-squares on F^2	
Data / restraints / parameters	9946 / 0 / 526	
Goodness-of-fit on F^2	1.018	
Final R indices [I>2sigma(I)]	R1 = 0.0558, wR2 = 0.1519	
R indices (all data)	R1 = 0.0970, wR2 = 0.1841	
Largest diff. peak and hole	0.346 and -0.434 $e.Å^{-3}$	

Table 1.44. Selected Bond Lengths (Å) for tetrakis(2,4,6-trimethylphenylimino)pyracene (15)

C1-C2	1.491(3)
C1-C14	1.543(3)
C1-N1	1.271(2)
C5-C6	1.493(3)
C6-C7	1.542(2)
C6-N2	1.269(2)
C7-C8	1.488(3)
C7-N3	1.272(2)
C13-C14	1.484(3)
C14-N4	1.267(2)

Table 1.45. Selected Bond Angles (°) for tetrakis(2,4,6-trimethylphenylimino)pyracene (15)

C1-C14-C13	106.62(15)
C1-C14-N4	121.47(16)
C2-C1-C14	106.68(15)
C2-C1-N1	132.29(17)
C5-C6-C7	106.47(15)
C5-C6-N2	131.83(17)
C6-C7-C8	106.92(15)
C6-C7-N3	121.96(17)
C7-C6-N2	121.64(16)
C8-C7-N3	131.10(17)
C13-C14-N4	131.91(17)
C14-C1-N1	120.91(17)

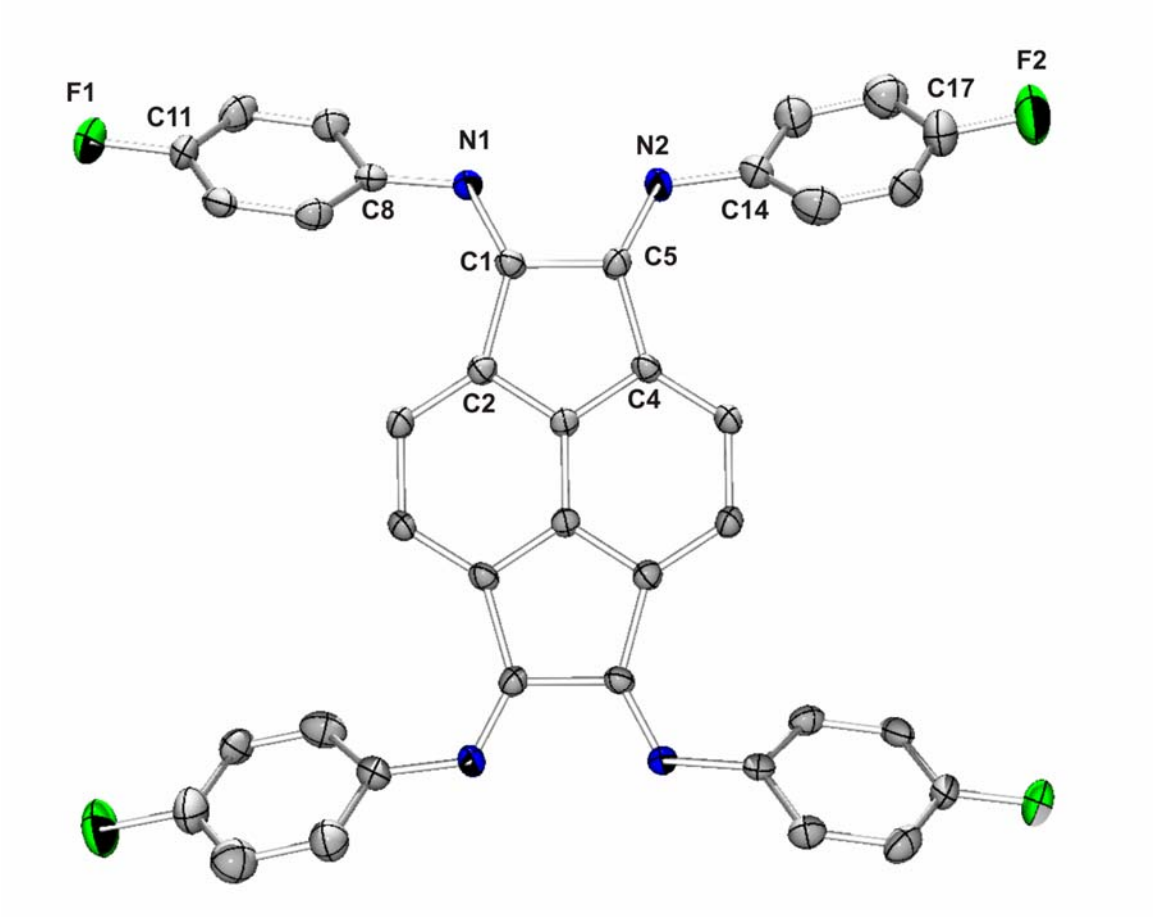

Figure 1.16. Molecular structure of 16 showing a partial numbering scheme. The thermal ellipsoids are shown at the 40% probability level. All hydrogen atoms have been omitted for clarity.

Table 1.46. Crystal data and structure refinement for 16.

Identification code	kvkv117a	
Empirical formula	C38 H20 F4 N4	
Formula weight	608.58	
Temperature	153(2) K	
Wavelength	0.71073 Å	
Crystal system	Monoclinic	
Space group	P21/c	
Unit cell dimensions	a = 11.328 Å	α= 90°.
	b = 8.222 Å	β= 98.61°.
	c = 14.696 Å	γ = 90°.
Volume	1353.3 $Å^3$	
Z	2	
Density (calculated)	1.493 Mg/m^3	
Absorption coefficient	0.108 mm^{-1}	
F(000)	624	
Crystal size	0.11 x 0.09 x 0.08 mm^3	
Theta range for data collection	1.82 to 25.00°.	
Index ranges	-13<=h<=13, -9<=k<=9, -17<=l<=17	
Reflections collected	3980	
Independent reflections	2379 [R(int) = 0.0482]	
Completeness to theta = 25.00°	99.6 %	
Absorption correction	None	
Refinement method	Full-matrix least-squares on F^2	
Data / restraints / parameters	2379 / 0 / 208	
Goodness-of-fit on F^2	1.076	
Final R indices [I>2sigma(I)]	R1 = 0.0881, wR2 = 0.2213	
R indices (all data)	R1 = 0.1407, wR2 = 0.2564	
Largest diff. peak and hole	1.019 and -0.308 $e.Å^{-3}$	

Table 1.47. Selected Bond Lengths (Å) for tetrakis(4-fluorophenylimino)pyracene (16)

C1-C2	1.500(6)
C1-C5	1.547(6)
C1-N1	1.266(5)
C4-C5	1.497(6)
C5-N2	1.253(6)
C8-N1	1.412(6)
C14-N2	1.436(6)
C11-F1	1.376(5)
C17-F2	1.359(6)

Table 1.48. Selected Bond Angles (°) for tetrakis(4-fluorophenylimino)pyracene (16)

C1-C5-C4	106.3(3)
C1-C5-N2	119.6(4)
C1-N1-C8	123.4(4)
C2-C1-C5	106.4(3)
C2-C1-N1	134.2(4)
C4-C5-N2	134.1(4)
C5-C1-N1	119.3(4)
C5-N2-C14	125.9(4)

Chapter 2

"BIAN-Supported Lanthanocene Complexes: Controlling the Metal→Ligand Transfer of 0, 1 or 2 Electrons"

Chapter 2 Introduction

Similar to the development of the 1,4-diazabutadiene (DAB) ligand class, early studies on the coordination chemistry of the bis(imino)acenaphthene (BIAN) ligand class began with the transition metals. Pioneering studies of BIAN-supported late transition metal complexes were reported by the research groups of Elsevier, Brookhart and Coates in the 1990's[4-6]. Such complexes were shown to serve as highly efficient catalysts for a variety of organic transformations[1, 11]. Recent years have seen a shift in BIAN studies toward their reactivity with a number of main group entities. While the exploration of transition metal-BIAN complexes has been focused on catalysis, several research groups have shown the propensity of the BIAN ligand class to undergo redox reactions with a wide variety of main group reagents[17, 18].

While the DAB ligand is capable of accepting up to two electrons, the naphthalene moiety of the BIAN ligand functions as an electron sink, allowing the uptake of up to four electrons into the ligand system. The BIAN ligand chemistry of the alkali and alkali earth metals has been studied extensively by Fedushkin *et al*[18]. Single-crystal X-ray diffraction studies of the four sequentially reduced anions[19] have shown that the first two electrons reside in the diazabutadiene fragment, while the subsequent two electrons are located in the naphthalene unit. These experimental observations are in accord with the relative energies of the LUMO and LUMO+1 as determined on the basis of DFT calculations.

While still in its relative infancy, several research groups have explored the p-block chemistry of the BIAN ligand and these studies have revealed fascinating variations in structure and redox behavior. An increasing number of Group 13-15 species have been shown to be capable of effecting one- or two-electron reduction of a variety of BIAN ligands. The propensity of such ligands to accept electrons has, for example, provided access to main group element derivatives in rare oxidation states[20] and shows considerable promise for future fruitful studies. The redox capabilities of the BIAN ligand can further serve as a model for the tetrakis(imino)pyracene (TIP) ligand. This bifunctional analogue of the DAB and BIAN ligand class would presumably be capable of supporting mixed valence systems or potentially functioning as a framework for electron transport through polymeric networks. As such, the topic of charge transfer chemistry in the context of the BIAN ligand was of fundamental interest in the present work.

There is a paucity of studies pertaining to charge transfer phenomena in lanthanide systems in the literature, owing largely to the prevalent +3 oxidation state of most lanthanide ions. However, in 2002, Andersen *et al*. reported a series of ytterbocene complexes supported by pyridine (py), bipyridine (bipy) and 1,10-phenanthroline (phen), of the types $[(Me_5C_5)_2Yb(py)_2]$, $[(Me_5C_5)_2Yb(bipy)]$ and $[(Me_5C_5)_2Yb(phen)]$, respectively (Scheme 2.01)[21].

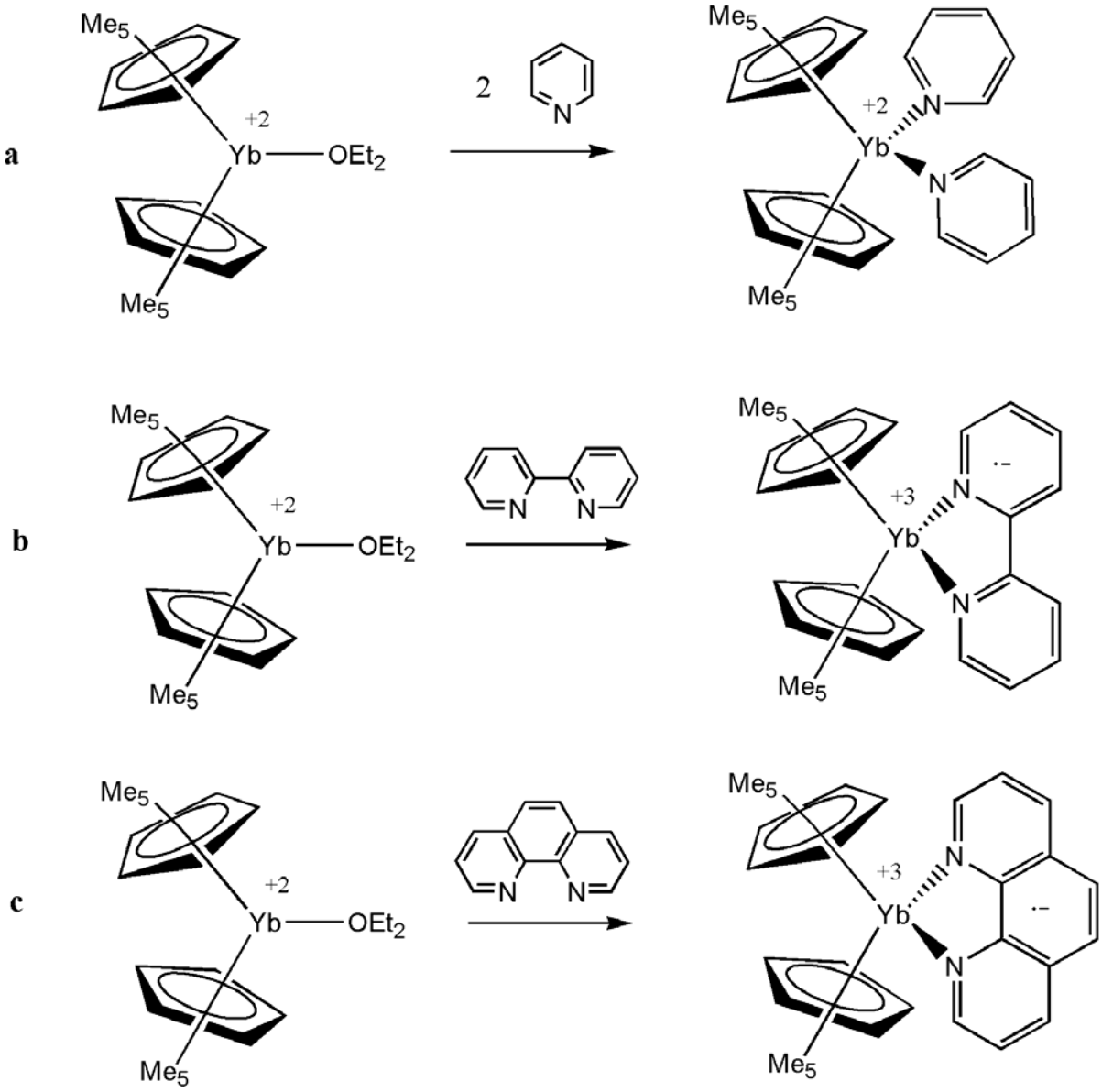

Scheme 2.01. The reaction of decamethylytterbocene with (a) pyridine, (b) bipyridine (c) 1,10-phenanthroline.

In the case of $[(Me_5C_5)_2Yb(py)_2]$, a diamagnetic product characteristic of the Yb(II) ion was observed. Interestingly, in the cases of $[(Me_5C_5)_2Yb(bipy)_2]$ and $[(Me_5C_5)_2Yb(phen)_2]$, a spontaneous charge transfer occurred resulting in reduction of the ligand and oxidation of the Yb ion to the +3 state.

In a subsequent study, John *et al*. reported similar results for decamethylytterbocene complexes supported by terpyridine ligands[22], thus providing additional examples of the charge transfer processes observed earlier by Andersen *et al.* More recently, studies conducted by Trifonov *et al*. and Andersen *et al.* involving DAB-supported decamethyllanthanocene complexes demonstrated the feasibility of controlling the charge transfer process by manipulation of the lanthanide or ligand stereo-electronics[23, 24].

At the outset of the present work, there were no examples of lanthanide-BIAN complexes in the literature. Recognizing that such compounds could potentially serve as both useful models for the electron interactions in bifunctional systems as well as serving as a potential source of new catalysts, a range of representative lanthanide-BIAN complexes was synthesized with the goal of gaining an enhanced understanding of the charge transfer processes in such systems. Specifically, the present work addresses the syntheses and reactivity studies of BIAN-supported decamethyllanthanocene complexes of the general form $(C_5Me_5)_2Ln$(R-BIAN) (Ln = Yb, Sm, Eu ; R = Dipp, Mes, p-F, p-OMe, ^{t}Bu) (Scheme 2.02). By careful selection of lanthanide and tuning of the steric and electronic properties of the ligand, it will be demonstrated that it is possible to control whether 0, 1 or 2 electrons are transferred from the lanthanide ion into the BIAN ligand.

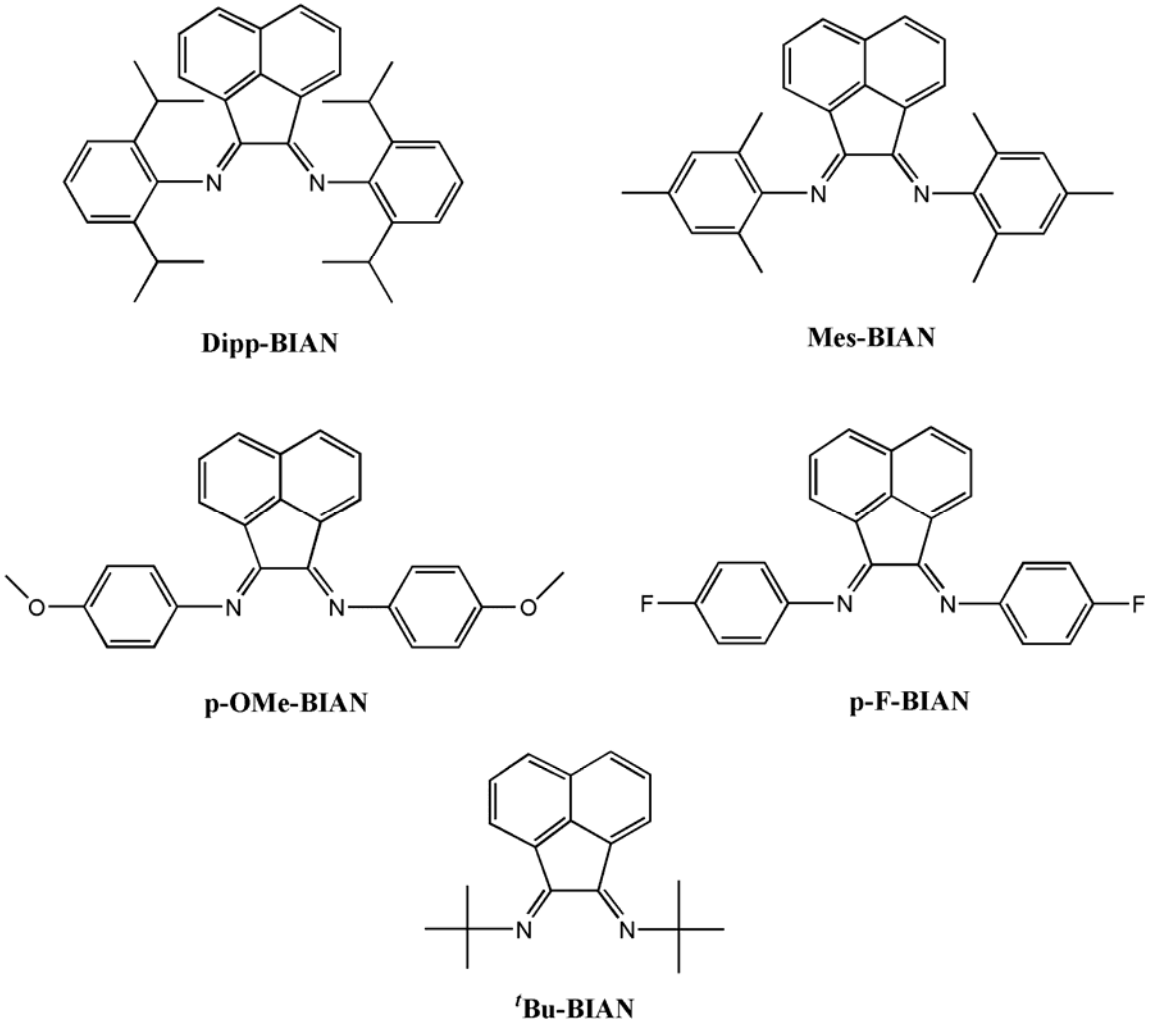

Scheme 2.02. BIAN ligands used in the present study.

Results and Discussion

Section 2.1 Introduction

It was evident from the publications of Andersen, Trifinov and John *et al.* that there exists a complex interplay of variables that ultimately determines the chemical fate of a lanthanide moiety supported by a nitrogen-donor ligand. As mentioned earlier, the choice of pyridine, bipyridine or 1,10-phenanthroline controlled whether a Yb(II) or a Yb(III) complex would be formed. Analogous studies of lanthanide complexes supported by DAB ligands demonstrated the effects of altering the cyclopentadienyl substituents or changing the R groups on the diimine framework.

Given that there are several known examples of lanthanide charge transfer chemistry in the literature coupled with the fact that the BIAN ligand typically undergoes facile reduction, it was anticipated that the majority, if not all, of the lanthanide-BIAN complexes would undergo a charge transfer process resulting in the corresponding Ln(III) complex of the anion radical BIAN ligand. Interestingly, however, conservation of the +2 oxidation state was observed in the cases of two decamethyleuropocene complexes. These $(C_5Me_5)_2$Eu-BIAN complexes therefore involved donor-acceptor bonding and no metal→ ligand electron transfer.

At the outset, a point of clarification should be made regarding the metrical parameters that were obtained by single-crystal X-ray diffraction. All discussion of the C-C and C-N bond distances relates to the bonds of the diazabutadiene (N-C-C-N) fragment of the BIAN ligand.

Synthesis and Characterization of $(C_5Me_5)_2Eu(^tBu\text{-}BIAN)$ (17)

The complex $(C_5Me_5)_2Eu(^tBu\text{-}BIAN)$ (**17**) was synthesized by the addition of toluene to an equimolar mixture of $(C_5Me_5)_2Eu\text{-}OEt_2$ and $^tBu\text{-}BIAN$. Following workup of the reaction mixture and removal of the solvent, a dark red solid was obtained in 78% yield. This solid was dissolved in a toluene/hexanes mixture and the resulting solution was stored at -15°C for 7 days, following which a small crop of dark red crystals of **17** suitable for X-ray diffraction experiments was isolated. The single-crystal X-ray diffraction study confirmed the identity of the product as the title compound shown in Figure 2.01. Details of the data collection, structure solution and refinement are compiled in Table 2.01 and selected metrical parameters are listed in Tables 2.02 and 2.03.

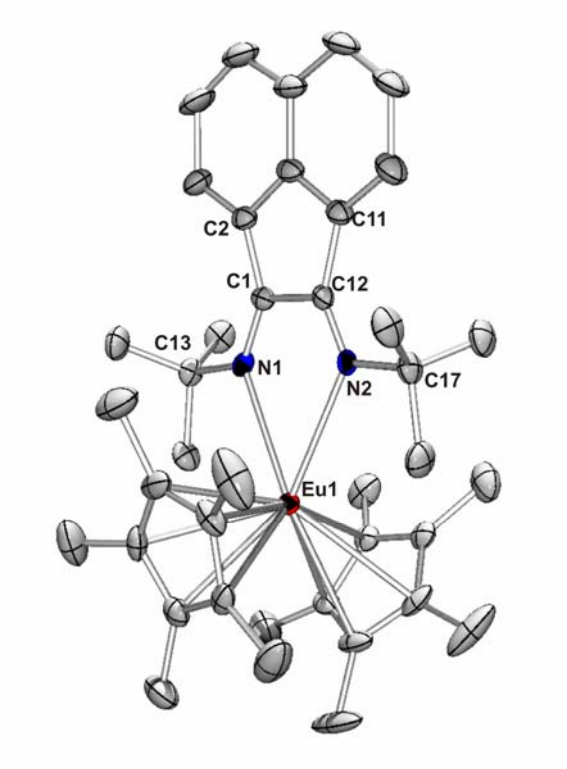

Figure 2.01. Molecular structure of 17 showing a partial numbering scheme. The thermal ellipsoids are shown at the 40% probability level. All hydrogen atoms have been omitted for clarity.

Compound **17** crystallizes in the monoclinic space group $P2_1/n$ with one molecule of toluene in the lattice. The most notable metrical parameters for **17** are the average C-N and C(1)-C(12) bond distances of 1.283(5) Å and 1.545(5) Å, respectively, which are nearly identical to those observed for the free ^{t}Bu-BIAN ligand (1.278(3) Å and 1.551(4) Å, respectively). The foregoing data imply that no metal→ligand charge transfer has occurred and thus implies the formation of a donor-acceptor complex. The average Eu-centroid distance for **17** of 2.672(5) Å is significantly longer than that found for $(C_5Me_5)_2$Eu-OEt_2 (2.527 Å)[25], which is consistent with a higher degree of electron density on the europium center and thus supports the notion that the +2 oxidation state of Eu is retained.

The IR spectrum of **17** reveals a sharp signal at 1636 cm^{-1} which falls in the region reported for C=N stretching frequencies. The solution state magnetic moment value for **17** is 6.98 BM as determined by the Evans method. While this value is slightly lower than the typical range associated with Eu(II) complexes (7.1-7.8 BM), it is significantly higher than the range reported for Eu(III) (3.4-3.6 BM), thus supporting the conclusion that the oxidation state of Eu in **17** is +2.

Synthesis and Characterization of $(C_5Me_5)_2$Eu(Mes-BIAN) (18)

The complex $(C_5Me_5)_2$Eu(Mes-BIAN) (**18**) was synthesized by treatment of Mes-BIAN with an equimolar quantity of $(C_5Me_5)_2$Eu-OEt_2 in toluene solution. A dark red solid was isolated in 82% yield following workup of the reaction mixture and removal of the solvent. A saturated solution of the crude solid in a toluene/hexanes solution was stored at -15°C for 7 days, affording a small crop of dark red crystals suitable for X-ray analysis. A single-crystal X-ray diffraction study confirmed the identity of the product as the title compound shown in Figure 2.02. Details of the data collection, structure solution

and refinement are compiled in Table 2.04 and pertinent metrical parameters are presented in Tables 2.05 and 2.06.

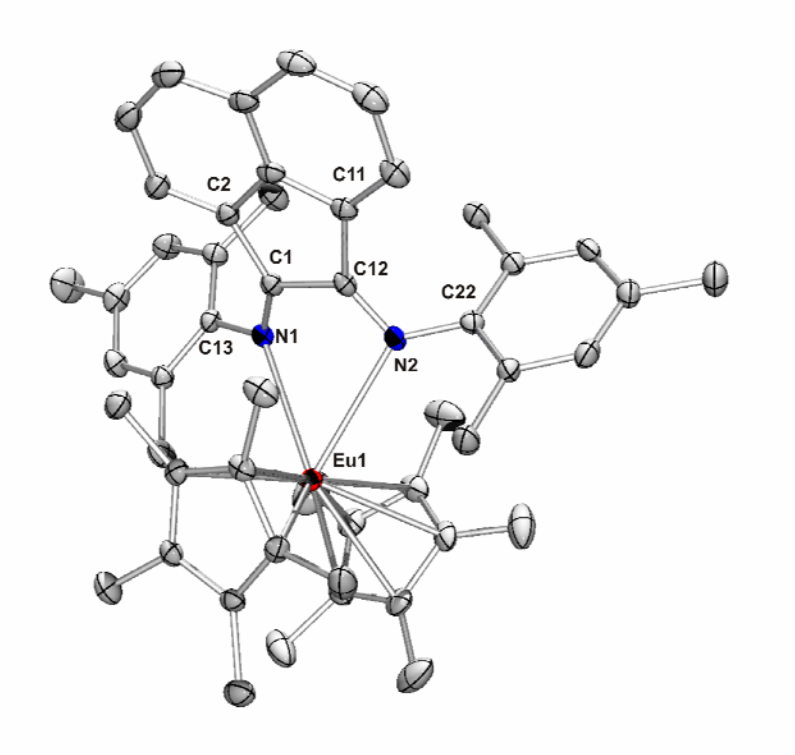

Figure 2.02. Molecular structure of 18 showing a partial numbering scheme. The thermal ellipsoids are shown at the 40% probability level. All hydrogen atoms and one molecule of toluene have been omitted for clarity.

Complex **18** crystallizes with one molecule of toluene in the monoclinic space group $P2_1/c$. As in the case of **17**, the bond distances of interest include the C(1)-C(12) distance of 1.531(5) Å and the average C-N distance of 1.285(5) Å, which imply bond orders of one and two, respectively. The fact that these metrical parameters are similar to those found for the free Mes-BIAN ligand (1.528(2) Å and 1.2662(16) Å, respectively[26]) strongly suggests that no metal→ligand charge transfer process has occurred. As in the case of **17**, the average Eu-centroid distance for **18** of 2.621(3) Å is significantly longer than the corresponding distance found for $(C_5Me_5)_2Eu\text{-}OEt_2$[25], thus providing further evidence of the retention of the +2 oxidation state for Eu.

The IR spectrum reveals a sharp stretch at 1631 cm^{-1} which falls in the region reported for C=N stretching frequencies. As determined by Evans method, the solution state magnetic moment value for **18** is 6.72 BM, implying a Eu oxidation state of +2.

Section 2.1 Conclusions

By treatment of $(C_5Me_5)_2Eu\text{-}OEt_2$ with ^{t}Bu-BIAN and Mes-BIAN, the complexes $(C_5Me_5)_2Eu(^t$Bu-BIAN) (**17**) and $(C_5Me_5)_2Eu$(Mes-BIAN) (**18**), respectively, were synthesized in good yields. The similarity of the C-C and C-N bond lengths in these complexes with respect to the corresponding free ligands indicates the formation of N→Eu donor-acceptor complexes. The observation of a C=N stretching vibration for both complexes lends further support to this bonding assignment, as does the solution state magnetic moment which indicates the presence of Eu(II) ions.

Given the entire Ln(II) series, the Eu(II) ion possesses the highest oxidation potential. The source of the extra stability associated with the +2 oxidation state stems from the presence of an f^7 half-filled shell. The removal of a single electron from Eu(II) is more energetically unfavorable than for any other Ln(II) ion. Moreover, the use of electron-donating ^{t}Bu and Mes substituents serves to enhance the electron density on the nitrogen atoms of the BIAN ligand, thus further inhibiting the Eu→ligand charge transfer process.

Section 2.2 Introduction

In the previous section, two BIAN-supported $(C_5Me_5)_2Eu$ complexes were discussed, both of which adopted a nitrogen→lanthanide donor-acceptor coordination mode. Given the aforementioned reluctance of the Eu(II) ion to undergo oxidation, the structures of **17** and **18** were not wholly unexpected. Recognizing that the decamethyleuropocene was capable of binding BIAN ligands in a donor-acceptor fashion, the question remained as to whether the one-electron transfer could be effected with different lanthanides and/or by control of the ligand stereo-electronics. Accordingly, the next section addresses the syntheses and structural assays of a series of Yb(III) and Sm(III) complexes supported by a variety of BIAN ligands. Two further examples of the analogous Eu(III) structures are also presented.

Synthesis and Characterization of $(C_5Me_5)_2Eu$(p-F-BIAN) (19)

The compound $(C_5Me_5)_2Eu$(p-F-BIAN) (**19**) was synthesized via the reaction of p-F-BIAN with an equimolar quantity of $(C_5Me_5)_2Eu\text{-}OEt_2$ in toluene solution. Following workup of the reaction mixture and solvent stripping, a dark green solid was isolated in 77% yield. Recrystallization of **19** was effected by storage of a toluene/hexanes solution at -15°C for 6 days. The resulting dark green crystals proved to be suitable for assay by single-crystal X-ray diffraction. The identity of the title compound shown in Figure 2.03 was confirmed on the basis of the X-ray data. Details of the data collection process, structure solution and refinement are presented in Table 2.07 and selected metrical parameters have been provided in Tables 2.08 and 2.09.

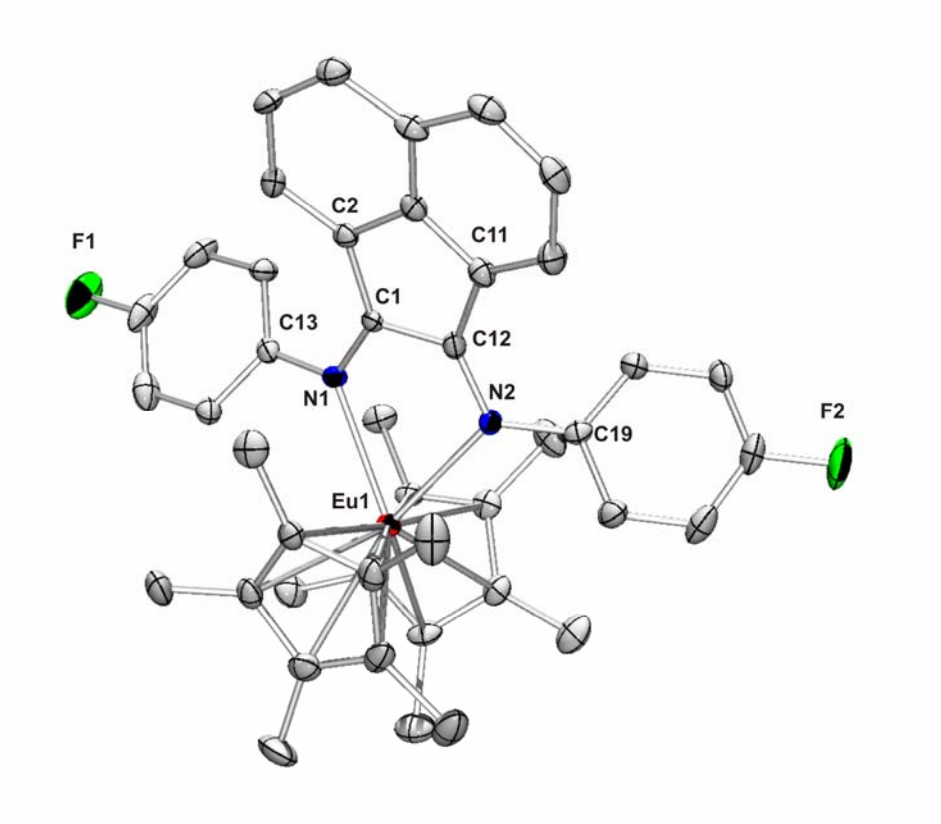

Figure 2.03. Molecular structure of 19 showing a partial numbering scheme. The thermal ellipsoids are shown at the 40% probability level. All hydrogen atoms have been omitted for clarity.

The single-crystal X-ray diffraction study revealed that **19** crystallizes in the monoclinic space group *Cc*. The salient bond distances are the C(1)-C(12) and C-N separations of 1.453(7) Å and 1.339(7) Å, respectively. Both of these bond distances are indicative of a bond order intermediate between those of single and double bonds, thereby implying the transfer of one electron from the Eu(II) center into the BIAN ligand. Further evidence stemmed from the average Eu-centroid distance of 2.450(7) Å, a value that is significantly shorter than the 2.527 Å value associated with $(C_5Me_5)_2Eu\text{-}OEt_2$[25]. Moreover, the deep green color of **19**, in contrast to the deep red color of **17** and **18**, lent qualitative support to the conclusion that Eu→ligand electron transfer had occurred. Further support for such a conclusion came from the absence of a feature in the C=N

stretching region in the IR spectrum and the solution state magnetic moment value of 2.80 BM as determined by the Evans method. While this value falls somewhat below the typical range observed for Eu(III) complexes (3.4-3.6 BM), it is distinctly different from the range of magnetic moments reported for Eu(II) complexes (7.1-7.8 BM). Finally, the ^{1}H NMR spectrum of **19** exhibited a resonance at δ -21.1, similar to a shift reported by Evans *et al.* for the (C_5Me_5) protons of the Eu(III) complex [(C_5Me_5)Eu($OCMe_3$)(μ-$OCMe_3$)$_2$[27]. Taken collectively, the foregoing data indicate that the oxidation state of Eu in **19** is +3 and that a one-electron charge transfer process has occurred.

Synthesis and Characterization of (C_5Me_5)$_2$Eu(p-OMe-BIAN) (20)

The compound (C_5Me_5)$_2$Eu(p-OMe-BIAN) was readily prepared by the treatment of one equivalent of p-OMe-BIAN with an equimolar quantity of (C_5Me_5)$_2$Eu-OEt_2 in toluene solution at ambient temperature. After workup of the reaction mixture and solvent stripping, a dark green solid was obtained in 87% yield. The crude solid was dissolved in a toluene/hexanes mixture and the resulting solution was stored at -15°C for 5 days, during which time a modest crop of dark green crystals suitable for X-ray diffraction experiments was formed. A single-crystal X-ray diffraction study verified the identity of the product as the title compound shown in Figure 2.04. Details pertaining to the data collection, structure solution and refinement are presented in Table 2.10 and a selection of pertinent metrical parameters is provided in Tables 2.11 and 2.12.

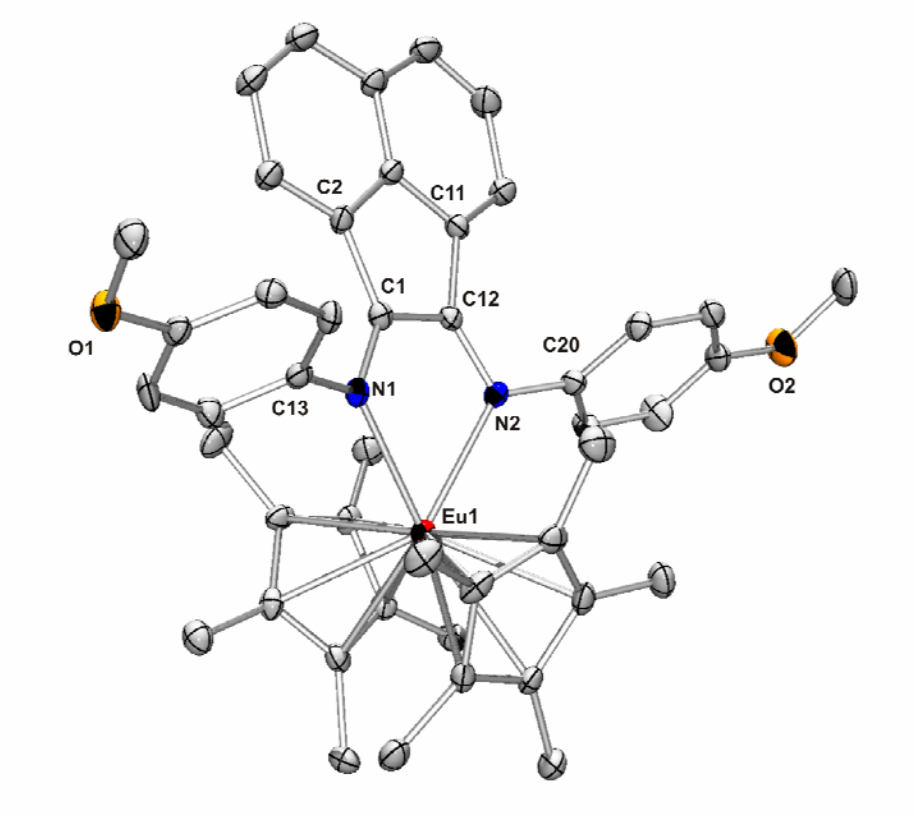

Figure 2.04. Molecular structure of 20 showing a partial numbering scheme. The thermal ellipsoids are shown at the 40% probability level. All hydrogen atoms and one molecule of toluene have been omitted for clarity.

Compound **20** crystallizes in the monoclinic space group $P2_1/n$ with one molecule of toluene. The C(1)-C(12) bond distance for **20** of 1.442(8) Å is significantly shorter than that found in the free p-OMe-BIAN ligand (1.527(2) Å) and the average C-N bond distance of 1.340(7) Å is appreciably longer than the value of 1.277(1) Å observed for the free ligand[28]. These disparities are suggestive of the transfer of one electron from divalent Eu into the BIAN ligand. Further support for this suggestion is provided by the fact that the average Eu-centroid distance of 2.442(4) Å is considerably shorter than that reported for $(C_5Me_5)_2Eu\text{-}OEt_2$[25], thus implying that one-electron oxidation of the metal has occurred, resulting in Eu(III). Additionally, the absence of an IR-active feature in the region reported for the C=N stretching vibration supports the foregoing conclusion, as does the solution state magnetic moment value for **20** of 3.55 BM as determined by the

Evans method. This magnetic moment value falls in the typical range that is anticipated for Eu(III) complexes (3.4-3.6 BM). As in the case of **19**, the ^{1}H NMR spectrum reveals a sharp signal at δ -21.3 providing further evidence for the occurrence of one-electron Eu→ligand charge transfer and formation of a BIAN radical anion complex of $(C_5Me_5)_2Eu^+$.

Synthesis and Characterization of $(C_5Me_5)_2Sm(^tBu\text{-}BIAN)$ (21)

The $(C_5Me_5)_2Sm(^tBu\text{-}BIAN)$ complex was synthesized by the addition of toluene to equimolar quantities of $(C_5Me_5)_2Sm\text{-}OEt_2$ and ^{t}Bu-BIAN. A dark green solid was obtained in 81% yield following workup of the reaction mixture and removal of the solvent. The crude solid was dissolved in a toluene/hexanes solution and stored at -15°C for one week, during which time a small crop of dark green crystals suitable for X-ray diffraction experiments was formed. On the basis of a single-crystal X-ray diffraction study, the anticipated structure of this compound was authenticated and is presented in Fig. 2.05. Details of the data collection, structure solution and refinement are collected in Table 2.13 and selected metrical parameters are presented in Tables 2.14 and 2.15.

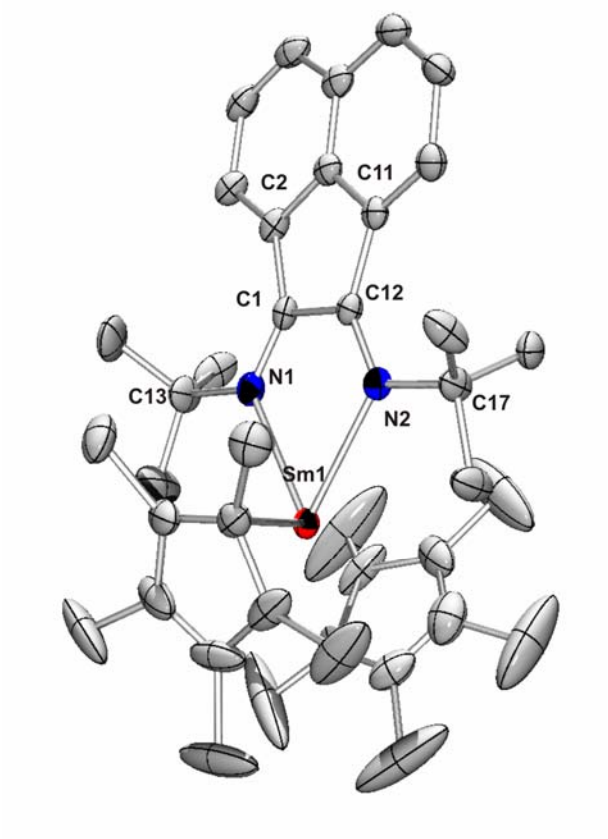

Figure 2.05. Molecular structure of 21 showing a partial numbering scheme. The thermal ellipsoids are shown at the 40% probability level. All hydrogen atoms have been omitted for clarity.

The single-crystal X-ray diffraction study revealed that **21** crystallizes in the monoclinic space group $P2_1/c$. The bond distance for C(1)-C(12) of 1.451(8) Å and the average C-N bond distance of 1.335(8) Å imply bond orders that are intermediate between one and two. The average Sm-centroid distance of 2.553(5) Å is similar to the value of 2.538 Å reported for $(C_5Me_5)_2Sm\text{-}OEt_2$[25]. Such a value would appear to favor assignment of the +2 oxidation state to the Sm ion. However, given the aforementioned N-C-C-N bond distances, it is more likely that a one-electron reduction has taken place. The accompanying color change to dark green is also indicative of one-electron metal→ligand transfer as observed in compounds **19** and **20**. Finally, the solution state magnetic moment value of 1.78 BM obtained by the Evans method falls near the region reported for Sm(III) ions (1.5-1.7 BM).

Synthesis and Characterization of $(C_5Me_5)_2Sm(Mes\text{-}BIAN)$ (22)

$(C_5Me_5)_2Sm(Mes\text{-}BIAN)$ was synthesized by the treatment of Mes-BIAN with an equimolar quantity of $(C_5Me_5)_2Sm\text{-}OEt_2$ in toluene solution. A dark green solid was isolated in 91% yield following workup of the reaction mixture and solvent stripping. The crude solid was dissolved in a toluene/hexanes mixture and the temperature of the resulting solution was reduced to -15°C. After 4 days, a small crop of dark green crystals suitable for X-ray analysis was obtained. A single-crystal X-ray diffraction study verified the identity of the product as the title compound shown in Figure 2.06. Details of the data collection process, structure solution and refinement are listed in Table 2.16 and relevant metrical parameters have been assembled in Tables 2.17 and 2.18.

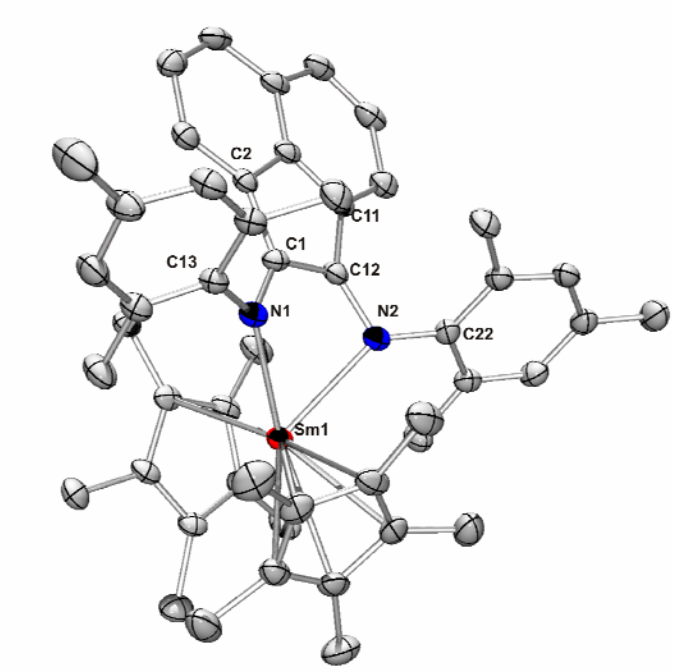

Figure 2.06. Molecular structure of 22 showing a partial numbering scheme. The thermal ellipsoids are shown at the 40% probability level. All hydrogen atoms have been omitted for clarity.

Compound **22** crystallizes in the triclinic space group *P-1*. A noteworthy aspect of the structure of **22** is the fact that the average C-N and C(1)-C(12) bond distances of

1.345(5) Å and 1.444(6) Å, respectively, differ significantly from those reported for the free Mes-BIAN ligand[26]. These bond lengths imply bond orders of between one and two, thus suggesting the formation of a BIAN radical anion. Akin to **21**, the average Sm-centroid distance of 2.490(3) Å is shorter than that reported for $(C_5Me_5)_2Sm\text{-}OEt_2$[25], thus providing a further indication of the presence of a Sm(III) ion.

Additional evidence that a metal→ligand charge transfer process had occurred stemmed from the absence of a feature in the C=N stretching region of the IR spectrum of **22**. The solution state magnetic moment value for **22** of 1.82 BM as determined by the Evans method furnished further evidence of the presence of a Sm(III) ion. The overall conclusion of this particular study is that **22** can best be described as a $(C_5Me_5)_2Sm(III)$ cation moiety supported by a Mes-BIAN radical anion ligand.

Synthesis and Characterization of $(C_5Me_5)_2Sm$(p-F-BIAN) (23)

The synthesis of $(C_5Me_5)_2Sm$(p-F-BIAN) was performed in an analogous fashion to that described for **22** using p-F-BIAN instead of Mes-BIAN. Workup of the reaction mixture and removal of solvent resulted in the isolation of a dark green solid in 84% yield. A small portion of the crude solid was dissolved in pentane and transferred to an NMR tube. This solution was allowed to slowly evaporate over the course of 10 days resulting in the formation of a small crop of green crystalline needles, the identity of which was established by single-crystal X-ray diffraction. The molecular structure is shown in Figure 2.07 and details regarding the data collection, structure solution and refinement are presented in Table 2.19. Pertinent metrical parameters are presented in Tables 2.20 and 2.21.

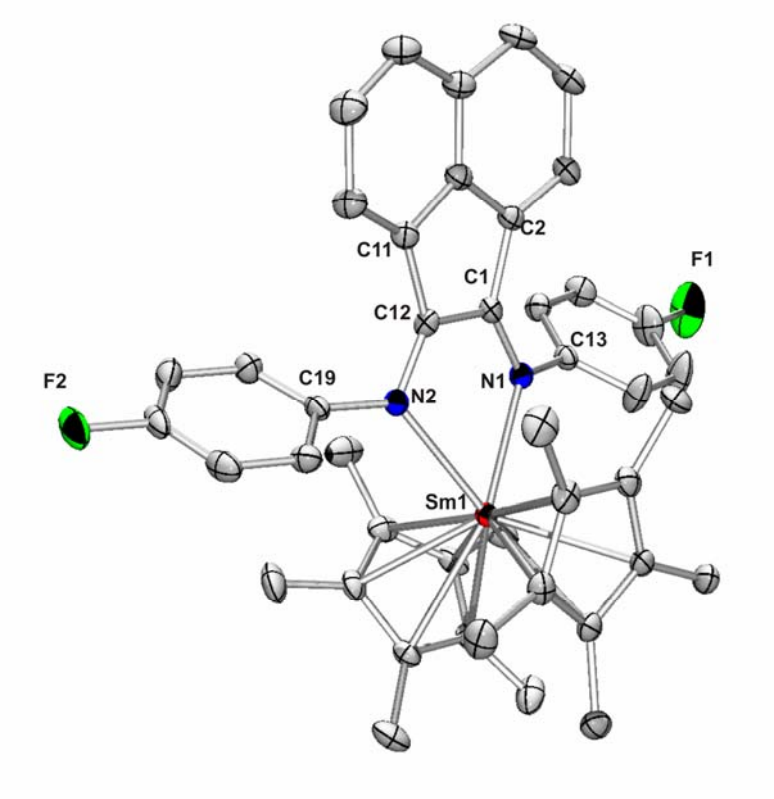

Figure 2.07. Molecular structure of 23 showing a partial numbering scheme. The thermal ellipsoids are shown at the 40% probability level. All hydrogen atoms have been omitted for clarity.

Compound **23** crystallizes in the triclinic space group *P-1*. The salient bond distances are the C(1)-C(12) distance of 1.442(5) Å and the average C-N bond distance of 1.341(5) Å, both of which imply bond orders between one and two. The average Sm-centroid distance of 2.449(4) Å is significantly shorter than the corresponding length in $(C_5Me_5)_2Sm\text{-}OEt_2$[25], thus suggesting an oxidation state of +3 for the Sm ion.

Inspection of the IR spectrum revealed the absence of a feature in the region reported for C=N stretching frequencies and the solution state magnetic moment value of 1.74 BM for **23** confirms the presence of a Sm(III) ion. It is concluded that a one-electron transfer has occurred, resulting in the formation of a $(C_5Me_5)_2Sm(III)$ cation supported by a p-F-BIAN radical anion.

Synthesis and Characterization of $(C_5Me_5)_2Sm$(p-OMe-BIAN) (24)

The compound $(C_5Me_5)_2Sm$(p-OMe-BIAN) (**24**) was synthesized and isolated in 93% yield from equimolar quantities of p-OMe-BIAN and $(C_5Me_5)_2Sm$-OEt_2 as described above for **23**. The crude green solid was dissolved in toluene and the resulting solution was stored at -15°C for 7 days. A crop of dark green crystals was isolated and proved to be suitable for single-crystal X-ray diffraction experiments. The structure of **24** is depicted in Figure 2.08 and details of the data collection, structure solution and refinement are presented in Table 2.22. A selection of relevant metrical parameters appears in Tables 2.23 and 2.24.

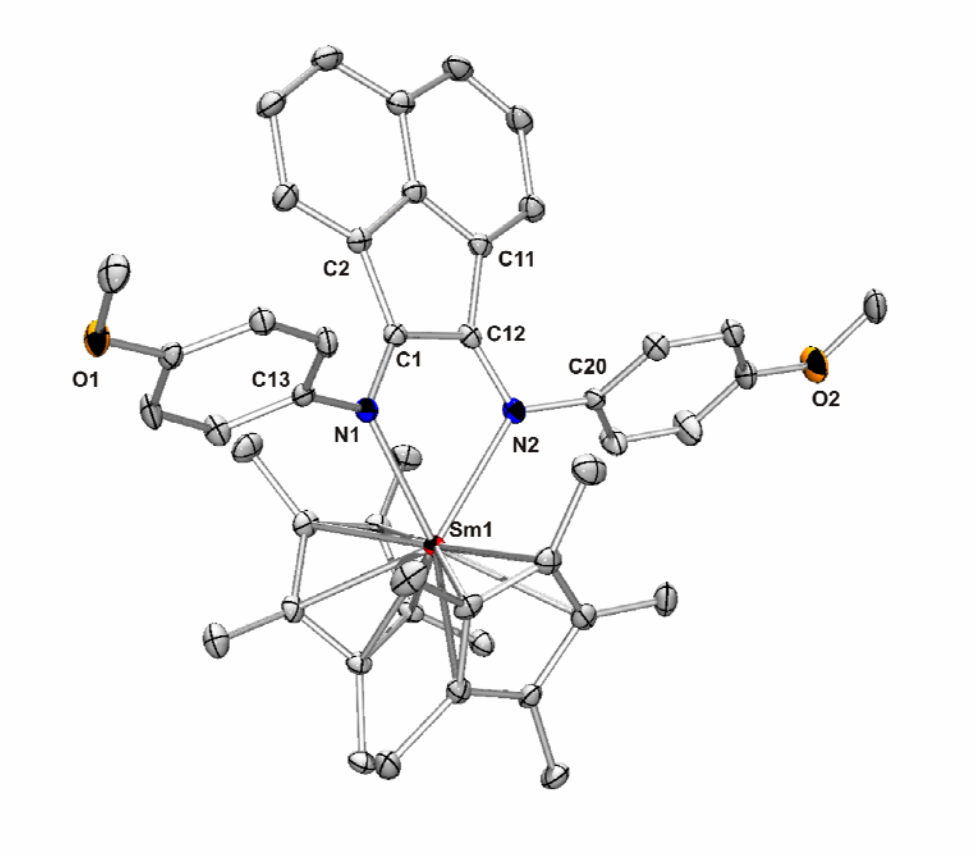

Figure 2.08. Molecular structure of 24 showing a partial numbering scheme. The thermal ellipsoids are shown at the 40% probability level. All hydrogen atoms have been omitted for clarity.

Compound **24** crystallizes in the triclinic space group *P-1*. As in the cases of other complexes that underwent one-electron metal→ligand charge transfer, the C(1)-C(12) bond distance of 1.446(5) Å and the average C-N bond distance of 1.336(5) Å imply bond orders intermediate between one and two. As expected, the average Sm-centroid distance of 2.455(3) Å for **24** is significantly shorter than that of the Sm(II) compound $(C_5Me_5)_2Sm\text{-}OEt_2$[25]. As in the cases of compounds **19**-**23**, the one electron metal→ligand charge transfer process was qualitatively evidenced by a color change from red to deep green.

As observed in the other BIAN-supported Sm(III) complexes, the IR spectrum is devoid of any peaks in the region anticipated for the C=N stretching region. The solution state magnetic moment value for **24** is 1.80 BM (Evans method), thus confirming the presence of a Sm(III) complex comprising a $(C_5Me_5)_2Sm^+$ moiety supported by a radical BIAN anion.

Synthesis and Characterization of $(C_5Me_5)_2Yb$(Mes-BIAN) (25)

The complex $(C_5Me_5)_2Yb$(Mes-BIAN) was synthesized and isolated in 94% yield from equimolar quantities of $(C_5Me_5)_2Yb\text{-}OEt_2$ and Mes-BIAN as described in **24**. The resulting dark green solid was isolated in 85% yield. This crude solid was dissolved in a toluene/hexanes mixture and stored at -15°C for one week. A suitable single-crystal was selected from the resulting crop of dark green crystals and subjected to X-ray analysis. The molecular structure is illustrated in Figure 2.09 and details of the data collection, structure solution and refinement have been summarized in Table 2.25. A selection of pertinent metrical parameters is presented in Tables 2.26 and 2.27.

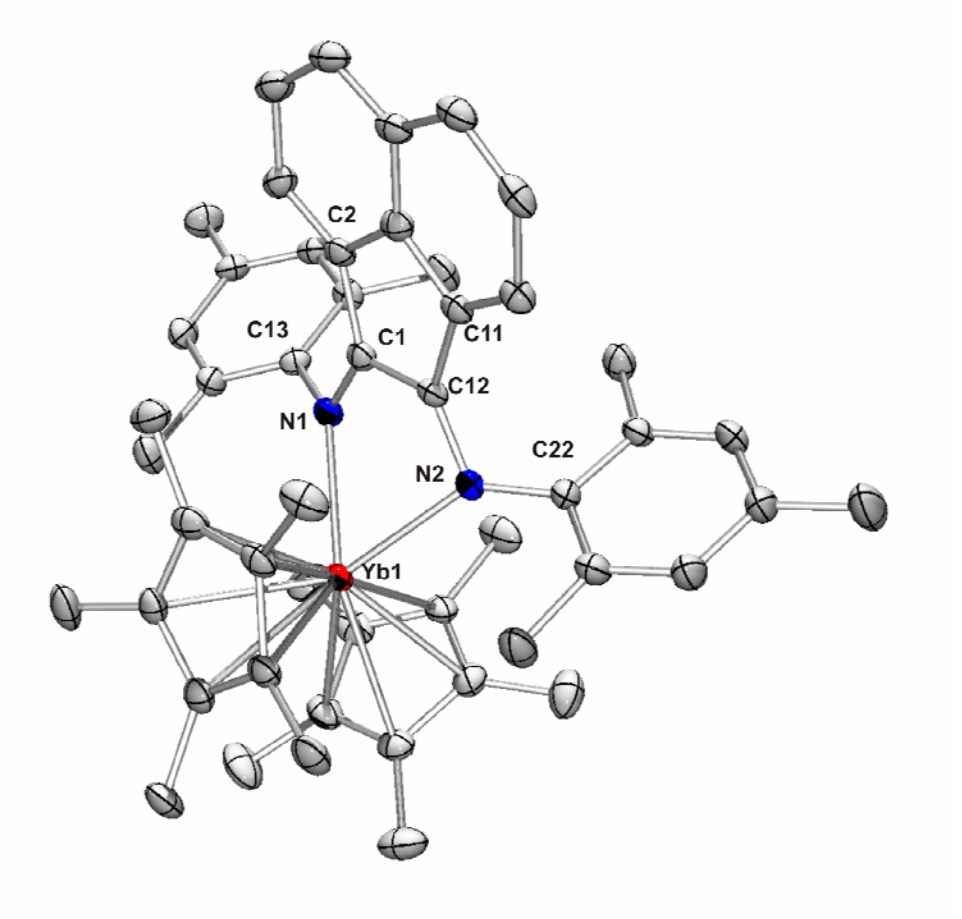

Figure 2.09. Molecular structure of 25 showing a partial numbering scheme. The thermal ellipsoids are shown at the 40% probability level. All hydrogen atoms have been omitted for clarity.

Compound **25** crystallizes in the triclinic space group *P-1*. As in the other cases of metal→ligand charge transfer the bond distances of 1.450(6) Å and 1.341(5) Å for the C(1)-C(12) and C-N bonds imply bond orders between one and two. Additionally, the average Yb-centroid distance of 2.392(3) Å is slightly shorter than the analogous distance of 2.412 Å reported for $(C_5Me_5)_2Yb\text{-}OEt_2$[29], thus suggesting the presence of a $(C_5Me_5)_2Yb(III)$ cation. As observed in the Sm(III) complexes **21-24**, there is an accompanying color change from red to deep green and no evidence for the presence of a C=N stretching vibration in the IR spectrum. The solution state magnetic moment value of **25** is 4.22 BM, indicative of the presence of Yb(III) ions (4.0-4.4 BM).

Synthesis and Characterization of $(C_5Me_5)_2Yb$(p-F-BIAN) (26)

The compound $(C_5Me_5)_2Yb$(p-F-BIAN) was synthesized from equimolar quantities of p-F-BIAN and $(C_5Me_5)_2Yb$-OEt_2 using the protocol described for **19-25**. Dark green solid **26** was isolated in 84% yield. This crude solid was purified by recrystallization from a toluene/hexanes mixture stored at -15°C for one week, which resulted in a small crop of green crystalline needles. One of these needles was selected for examination by single-crystal X-ray diffraction analysis. The molecular structure is presented in Figure 2.10 and details regarding the data collection, structure solution and refinement have been summarized in Table 2.28. A selection of pertinent metrical parameters appears in Tables 2.29 and 2.30.

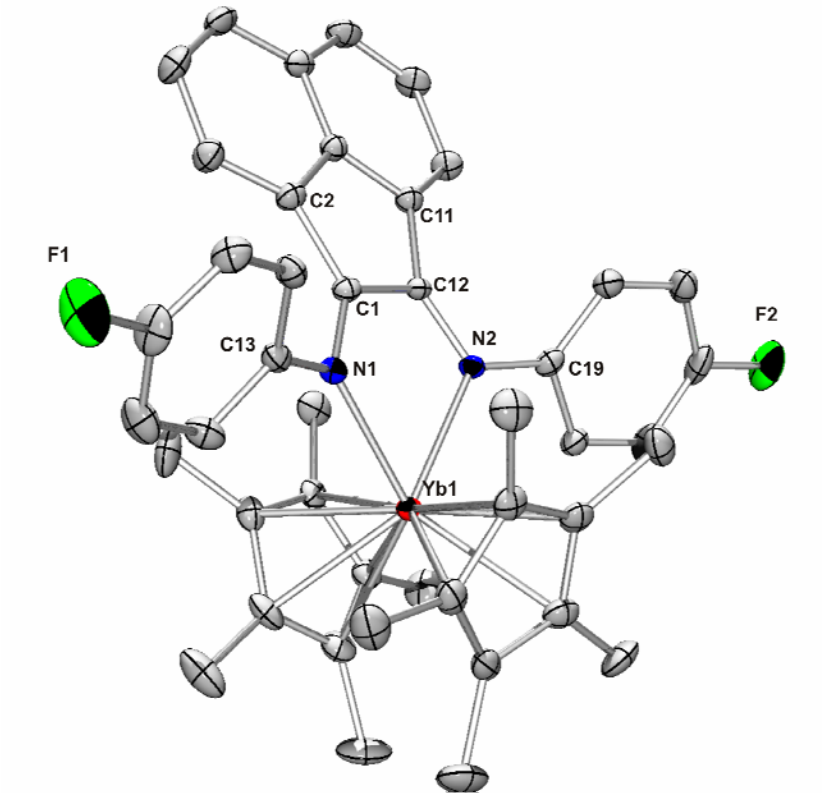

Figure 2.10. Molecular structure of 26 showing a partial numbering scheme. The thermal ellipsoids are shown at the 40% probability level. All hydrogen atoms have been omitted for clarity.

Compound **26** crystallizes in the monoclinic space group *Cc*. As in the other cases of single-electron metal→ligand transfer reactions the C(1)-C(12) distance of 1.432(5) Å and average C-N bond distance of 1.344(5) Å fall between those anticipated for single and double bonds. As expected, the observed average Yb-centroid distance of 2.357(3) Å, is significantly shorter than that reported for $(C_5Me_5)_2Yb\text{-}OEt_2$[29]. The accompanying color change from red to deep green is also indicative of the BIAN radical formation as observed in compounds **19-25**. No feature corresponding to a C=N stretching vibration was evident in the IR spectrum. The solution state magnetic moment value of 3.71 BM for **26** further supports the assignment of the +3 oxidation state.

Synthesis and Characterization of $(C_5Me_5)_2Yb$(p-OMe-BIAN) (27)

The $(C_5Me_5)_2Yb$(p-OMe-BIAN) complex was synthesized in 88% yield from $(C_5Me_5)_2Yb\text{-}OEt_2$ and p-OMe-BIAN as described for **26**. Recrystallization of the crude solid from a toluene/hexanes solution stored at -15°C for 7 days afforded a crop of dark green crystals suitable for analysis by single-crystal X-ray diffraction. The molecular structure of **27** is presented in Figure 2.11 and details of the data collection, structure solution and refinement can be found in Table 2.31 with a companion sampling of relevant metrical parameters in Tables 2.32 and 2.33.

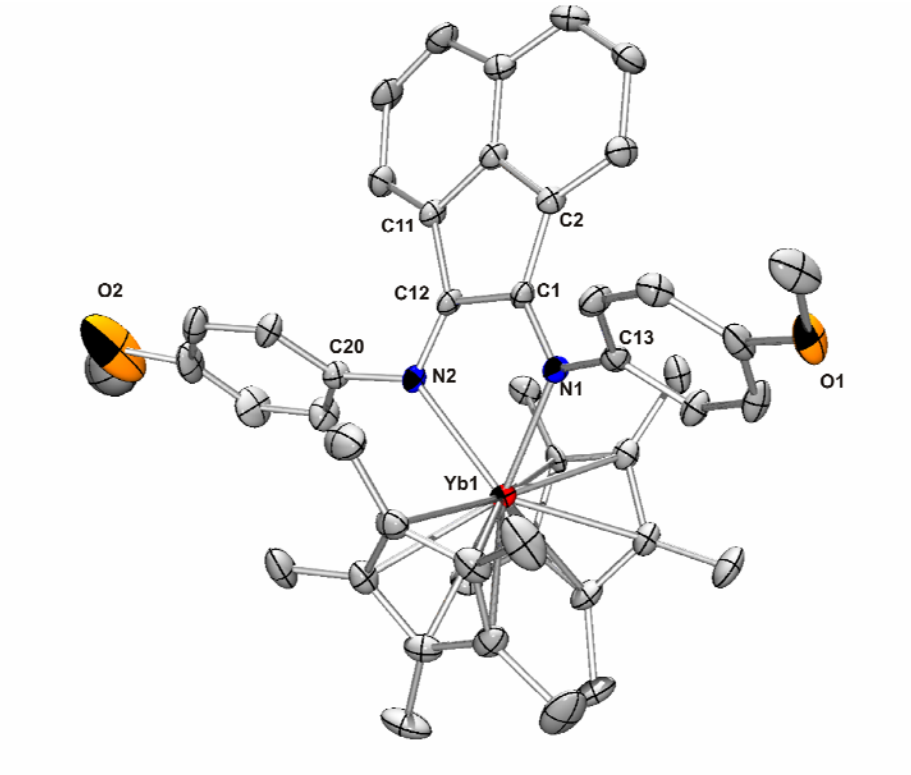

Figure 2.11. Molecular structure of 27 showing a partial numbering scheme. The thermal ellipsoids are shown at the 40% probability level. All hydrogen atoms have been omitted for clarity.

Compound **27** crystallizes in the monoclinic space group *C2/c*. As in the other complexes that undergo a metal→ligand charge transfer, this process is evidenced by a C(1)-C(12) bond distance of 1.448(8) Å and an average C-N distance of 1.338(8) Å, which collectively indicate bond orders intermediate between one and two. Consistent with the presence of a Yb(III) cation, the average Yb-centroid distance is 2.346(4) Å. Again, as with the other compounds discussed in this section, absence of a C=N IR stretching mode and the characteristic color change from red to deep green confirm that a charge transfer process has taken place. Lastly, the magnetic moment value of 3.91 BM obtained for **27** indicates the presence of Yb(III) ions, further supporting the notion that charge transfer has occurred.

Section 2.2 Conclusions

The reactions of $(C_5Me_5)_2$Eu-OEt_2 with p-F-BIAN and p-OMe-BIAN, and of $(C_5Me_5)_2$Sm-OEt_2 with tBu-BIAN, Mes-BIAN, p-F-BIAN and p-OMe-BIAN, and of $(C_5Me_5)_2$Yb-OEt_2 with Mes-BIAN, p-F-BIAN and p-OMe-BIAN, each resulted in single electron metal→ligand electron transfer and formation of the $(C_5Me_5)_2$Ln(III) complex of the anion radical of the respective BIAN ligand:

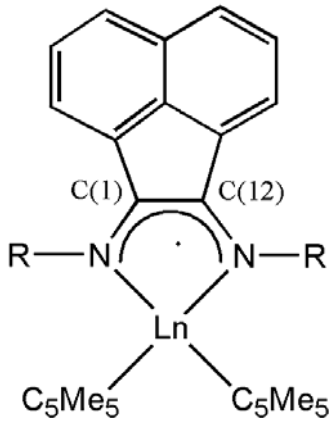

In each case, the single-electron transfer was evidenced by a reduction in the C(1)-C(12) bond distance and elongation of the corresponding C-N bond distances. The magnitude of these distances implies the presence of bond orders between one and two (Scheme 2.03). The new bond distances are in accord with the canonical form shown above with a delocalization of the transferred electron across the N-C-C-N fragment. Further evidence for the absence of a carbon-nitrogen double bond in complexes **19**-**27**

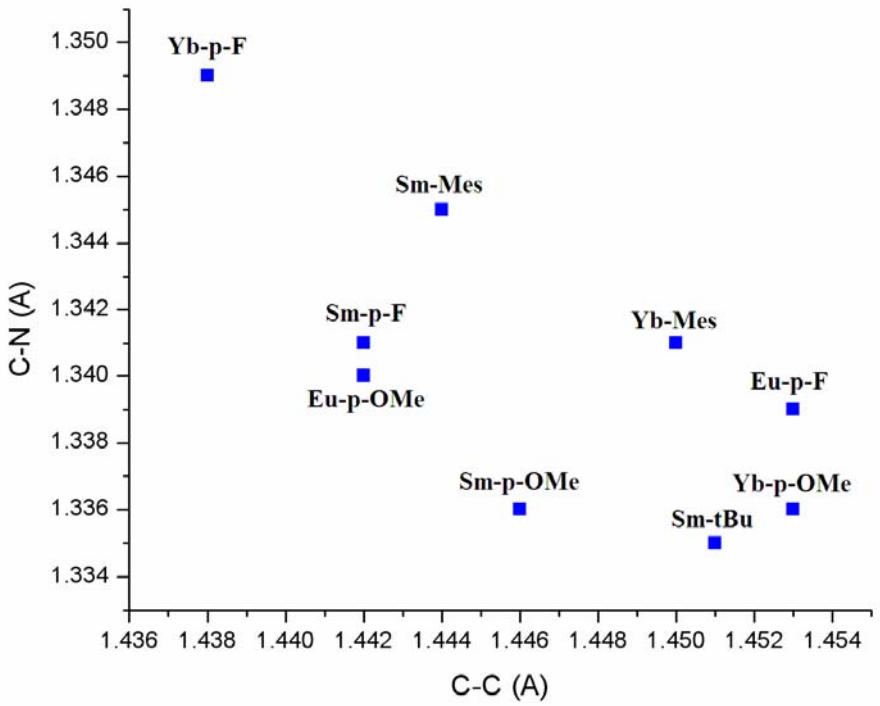

Scheme 2.03. Ln-BIAN Metrical Parameters [C-N (Å) vs C-C (Å)].

stemmed from the absence of a C=N stretching vibration in the 1630 cm^{-1} region of the IR spectra. Finally, magnetic moment measurements obtained via the Evans method further corroborated the conclusion that complexes **19**-**27** feature Ln(III) ions.

It is clear from the foregoing experimental evidence that the choice of BIAN substituent has a direct bearing on the product formed when a BIAN ligand is treated with $(C_5Me_5)_2Eu\text{-}OEt_2$. In contrast to the electron donating ^{t}Bu and Mes substituents, the presence of p-F or p-OMe substituents on the BIAN ligand induce a one-electron charge transfer from the Eu(II) center into the supporting BIAN ligand. Changes in the electron donating or electron withdrawing characteristics of the substituted BIAN ligand appears to have no influence on the spontaneous metal→ligand charge transfer processes from the standpoint of the Sm(II)→Sm(III) and Yb(II)→Yb(III) oxidation processes. Despite the

use of a wide range of electron donating and withdrawing BIAN substituents, the one electron charge transfer process is always observed, resulting in corresponding BIAN-supported lanthanide(III) complexes.

Section 2.3 Introduction

Recently, Evans *et al*. have introduced the concept of sterically induced reduction (SIR) chemistry. This method employs extreme steric crowding and represents a new way of generating reductive pathways. Accordingly, it was of interest to explore the consequences of using very bulky substituents on a BIAN ligand system. The present section addresses the outcomes of the reaction of the Dipp-BIAN ligand with $(C_5Me_5)_2Sm\text{-}OEt_2$ or $(C_5Me_5)_2Yb\text{-}OEt_2$. It will be shown that both reactions proceed by a SIR process. The overall result is that a two-electron reduction of the BIAN ligand takes place, and $(C_5Me_5)_2$ and a BIAN-supported Ln(III) complex are formed. Model studies showed that the 2,6-diisopropylphenyl (Dipp) ligand would be ideal for this purpose.

Synthesis and Characterization of $(C_5Me_5)(THF)Sm$(Dipp-BIAN) (28)

The complex $(C_5Me_5)(THF)Sm$(Dipp-BIAN) was synthesized by treatment of Dipp-BIAN with an equimolar quantity of $(C_5Me_5)_2Sm\text{-}OEt_2$ in a toluene/THF solution. A deep blue-green solid was isolated in 70% yield following workup of the reaction mixture. The crude solid was dissolved in a toluene/hexanes solution and the resulting solution was stored at -15°C for one week, affording a modest crop of dark blue-green crystals suitable for X-ray diffraction experiments. The molecular structure of **28** is illustrated in Figure 2.12. Details involving the data collection process, structure solution

and refinement are presented in Table 2.34 and a selection of pertinent metrical parameters appears in Tables 2.35 and 2.36.

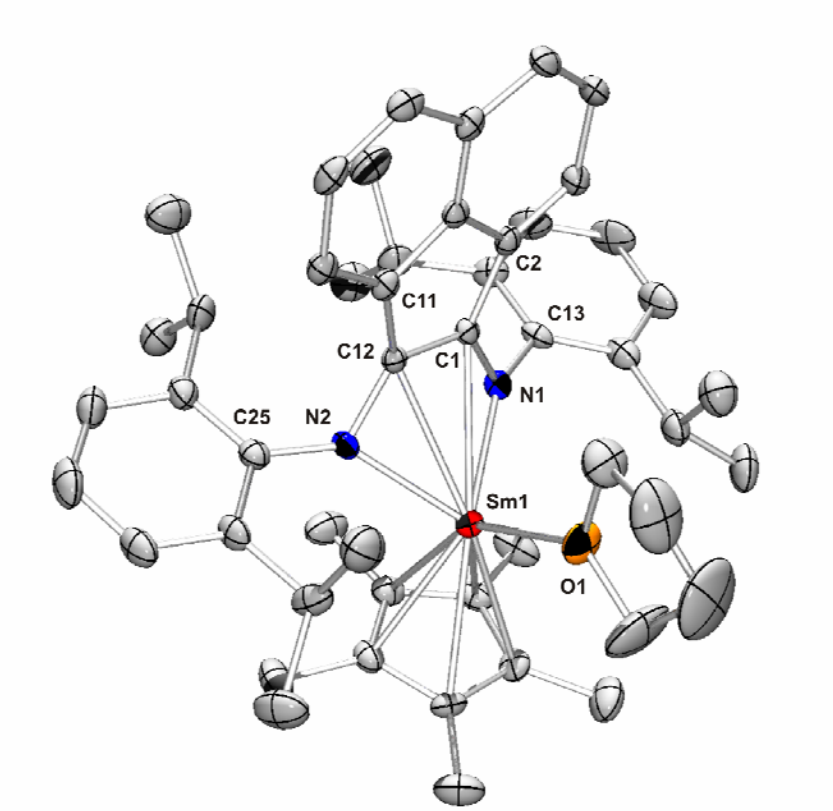

Figure 2.12. Molecular structure of 28 showing a partial numbering scheme. The thermal ellipsoids are shown at the 40% probability level. All hydrogen atoms have been omitted for clarity.

The single-crystal X-ray diffraction study revealed that **28** crystallizes in the monoclinic space group $P2_1/n$. One of the salient features of the molecular structure relates to the bond distances of C(1)-C(12) (1.414(6) Å) and the C-N bonds (1.396(5) Å) which imply bond orders of two and one, respectively. These values are markedly different than those of the free Dipp-BIAN ligand (1.530(2) Å and 1.280(1) Å, respectively)[30] and also different than the values discussed earlier for complexes **19**-**27**.

The average Sm-centroid distance of 2.422(4) Å for **28** is slightly shorter than that reported for $(C_5Me_5)_2Sm\text{-}OEt_2$[25].

It is likely that the reaction of $(C_5Me_5)_2Sm\text{-}OEt_2$ with Dipp-BIAN proceeds *via* initial displacement of diethyl ether to form $(C_5Me_5)_2Sm(II)$(Dipp-BIAN), followed by intramolecular electron transfer to generate $(C_5Me_5)_2Sm(III)$(Dipp-BIAN$^-$), which then eliminates $(C_5Me_5)^-$. In turn, $(C_5Me_5)^-$ transfers the second electron to the singly-reduced BIAN ligand. Support for this idea stems from the detection of the oxidized product, $(C_5Me_5)_2$, in the reaction mixture by ^{1}H NMR spectroscopy. This type of SIR process has been elegantly investigated by Evans and Davis[31].

Synthesis and Characterization of (C_5Me_5)(THF)Yb(Dipp-BIAN) (29)

The complex (C_5Me_5)(THF)Yb(Dipp-BIAN) was synthesized by treatment of $(C_5Me_5)_2Yb\text{-}OEt_2$ with an equimolar quantity of Dipp-BIAN in a toluene/THF solution. Following workup of the reaction mixture and solvent stripping, a deep blue-green solid was obtained in 72% yield. A small quantity of the crude solid was dissolved in THF and the resulting solution allowed to slowly evaporate over the course of 7 days. After this period, a small crop of large blue crystals was isolated. Structural authentication of the title compound, shown in Figure 2.13, was confirmed on the basis of a single-crystal X-ray diffraction study. Details of the data collection, structure solution and refinement are presented in Table 2.37 and a selection of pertinent metrical parameters is provided in Tables 2.38 and 2.39.

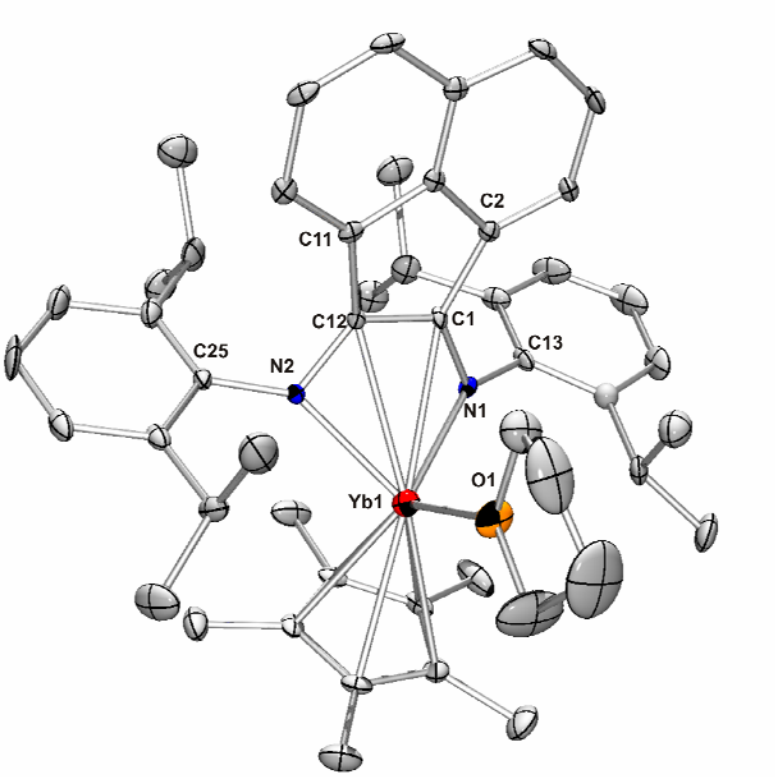

Figure 2.13. Molecular structure of 29 showing a partial numbering scheme. The thermal ellipsoids are shown at the 40% probability level. All hydrogen atoms have been omitted for clarity.

Compound **29** crystallizes in the monoclinic space group $P2_1/n$. The pertinent C(1)-C(12) and C-N bond distances of 1.420(6) Å and 1.391(5) Å are similar to those observed for **28**, implying bond orders of two and one, respectively. The average Yb-centroid distance of 2.402(4) Å is slightly shorter than that found in $(C_5Me_5)_2$Yb-OEt_2[29], yielding further evidence for a Yb(III) cation.

It is likely that the reaction of $(C_5Me_5)_2$Yb-OEt_2 with Dipp-BIAN proceeds in a similar fashion to that described for **28**. Thus, following initial displacement of diethyl ether and formation of $(C_5Me_5)_2$Yb(II)(Dipp-BIAN), the intramolecular electron transfer to generate $(C_5Me_5)_2$Sm(III)(Dipp-BIAN$^-$) proceeds. The expelled $(C_5Me_5)^-$ then transfers the second electron to the singly-reduced BIAN ligand. As in the case of **28**, $(C_5Me_5)_2$ is detected in the reaction mixture by ^{1}H NMR spectroscopy.

Section 2.3 Conclusions

Two BIAN-supported lanthanide complexes have been prepared featuring a two electron reduction of the BIAN ligand. Treatment of Dipp-BIAN with $(C_5Me_5)_2Sm\text{-}OEt_2$ or $(C_5Me_5)_2Yb\text{-}OEt_2$ resulted in the formation of products of the general form:

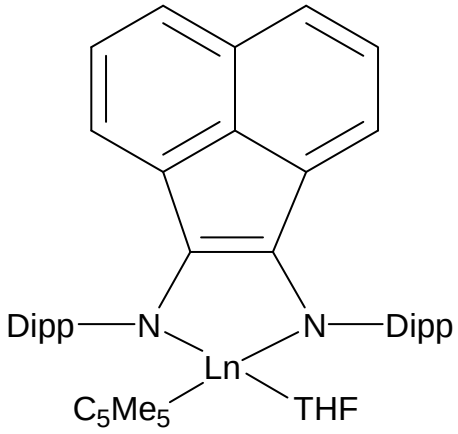

Both **28** and **29** feature shortened C-C bond lengths indicative of a bond order of two and average C-N bond distances that establish a bond order of one. Inspection of the IR spectra of both complexes reveals an absence of any peaks associated with C=N stretching frequencies, further supporting the proposed charge transfer process.

As indicated in Scheme 2.04, along with the complexes exhibiting the transfer of 0 or 1 electrons, **28** and **29** can be clearly differentiated on the basis of their metrical parameters.

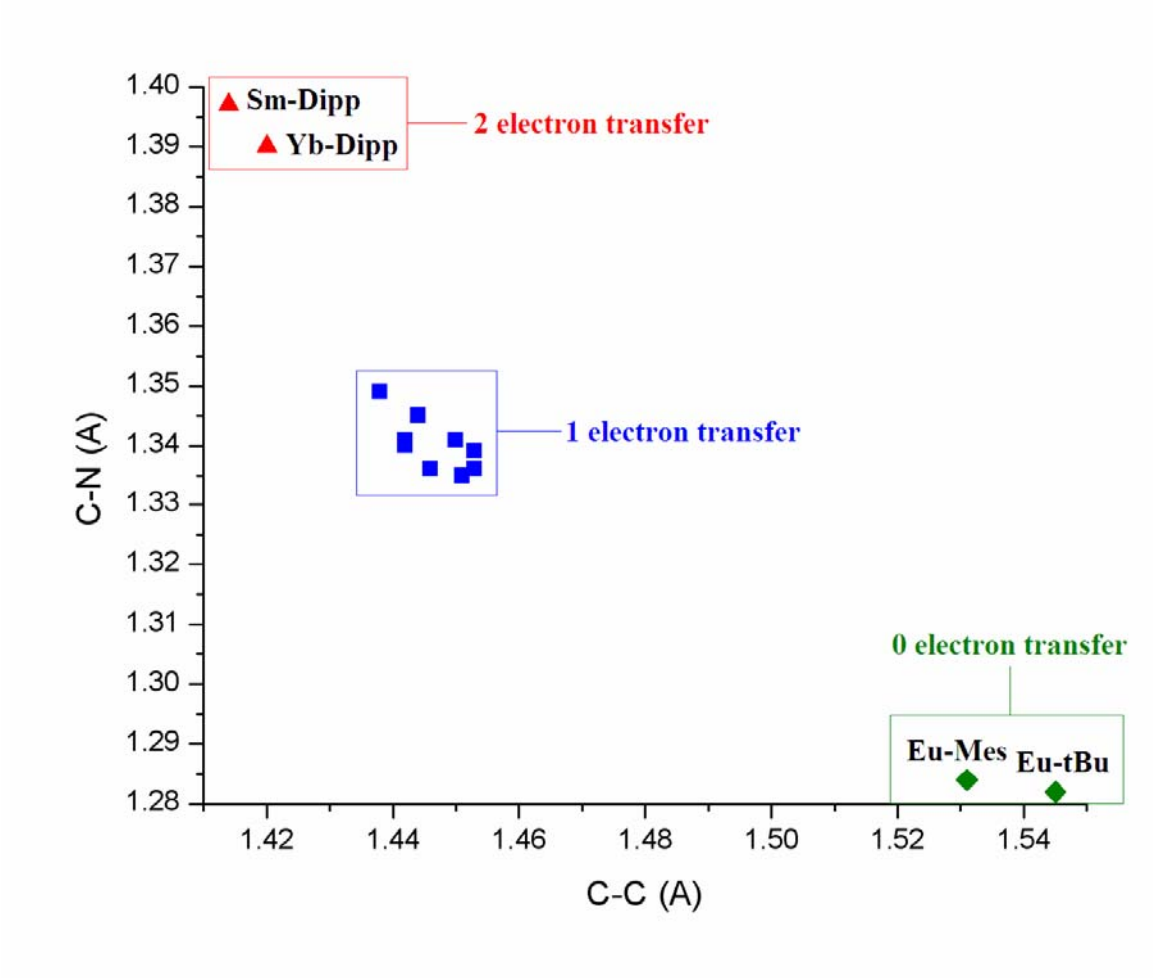

Scheme 2.04. Ln-BIAN Metrical Parameters [C-N (Å) vs C-C (Å)].

The most striking structural feature of both **28** and **29** is the displacement of a (C_5Me_5) substituent and its replacement by a THF molecule. It is evident that a sterically induced reduction (SIR) process has taken place due to the presence of very bulky diisopropylphenyl substituents, which prompt the elimination of a $(C_5Me_5)^-$ anion. This reactivity pattern is clearly absent in the cases of the less sterically-demanding BIAN ligands that were employed in the syntheses of complexes **17-27**. It is interesting to note that no reaction takes place when $(C_5Me_5)_2Eu\text{-}OEt_2$ is treated with the Dipp-BIAN

ligand. Despite changes of solvent, reaction stoichiometry or reaction conditions, the attempted reaction invariably resulted in the isolation of starting materials.

While not the topic of the present study, compounds **28** and **29** could represent a rational synthetic route to potentially highly active catalytic species. An alternate synthetic scheme was also employed using only toluene as the reaction solvent, in order to avoid the coordination of the THF molecule. Multiple attempts to grow crystalline materials were successful. However, in all instances the samples proved to be extremely unstable with respect to contact with air. This instability rendered structural characterization by single-crystal X-ray diffraction impossible. The pronounced instability of this product suggests that the solvent-free analogues of **28** and **29** are the products of the THF-free reaction. It is anticipated that the vacant lanthanide coordination site could potentially serve as a viable, highly active reaction site in catalytic pathways.

Experimental Section

General Procedures

The solvents toluene, THF, hexanes and pentane were distilled over sodium with sodium benzophenone ketyl indicator and degassed prior to use. An M-Braun argon-filled drybox was employed for the manipulation of all air-sensitive solid reagents. All reactions requiring anaerobic conditions were performed using standard Schlenk or drybox techniques. All glassware was dried at least 24 h in a 120°C oven prior to use.

The compounds Dipp-BIAN[30], Mes-BIAN[26], ^{t}Bu-BIAN[14], p-F-BIAN[11], p-OMe-BIAN[28], $(C_5Me_5)_2Eu\text{-}OEt_2$[25], $(C_5Me_5)_2Sm\text{-}OEt_2$[25] and $(C_5Me_5)_2Yb\text{-}OEt_2$[29] were synthesized according to literature procedures.

Physical Measurements

Low resolution CI mass spectra were collected on a Finnigan MAT TSQ-700 mass spectrometer. High resolution mass spectra were collected on a VG Analytical ZAB-VE sector instrument. All ^{1}H and ^{19}F NMR spectra were recorded at 295K on a Varian 300 MHz NMR spectrometer (^{1}H, 300 MHz; ^{19}F, 470 MHz). Deuterated solvents were obtained from Cambridge Isotopes and stored over molecular sieves prior to use. ^{1}H spectra are reported relative to tetramethylsilane and referenced to solvent. Melting points were obtained on a Fisher-Johns apparatus and are reported uncorrected.

X-Ray Crystallography

The X-ray data were collected on a Nonius Kappa CCD diffractometer equipped with an Oxford Cryostream liquid nitrogen cooling stream. All structure determinations and refinements were performed at the University of Texas at Austin. Samples were covered in mineral oil and mounted on a nylon thread loop prior to data collection. All data collection were performed at 153(2) K using graphite monochromated Mo Kα radiation (λ = 0.71073). A correction was applied for Lorentz-polarization in each case. All structures were solved by direct methods and refined by full-matrix least squares on F^2 using the Siemens SHELXL PLUS 5.0 (PC) software package. All hydrogen atoms were either placed in calculated positions (C-H = 0.96 Å) and refined using a riding model and a general isotropic thermal parameter or manually assigned. The total number of reflections, collection ranges and final R-values for each molecule are listed in the appropriate crystallographic data tables.

Preparation of $(C_5Me_5)_2Eu(^tBu\text{-}BIAN)$ (17)

Toluene (25 mL) was added to a flask charged with ^{t}Bu-BIAN (0.059 g, 0.20 mmol) and $(C_5Me_5)_2Eu\text{-}OEt_2$ (0.100 g, 0.20 mmol) and the resulting reddish-brown solution was stirred for 12 h. The solvent was then removed affording a dark red-brown solid. The resulting crude solid was dissolved in a 4:1 toluene/hexanes mixture, filtered and stored at -15°C for 7 days, affording a small crop of red-brown blocks. Yield 0.112 g (78.3%). MS (CI^+, CH_4): *m/z* 715; HRMS (CI^+, CH_4): calcd for $C_{50}H_{54}N_2Eu$ *m/z* 713.3486; found, 713.3486; Magnetic moment (Evans Method): 6.98 BM.

Preparation of $(C_5Me_5)_2Eu$(Mes-BIAN) (18)

Toluene (25 mL) was added to a flask charged with Mes-BIAN (0.083 g, 0.20 mmol) and $(C_5Me_5)_2Eu\text{-}OEt_2$ (0.100 g, 0.20 mmol) and the resulting reddish-brown solution was stirred for 12 h. The solvent was then removed affording a dark red-brown solid. Yield 0.137 g (82%). The crude product was dissolved in a 4:1 toluene/hexanes mixture, filtered and stored at -15°C for 7 days, affording a crop of dark red crystalline blocks. Magnetic moment (Evans Method): 6.72 BM IR (cm^{-1}): 2962b, 1636b, 1474s, 1437b, 1375s, 1261s, 1091s, 1028s, 800s.

Preparation of $(C_5Me_5)_2Eu$(p-F-BIAN) (19)

Toluene (25 mL) was added to a flask charged with p-F-BIAN (0.074 g, 0.20 mmol) and $(C_5Me_5)_2Eu\text{-}OEt_2$ (0.100 g, 0.20 mmol) and the resulting deep green solution was stirred

for 12 h. Solvent stripping resulted in the isolation of a dark green solid. Yield 0.122 g (77.2%). The crude solid was dissolved in a 4:1 toluene/hexanes solution, filtered and stored at -15°C for 7 days, affording a small crop of crystalline green rods.

^{1}H NMR ($CDCl_3$): δ -21.7 (s, C_5Me_5); MS (CI^+, CH_4): *m/z* 790.9; Magnetic moment (Evans Method): 2.80 BM; IR (cm^{-1}): 2963s, 1499s, 1261s, 1091s, 800s.

Preparation of $(C_5Me_5)_2$Eu(p-OMe-BIAN) (20)

Toluene (25 mL) was adder to a flask charged with p-OMe-BIAN (0.079 g, 0.20 mmol) and $(C_5Me_5)_2$Eu-OEt_2 (0.100 g, 0.20 mmol) and the resulting deep green solution was stirred for 12 h. Solvent stripping then afforded a dark green solid. Yield 0.141 g (86.6%). The crude solid was dissolved in a 4:1 toluene/hexanes solution, filtered and stored at -15°C for 7 days, affording a crop of green-brown crystalline blocks.

^{1}H NMR ($CDCl_3$): δ -21.3 (s, C_5Me_5); Magnetic moment (Evans Method): 3.55 BM.

Preparation of $(C_5Me_5)_2$Sm(^{t}Bu-BIAN) (21)

Toluene (25 mL) was added to a flask charged with ^{t}Bu-BIAN (0.059 g, 0.20 mmol) and $(C_5Me_5)_2$Sm-OEt_2 (0.100 g, 0.20 mmol) and the resulting deep green solution was stirred for 12 h. Subsequent removal of solvent afforded a dark green solid. Yield 0.115 g (80.6%). The crude solid was dissolved in a 4:1 toluene/hexanes solution, filtered and stored at -15°C for 6 days, affording a very small crop of green crystalline rods.

MS (CI^+, CH_4): *m/z* 712; Magnetic moment (Evans Method): 1.78 BM.

Preparation of $(C_5Me_5)_2Sm$(Mes-BIAN) (22)

Toluene (25 mL) was added to a flask charged with Mes-BIAN (0.083 g, 0.20 mmol) and $(C_5Me_5)_2Sm$-OEt_2 (0.100 g, 0.20 mmol) and the resulting deep green solution was stirred for 12 h. Solvent stripping resulted in the isolation of a dark green solid. Yield 0.152 g (90.8%). The crude solid was dissolved in a 4:1 toluene/hexanes solution, filtered and stored at -15°C for 5 days, affording a moderate crop of green crystalline blocks.

MS (CI^+, CH_4): *m/z* 841; HRMS (CI^+, CH_4): calcd for $C_{50}H_{58}N_2Sm$ *m/z* 830.3714; found, 830.3720; Magnetic moment (Evans Method): 1.82 BM; IR (cm^{-1}): 2963s, 1261s, 1090s, 800s.

Preparation of $(C_5Me_5)_2Sm$(p-F-BIAN) (23)

Toluene (25 mL) was added to a flask charged with p-F-BIAN (0.074 g, 0.20 mmol) and $(C_5Me_5)_2Sm$-OEt_2 (0.100 g, 0.20 mmol) and the resulting deep green solution was stirred for 12 h. Stripping of the solvent afforded a dark green solid. Yield 0.132 g (83.7%). The crude solid was dissolved in pentane and transferred to an NMR tube. The solution was slowly evaporated over the course of 10 days to afford a small crop of green crystalline needles.

Magnetic moment (Evans Method): 1.74 BM; IR (cm^{-1}): 2963s, 1261s, 1093s, 1020s, 800s.

Preparation of $(C_5Me_5)_2Sm$(p-OMe-BIAN) (24)

Toluene (25 mL) was added to a flask charged with p-OMe-BIAN (0.079 g, 0.20 mmol) and $(C_5Me_5)_2Sm$-OEt_2 (0.100 g, 0.20 mmol) and the resulting deep green solution was stirred for 12 h. The solvent was stripped subsequently resulting in a dark green solid. Yield 0.151 g (92.9%). The crude solid was dissolved in a 4:1 toluene/hexanes solution, filtered and stored at -15°C for 7 days, affording a crop of green crystals.

Magnetic moment (Evans Method): 1.80 BM.

Preparation of $(C_5Me_5)_2Yb$(Mes-BIAN) (25)

Toluene (25 mL) was added to a flask charged with Mes-BIAN (0.079 g, 0.19 mmol) and $(C_5Me_5)_2Yb$-OEt_2 (0.100 g, 0.19 mmol) and the resulting deep green solution stirred for 12 h. The reaction solvent was removed affording a dark green solid. Yield 0.154 g (94.3%). The crude solid was dissolved in a 4:1 toluene/hexanes solution, filtered and stored at -15°C for 4 days, affording a small crop of green crystals.

MS (CI^+, CH_4): *m/z* 859 $[M+H]^+$; Magnetic moment (Evans method): 4.22 BM; IR (cm^{-1}): 2963s, 1261s, 1093s, 1020s, 799s.

Preparation of $(C_5Me_5)_2Yb$(p-F-BIAN) (26)

Toluene (25 mL) was added to a flask charged with p-F-BIAN (0.070 g, 0.19 mmol) and $(C_5Me_5)_2Yb$-OEt_2 (0.100 g, 0.19 mmol) and the resulting deep green solution was stirred for 12 h. The solvent was removed subsequently affording a dark green solid. Yield

0.130 g (84.3%). The crude solid was dissolved in a 4:1 toluene/hexanes mixture, filtered and stored at -15°C for 7 days, affording a crop of green needles.

MS (CI^+, CH_4): *m/z* 812; HRMS (CI^+, CH_4): calcd for $C_{44}H_{44}N_2F_2Yb$ *m/z* 808.2823; found, 808.2820; EA: calcd %C: 59.68, %H: 4.97, %N: 3.16; found, %C: 61.51, %H: 5.38, %N 2.59; Magnetic moment (Evans method): 3.71 BM; IR (cm^{-1}): 2915t, 1498s, 1442s, 1425s.

Preparation of $(C_5Me_5)_2Yb$(p-OMe-BIAN) (27)

Toluene (25 mL) was added to a flask charged with p-OMe-BIAN (0.076 g, 0.19 mmol) and $(C_5Me_5)_2Yb$-OEt_2 (0.100 g, 0.19 mmol) and the resulting deep green solution was stirred for 12 h. Solvent stripping resulted in the isolation of a dark green solid. Yield 0.140 g (88.2%). The green solid was dissolved in a 4:1 toluene/hexanes solution, filtered and stored at -15°C for 5 days, affording a crop of large green blocks.

Magnetic moment (Evans method): 3.91 BM.

Preparation of (C_5Me_5)(THF)Sm(Dipp-BIAN) (28)

Dipp-BIAN (0.101 g, 0.20 mmol) and $(C_5Me_5)_2Sm$-OEt_2 (0.100 g, 0.20 mmol) were dissolved in a 9:1 toluene/THF mixture (20 mL) and stirred together as a deep blue-green solution for 12 h. The solvent was then removed affording a dark blue powder. Yield 0.121 g (70.1%). Crystals were grown from a saturated 4:1 toluene/hexanes solution stored at -15°C for 7 days.

Preparation of (C_5Me_5)(THF)Yb(Dipp-BIAN) (29)

Dipp-BIAN (0.097 g, 0.19 mmol) and $(C_5Me_5)_2Yb\text{-}OEt_2$ (0.100 g, 0.19 mmol) were dissolved in a 9:1 toluene/THF mixture (20 mL) and stirred together as a deep blue-green solution for 12 h. Solvent stripping afforded a dark blue powder. Yield 0.127 g (72.3%). A small portion of the crude solid was dissolved in THF and transferred to an NMR tube. The solution was allowed to slowly evaporate over the course of 7 days, affording large blue crystalline blocks of **29**.

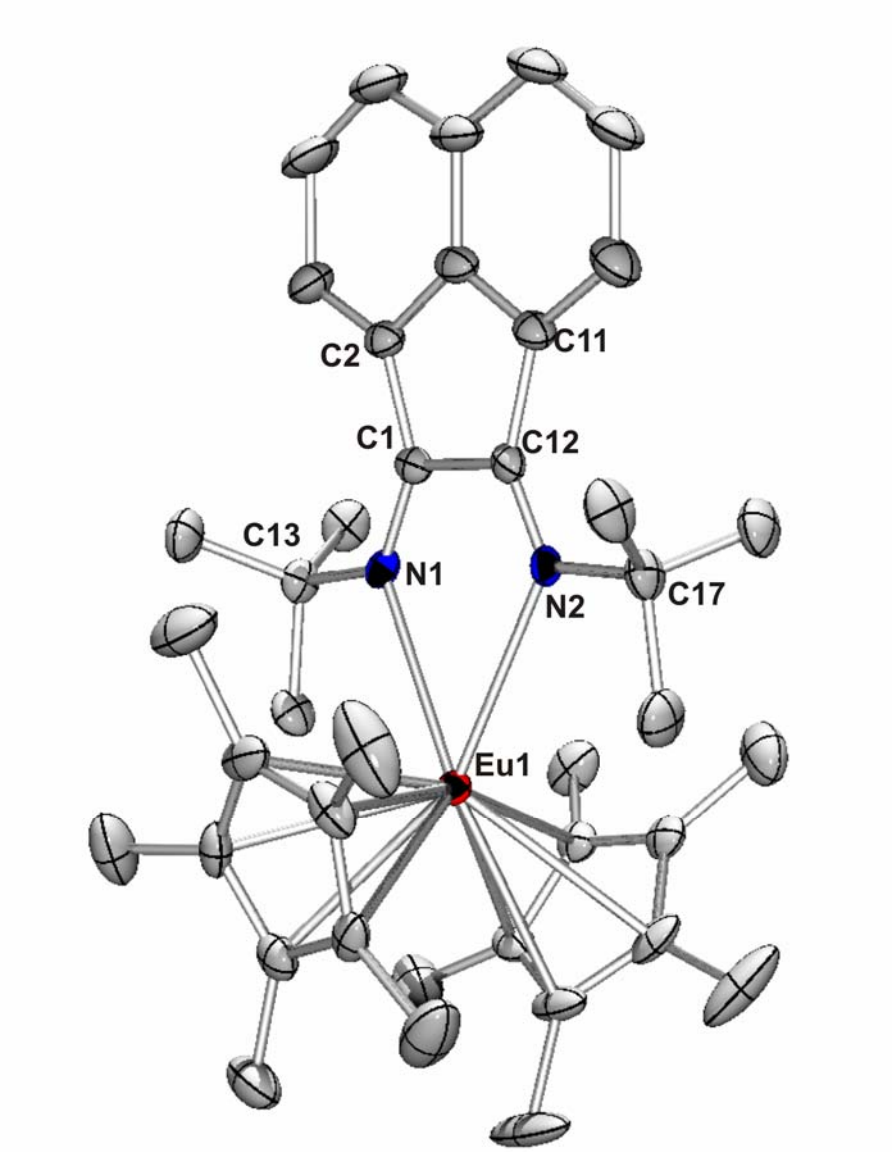

Figure 2.01. Molecular structure of 17 showing a partial numbering scheme. The thermal ellipsoids are shown at the 40% probability level. All hydrogen atoms have been omitted for clarity.

Table 2.01. Crystal data and structure refinement for 17.

Identification code	kvjm007	
Empirical formula	C40 H54 Eu N2	
Formula weight	714.81	
Temperature	153(2) K	
Wavelength	0.71069 Å	
Crystal system	Monoclinic	
Space group	P21/n	
Unit cell dimensions	a = 10.250(5) Å	α= 90.000(5)°.
	b = 18.436(5) Å	β= 94.739(5)°.
	c = 23.258(5) Å	γ = 90.000(5)°.
Volume	4380(3) $Å^3$	
Z	4	
Density (calculated)	1.084 Mg/m^3	
Absorption coefficient	1.455 mm^{-1}	
F(000)	1484	
Crystal size	0.14 x 0.12 x 0.10 mm^3	
Theta range for data collection	1.76 to 27.49°.	
Index ranges	-13<=h<=13, -22<=k<=23, -30<=l<=30	
Reflections collected	16943	
Independent reflections	10026 [R(int) = 0.0357]	
Completeness to theta = 27.49°	99.7 %	
Absorption correction	None	
Refinement method	Full-matrix least-squares on F^2	
Data / restraints / parameters	10026 / 0 / 402	
Goodness-of-fit on F^2	0.946	
Final R indices [I>2sigma(I)]	R1 = 0.0416, wR2 = 0.1103	
R indices (all data)	R1 = 0.0628, wR2 = 0.1194	
Largest diff. peak and hole	2.285 and -0.983 $e.Å^{-3}$	

Table 2.02. Selected Bond Lengths (Å) for $(C_5Me_5)_2Eu(^tBu\text{-}BIAN)$ (17)

C1-C2	1.491(5)
C1-C12	1.545(5)
C1-N1	1.278(5)
C11-C12	1.478(5)
C12-N2	1.287(5)
C13-N1	1.500(5)
C17-N2	1.502(5)
N1-Eu1	2.768(3)
N2-Eu1	2.797(3)
Eu1-cent1	2.668(5)
Eu1-cent2	2.675(5)

Table 2.03. Selected Bond Angles (°) for $(C_5Me_5)_2Eu(^tBu\text{-}BIAN)$ (17)

C1-C12-C11	106.7(3)
C1-C12-N2	117.8(3)
C1-N1-C13	123.1(3)
C1-N1-Eu1	121.6(2)
C2-C1-C12	105.6(3)
C12-C1-N1	119.3(3)
C12-N2-C17	123.5(3)
C12-N2-Eu1	120.9(2)
N1-Eu1-N2	59.74(9)
N1-Eu1-cent1	108.22(2)
N1-Eu1-cent2	114.55(2)
N2-Eu1-cent1	106.27(2)
N2-Eu1-cent2	115.60(2)

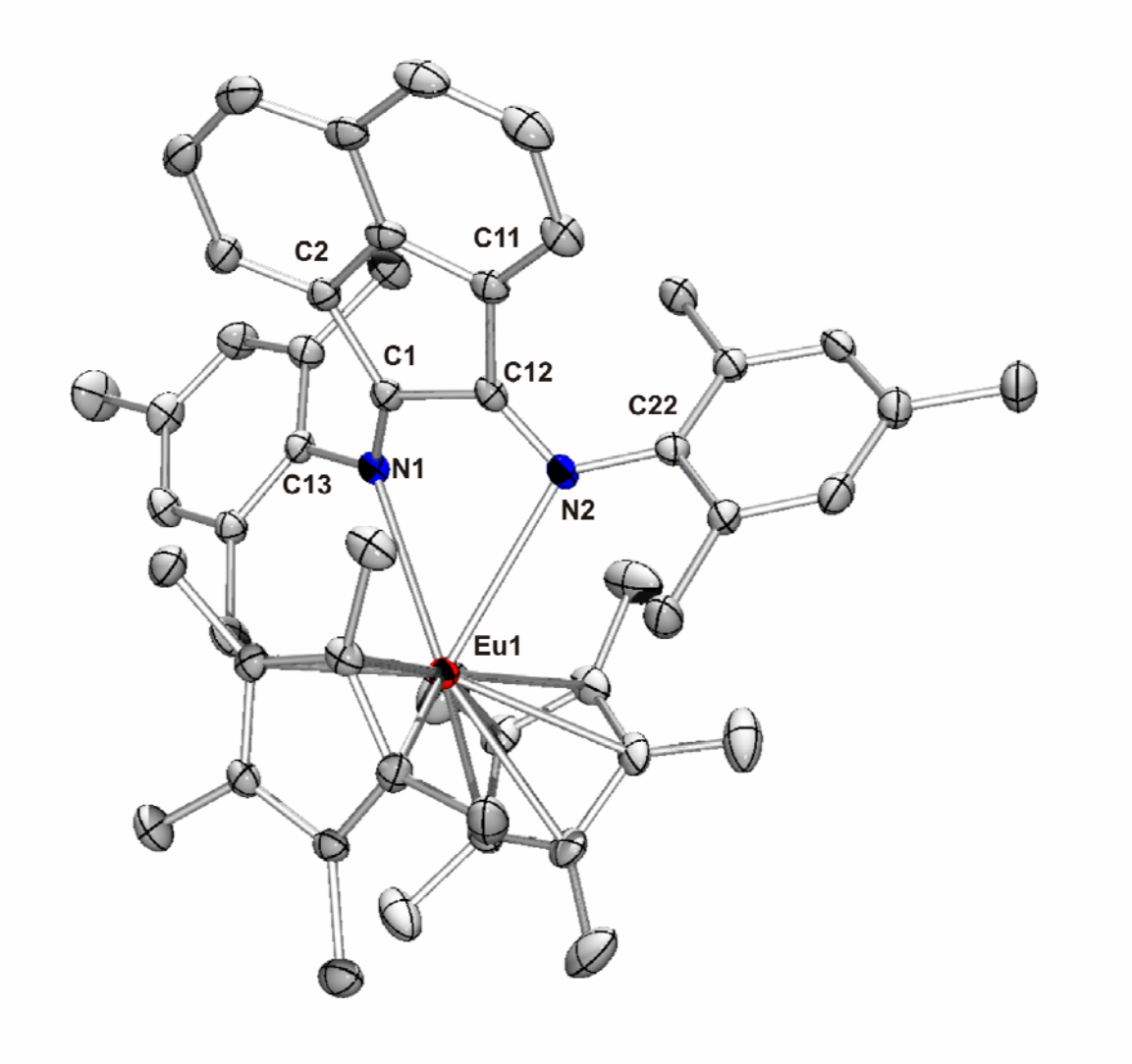

Figure 2.02. Molecular structure of 18 showing a partial numbering scheme. The thermal ellipsoids are shown at the 40% probability level. All hydrogen atoms have been omitted for clarity.

Table 2.04. Crystal data and structure refinement for 18.

Identification code	kvgr052	
Empirical formula	C57 H66 Eu N2	
Formula weight	931.08	
Temperature	153(2) K	
Wavelength	0.71069 Å	
Crystal system	Monoclinic	
Space group	P21/c	
Unit cell dimensions	a = 18.004(5) Å	α= 90.000(5)°.
	b = 15.727(5) Å	β= 112.209(5)°.
	c = 17.710(5) Å	γ = 90.000(5)°.
Volume	4643(2) $Å^3$	
Z	4	
Density (calculated)	1.332 Mg/m^3	
Absorption coefficient	1.390 mm^{-1}	
F(000)	1940	
Crystal size	0.18 x 0.11 x 0.05 mm^3	
Theta range for data collection	1.78 to 27.51°.	
Index ranges	-23<=h<=23, -18<=k<=20, -22<=l<=23	
Reflections collected	17590	
Independent reflections	10579 [R(int) = 0.0330]	
Completeness to theta = 27.51°	99.2 %	
Absorption correction	None	
Refinement method	Full-matrix least-squares on F^2	
Data / restraints / parameters	10579 / 0 / 559	
Goodness-of-fit on F^2	1.354	
Final R indices [I>2sigma(I)]	R1 = 0.0423, wR2 = 0.0903	
R indices (all data)	R1 = 0.0697, wR2 = 0.1197	
Extinction coefficient	0.0080(2)	
Largest diff. peak and hole	2.914 and -0.904 $e.Å^{-3}$	

Table 2.05. Selected Bond Lengths (Å) for $(C_5Me_5)_2Eu$(Mes-BIAN) (18)

C1-C2	1.481(5)
C1-C12	1.531(5)
C1-N1	1.280(5)
C11-C12	1.480(5)
C12-N2	1.289(5)
C13-N1	1.440(5)
C22-N2	1.437(5)
N1-Eu1	2.825(3)
N2-Eu1	2.829(3)
Eu1-cent1	2.554(3)
Eu1-cent2	2.681(3)

Table 2.06. Selected Bond Angles (°) for $(C_5Me_5)_2Eu$(Mes-BIAN) (18)

C1-C12-C11	106.2(3)
C1-C12-N2	120.3(3)
C1-N1-C13	117.8(3)
C1-N1-Eu1	104.5(2)
C2-C1-C12	107.0(3)
C12-C1-N1	120.9(3)
C12-N2-C17	119.4(3)
C12-N2-Eu1	103.0(2)
N1-Eu1-N2	60.33(9)
N1-Eu1-cent1	109.47(3)
N1-Eu1-cent2	110.60(3)
N2-Eu1-cent1	102.37(3)
N2-Eu1-cent2	114.45(3)

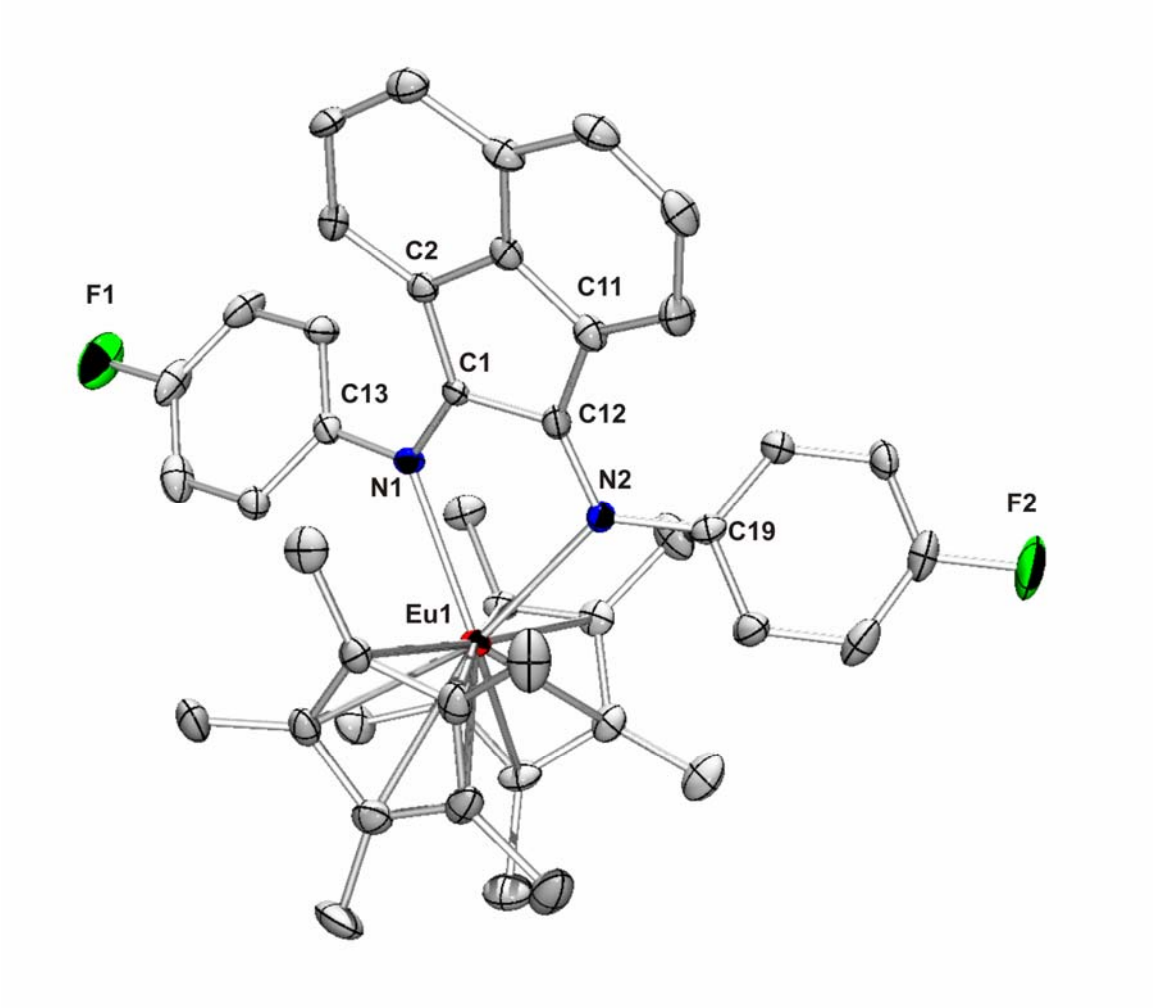

Figure 2.03. Molecular structure of 19 showing a partial numbering scheme. The thermal ellipsoids are shown at the 40% probability level. All hydrogen atoms have been omitted for clarity.

Table 2.07. Crystal data and structure refinement for 19.

Identification code	kvkv003c	
Empirical formula	C44 H44 Eu F2 N2	
Formula weight	790.77	
Temperature	153(2) K	
Wavelength	0.71073 Å	
Crystal system	Monoclinic	
Space group	Cc	
Unit cell dimensions	a = 21.972(5) Å	α= 90.000(5)°.
	b = 10.238(5) Å	β= 119.046(5)°.
	c = 18.282(5) Å	γ = 90.000(5)°.
Volume	3595(2) $Å^3$	
Z	4	
Density (calculated)	1.461 Mg/m^3	
Absorption coefficient	1.789 mm^{-1}	
F(000)	1612	
Crystal size	0.10 x 0.09 x 0.06 mm^3	
Theta range for data collection	3.43 to 27.52°.	
Index ranges	-28<=h<=27, -13<=k<=12, -23<=l<=23	
Reflections collected	11969	
Independent reflections	7709 [R(int) = 0.0297]	
Completeness to theta = 27.52°	99.7 %	
Absorption correction	None	
Refinement method	Full-matrix least-squares on F^2	
Data / restraints / parameters	7709 / 2 / 452	
Goodness-of-fit on F^2	1.052	
Final R indices [I>2sigma(I)]	R1 = 0.0370, wR2 = 0.0807	
R indices (all data)	R1 = 0.0472, wR2 = 0.0856	
Absolute structure parameter	0.00	
Largest diff. peak and hole	2.702 and -1.160 $e.Å^{-3}$	

Table 2.08. Selected Bond Lengths (Å) for $(C_5Me_5)_2Eu$(p-F-BIAN) (19)

C1-C2	1.483(7)
C1-C12	1.453(7)
C1-N1	1.336(7)
C11-C12	1.472(7)
C12-N2	1.341(7)
C13-N2	1.403(7)
C19-N1	1.407(7)
N1-Eu1	2.434(4)
N2-Eu1	2.451(5)
Eu1-cent1	2.437(7)
Eu1-cent2	2.462(7)

Table 2.09. Selected Bond Angles (°) for $(C_5Me_5)_2Eu$(p-F-BIAN) (19)

C1-C12-C11	107.9(4)
C1-C12-N2	119.3(5)
C1-N1-C19	118.5(4)
C1-N1-Eu1	111.6(3)
C2-C1-C12	107.9(4)
C12-C1-N1	120.8(5)
C12-N2-C13	121.2(4)
C12-N2-Eu1	112.7(3)
C13-N2-Eu1	125.7(3)
C19-N1-Eu1	129.9(3)
N1-Eu1-N2	69.75(15)
N1-Eu1-cent1	106.99(3)
N1-Eu1-cent2	106.36(3)
N2-Eu1-cent1	109.15(3)
N2-Eu1-cent2	106.86(3)

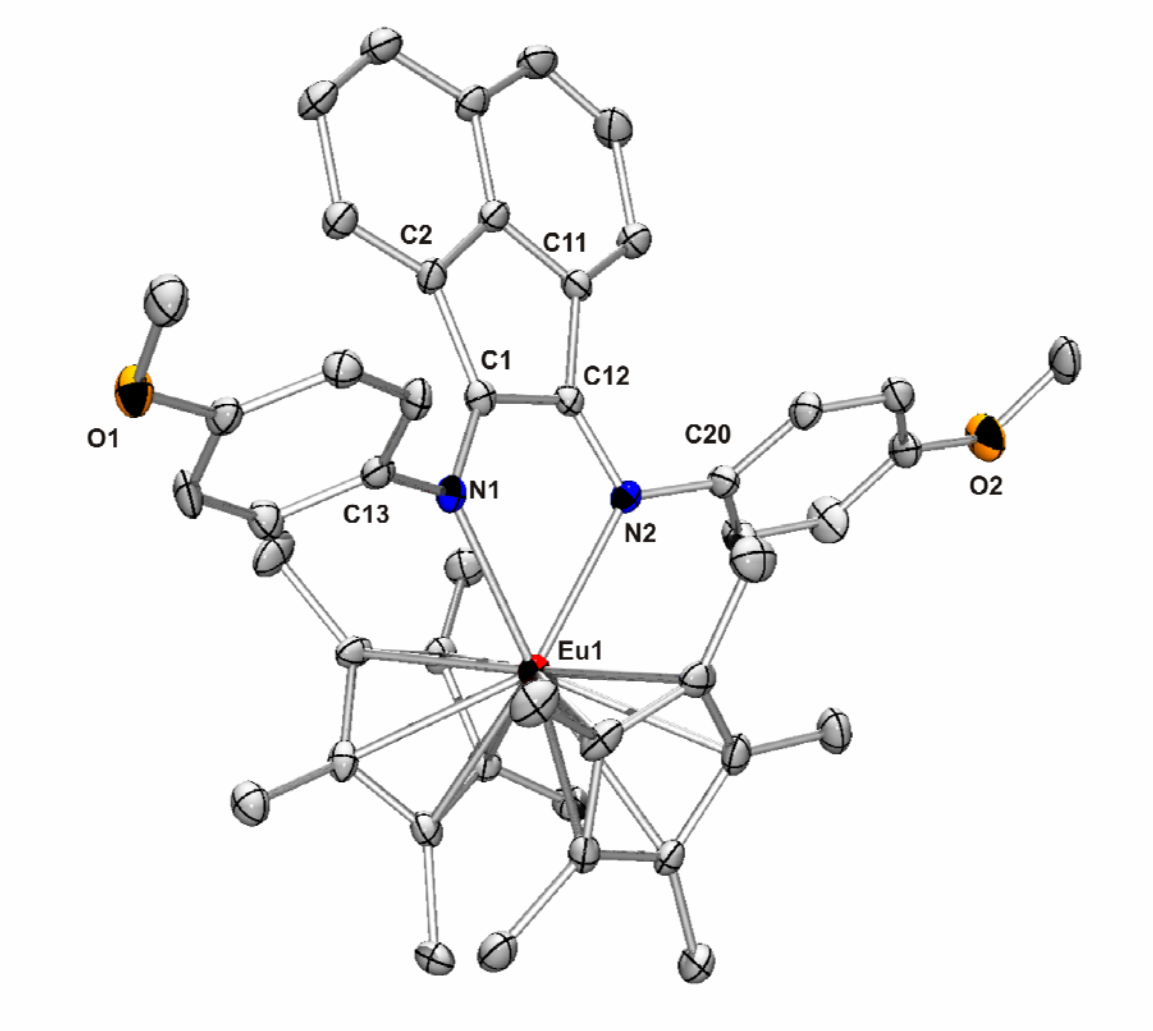

Figure 2.04. Molecular structure of 20 showing a partial numbering scheme. The thermal ellipsoids are shown at the 40% probability level. All hydrogen atoms have been omitted for clarity.

Table 2.10. Crystal data and structure refinement for 20.

Identification code	kvkv009e	
Empirical formula	C46 H50 Eu N2 O2	
Formula weight	814.88	
Temperature	153(2) K	
Wavelength	0.71073 Å	
Crystal system	Triclinic	
Space group	P-1	
Unit cell dimensions	a = 9.5567(19) Å	α= 101.15(3)°.
	b = 10.286(2) Å	β= 94.09(3)°.
	c = 20.283(4) Å	γ = 104.01(3)°.
Volume	1883.4(7) $Å^3$	
Z	2	
Density (calculated)	1.437 Mg/m^3	
Absorption coefficient	1.706 mm^{-1}	
F(000)	838	
Crystal size	0.20 x 0.20 x 0.10 mm^3	
Theta range for data collection	1.03 to 27.46°.	
Index ranges	-12<=h<=12, -13<=k<=12, -26<=l<=26	
Reflections collected	12045	
Independent reflections	8520 [R(int) = 0.0398]	
Completeness to theta = 27.46°	98.8 %	
Absorption correction	None	
Refinement method	Full-matrix least-squares on F^2	
Data / restraints / parameters	8520 / 0 / 472	
Goodness-of-fit on F^2	1.052	
Final R indices [I>2sigma(I)]	R1 = 0.0476, wR2 = 0.0989	
R indices (all data)	R1 = 0.0872, wR2 = 0.1361	
Largest diff. peak and hole	2.192 and -1.744 $e.Å^{-3}$	

Table 2.11. Selected Bond Lengths (Å) for $(C_5Me_5)_2Eu$(p-OMe-BIAN) (20)

C1-C2	1.486(7)
C1-C12	1.442(8)
C1-N1	1.345(6)
C11-C12	1.494(7)
C12-N2	1.334(7)
C13-N1	1.423(7)
C20-N2	1.433(7)
N1-Eu1	2.456(4)
N2-Eu1	2.454(4)
Eu1-cent1	2.446(4)
Eu1-cent2	2.437(4)

Table 2.12. Selected Bond Angles (°) for $(C_5Me_5)_2Eu$(p-OMe-BIAN) (20)

C1-C12-C11	107.5(4)
C1-C12-N2	130.4(5)
C1-N1-C13	116.1(4)
C1-N1-Eu1	111.2(4)
C2-C1-C12	108.1(4)
C12-C1-N1	121.5(5)
C12-N2-C20	115.3(4)
C12-N2-Eu1	111.0(3)
C13-N1-Eu1	132.7(3)
C20-N2-Eu1	133.7(3)
N1-Eu1-N2	70.84(15)
N1-Eu1-cent1	107.64(3)
N1-Eu1-cent2	109.36(3)
N2-Eu1-cent1	107.38(3)
N2-Eu1-cent2	109.43(3)

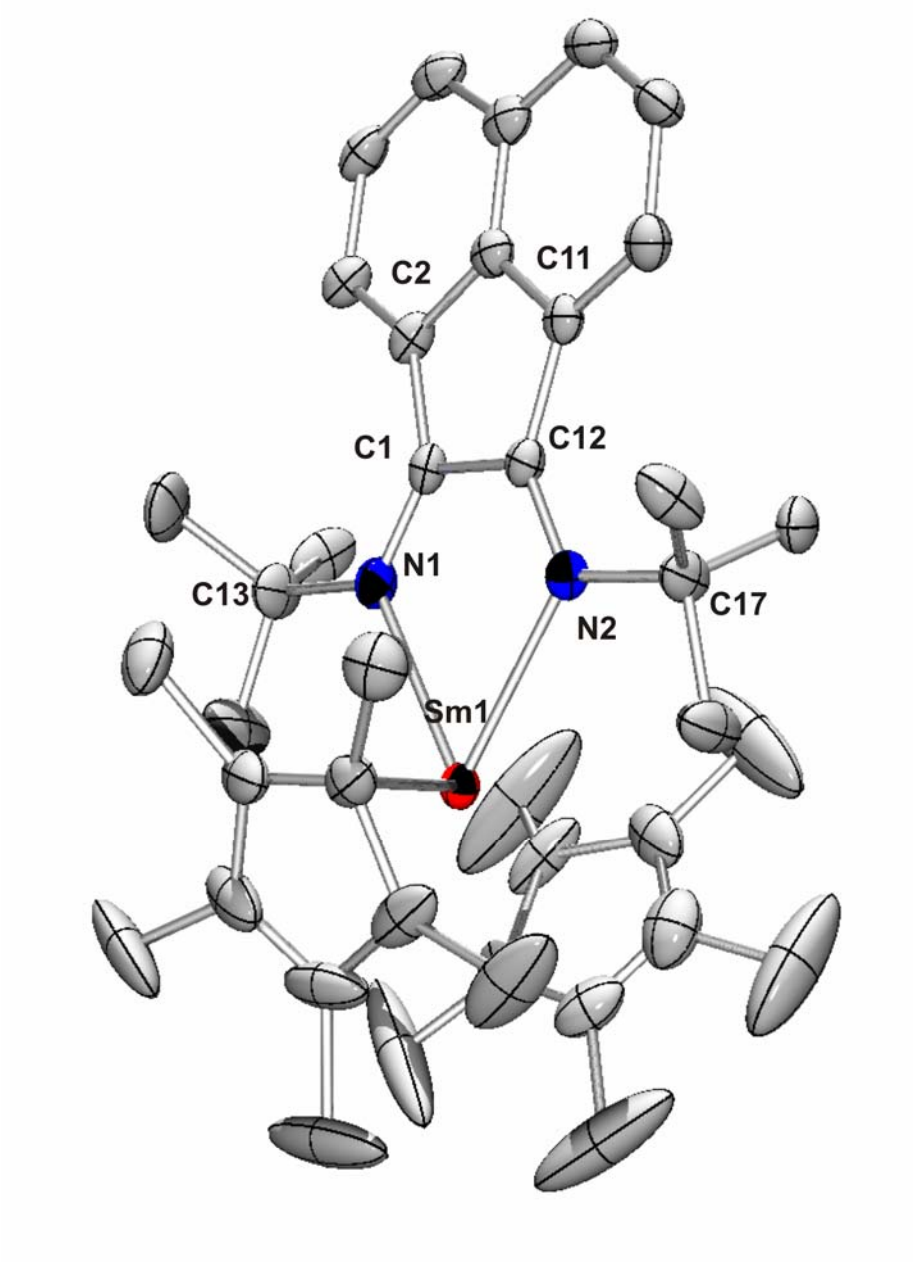

Figure 2.05. Molecular structure of 21 showing a partial numbering scheme. The thermal ellipsoids are shown at the 40% probability level. All hydrogen atoms have been omitted for clarity.

Table 2.13. Crystal data and structure refinement for 21.

Identification code	kvkv006a	
Empirical formula	C40 H54 N2 Sm	
Formula weight	713.20	
Temperature	153(2) K	
Wavelength	0.71073 Å	
Crystal system	Monoclinic	
Space group	P21/c	
Unit cell dimensions	a = 18.640(4) Å	α= 90°.
	b = 10.563(2) Å	β= 97.49(3)°.
	c = 17.493(4) Å	γ = 90°.
Volume	3414.8(12) $Å^3$	
Z	4	
Density (calculated)	1.387 Mg/m^3	
Absorption coefficient	1.749 mm^{-1}	
F(000)	1480	
Crystal size	0.25 x 0.10 x 0.10 mm^3	
Theta range for data collection	1.10 to 27.46°.	
Index ranges	-24<=h<=24, -13<=k<=12, -22<=l<=22	
Reflections collected	12820	
Independent reflections	7785 [R(int) = 0.0517]	
Completeness to theta = 27.46°	99.5 %	
Absorption correction	None	
Max. and min. transmission	0.8445 and 0.6689	
Refinement method	Full-matrix least-squares on F^2	
Data / restraints / parameters	7785 / 60 / 405	
Goodness-of-fit on F^2	1.020	
Final R indices [I>2sigma(I)]	R1 = 0.0574, wR2 = 0.1419	
R indices (all data)	R1 = 0.1018, wR2 = 0.1666	
Extinction coefficient	0.0006(3)	
Largest diff. peak and hole	1.831 and -1.505 $e.Å^{-3}$	

Table 2.14. Selected Bond Lengths (Å) for $(C_5Me_5)_2Sm(^tBu\text{-}BIAN)$ (21)

C1-C2	1.491(9)
C1-C12	1.451(8)
C1-N1	1.335(8)
C11-C12	1.497(8)
C12-N2	1.335(7)
C13-N2	1.494(7)
C17-N1	1.511(8)
N1-Sm1	2.520(5)
N2-Sm1	2.507(5)
Sm1-cent1	2.573(5)
Sm1-cent2	2.532(5)

Table 2.15. Selected Bond Angles (°) for $(C_5Me_5)_2Sm(^tBu\text{-}BIAN)$ (21)

C1-C12-C11	107.4(5)
C1-C12-N2	119.1(5)
C1-N1-C17	121.2(5)
C1-N1-Sm1	117.2(4)
C2-C1-C12	107.5(5)
C12-C1-N1	119.3(5)
C12-N2-C13	120.5(5)
C12-N2-Sm1	117.8(4)
C13-N2-Sm1	121.5(3)
C17-N1-Sm1	121.6(4)
N1-Sm1-N2	66.47(16)
N1-Sm1-cent1	113.74(3)
N1-Sm1-cent2	110.83(3)
N2-Sm1-cent1	112.83(3)
N2-Sm1-cent2	108.91(3)

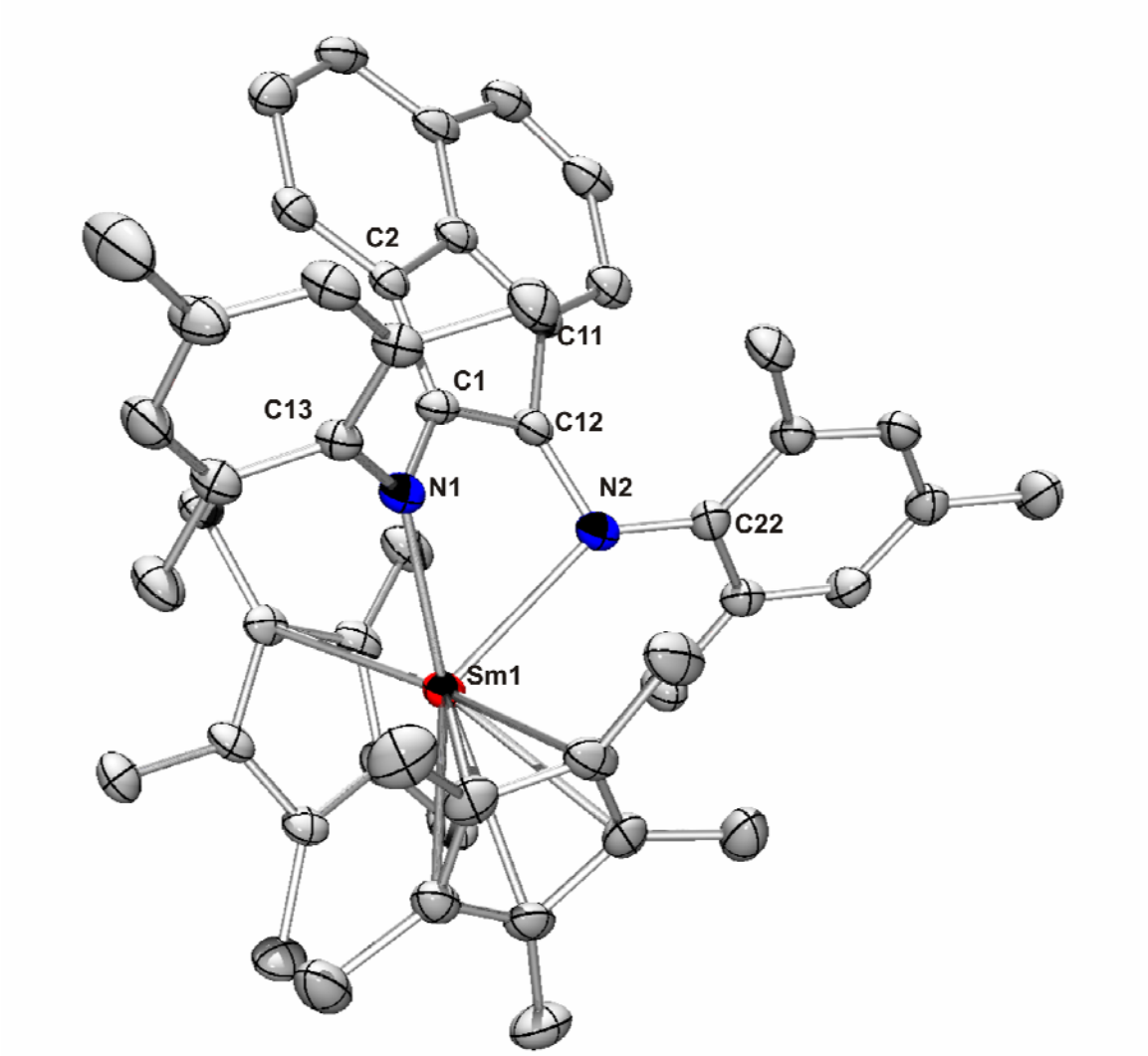

Figure 2.06. Molecular structure of 22 showing a partial numbering scheme. The thermal ellipsoids are shown at the 40% probability level. All hydrogen atoms have been omitted for clarity.

Table 2.16. Crystal data and structure refinement for 22.

Identification code	kvkv002	
Empirical formula	C50 H58 N2 Sm	
Formula weight	837.33	
Temperature	153(2) K	
Wavelength	0.71073 Å	
Crystal system	Triclinic	
Space group	P-1	
Unit cell dimensions	a = 12.319(5) Å	α= 70.589(5)°.
	b = 14.294(5) Å	β= 82.726(5)°.
	c = 16.910(5) Å	γ = 69.084(5)°.
Volume	2623.2(16) $Å^3$	
Z	2	
Density (calculated)	1.060 Mg/m^3	
Absorption coefficient	1.147 mm^{-1}	
F(000)	868	
Crystal size	0.09 x 0.09 x 0.08 mm^3	
Theta range for data collection	2.03 to 27.51°.	
Index ranges	-15<=h<=16, -18<=k<=18, -21<=l<=21	
Reflections collected	17880	
Independent reflections	11973 [R(int) = 0.0373]	
Completeness to theta = 27.51°	99.3 %	
Absorption correction	None	
Refinement method	Full-matrix least-squares on F^2	
Data / restraints / parameters	11973 / 0 / 494	
Goodness-of-fit on F^2	0.961	
Final R indices [I>2sigma(I)]	R1 = 0.0491, wR2 = 0.1107	
R indices (all data)	R1 = 0.0857, wR2 = 0.1216	
Largest diff. peak and hole	1.853 and -0.960 $e.Å^{-3}$	

Table 2.17. Selected Bond Lengths (Å) for $(C_5Me_5)_2Sm$(Mes-BIAN) (22)

C1-C2	1.484(6)
C1-C12	1.444(6)
C1-N1	1.352(5)
C11-C12	1.478(5)
C12-N2	1.338(5)
C13-N2	1.430(5)
C22-N1	1.425(5)
N1-Sm1	2.530(3)
N2-Sm1	2.501(3)
Sm1-cent1	2.536(3)
Sm1-cent2	2.443(3)

Table 2.18. Selected Bond Angles (°) for $(C_5Me_5)_2Sm$(Mes-BIAN) (22)

C1-C12-C11	107.9(3)
C1-C12-N2	123.1(3)
C1-N1-C22	117.4(3)
C1-N1-Sm1	99.6(2)
C2-C1-C12	107.4(3)
C12-C1-N1	123.5(3)
C12-N2-C13	114.3(3)
C12-N2-Sm1	101.1(3)
C13-N2-Sm1	143.6(2)
C22-N1-Sm1	142.0(2)
N1-Sm1-N2	71.01(11)
N1-Sm1-cent1	112.64(3)
N1-Sm1-cent2	107.34(3)
N2-Sm1-cent1	113.60(3)
N2-Sm1-cent2	104.81(3)

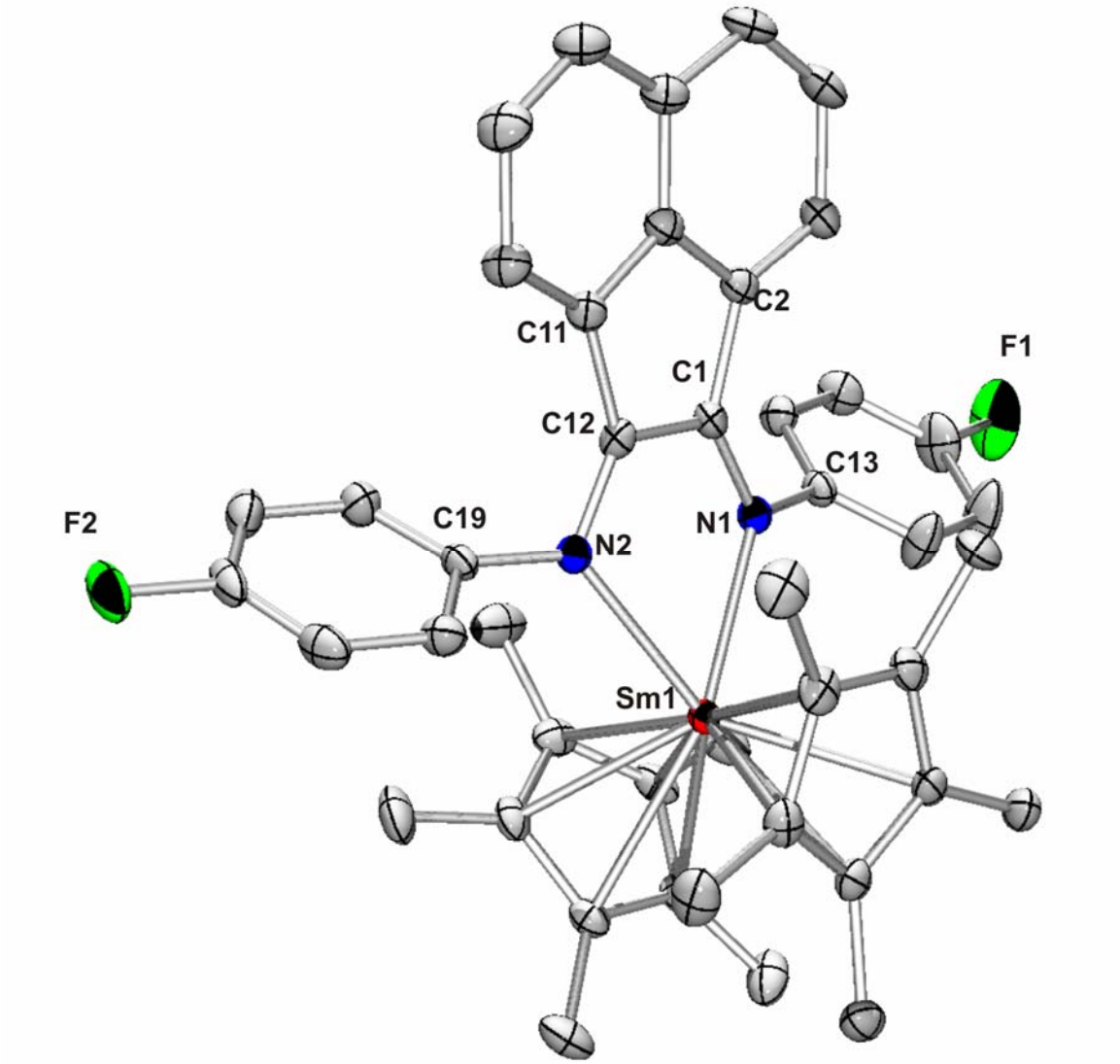

Figure 2.07. Molecular structure of 23 showing a partial numbering scheme. The thermal ellipsoids are shown at the 40% probability level. All hydrogen atoms have been omitted for clarity.

Table 2.19. Crystal data and structure refinement for 23.

Identification code	kvkv005	
Empirical formula	C44 H44 F2 N2 Sm	
Formula weight	789.16	
Temperature	153(2) K	
Wavelength	0.71073 Å	
Crystal system	Triclinic	
Space group	P-1	
Unit cell dimensions	a = 9.542(5) Å	α= 92.617(5)°.
	b = 10.183(5) Å	β= 96.042(5)°.
	c = 19.192(5) Å	γ = 101.227(5)°.
Volume	1814.8(14) $Å^3$	
Z	2	
Density (calculated)	1.444 Mg/m^3	
Absorption coefficient	1.661 mm^{-1}	
F(000)	804	
Crystal size	0.25 x 0.20 x 0.10 mm^3	
Theta range for data collection	1.07 to 27.48°.	
Index ranges	-11<=h<=12, -13<=k<=11, -24<=l<=21	
Reflections collected	12112	
Independent reflections	8266 [R(int) = 0.0296]	
Completeness to theta = 27.48°	99.4 %	
Absorption correction	None	
Refinement method	Full-matrix least-squares on F^2	
Data / restraints / parameters	8266 / 0 / 452	
Goodness-of-fit on F^2	1.189	
Final R indices [I>2sigma(I)]	R1 = 0.0351, wR2 = 0.0845	
R indices (all data)	R1 = 0.0477, wR2 = 0.1024	
Largest diff. peak and hole	1.703 and -1.326 e.$Å^{-3}$	

Table 2.20. Selected Bond Lengths (Å) for $(C_5Me_5)_2Sm$(p-F-BIAN) (23)

C1-C2	1.483(5)
C1-C12	1.442(5)
C1-N1	1.341(5)
C11-C12	1.490(5)
C12-N2	1.341(4)
C13-N1	1.426(4)
C19-N2	1.427(4)
N1-Sm1	2.466(3)
N2-Sm1	2.474(3)
Sm1-cent1	2.456(3)
Sm1-cent2	2.441(3)

Table 2.21. Selected Bond Angles (°) for $(C_5Me_5)_2Sm$(p-F-BIAN) (23)

C1-C12-C11	107.9(3)
C1-C12-N2	121.7(3)
C1-N1-C13	118.3(3)
C1-N1-Sm1	112.1(2)
C2-C1-C12	107.7(3)
C12-C1-N1	120.8(3)
C12-N2-C19	117.1(3)
C12-N2-Sm1	111.5(3)
C13-N1-Sm1	129.6(2)
C19-N2-Sm1	131.4(2)
N1-Sm1-N2	69.99(10)
N1-Sm1-cent1	107.11(3)
N1-Sm1-cent2	109.02(3)
N2-Sm1-cent1	106.78(3)
N2-Sm1-cent2	109.47(3)

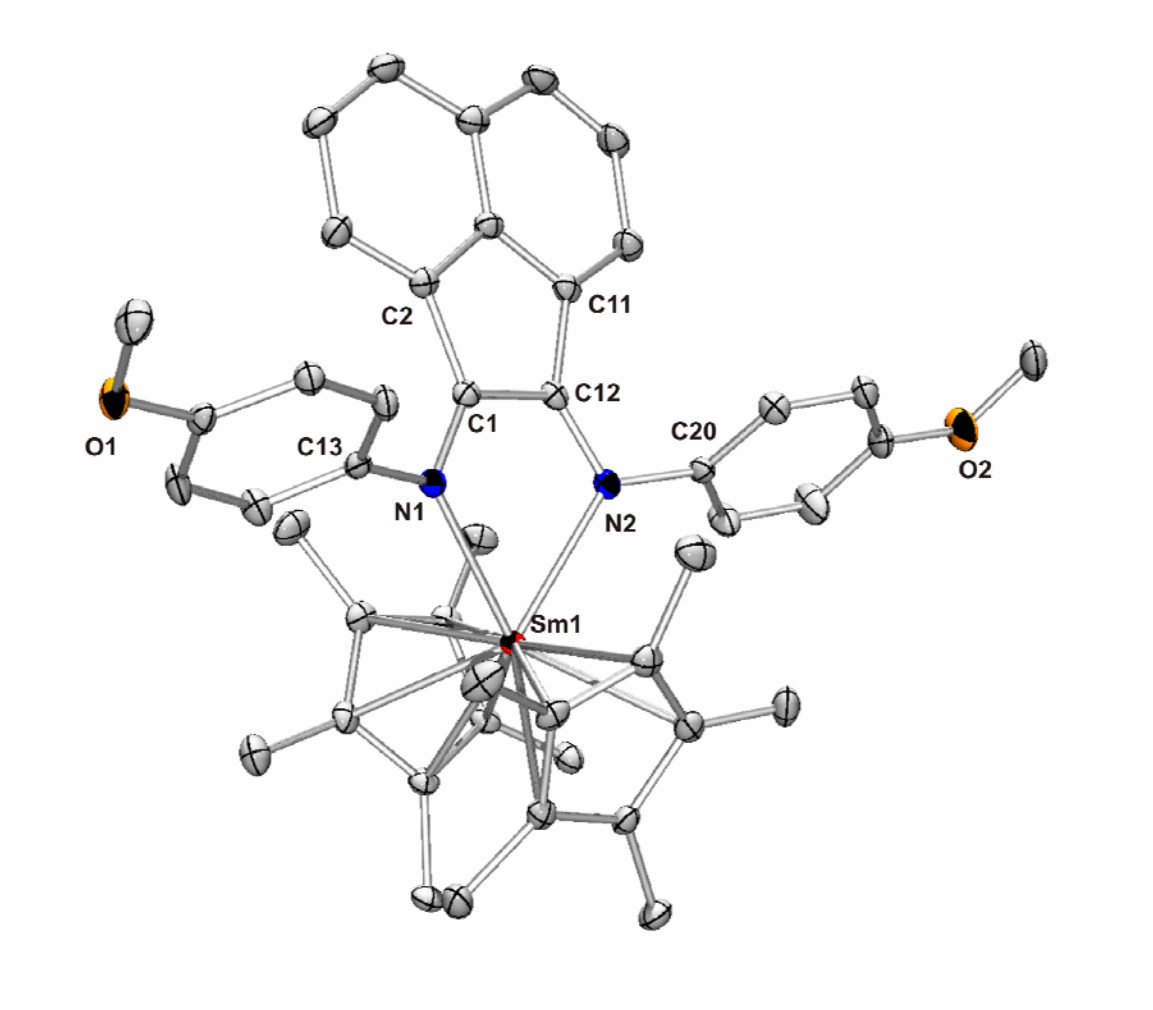

Figure 2.08. Molecular structure of 24 showing a partial numbering scheme. The thermal ellipsoids are shown at the 40% probability level. All hydrogen atoms have been omitted for clarity.

Table 2.22. Crystal data and structure refinement for 24.

Identification code	kvkv010b	
Empirical formula	C46 H50 N2 O2 Sm	
Formula weight	813.28	
Temperature	153(2) K	
Wavelength	0.71073 Å	
Crystal system	Triclinic	
Space group	P-1	
Unit cell dimensions	a = 9.560(5) Å	α= 101.103(5)°.
	b = 10.291(5) Å	β= 94.137(5)°.
	c = 20.298(5) Å	γ = 104.020(5)°.
Volume	1886.3(14) $Å^3$	
Z	2	
Density (calculated)	1.432 Mg/m^3	
Absorption coefficient	1.597 mm^{-1}	
F(000)	836	
Crystal size	0.20 x 0.15 x 0.07 mm^3	
Theta range for data collection	1.03 to 27.49°.	
Index ranges	-9<=h<=12, -13<=k<=12, -26<=l<=25	
Reflections collected	12435	
Independent reflections	8588 [R(int) = 0.0234]	
Completeness to theta = 27.49°	99.2 %	
Absorption correction	None	
Refinement method	Full-matrix least-squares on F^2	
Data / restraints / parameters	8588 / 0 / 472	
Goodness-of-fit on F^2	1.270	
Final R indices [I>2sigma(I)]	R1 = 0.0348, wR2 = 0.0947	
R indices (all data)	R1 = 0.0415, wR2 = 0.1115	
Largest diff. peak and hole	1.461 and -1.336 $e.Å^{-3}$	

Table 2.23. Selected Bond Lengths (Å) for $(C_5Me_5)_2Sm$(p-OMe-BIAN) (24)

C1-C2	1.489(5)
C1-C12	1.446(5)
C1-N1	1.336(5)
C11-C12	1.488(5)
C12-N2	1.336(5)
C13-N1	1.433(5)
C20-N2	1.433(5)
N1-Sm1	2.462(3)
N2-Sm1	2.464(3)
Sm1-cent1	2.455(3)
Sm1-cent2	2.456(3)

Table 2.24. Selected Bond Angles (°) for $(C_5Me_5)_2Sm$(p-OMe-BIAN) (24)

C1-C12-C11	107.8(3)
C1-C12-N2	122.2(3)
C1-N1-C13	116.3(3)
C1-N1-Sm1	111.1(2)
C2-C1-C12	107.7(3)
C12-C1-N1	121.3(3)
C12-N2-C20	115.8(3)
C12-N2-Sm1	110.5(2)
C13-N1-Sm1	132.7(2)
C20-N2-Sm1	133.7(2)
N1-Sm1-N2	70.78(11)
N1-Sm1-cent1	108.98(3)
N1-Sm1-cent2	107.73(3)
N2-Sm1-cent1	109.31(3)
N2-Sm1-cent2	107.44(3)

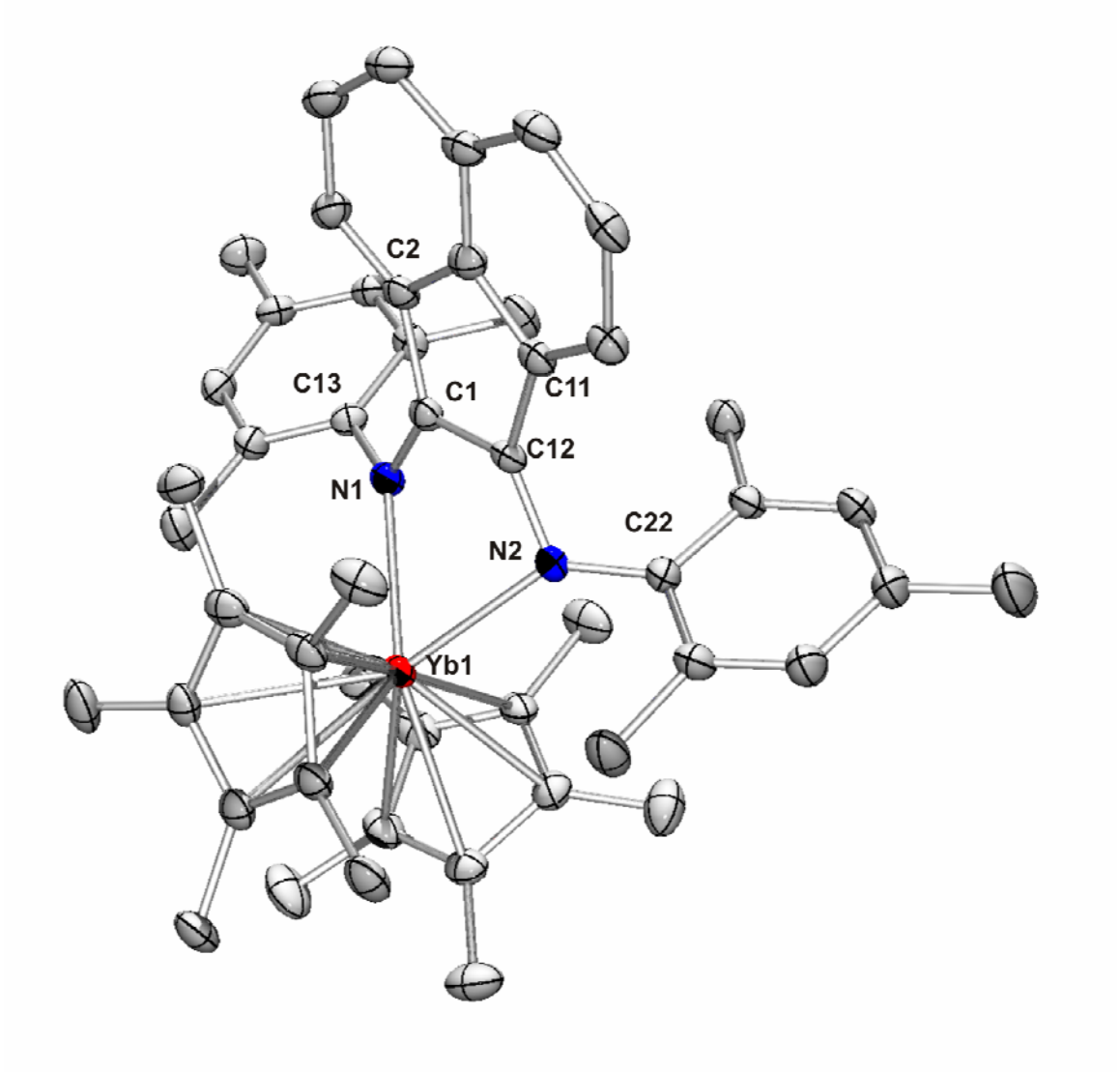

Figure 2.09. Molecular structure of 25 showing a partial numbering scheme. The thermal ellipsoids are shown at the 40% probability level. All hydrogen atoms have been omitted for clarity.

Table 2.25. Crystal data and structure refinement for 25.

Identification code	kvgr069	
Empirical formula	C50 H58 N2 Yb	
Formula weight	860.02	
Temperature	153(2) K	
Wavelength	0.71073 Å	
Crystal system	Triclinic	
Space group	P-1	
Unit cell dimensions	a = 12.471(3) Å	α= 71.20(3)°.
	b = 13.984(3) Å	β= 83.28(3)°.
	c = 16.862(3) Å	γ = 68.41(3)°.
Volume	2588.4(12) $Å^3$	
Z	2	
Density (calculated)	1.103 Mg/m^3	
Absorption coefficient	1.835 mm^{-1}	
F(000)	884	
Crystal size	0.25 x 0.21 x 0.20 mm^3	
Theta range for data collection	2.03 to 27.50°.	
Index ranges	-15<=h<=16, -14<=k<=18, -21<=l<=21	
Reflections collected	17009	
Independent reflections	11718 [R(int) = 0.0247]	
Completeness to theta = 27.50°	98.5 %	
Absorption correction	Semi-empirical from equivalents	
Max. and min. transmission	0.693 and 0.638	
Refinement method	Full-matrix least-squares on F^2	
Data / restraints / parameters	11718 / 0 / 494	
Goodness-of-fit on F^2	1.072	
Final R indices [I>2sigma(I)]	R1 = 0.0415, wR2 = 0.1104	
R indices (all data)	R1 = 0.0494, wR2 = 0.1135	
Largest diff. peak and hole	2.647 and -0.994 $e.Å^{-3}$	

Table 2.26. Selected Bond Lengths (Å) for $(C_5Me_5)_2Yb$(Mes-BIAN) (25)

C1-C2	1.473(5)
C1-C12	1.450(6)
C1-N1	1.342(5)
C10-C12	1.484(5)
C12-N2	1.339(5)
C13-N1	1.441(5)
C22-N2	1.431(5)
N1-Yb1	2.440(3)
N2-Yb1	2.422(3)
Yb1-cent1	2.343(3)
Yb1-cent2	2.447(3)

Table 2.27. Selected Bond Angles (°) for $(C_5Me_5)_2Yb$(Mes-BIAN) (25)

C1-C12-C10	107.9(3)
C1-C12-N2	123.3(3)
C1-N1-C13	115.6(3)
C1-N1-Yb1	107.8(2)
C2-C1-C12	107.6(3)
C12-C1-N1	122.0(3)
C12-N2-C22	114.5(3)
C12-N2-Yb1	101.6(2)
C13-N1-Yb1	142.3(2)
C22-N2-Yb1	101.6(2)
N1-Yb1-N2	73.09(11)
N1-Yb1-cent1	108.25(3)
N1-Yb1-cent2	111.24(3)
N2-Yb1-cent1	107.23(3)
N2-Yb1-cent2	111.67(3)

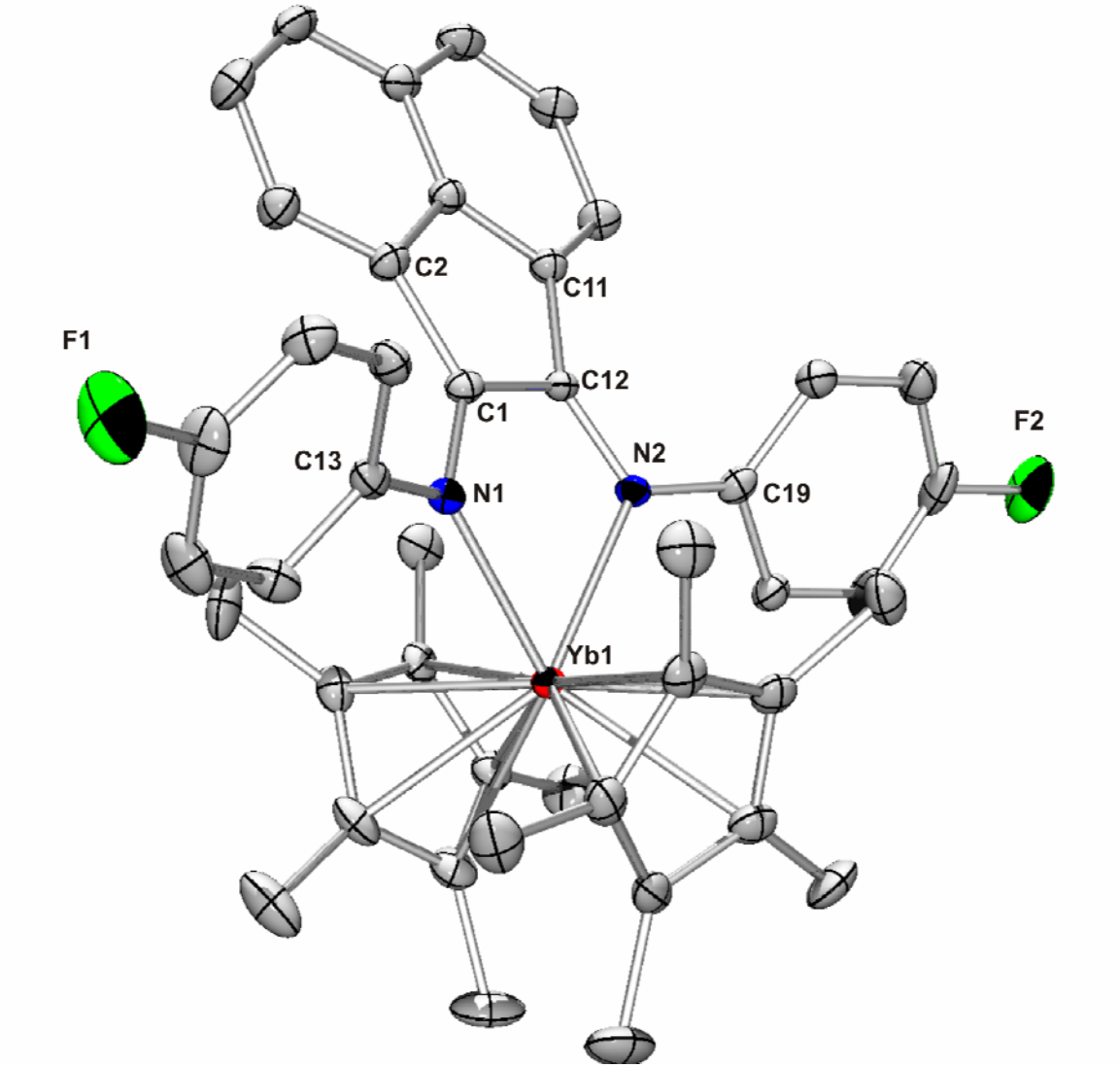

Figure 2.10. Molecular structure of 26 showing a partial numbering scheme. The thermal ellipsoids are shown at the 40% probability level. All hydrogen atoms have been omitted for clarity.

Table 2.28. Crystal data and structure refinement for 26.

Identification code	kvkv004	
Empirical formula	C44 H44 F2 N2 Yb	
Formula weight	811.85	
Temperature	153(2) K	
Wavelength	0.71073 Å	
Crystal system	Monoclinic	
Space group	Cc	
Unit cell dimensions	a = 21.767(5) Å	α= 90.000(5)°.
	b = 10.210(5) Å	β= 118.767(5)°.
	c = 18.120(5) Å	γ = 90.000(5)°.
Volume	3530(2) $Å^3$	
Z	4	
Density (calculated)	1.528 Mg/m^3	
Absorption coefficient	2.694 mm^{-1}	
F(000)	1640	
Crystal size	0.20 x 0.15 x 0.10 mm^3	
Theta range for data collection	3.45 to 27.46°.	
Index ranges	-27<=h<=28, -12<=k<=13, -23<=l<=22	
Reflections collected	9866	
Independent reflections	6498 [R(int) = 0.0274]	
Completeness to theta = 27.46°	99.0 %	
Absorption correction	None	
Refinement method	Full-matrix least-squares on F^2	
Data / restraints / parameters	6498 / 2 / 453	
Goodness-of-fit on F^2	1.088	
Final R indices [I>2sigma(I)]	R1 = 0.0234, wR2 = 0.0495	
R indices (all data)	R1 = 0.0276, wR2 = 0.0511	
Absolute structure parameter	-0.015(7)	
Extinction coefficient	0.00118(9)	
Largest diff. peak and hole	1.635 and -0.555 $e.Å^{-3}$	

Table 2.29. Selected Bond Lengths (Å) for $(C_5Me_5)_2Yb$(p-F-BIAN) (26)

C1-C2	1.480(5)
C1-C12	1.432(5)
C1-N2	1.334(5)
C11-C12	1.482(5)
C12-N1	1.351(5)
C13-N1	1.417(5)
C19-N2	1.403(5)
N1-Yb1	2.345(3)
N2-Yb1	2.339(3)
Yb1-cent1	2.371(3)
Yb1-cent2	2.344(3)

Table 2.30. Selected Bond Angles (°) for $(C_5Me_5)_2Yb$(p-F-BIAN) (26)

C1-C12-C11	108.6(3)
C1-C12-N1	120.8(3)
C1-N2-C19	121.2(3)
C1-N2-Yb1	112.3(3)
C2-C1-C12	108.1(3)
C12-C1-N2	118.7(3)
C12-N1-C13	117.3(3)
C12-N1-Yb1	110.5(3)
C13-N1-Yb1	132.2(2)
C19-N2-Yb1	126.3(3)
N1-Yb1-N2	72.37(12)
N1-Yb1-cent1	106.38(3)
N1-Yb1-cent2	107.04(3)
N2-Yb1-cent1	106.24(3)
N2-Yb1-cent2	109.28(3)

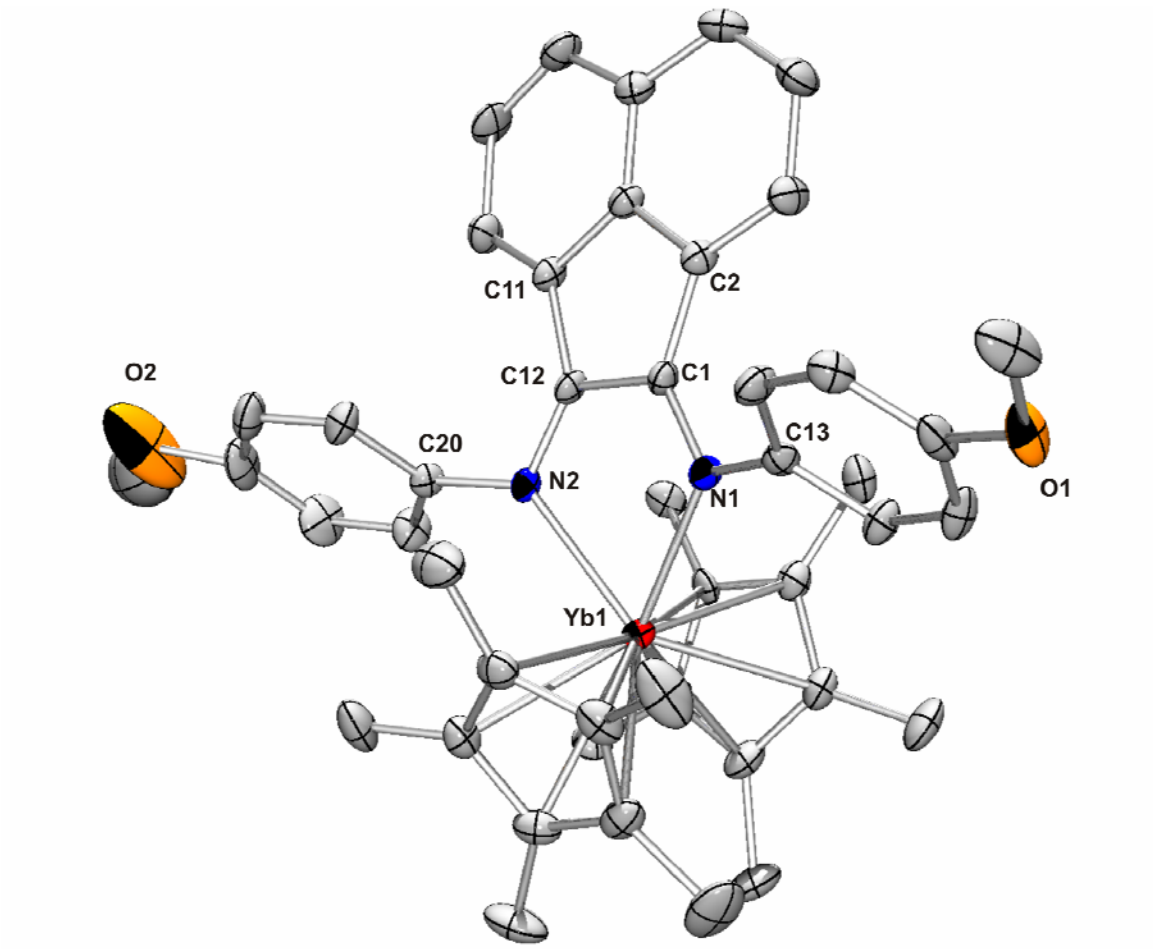

Figure 2.11. Molecular structure of 27 showing a partial numbering scheme. The thermal ellipsoids are shown at the 40% probability level. All hydrogen atoms have been omitted for clarity.

Table 2.31. Crystal data and structure refinement for 27.

Identification code	kvkv043sq	
Empirical formula	C48 H50 N2 O2 Yb	
Formula weight	859.94	
Temperature	153(2) K	
Wavelength	0.71073 Å	
Crystal system	Monoclinic	
Space group	C2/c	
Unit cell dimensions	a = 45.662(9) Å	α= 90°.
	b = 10.337(2) Å	β= 105.78(3)°.
	c = 18.349(4) Å	γ = 90°.
Volume	8334(3) $Å^3$	
Z	8	
Density (calculated)	1.371 Mg/m^3	
Absorption coefficient	2.283 mm^{-1}	
F(000)	3504	
Crystal size	0.20 x 0.15 x 0.15 mm^3	
Theta range for data collection	1.85 to 27.31°.	
Index ranges	-57<=h<=58, -13<=k<=12, -23<=l<=23	
Reflections collected	16123	
Independent reflections	9306 [R(int) = 0.0421]	
Completeness to theta = 27.31°	99.0 %	
Absorption correction	None	
Refinement method	Full-matrix least-squares on F^2	
Data / restraints / parameters	9306 / 0 / 471	
Goodness-of-fit on F^2	1.163	
Final R indices [I>2sigma(I)]	R1 = 0.0564, wR2 = 0.1170	
R indices (all data)	R1 = 0.0789, wR2 = 0.1228	
Largest diff. peak and hole	1.506 and -1.340 e.$Å^{-3}$	

Table 2.32. Selected Bond Lengths (Å) for $(C_5Me_5)_2Yb$(p-OMe-BIAN) (27)

C1-C2	1.487(8)
C1-C12	1.448(8)
C1-N1	1.328(8)
C11-C12	1.476(8)
C12-N2	1.347(8)
C13-N1	1.423(7)
C20-N2	1.422(8)
N1-Yb1	2.360(5)
N2-Yb1	2.344(5)
Yb1-cent1	2.335(3)
Yb1-cent2	2.357(3)

Table 2.33. Selected Bond Angles (°) for $(C_5Me_5)_2Yb$(p-OMe-BIAN) (27)

C1-C12-C11	108.0(5)
C1-C12-N2	120.6(5)
C1-N1-C13	116.4(5)
C1-N1-Yb1	110.0(4)
C2-C1-C12	107.4(5)
C12-C1-N1	121.4(5)
C12-N1-C20	118.2(5)
C12-N2-Yb1	110.1(4)
C13-N1-Yb1	133.5(4)
C20-N2-Yb1	131.6(4)
N1-Yb1-N2	78.83(18)
N1-Yb1-cent1	107.53(3)
N1-Yb1-cent2	107.07(3)
N2-Yb1-cent1	108.81(3)
N2-Yb1-cent2	106.98(3)

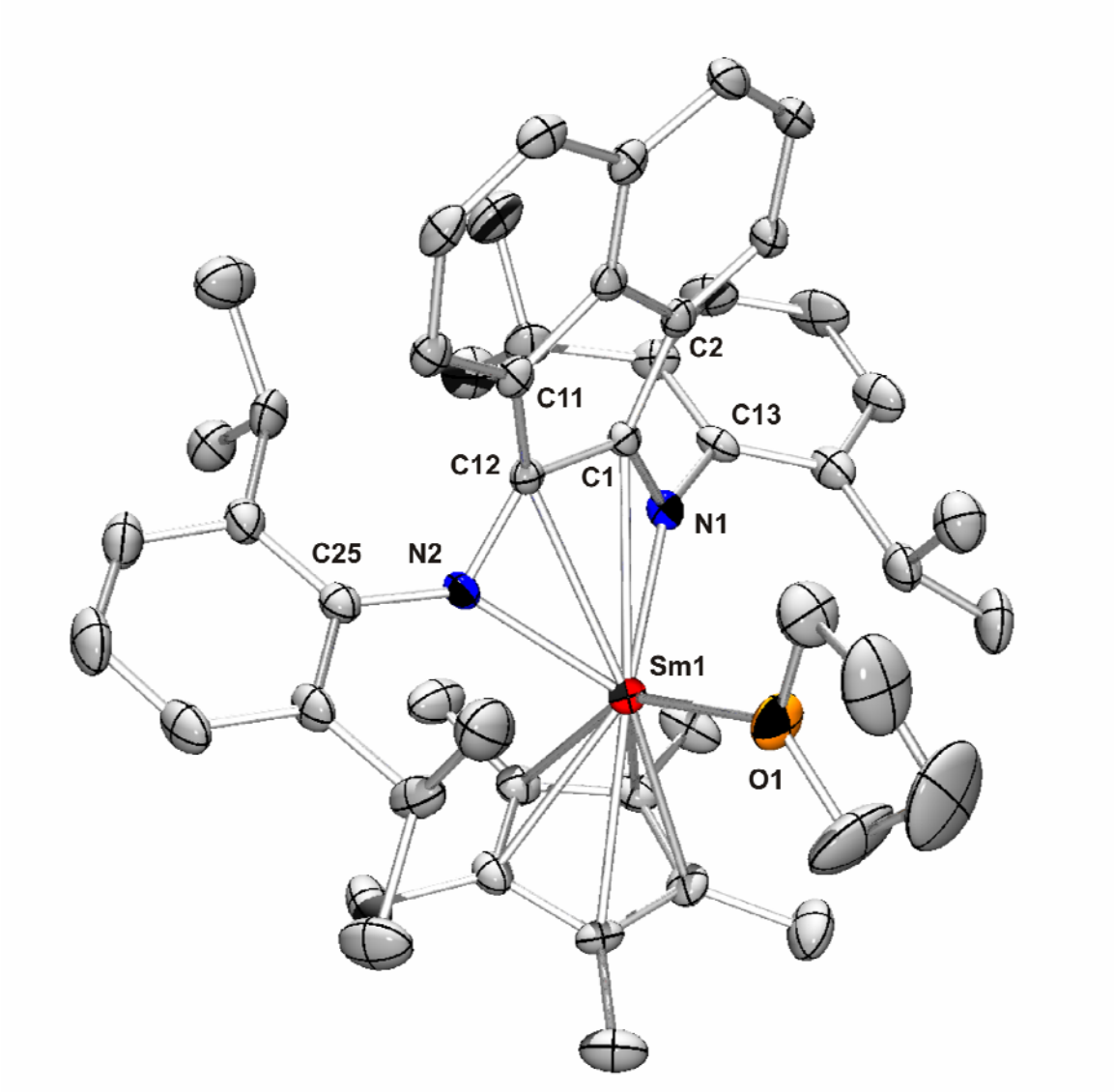

Figure 2.12. Molecular structure of 28 showing a partial numbering scheme. The thermal ellipsoids are shown at the 40% probability level. All hydrogen atoms have been omitted for clarity.

Table 2.34. Crystal data and structure refinement for 28.

Identification code	kvkv011	
Empirical formula	C50 H63 N2 O Sm	
Formula weight	858.37	
Temperature	153(2) K	
Wavelength	0.71073 Å	
Crystal system	Monoclinic	
Space group	P21/n	
Unit cell dimensions	a = 10.856(5) Å	α= 90.000(5)°.
	b = 20.426(5) Å	β= 103.851(5)°.
	c = 20.153(5) Å	γ = 90.000(5)°.
Volume	4339(3) $Å^3$	
Z	4	
Density (calculated)	1.314 Mg/m^3	
Absorption coefficient	1.391 mm^{-1}	
F(000)	1788	
Crystal size	0.20 x 0.20 x 0.15 mm^3	
Theta range for data collection	1.44 to 27.49°.	
Index ranges	-14<=h<=14, -26<=k<=24, -26<=l<=26	
Reflections collected	16826	
Independent reflections	9858 [R(int) = 0.0502]	
Completeness to theta = 27.49°	99.0 %	
Absorption correction	None	
Refinement method	Full-matrix least-squares on F^2	
Data / restraints / parameters	9858 / 0 / 500	
Goodness-of-fit on F^2	1.053	
Final R indices [I>2sigma(I)]	R1 = 0.0416, wR2 = 0.0863	
R indices (all data)	R1 = 0.0898, wR2 = 0.1189	
Largest diff. peak and hole	1.653 and -1.026 $e.Å^{-3}$	

Table 2.35. Selected Bond Lengths (Å) for (C_5Me_5)(THF)Sm(Dipp-BIAN) (28)

C1-C2	1.478(6)
C1-C12	1.414(6)
C1-N1	1.387(5)
C11-C12	1.479(6)
C12-N2	1.405(5)
C13-N1	1.420(5)
C25-N2	1.414(5)
N1-Sm1	2.269(3)
N2-Sm1	2.232(4)
O1-Sm1	2.451(3)
Sm1-cent	2.422(3)

Table 2.36. Selected Bond Angles (°) for (C_5Me_5)(THF)Sm(Dipp-BIAN) (28)

C1-C12-C11	108.3(3)
C1-C12-N2	124.4(4)
C1-N1-C13	119.5(3)
C1-N1-Sm1	92.4(2)
C2-C1-C12	108.0(3)
C12-C1-N1	124.2(4)
C12-N2-C25	116.8(3)
C12-N2-Sm1	92.6(2)
C13-N1-Sm1	145.9(3)
C25-N2-Sm1	149.7(3)
N1-Sm1-N2	83.15(12)
N1-Sm1-cent	115.47(3)
N1-Sm1-O1	107.27(12)
N2-Sm1-cent	113.21(3)
N2-Sm1-O1	106.02(12)
O1-Sm1-cent	123.95(3)

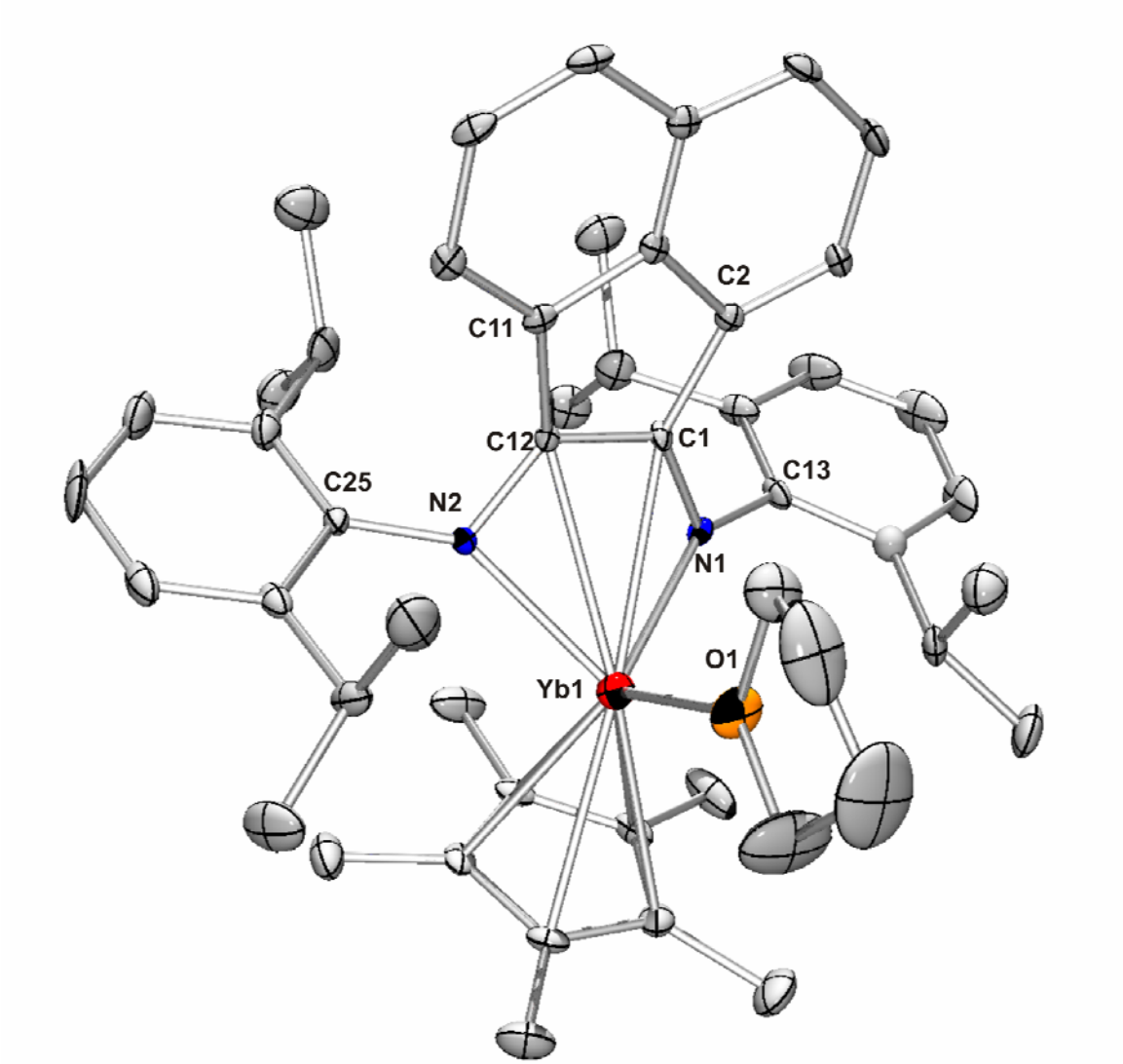

Figure 2.13. Molecular structure of 29 showing a partial numbering scheme. The thermal ellipsoids are shown at the 40% probability level. All hydrogen atoms have been omitted for clarity.

Table 2.37. Crystal data and structure refinement for 29.

Identification code	kvkv012	
Empirical formula	C50 H63 N2 O Yb	
Formula weight	881.06	
Temperature	153(2) K	
Wavelength	0.71073 Å	
Crystal system	Monoclinic	
Space group	P21/n	
Unit cell dimensions	a = 10.859(5) Å	α= 90.000(5)°.
	b = 20.424(5) Å	β= 103.830(5)°.
	c = 20.148(5) Å	γ = 90.000(5)°.
Volume	4339(3) $Å^3$	
Z	4	
Density (calculated)	1.349 Mg/m^3	
Absorption coefficient	2.193 mm^{-1}	
F(000)	1820	
Crystal size	0.20 x 0.14 x 0.09 mm^3	
Theta range for data collection	2.31 to 27.46°.	
Index ranges	-14<=h<=14, -24<=k<=26, -26<=l<=26	
Reflections collected	18217	
Independent reflections	9875 [R(int) = 0.0364]	
Completeness to theta = 27.46°	99.5 %	
Absorption correction	None	
Refinement method	Full-matrix least-squares on F^2	
Data / restraints / parameters	9875 / 0 / 495	
Goodness-of-fit on F^2	1.037	
Final R indices [I>2sigma(I)]	R1 = 0.0467, wR2 = 0.1354	
R indices (all data)	R1 = 0.0729, wR2 = 0.1513	
Largest diff. peak and hole	2.580 and -0.998 $e.Å^{-3}$	

Table 2.38. Selected Bond Lengths (Å) for (C_5Me_5)(THF)Yb(Dipp-BIAN) (29)

C1-C2	1.481(6)
C1-C12	1.420(6)
C1-N1	1.398(5)
C11-C12	1.488(6)
C12-N2	1.385(6)
C13-N1	1.433(6)
C25-N2	1.424(5)
N1-Yb1	2.222(4)
N2-Yb1	2.265(4)
O1- Yb1	2.456(3)
Yb1-cent	2.422(4)

Table 2.39. Selected Bond Angles (°) for (C_5Me_5)(THF)Yb(Dipp-BIAN) (29)

C1-C12-C11	108.0(4)
C1-C12-N2	123.7(4)
C1-N1-C13	116.6(4)
C1-N1-Yb1	93.0(3)
C2-C1-C12	107.7(4)
C12-C1-N1	124.1(4)
C12-N2-C25	119.4(4)
C12-N2-Yb1	92.8(2)
C13-N1-Yb1	149.5(3)
C25-N2-Yb1	145.4(3)
N1-Yb1-N2	82.99(13)
N1-Yb1-cent1	113.22(3)
N1-Yb1-O1	105.89(14)
N2-Yb1-cent1	115.47(3)
N2-Yb1-O1	107.32(13)
O1-Yb1-cent	124.12(3)

Chapter 3

"Reactivity of the Tetrakis(imino)pyracene (TIP) Ligand Class"

Chapter 3 Introduction

Studies involving poly(pyridyl) adducts of ytterbocene have inspired the synthesis of bimetallic f-element systems displaying a range of interesting properties, such as the magnetic and electronic interactions between the f-element centers and the role of the bridging ligand in the mediation of such interactions. The potential to achieve high molecular magnetic moments stems from the presence of multiple lanthanide ions which have the ability to communicate through the appropriate orbitals of the bridging ligand. Linking discreet lanthanide ions through π-bonded ligand systems serves to promote such electronic interactions, leading to *e.g.* molecular wires and molecular magnets. Most pertinent to the current chapter are the studies conducted by John *et al.*[22, 32, 33] involving bis(ytterbocene) complexes with bis(polypyridyl) bridging ligands. Specifically, these studies involved a series of decamethylytterbocene complexes supported by a variety of conformationally diverse bis(terpyridyl) and bis(bipyridyl) ligands as summarized in Scheme 3.01. Analysis of the cyclic voltammagrams of these complexes revealed that they undergo two ligand-based oxidation events and two ytterbium-based reductions. The difference in potential between the reduction waves is a diagnostic of the degree of electronic interaction between the lanthanide centers. The highest degree of intramolecular electronic communication was found for those complexes with the greatest separation in reduction potentials. For example, the complex of ligand **A** exhibited a peak differential of 0.60 V, while the corresponding value for **F** was 0.09 V.

These authors concluded that the metallic species bridged by rigid, planar ligands with extensive orbital overlap result in the highest degree of electronic communication between metal centers.

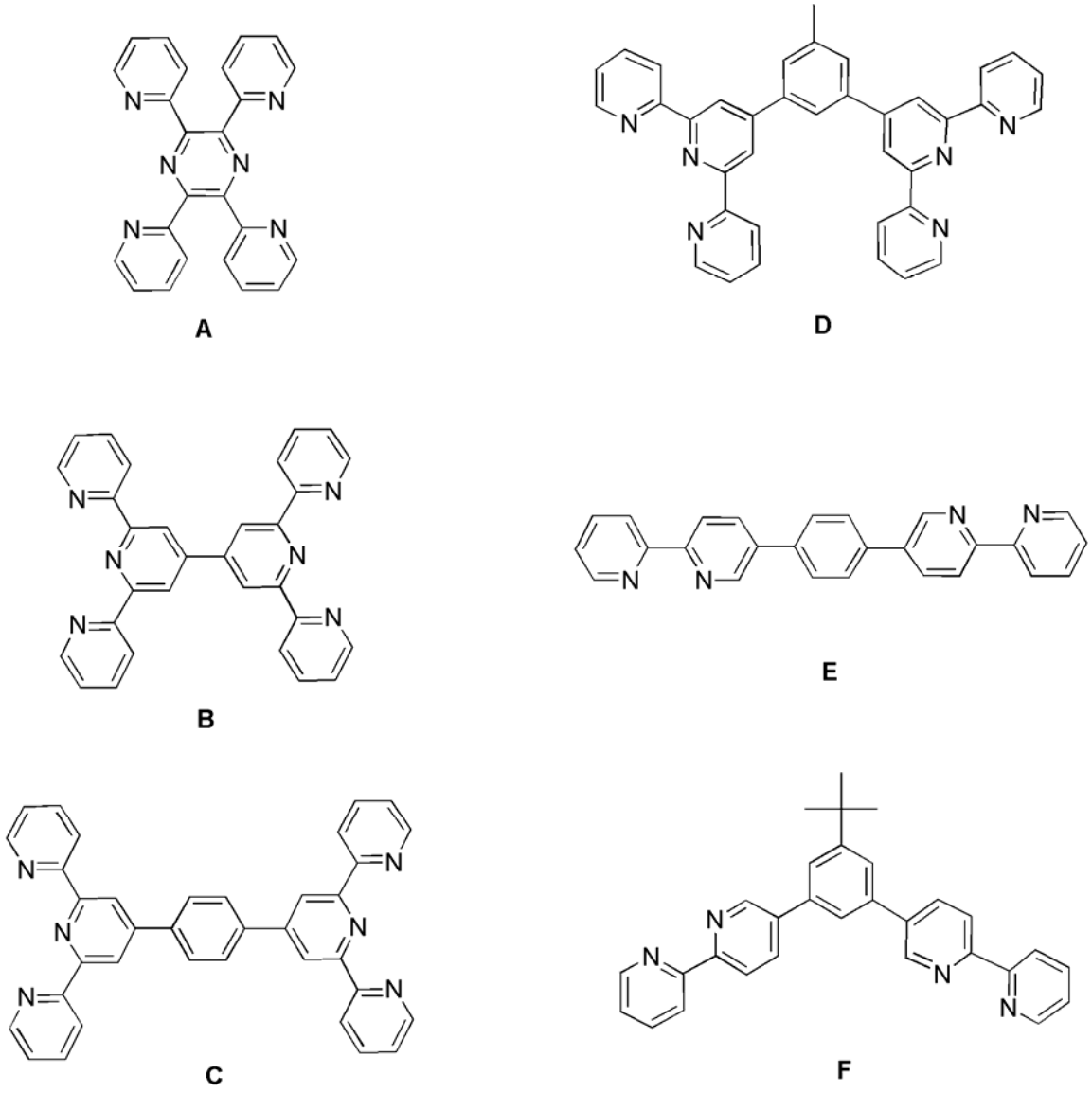

Scheme 3.01. Bifunctional bis(terpyridine) [A-D] and bis(bipyridyl) [E-F] ligands employed in the John *et al.* studies.

In order to apply the approach of John *et al*. to the current work, the logical next step was the development of a bifunctional ligand of the BIAN-type. The advantages of such a bifunctional ligand would be the high degree of ligand rigidity and the tunability of the stereo-electronic properties of the substituents. It became evident that a ligand based on a pyracene backbone would most closely mimic the BIAN framework. This approach resulted in the design and synthesis of the tetrakis(imino)pyracene (TIP) ligand, the synthesis of which is described in Section 1.3. The synthetic route to the ligand precursor, 1,2,7,8-tetraketopyracene, is shown in Scheme 3.02[16].

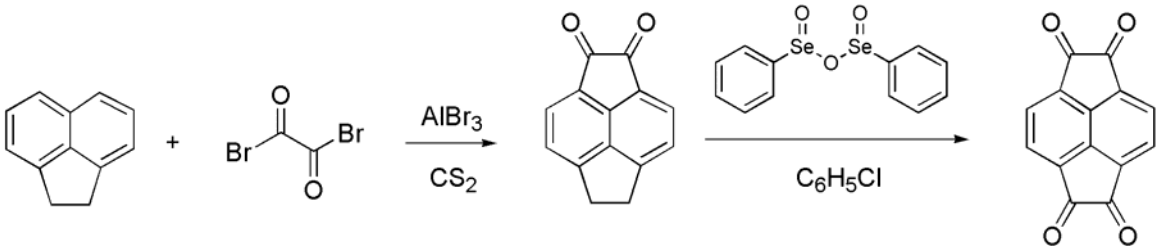

Scheme 3.02. Synthetic route to 1,2,7,8-tetraketopyracene.

It was envisioned that the TIP ligand could serve as a redox-active scaffold for the development of *e.g.* new molecular wires, metallopolymers and bimetallic catalysts. The TIP ligand is proving to be highly versatile and capable of supporting a wide array of main group and lanthanide fragments. Probably, its most useful functions are as a framework for promoting electron communication between redox-active species and as a scaffold for the formation of new polymeric materials.

Of further import is the recent wealth of research pertaining to graphene-type systems that has recently appeared in the literature. Graphene can be regarded as a thin

planar sheet of sp^2 hybridized carbon atoms densely packed in a honeycomb fashion. The more than 1,000 papers published on this subject since 2007 have gained graphene increasingly widespread attention from the scientific community[34]. Interest in this subject has blossomed as a result of the unique properties of the material, which include its superior tensile strength and extended conjugation. These extraordinary mechanical and electronic properties render graphene desirable for applications in such areas as advanced composites and electronics. While the TIP ligand is a mere fraction of the size of a traditional graphene unit, it can be viewed as a small functionalized graphene fragment. Studies on this small scale may prove useful in the broader context of understanding the electron transport mechanisms in graphene-type systems.

Results and Discussion

Section 3.1 Introduction

The TIP ligand has proved to be of value in terms of its ability to function as a support for a significant number of main group and transition metal species. While the primary interest in this ligand is focused on the synthesis and properties of redox-active complexes, a variety of other potential applications exist. For example, several diimine-supported late transition metal complexes are known to be highly efficient catalysts for olefin polymerization and a number of industrially important organic transformations[1, 11]. Furthermore, given that a number of transition metal BIAN complexes have been shown to exist as dimers in the solid state[30, 35], a logical expectation would be the possibility of forming metallopolymers based on bridging TIP ligands. In the context of donor-acceptor complexes involving main group element moieties, the BIAN ligand has proved to be effective for the capture of the previously unknown TeI_2 molecule[36] and has also shown the ability to support a number of novel Group 13 cations[20, 37]. The foregoing applications of the BIAN ligand provided the motivation to explore the syntheses of a number of donor-acceptor complexes of the TIP ligand involving both transition metal and main group entities.

Synthesis and Characterization of $(PdX_2)_2$(Dipp-TIP) [X = Cl (30), Br (31)]

The $(PdX_2)_2$(Dipp-TIP) (X = Cl, Br) complexes **30** and **31** were synthesized by treatment of one equivalent of the Dipp-TIP ligand with two equivalents of the appropriate palladium(II)halide in hot acetonitrile solution. Workup of each reaction mixture resulted in the isolation of dark red solids **30** and **31** in yields of 75-80%. Recrystallization of the crude solids was accomplished by slow evaporation of saturated

dichloromethane solutions of **30** and **31** over 4 days, affording small crops of dark red crystals. Both new compounds were structurally authenticated on the basis of single-crystal X-ray diffraction studies and the pertinent structures are displayed in Figures 3.01 and 3.02, respectively. Details of the data collection, structure solution and refinement for both structures are compiled in Tables 3.01 (**30**) and 3.04 (**31**) and selections of pertinent metrical parameters are provided in Tables 3.02, 3.03 (**30**), 3.05 and 3.06 (**31**).

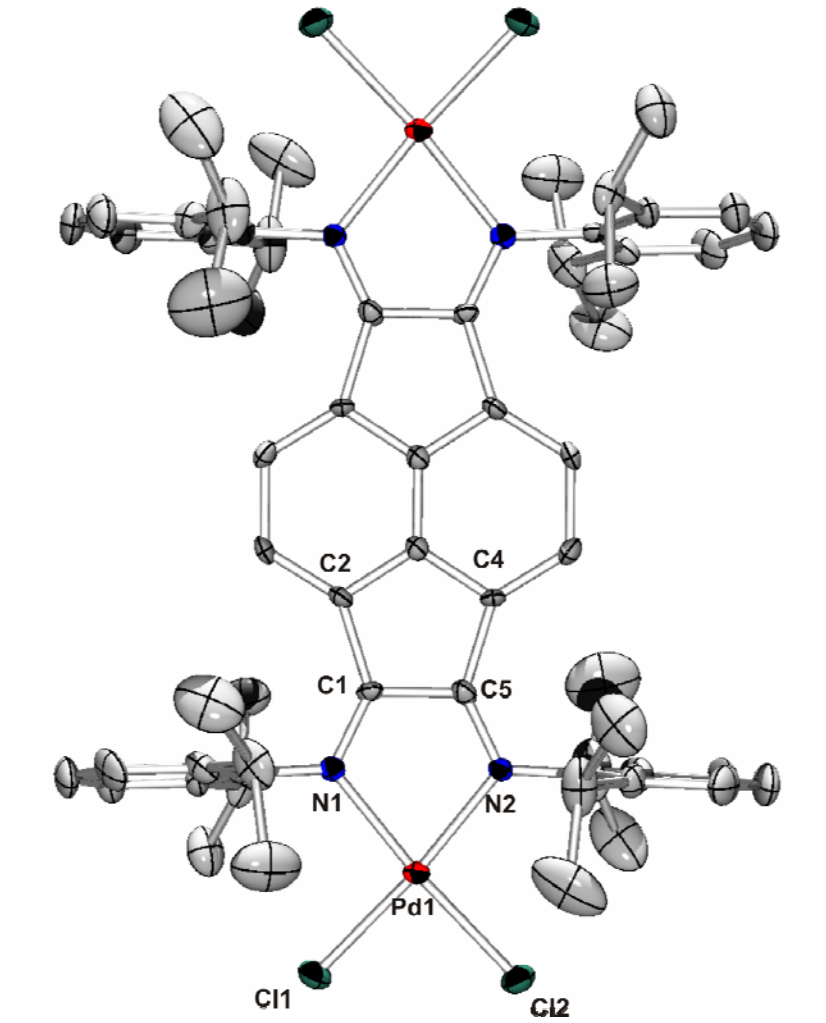

Figure 3.01. Molecular structure of 30 showing a partial numbering scheme. The thermal ellipsoids are shown at the 40% probability level. All hydrogen atoms and two molecules of dichloromethane have been omitted for clarity.

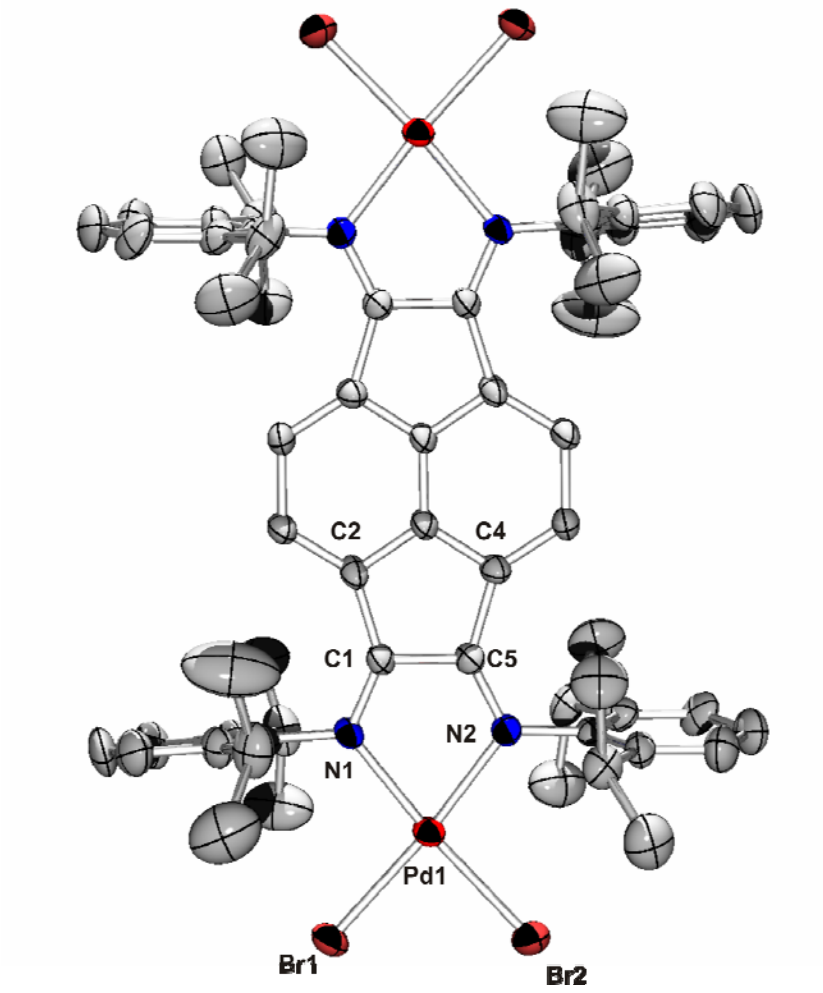

Figure 3.02. Molecular structure of 31 showing a partial numbering scheme. The thermal ellipsoids are shown at the 40% probability level. All hydrogen atoms have been omitted for clarity.

As mentioned earlier, BIAN-supported palladium and other late transition metal complexes have found utility as efficient catalysts for both olefin polymerization and also for a number of important organic transformations. Given the successful application of such complexes in the realm of catalysis, the bimetallic TIP-supported complexes **30** and **31** were synthesized with a long-term goal of assessing their activities and comparing them with those of the known BIAN analogues. However, thus far, **30** and **31** have only been characterized on the basis of single-crystal X-ray diffraction, along with IR, and ^{1}H NMR spectroscopic data, and at this point, their catalytic properties have not been

investigated. Both **30** and **31** crystallize in the orthorhombic space group *Pbca*, the former with two molecules of dichloromethane. The nearly identical average C-N bond lengths in **30** and **31** of 1.289(10) Å and 1.289(7) Å imply a bond order of two. The respective C(1)-C(5) bond lengths of 1.484(10) Å and 1.503(7) Å deviate somewhat from those reported for the free Dipp-TIP ligand (1.549(4) Å)[38]. While the compression of the C-C bond suggests potential electron transfer, when taken in conjunction with the C-N bond lengths, it is likely that the C-C bond order is one and that no charge transfer process has occurred. However, the relatively large R(int) value of 0.1078 for **30** along with the high esd values renders an accurate assessment of the bond orders difficult solely on the basis of X-ray data. Nevertheless, additional supporting evidence for the proposed bonding mode stems from the IR spectrum of **30**, which features a peak at 1625 cm^{-1}, which is indicative of the presence of C=N bonds. A virtually identical stretching frequency was observed in the case of **31** (1627 cm^{-1}), hence it is concluded that both complexes feature N→Pd donor-acceptor bonding.

Synthesis and Characterization of $[(CuBr)_2(Dipp\text{-}TIP)]_n$ (32)

The metallopolymer $[(CuBr)_2(Dipp\text{-}TIP)]_n$ (**32**) was synthesized by treatment of two equivalents of $CuBr_2$ with one equivalent of Dipp-TIP in THF/methanol solution. The resulting dark green precipitate was obtained in 72% yield. Recrystallization of the crude solid was not possible due to the pronounced insolubility of the resulting product. However, single crystals suitable for X-ray diffraction were obtained by layering two equivalents of $CuBr_2$ in methanol solution over a solution that contained one equivalent of Dipp-TIP in THF. Over the course of 6 days, a crop of small dark green crystals was formed at the solvent interface. The product was subjected to single-crystal X-ray analysis and shown to be a metallopolymer of composition $[(CuBr)_2(Dipp\text{-}TIP)]_n$. A

representative section of the polymeric chain is presented in Figure 3.03. Details of the data collection, structure solution and refinement are provided in Table 3.07 and relevant metrical parameters are displayed in Tables 3.08 and 3.09.

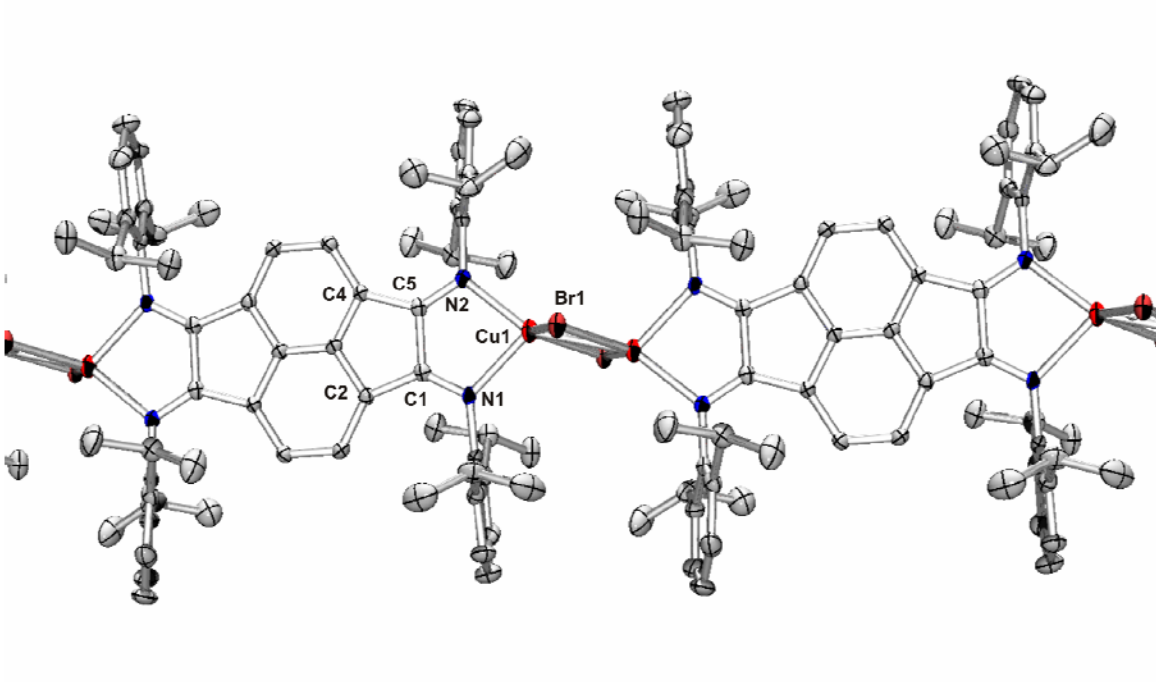

Figure 3.03. Molecular structure of metallopolymer 32 showing a partial numbering scheme. The thermal ellipsoids are shown at the 40% probability level. All hydrogen atoms and one molecule of THF have been omitted for clarity.

The potential for the TIP ligand to serve as a bridging ligand is demonstrated by the isolation of the polymer **32**. The average C-N and C-C bond distances for **32** of 1.275(7) Å and 1.504(8) Å, respectively, imply the existence of a donor-acceptor bonding between the imino nitrogens and the Cu(I) centers. Structurally, **32** features essentially planar [Cu(Dipp-TIP)Cu] moieties which are linked in an orthogonal fashion to rhomboids of Cu_2Br_2. It is interesting to note that the reaction proceeds with reduction of Cu(II)→Cu(I) with concomitant formation of Br_2. However, it is evident both from the foregoing observations and the metrical parameters for the polymer that no redox processes have taken place in the TIP ligand.

The extremely poor solubility of **32** necessitated a very lengthy acquisition time (24 h) for the ^{1}H NMR data. Nevertheless, the resulting spectrum displayed all the anticipated resonances, albeit broadened due to the polymeric nature of the product. Further supporting spectroscopic evidence was gleaned from the low resolution mass spectrum (CI+) of **32**, which features a prominent peak at *m/z* 1156, that corresponds to the value anticipated for the monomeric unit [CuBr(Dipp-TIP)CuBr]. Less intense peaks were detected at *m/z* 2312 and 3468, and correspond to the values calculated for the dimeric and trimeric units, respectively.

Given the bridging geometry of the TIP ligand and the propensity of the BIAN ligand to form dimers with a variety of transition metal entities, it is expected that a number of other TIP-supported metallopolymers could be readily synthesized by employing this facile synthetic method.

Synthesis and Characterization of $[(BCl_2)_2$(Dipp-TIP)$][BCl_4]_2$ (33)

Treatment of one equivalent of the Dipp-TIP ligand with four equivalents of BCl_3 in dichloromethane solution resulted in the formation of $[(BCl_2)_2$(Dipp-TIP)$][BCl_4]_2$ (**33**). Analytically pure **33** was isolated as a green powder in high yield (93%) upon workup of the reaction mixture. A small crop of single crystals of **33** was obtained by recrystallization of the powder from dichloromethane solution at -15°C. A suitable single crystal of **33** was selected and used for X-ray analysis. Details of the data collection, structure solution and refinement are compiled in Table 3.10 and a selection of relevant structural data of **33** is presented in Tables 3.11 and 3.12.

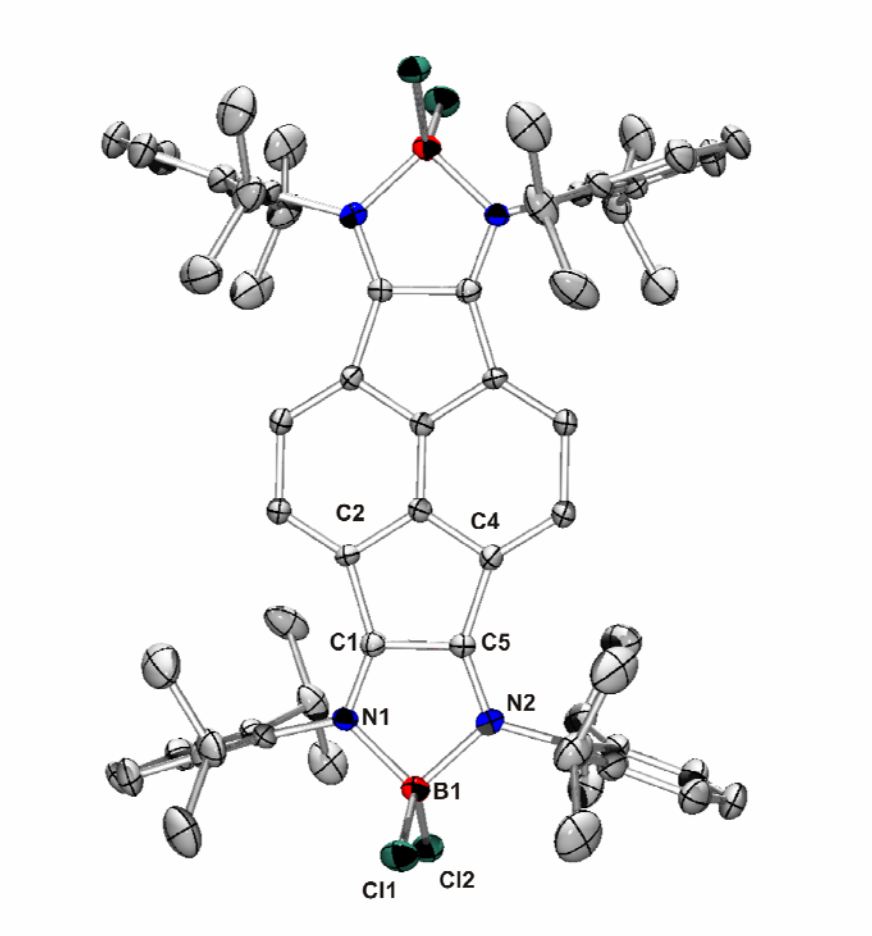

Figure 3.04. Molecular structure of the cation of 33 showing a partial numbering scheme. The thermal ellipsoids are shown at the 40% probability level. All hydrogen atoms and three molecules of dichloromethane have been omitted for clarity.

Compound **33** represents the first main group complex of the TIP ligand class. Single-crystal X-ray analysis revealed that **33** crystallizes in the monoclinic space group $P2_1/n$ with three molecules of dichloromethane. The solid state consists of an assembly of one $[(BCl_2)_2$Dipp-TIP$]^{2+}$ dication and two $[BCl_4]^-$ counterions. The average C-N and C(1)-C(5) bond distances for **33** of 1.281(9) Å and 1.501(10) Å, respectively, imply bond orders of two and one, respectively, thus indicating that both of the diimine functionalities form donor-acceptor bonds to a $[BCl_2]^+$ moiety. Both BN_2C_2 rings are essentially planar, as in the case of the analogous mononuclear BIAN complex[37]. Thus,

the formation of **33** indicates that the monofunctional Dipp-BIAN and bifunctional Dipp-TIP ligands undergo similar reactions with BCl_3, namely via heterolysis into $[BCl_2]^+$ and $[BCl_4]^-$ ions.

Synthesis and Characterization of $(TeI_2)_2$(Dipp-TIP) (34)

It is known that the Dipp-BIAN ligand forms the product (Dipp-BIAN)TeI_2 upon treatment with TeI_4[36]. This complex is of interest because TeI_2 does not exist in the solid state (but is stable in the vapor phase). It was therefore pertinent to explore the reaction of the bifunctional Dipp-TIP ligand with TeI_4 to determine whether the Te(IV)→Te(II) reduction would occur in a similar fashion to that of the analogous BIAN product. Reaction of the Dipp-TIP ligand with two equivalents of TeI_4 in dichloromethane resulted, after workup of the reaction mixture, in isolation of an analytically pure blue-green powder in 79% yield. Recrystallization of the crude solid from a saturated dichloromethane/hexanes solution resulted in the formation of a moderate crop of blue-green crystals. A single-crystal X-ray diffraction experiment was carried out and the resulting molecular structure is shown in Figure 3.05. Details regarding the data collection, structure solution and refinement are provided in Table 3.13 and a number of selected metrical parameters are listed in Tables 3.14 and 3.15.

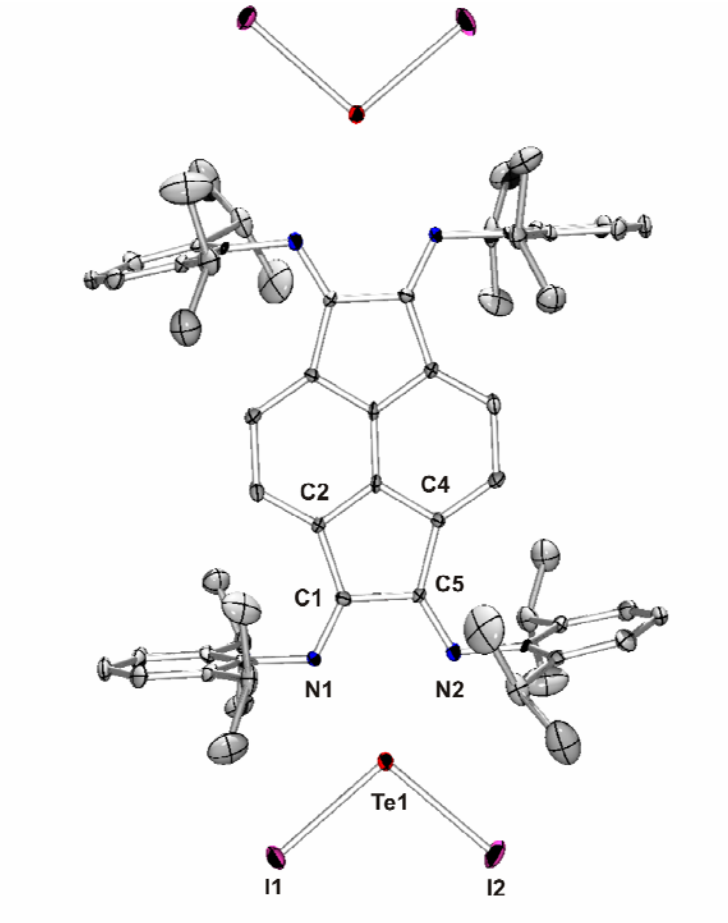

Figure 3.05. Molecular structure of 34 showing a partial numbering scheme. The thermal ellipsoids are shown at the 40% probability level. All hydrogen atoms and two molecules of dichloromethane have been omitted for clarity.

The average C-N and C-C bond distances for **34** of 1.285(5) Å and 1.509(6) Å, respectively, are similar to those reported for the free Dipp-TIP ligand[38], thus implying bond orders of two and one, respectively. A further objective of the synthesis of **34** was to explore the possibility that it could serve as a precursor to an unprecedented ditellurium tetracation. This is being investigated currently by treatment of **34** with a variety of halide ion abstraction reagents. Parallel studies are also being carried out with the (Dipp-BIAN)TeI_2 complex with the objective of preparing the corresponding tellurium dication.

Synthesis and Characterization of $(InX_3)_2$(Dipp-TIP) [X = Cl (35), Br (36), I (37)]

The compounds $(InX_3)_2$(Dipp-TIP) [X = Cl (**35**), Br (**36**), I (**37**)] were obtained by addition of dichloromethane to one equivalent of Dipp-TIP and two equivalents of the appropriate indium(III)halide. Following workup of the reaction mixtures, analytically pure orange-red solids were isolated in high yields (80-90%). Crystals of each compound that were suitable for analysis by single-crystal X-ray diffraction were obtained from saturated dichloromethane/hexanes solutions stored at room temperature for 3 days. Figures 3.06-3.08 depict the molecular structures of the three complexes as determined by single-crystal X-ray diffraction methods. Details of the data collection, structure solution and refinement are compiled in Tables 3.16 (**35**), 3.19 (**36**) and 3.22 (**37**) and a selection of metrical parameters is presented in Tables 3.17-3.18 (**35**), 3.20-3.21 (**36**) and 3.23-3.24 (**37**).

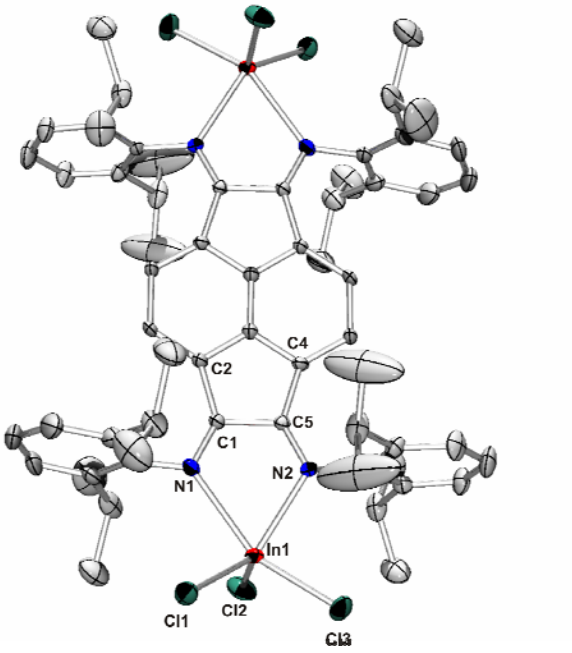

Figure 3.06. Molecular structure of 35 showing a partial numbering scheme. The thermal ellipsoids are shown at the 40% probability level. All hydrogen atoms and two molecules of dichloromethane have been omitted for clarity.

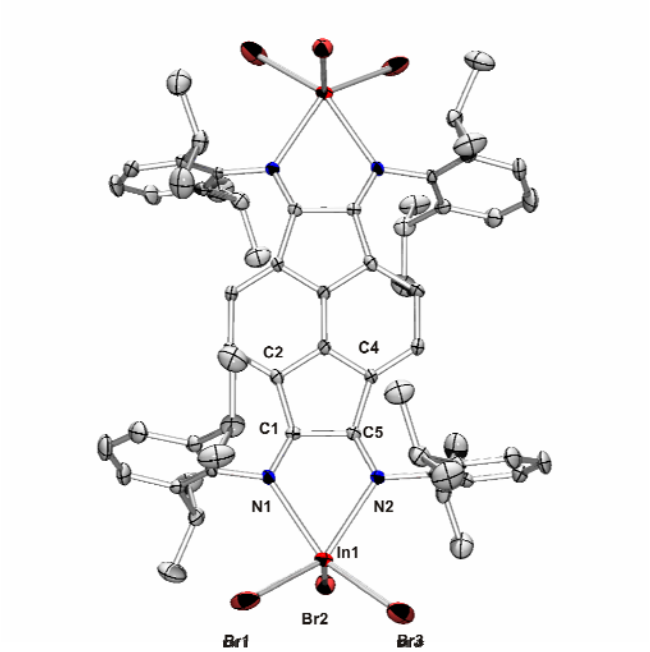

Figure 3.07. Molecular structure of 36 showing a partial numbering scheme. The thermal ellipsoids are shown at the 40% probability level. All hydrogen atoms and two molecules of dichloromethane have been omitted for clarity.

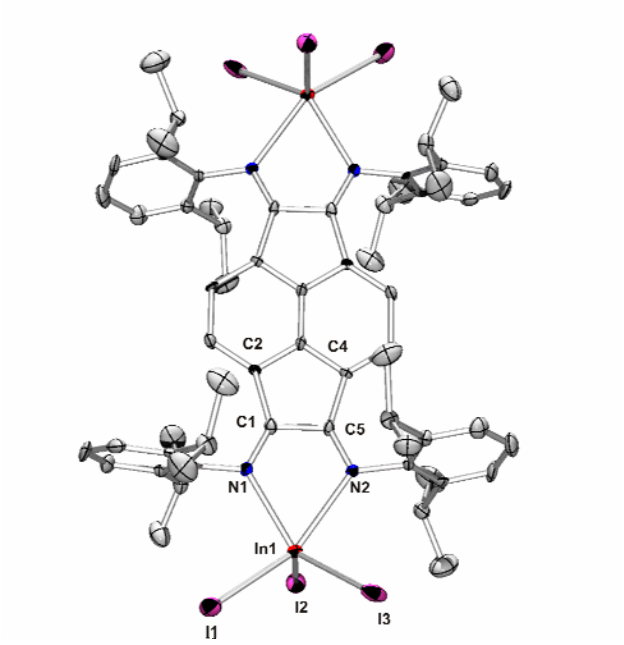

Figure 3.08. Molecular structure of 37 showing a partial numbering scheme. The thermal ellipsoids are shown at the 40% probability level. All hydrogen atoms and two molecules of dichloromethane have been omitted for clarity.

As expected the bond angles and bond distances are very similar for all three structures. The average C-N bond distances of 1.273(5) Å (**35**), 1.275(5) Å (**36**) and 1.279(5) Å (**37**) are all close to that reported for the free Dipp-TIP ligand[38] and imply a bond order of two. Correspondingly, the C(1)-C(5) bond distances of 1.541(6) Å (**35**), 1.529(5) Å (**36**) and 1.523(6) Å (**37**) imply a bond order of one for each complex, hence in each case the indium trihalide is anchored to the TIP ligand framework by N→In donor-acceptor bonds. Complexes **35-37** exhibit donor-acceptor character and indicate retention of In(III) ions.

Interestingly, the low resolution mass spectra of all three complexes exhibit a parent peak corresponding to the monometallic species. Based on the crystallographic data and the high symmetry evidenced by the ^{1}H NMR spectra, the likely explanation for this anomaly is the harsh nature of the ionization technique which results in the elimination of one of the two InX_3 molecules.

Future studies involving **37** are currently underway and involve iodide abstraction experiments, the goal of which is to synthesize novel indium-based cationic complexes. A further objective is to attempt the preparation of new main group metallopolymers by reduction of **35-37**.

Section 3.1 Conclusions

The donor-acceptor complexes **30** and **31** were prepared by treatment of the Dipp-TIP ligand with two equivalents of $PdCl_2$ and $PdBr_2$, respectively. Both reactions are high yielding and result in complexes that feature two palladium centers. It is expected that these compounds could find utility as catalysts for a number of organic transformations. However, such catalytic studies have not yet been attempted and

comparison of the activities of these bimetallic catalysts with those of the analogous monometallic BIAN analogues would be of interest.

One of the most intriguing TIP complexes synthesized thus far is that of **32**. Prepared from the Dipp-TIP ligand and two equivalents of $CuBr_2$, the polymeric nature of the complex was evident from the extremely poor solubility in a wide variety of polar solvents. The single-crystal X-ray structure revealed the formation of a polymer based on the monomeric [CuBr(Dipp-TIP)CuBr] unit. Compound **32** represents the first polymer based on a BIAN-type framework and superbly exploits the bifunctionality of the TIP ligand as a means of metallopolymer assembly.

Moving to the main group elements, the "heterolysis salt" $[(BCl_2)_2$(Dipp-TIP)$][BCl_4]_2$**, 33,** resulted from the addition of the Dipp-TIP ligand to four equivalents of BCl_3. The structure can be regarded as that of a diboron dication and could potentially serve as a precursor for the synthesis of an unprecedented diboron tetracation.

The compound $(TeI_2)_2$(Dipp-TIP) (**34**) can be synthesized from the reaction of the Dipp-TIP ligand with two equivalents of TeI_4. While the immediate structure represents a bifunctional version of the known BIAN analogue, (Dipp-BIAN)TeI_2, the potential utility of complex **34** lies in the prospect of halide abstraction. Studies involving iodide abstraction are currently underway, the purpose being to attempt the synthesis of the first ditellurium tetracation. Aside from the fundamental novelty of such a compound, the complex could also serve as a highly potent catalyst. Preliminary studies of the analogous monometallic BIAN complex have thus far shown the ability of the product to polymerize THF. This observation suggests the intermediacy of a cationic species.

The complexes of general form $(InX_3)_3$(DippTIP) [X = Cl (**35**), Br (**36**), I (**37**)], were prepared by treatment of the Dipp-TIP ligand with two equivalents of the respective indium(III)halide. All three complexes were synthesized in high yield and exhibit N→In donor-acceptor bonding. Halide ion abstraction studies of **37** to form TIP-based indium

cations are ongoing with the two-fold purpose of synthesizing novel main group catalysts and precursors for potential main group metallopolymers.

Section 3.2 Introduction

A series of reactions of the BIAN ligand with a wide variety of main group species has resulted in the isolation of several compounds that feature these elements in unusual oxidation states. For instance, Cowley *et al*. have used the BIAN ligand for capture of an elusive P(I) cation[20] and Fedushkin *et al*. have shown the utility of the poly-alkali salts of the BIAN ligand as reagents for metathetical reactions that generate *e.g.* BIAN-supported germylenes[39]. The potential applications of the TIP ligand complement those of the BIAN ligand but have the further advantages of supporting systems with intramolecular electronic communication as well as the synthesis of redox-active metallopolymers.

One of the primary goals of the studies detailed in Chapter 2 was the elucidation of the metal→ligand charge transfer processes associated with BIAN-supported lanthanocene complexes. By extending these studies to the TIP ligand, it seemed reasonable to expect the formation of TIP complexes bearing two lanthanide moieties, each of which would be capable of transferring one electron into the ligand manifold. The interest in this type of complex would be focused on the ability of the TIP ligand to accept electrons into the π-system and to explore the possibility that such electrons interact with each other.

Synthesis and Characterization of $[(BI)_2(Dipp\text{-}TIP)][I_5]$ (38)

The compound $[(BI)_2(Dipp\text{-}TIP)][I_5]$ (**38**) was synthesized by the treatment of Dipp-TIP with a two-fold excess of BI_3 in dichloromethane solution. A green solid was isolated in 70% yield following workup of the reaction mixture. Recrystallization of the crude solid from dichloromethane solution resulted in a small crop of dark green crystals. A single-crystal X-ray diffraction study revealed the molecular structure shown in Figure 3.09. Details of the data collection, structure solution and refinement are assembled in Table 3.25 and a selection of pertinent metrical parameters is provided in Tables 3.26 and 3.27.

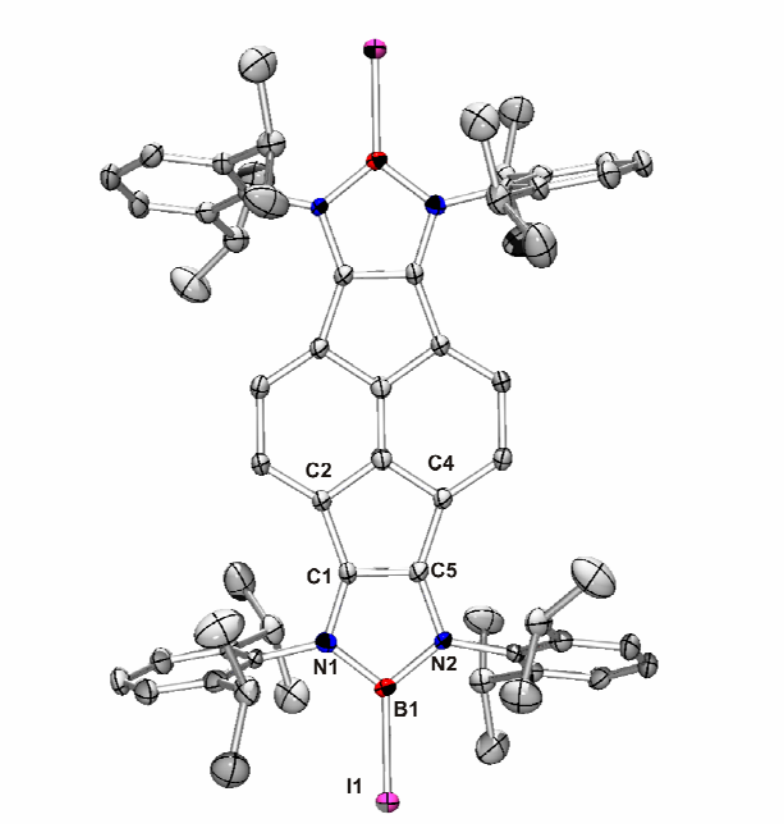

Figure 3.09. Molecular structure of the cation of 38 showing a partial numbering scheme. The thermal ellipsoids are shown at the 40% probability level. All hydrogen atoms and three molecules of dichloromethane have been omitted for clarity.

Interestingly, the structure of **38** features an $[I_5]^-$ anion, thus implying the presence of a positively charged TIP moiety. The average C-N bond distance of 1.372(7) Å and a C-C bond distance of 1.401(7) Å suggest assignment of C-N and C-C bond orders of one and two, respectively. However, this scenario renders assignment of a positive charge on the TIP complex problematic. Given the inability to acquire ^{1}H NMR spectroscopic data, it is reasonable to assume that the compound is paramagnetic and that a total of three electrons have been transferred from the two boron ions into the TIP ligand manifold. In this scenario, the complex would be regarded as a TIP-based radical cation. The most intense spectral peaks in the low resolution mass spectrum correspond to the $[(BI)_2(Dipp\text{-}TIP)]^+$ cation.

Synthesis and Characterization of $[(K(THF)_3)_2(Dipp\text{-}TIP)]$ (39)

The complex $[(K(THF)_3)_2(Dipp\text{-}TIP)]$ (**39**) was the sole product of the reaction of Dipp-TIP with two equivalents of potassium metal in THF solution. Following workup of the reaction mixture, **39** was isolated as a green solid in 86% yield. Crystals of **39** were grown from a saturated THF solution and examined by single-crystal X-ray diffraction. This experiment confirmed the identity of the product as the title compound shown in Figure 3.10. Details of the data collection, structure solution and refinement are compiled in Table 3.28. Selected metrical parameters are presented in Tables 3.29 and 3.30.

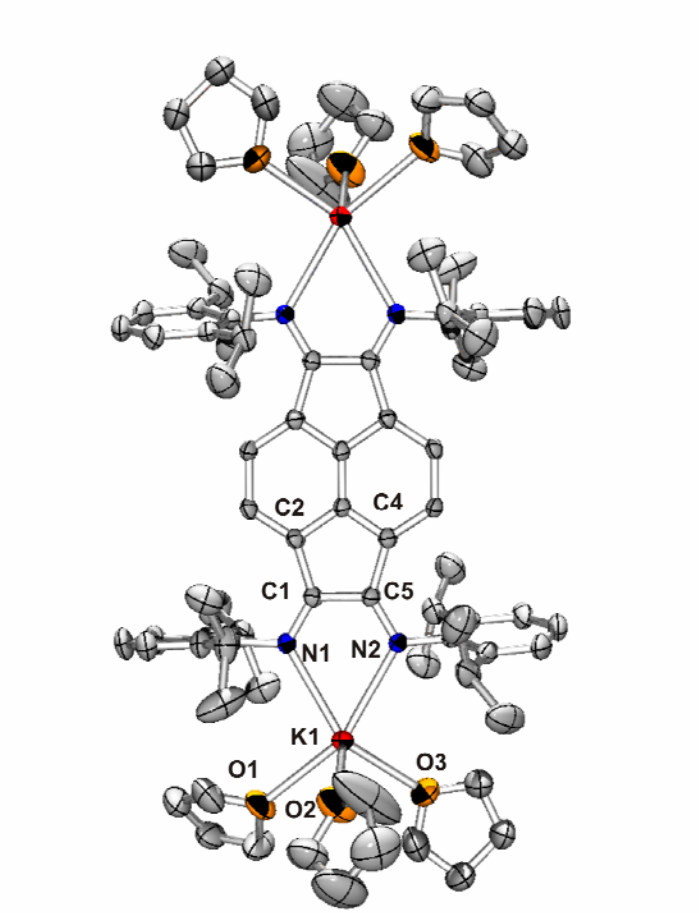

Figure 3.10. Molecular structure of 39 showing a partial numbering scheme. The thermal ellipsoids are shown at the 40% probability level. All hydrogen atoms have been omitted for clarity.

The crystal structure reveals the presence of a $K(THF)_3$ moiety bonded to either end of the TIP ligand. The structure of the H_4TIP ligand and the products of the sequential addition of two electrons were modelled under idealized D_{2h} symmetry by means of DFT/B3LYP calculations. The addition of two electrons to H_4TIP resulted in a computed C-N bond distance of 1.3294 Å and a computed C-C bond distance of 1.5040 Å. The observed average C-N and C(1)-C(5) bond distances in **39** of 1.312(7) Å and 1.485(6) Å, respectively, correlate well with the theoretical values and imply bond orders between one and two. Furthermore, the 0.021 Å contraction of the central C-C bond of the naphthalene fragment for **39** was also modelled satisfactorily. Overall, the foregoing

metrical parameters are consistent with the view that single-electron transfer has taken place at both diimine functionalities.

More detailed information was gleaned by interpretation of the ^{1}H NMR spectrum. Given that singly-reduced BIAN ligands are paramagnetic due to the presence of one unpaired electron, it was reasonable to expect that the corresponding reaction with the TIP ligand would result in two paramagnetic ends of the complex. However, the ^{1}H NMR spectrum of **39** consists of clearly distinguishable peaks, the chemical shifts of which are consistent with a diamagnetic product. It is evident that the two electrons pair, resulting in the formation of the observed diamagnetic complex. Based on the aforementioned work of John *et al.*[22], it was expected that the highly planar TIP ligand would provide a suitable framework for high electronic communication. Compound **39** is the first example where this feature is clearly observed in a TIP complex.

Synthesis and Characterization of $[(P)_2$(Dipp-TIP)$][I_3]_2$ (40)

The complex $[(P)_2$(Dipp-TIP)$][I_3]_2$ (**40**) was synthesized by treatment of one equivalent of Dipp-TIP with two equivalents of PI_3 in dichloromethane solution. A dark red powder was isolated in 84% yield following workup of the reaction mixture. Following recrystallization of the crude solid from a dichloromethane/hexanes solution, the molecular structure of **40** was established on the basis of a single-crystal X-ray diffraction study. Details of the data collection, structure solution and refinement are compiled in Table 3.31 and relevant metrical parameters are displayed in Tables 3.32 and 3.33.

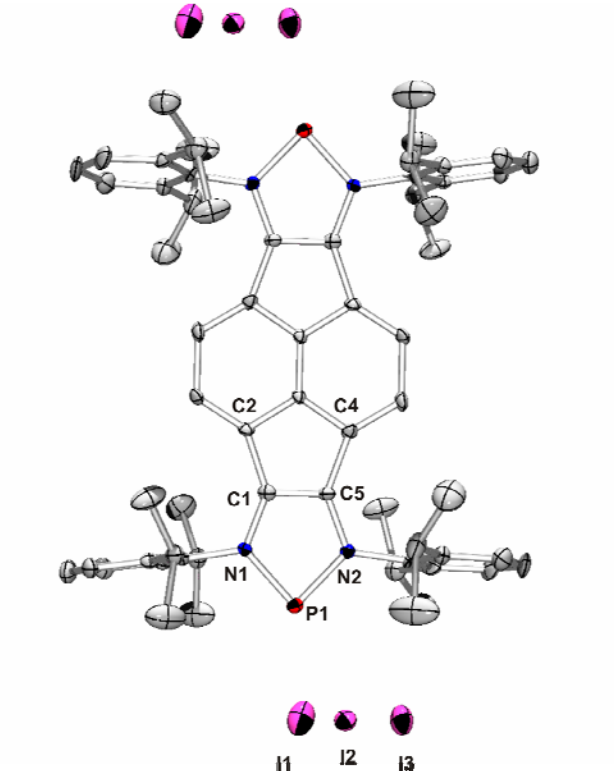

Figure 3.11. Molecular structure of 40 showing a partial numbering scheme. The thermal ellipsoids are shown at the 40% probability level. All hydrogen atoms and two dichloromethane molecules have been omitted for clarity.

Complex **40** crystallizes in the monoclinic space group $P2_1/c$ with two molecules of dichloromethane. The average C-N and C(1)-C(5) bond distances for **40** of 1.353(7) Å and 1.395(9) Å, respectively, imply bond orders of one and two, respectively. It is evident that a two-electron reduction occurs on either end of the molecule resulting in a TIP tetraanion. The complex can be regarded as a bis(phosphenium)cation accompanied by a pair of triiodide counterions.

The ^{1}H NMR spectrum of **40** comprises a clean set of resonances corresponding to those anticipated on the basis of the X-ray crystal structure, thus indicating that the product is diamagnetic. Furthermore, the diamagnetic nature of **40** suggests that the four electrons donated by the P ions are paired in the ligand manifold. Compound **40** represents the first example of a TIP ligand reduced by four electrons and thus further highlights the chemical versatility of the TIP ligand class.

Synthesis and Characterization of $[(C_5Me_5)_2Eu]_2$(p-F-TIP) (41)

The $[(C_5Me_5)_2Eu]_2$(p-F-TIP) (**41**) complex was synthesized by treatment of one equivalent of p-F-TIP with two equivalents of $(C_5Me_5)_2Eu\text{-}OEt_2$ in toluene solution. Following workup of the reaction, a dark red powder was isolated in 83% yield. A small crop of dark red crystals of **41** was obtained by recrystallization of the crude solid from a toluene/hexanes solution. One such crystal was examined by single-crystal X-ray diffraction and the molecular structure is depicted in Figure 3.12. Details of the data collection, structure solution and refinement are presented in Table 3.34 and pertinent metrical parameters are compiled in Tables 3.35 and 3.36.

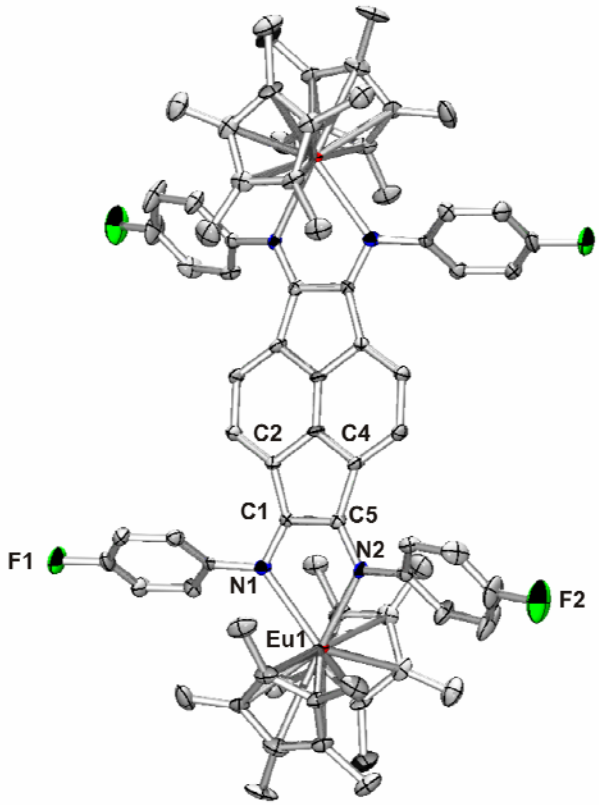

Figure 3.12. Molecular structure of 41 showing a partial numbering scheme. The thermal ellipsoids are shown at the 40% probability level. All hydrogen atoms and two molecules of toluene have been omitted for clarity.

The average C-N bond distance of 1.326(9) Å and the C(1)-C(5) bond distance of 1.480(10) Å imply bond orders of between one and two. On the basis of these metrical parameters and those of the analogous BIAN product [$(C_5Me_5)_2$Eu(p-F-BIAN)], it is evident that a one-electron reduction occurs on both ends of the molecule resulting in the formation of a p-F-TIP dianion. Both $(C_5Me_5)_2$Eu moieties evidently undergo significant steric repulsion from the p-F-phenyl substituents as evidenced by the average angle between the N(1)-Eu(1)-N(2) and N(1)-C(1)-C(5)-N(2) planes of 19.2(2)°, which imply a significant deviation of the Eu(III) ions from the ligand plane. Interestingly, and in contrast to the deep green color associated with the lanthanide-BIAN charge transfer products **19**-**27**, complex **41** is dark red-brown in color.

It was possible to detect a resonance at δ -21.9 in the ^{1}H NMR spectrum of **41**, attributable to the (C_5Me_5) protons. Evans *et al.* have reported a similar shift of δ -19.7 for Eu(III) complexes bearing (C_5Me_5) groups[27]. Preliminary solution state magnetic moment measurements obtained *via* the Evans method gave a value of 3.86 BM. Taken collectively, it is evident from the magnetic and spectral data that each $(C_5Me_5)_2$Eu moiety serves as a one electron reductant, thereby resulting in two $(C_5Me_5)_2$Eu(III) moieties supported by a doubly-reduced TIP ligand. Presumably, the presence of the electron withdrawing p-F substituents on the TIP ligand serves to facilitate this redox process.

Section 3.2 Conclusions

The complex [$(BI)_2$(Dipp-TIP)][I_5] (**38**) was prepared from the reaction of the Dipp-TIP ligand with two equivalents of BI_3. The X-ray crystal structure features an $[I_5]^-$ anion, thus implying a positively charged TIP complex. The average C-N and C-C bond distances suggest that transfer of three electrons from the BI fragments into the TIP

ligand has occurred. Since the electronic structure of **38** is not completely understood at the present time, further studies are in progress.

The dipotassium TIP complex $[(K(THF)_3)_2(Dipp\text{-}TIP)]$ (**39**) was synthesized by the addition of two equivalents of potassium metal to the Dipp-TIP ligand. The structure of **39** features two $K(THF)_3$ moieties attached to either end of the ligand. The resulting doubly-reduced TIP ligand is diamagnetic, thus indicating that the electrons pair up in the TIP ligand manifold. The bond lengths of **39** correlate well with the theoretical values modeled by the sequential addition of two electrons to the H_4TIP ligand. It is anticipated that **39** will serve as a useful reagent for the synthesis of novel TIP-supported transition metal and main group complexes. It may also find utility in the direct synthesis of TIP-based metallopolymers.

The addition of two equivalents of PI_3 to the Dipp-TIP ligand resulted in the formation of $[(P)_2(Dipp\text{-}TIP)][I_3]_2$ (**40**). The structure is best regarded as that of a bis(phosphenium) dication and represents the first example of a TIP tetraanion.

Finally, the $[(C_5Me_5)_2Eu]_2$(p-F-TIP) (**41**) complex was synthesized by the addition of two equivalents of $(C_5Me_5)_2Eu\text{-}OEt_2$ to the p-F-TIP ligand. The product features a $(C_5Me_5)_2Eu$ unit bonded to either end of the TIP ligand. Analysis of the bond distances indicates that one electron has been transferred from each Eu(II) ion, resulting in a complex that can be regarded as a TIP dianion coordinated to two $(C_5Me_5)_2Eu^+$ units. As in the case of the analogous monometallic BIAN complex, **19,** the ^{1}H NMR spectrum of **41** reveals a sharp signal at δ -21.3, thus providing further evidence for the occurrence of Eu→ligand charge transfers and formation of the TIP dianion complex.

Experimental Section

General Considerations. All manipulations were performed in a dry and oxygen-free argon atmosphere by using standard Schlenk or glove-box techniques. Toluene, THF and hexanes were dried over Na and freshly distilled prior to use. Dichloromethane was dried over CaH_2 and freshly distilled prior to use. All transition metal and main group starting materials were used without further purification from Aldrich or Strem. The starting materials $(C_5Me_5)_2Eu\text{-}OEt_2$[25] and Dipp-TIP[38] were synthesized according to published procedures.

Physical Measurements. Low-resolution CI mass spectra were collected on a Finnigan MAT TSQ-700 mass spectrometer. High resolution mass spectra were acquired on a VG Analytical ZAB-VE sector instrument. All ^{1}H, ^{11}B and ^{31}P NMR spectra were recorded at 295 K on a Varian 300 MHz NMR spectrometer. Deuterated solvents were obtained from Cambridge Isotopes and stored over molecular sieves prior to use. The ^{1}H spectra are reported relative to tetramethylsilane and referenced to solvent. The ^{11}B and ^{31}P spectra are reported relative to $BF_3{\cdot}OEt_2$ and H_3PO_4, respectively. Melting points were obtained on a Fisher-Johns apparatus and are reported uncorrected.

X-Ray Crystallography. The X-ray data were collected on a Nonius Kappa CCD diffractometer equipped with an Oxford Cryostream liquid nitrogen cooling stream. Samples were covered with mineral oil and mounted on a nylon thread loop prior to data collection. All data collections were performed at 153(2) K using graphite-monochromated Mo Kα radiation (λ = 0.71073 Å). A correction was applied for Lorentz-polarization in each case. All structures were solved by direct methods and refined by full-matrix least squares on F^2 using the Siemens SHELXL PLUS 5.0 (PC) software package[5]. All hydrogen atoms were either placed in calculated positions (C-H = 0.96 Å) and refined using a riding model and a general isotropic thermal parameter or assigned manually.

Preparation of $(PdCl_2)_2$(Dipp-TIP) (30)

To a flask charged with Dipp-TIP (0.030 g, 0.034 mmol) and $PdCl_2$ (0.012 g, 0.069 mmol) was added acetonitrile (10 mL) and the resulting mixture was stirred at reflux for 1 h. Cooling of the reaction mixture and stripping of solvent afforded a red solid. The crude solid was washed with deionized water (5 mL) and cold diethyl ether (2 mL) and dried, resulting in an analytically pure red powder. The solid was dissolved in dichloromethane, filtered and allowed to slowly evaporate over 3 days, affording a crop of red crystalline blocks. Yield 0.112 g (78.3%).

MS (CI^+, CH_4): *m/z* 1227 $[M+H]^+$; HRMS (CI^+, CH_4): calcd for $C_{62}H_{72}N_4Pd_2Cl_4$ *m/z* 1227.3122; found, 1227.3130; ^1H NMR (CD_2Cl_2): δ 0.90 (d, 24H, CH_3), 1.45 (d, 24H, CH_3), 3.31 (sept, 8H, -CH), 6.50 (d, 4H, NapC-H), 7.38 (d, 8H, Ar-H), 7.55 (t, 4H, Ar-H); IR (cm^{-1}): 1771s, 1625s, 1601s, 1586, 1458, 1440, 1300, 1187, 1064; mp 299(d).

Preparation of $(PdBr_2)_2$(Dipp-TIP) (31)

To a flask charged with Dipp-TIP (0.030 g, 0.034 mmol) and $PdBr_2$ (0.037 g, 0.069 mmol) was added acetonitrile (10 mL) and the resulting mixture was stirred at reflux for 45 min. Cooling of the reaction mixture and stripping of solvent afforded a dark red solid which was washed with deionized water (5 mL) and cold diethyl ether (2 mL) and dried, resulting in an analytically pure red powder. The solid was dissolved in dichloromethane, filtered and allowed to slowly evaporate for 3 days, affording a crop of dark red crystalline blocks. Yield 0.053 g (79.1%).

MS (CI^+, CH_4): *m/z* 1405 $[M+H]^+$; HRMS (CI^+, CH_4): calcd for $C_{62}H_{72}N_4Pd_2Br_4$ *m/z* 1405.2332; found, 1405.2326; ^1H NMR (CD_2Cl_2): δ 0.86 (d, 24H, CH_3), 1.44 (d, 24H, CH_3), 3.29 (sept, 8H, -CH), 6.46 (d, 4H, NapC-H), 7.37 (d, 8H, Ar-H), 7.51 (t, 4H, Ar-H); IR (cm^{-1}): 1722s, 1627s, 1603s, 1586s, 1451, 1441s, 1364, 1296, 1187s, 1065s; mp 291(d).

Preparation of $[(CuBr)_2(Dipp\text{-}TIP)]_n$ (32)

$CuBr_2$ (2.60 mg, 0.0115 mmol) was dissolved in ethanol (2 mL) and added to an NMR tube. A THF (2 mL) solution of Dipp-TIP (5.00 mg, 0.0057 mmol) was layered on top of the ethanolic solution and the system sealed and stored at room temperature for 7 days, during which time green crystals were observed to be growing at the solvent interface. After a period of 2 weeks, a crop of green crystals had collected at the bottom of the tube and was isolated by filtration. Yield 5.5 mg (72.1%).

MS (CI^+, CH_4): *m/z* 1156 $[M+H]^+$; HRMS (CI^+, CH_4): calcd for $C_{62}H_{72}Cu_2Br_2$ *m/z* 1156.2716; found, 1156.2726; ^1H NMR (CD_3CN): δ 0.83 (b, s, 24H), 1.24 (b, s, 24H), 3.08 (b, s, 8H), 6.41 (b, s, 4H), 7.37 (b, s, 12H).

Preparation of $[(BCl_2)_2(Dipp\text{-}TIP)][BCl_4]_2$ (33)

BCl_3 (0.20 mL [0.202 mmol] of 1.0 M solution in hexanes) was added to a flask charged with Dipp-TIP (0.044 g, 0.050 mmol) in dichloromethane (20 mL) and the resulting deep green solution was stirred for 12 h. Solvent stripping afforded a green solid that was

recrystallized from a saturated dichloromethane solution stored at -15°C for 7 days. Yield 0.063 g (93.2%).

MS (CI^+, CH_4): *m/z* 1036 $[M+H]^+$; HRMS (CI^+, CH_4): calcd for $C_{62}H_{72}B_2Cl_4$ *m/z* 1037.6367; found, 1037.6360; ^1H NMR (CD_2Cl_2): δ 0.93 (d, 24H), 1.33 (d, 24H), 3.15 (sept, 8H), 6.83 (d, 4H), 7.44 (br, m, 12H); ^{11}B NMR (CD_2Cl_2): δ 13.81.

Preparation of [$(TeI_2)_2$(Dipp-TIP)] (34)

Dichloromethane (40 mL) was added to a flask charged with Dipp-TIP (0.03 g, 0.034 mmol) and TeI_4 (0.044 g, 0.069 mmol) and the resulting blue-green solution was stirred for 12 h. The solvent was stripped and the crude solid rinsed with hexanes (3 x 10 mL) to remove residual iodine. A saturated 4:1 dichloromethane/hexanes solution of the crude solid was filtered and stored at -15°C for 6 days, affording a crop of blue-green crystalline blocks. Yield 0.044 g (79.0%).

MS (CI^+, CH_4): *m/z* 1635 $[M+H]^+$; ^1H NMR (CD_2Cl_2): δ 0.96 (d, 24H, CH_3), 1.36 (d, 24H, CH_3), 3.00 (sept, 8H, -CH), 6.77 (d, 4H, NapC-H), 7.44 (b, 8H, Ar-H), 8.16 (t, 4H, Ar-H); IR (cm^{-1}): 3054s, 2987s, 1604s, 1551s, 1422s, 1265s, 896, 739s.

Preparation of [$(InCl_3)_2$(Dipp-TIP)] (35)

Dichloromethane (20 mL) was added to a flask charged with Dipp-TIP (0.025 g, 0.029 mmol) and $InCl_3$ (0.013 g, 0.059 mmol) and the resulting orange mixture was stirred for 12 h. The solvent was stripped and the crude solid dissolved in a minimal volume of a

4:1 dichloromethane/hexanes solution. The resulting red solution was filtered and stored at room temperature for 5 days, affording a crop of red crystals. Yield 0.032 g (84.3%). MS (CI^+, CH_4): *m/z* 1094 (M-$InCl_3$) $[M+H]^+$; ^1H NMR ($CDCl_3$): δ 0.69 (d, 24H, CH_3), 1.31 (d, 24H, CH_3), 2.95 (sept, 8H, -CH), 6.54 (d, 4H, NapC-H), 7.30 (b, 8H, Ar-H), 7.45 (t, 4H, Ar-H); IR (cm^{-1}): 1727s, 1631s, 1462, 1362s, 1073s, 748s.

Preparation of [$(InBr_3)_2$(Dipp-TIP)] (36)

Dichloromethane (20 mL) was added to a flask charged with Dipp-TIP (0.025 g, 0.029 mmol) and $InBr_3$ (0.021 g, 0.059 mmol) and the resulting orange mixture was stirred for 12 h. Following solvent stripping, the resulting crude solid was recrystallized from a saturated 4:1 dichloromethane/hexanes solution stored at room temperature for 5 days. Yield 0.041 g (89.1%).

MS (CI^+, CH_4): *m/z* 1226 (M-$InBr_3$) $[M+H]^+$; ^1H NMR ($CDCl_3$): δ 0.75 (d, 24H, CH_3), 1.30 (d, 24H, CH_3), 2.94 (sept, 8H, -CH), 6.58 (d, 4H, NapC-H), 7.35 (b, 8H, Ar-H), 7.49 (t, 4H, Ar-H); IR (cm^{-1}): 1655s, 1617s, 1460s, 1360, 1093, 1020, 797s.

Preparation of [$(InI_3)_2$(Dipp-TIP)] (37)

Dichloromethane (20 mL) was added to a flask charged with Dipp-TIP (0.025 g, 0.029 mmol) and InI_3 (0.030 g, 0.060 mmol) and the resulting orange mixture was stirred for 12 h. Solvent stripping resulted in isolation of a red-orange solid. The crude solid was

recrystallized from a saturated 4:1 dichloromethane/hexanes solution stored at room temperature for 5 days. Yield 0.048 g (87.2%).

MS (CI^+, CH_4): *m/z* 1368 (M-InI_3) $[M+H]^+$; ^1H NMR ($CDCl_3$): δ 0.66 (d, 24H, CH_3), 1.35 (d, 24H, CH_3), 2.95 (sept, 8H, -CH), 6.61 (d, 4H, NapC-H), 7.40 (b, 8H, Ar-H), 7.53 (t, 4H, Ar-H); IR (cm^{-1}): 1660s, 1611s, 1584, 1459s, 1365, 896, 739s.

Preparation of $[(BI)_2$(Dipp-TIP)$][I_5]$ (38)

Dichloromethane (25 mL) was added to a flask charged with Dipp-TIP (0.050 g, 0.057 mmol) and BI_3 (0.045 g, 0.115 mmol) and the resulting deep green solution stirred for 12 h. Removal of solvent resulted in a dark green solid which was dissolved in a minimal volume of a 5:1 dichloromethane/hexanes solution. Storage for 4 days at-15°C resulted in a crop of green crystalline blocks of **38**. Yield 0.071 g (69.9%).

MS (CI^+, CH_4): *m/z* 1149 $[M+H]^+$; HRMS (CI^+, CH_4): calcd for $C_{62}H_{72}N_4I_2B_2$ *m/z* 1146.4105; found, 1146.4105; magnetic moment (Evans method), 1.74 BM.

Preparation of $[(K(THF)_3)_2$(Dipp-TIP)] (39)

THF (45 mL) was added to a flask charged with Dipp-TIP (0.033 g, 0.038 mmol) and freshly cut potassium metal (0.003 g, 0.077 mmol). The resulting reaction mixture was stirred for 24 h. Stripping of solvent resulted in an analytically pure dark green solid which was recrystallized from a 1:1 THF/toluene mixture stored at -15°C for 6 days. Yield 0.045 g (85.6%).

^{1}H NMR (CD_2Cl_2): δ 0.91 (b, 24H, Me-H), 1.17 (b, 24H, Me-H), 1.82 (b, 24H, THF), 2.86 (sept, 8H, Me_2C-H), 3.68 (b, 24H, THF), 6.44 (b, 4H, Nap-H), 7.23 (b, 12H, Ar-H).

Preparation of $[(P)_2$(Dipp-TIP)$][I_3]_2$ (40)

Dichloromethane (30 mL) was added to a flask charged with Dipp-TIP (0.025 g, 0.029 mmol) and PI_3 (0.024 g, 0.058 mmol) and the resulting green-brown solution was stirred for 12 h. Following solvent stripping, a dark red-brown solid was isolated. The crude solid was dissolved in a 9:1 dichloromethane/hexanes solution, filtered and stored at -15°C for 6 days, affording a crop of dark red crystalline blocks of **40**. Yield 0.041 g (83.7%).

MS (CI^+, CH_4): *m/z* 935 $[M+H]^+$; HRMS (CI^+, CH_4): calcd for $C_{62}H_{72}N_4P_2$ *m/z* 934.5238; found, 934.5232; ^{1}H NMR ($CDCl_3$): δ 1.23 (d, 24H, CH_3), 1.33 (d, 24H, CH_3), 3.01 (sept, 8H, -CH), 5.92 (d, 4H, NapC-H), 7.43 (b, 8H, Ar-H), 7.63 (t, 4H, Ar-H); ^{31}P NMR ($CDCl_3$): δ 237.7.

Preparation of $[(C_5Me_5)_2Eu]_2$(p-F-TIP) (41)

Toluene (30 mL) was added to a flask charged with p-F-TIP (0.025 g, 0.041 mmol) and $(C_5Me_5)_2$Eu-OEt_2 (0.041 g, 0.083 mmol) and the resulting red-brown solution was stirred for 12 h. Solvent stripping resulted in isolation of a dark red-brown powder. The crude solid was recrystallized from a saturated 9:1 toluene/hexanes solution stored at -15°C for 6 days. Yield 0.049 g (83.1%).

^{1}H NMR ($CDCl_3$): δ -21.9 (s, C_5Me_5); magnetic moment (Evans method) 3.86 BM.

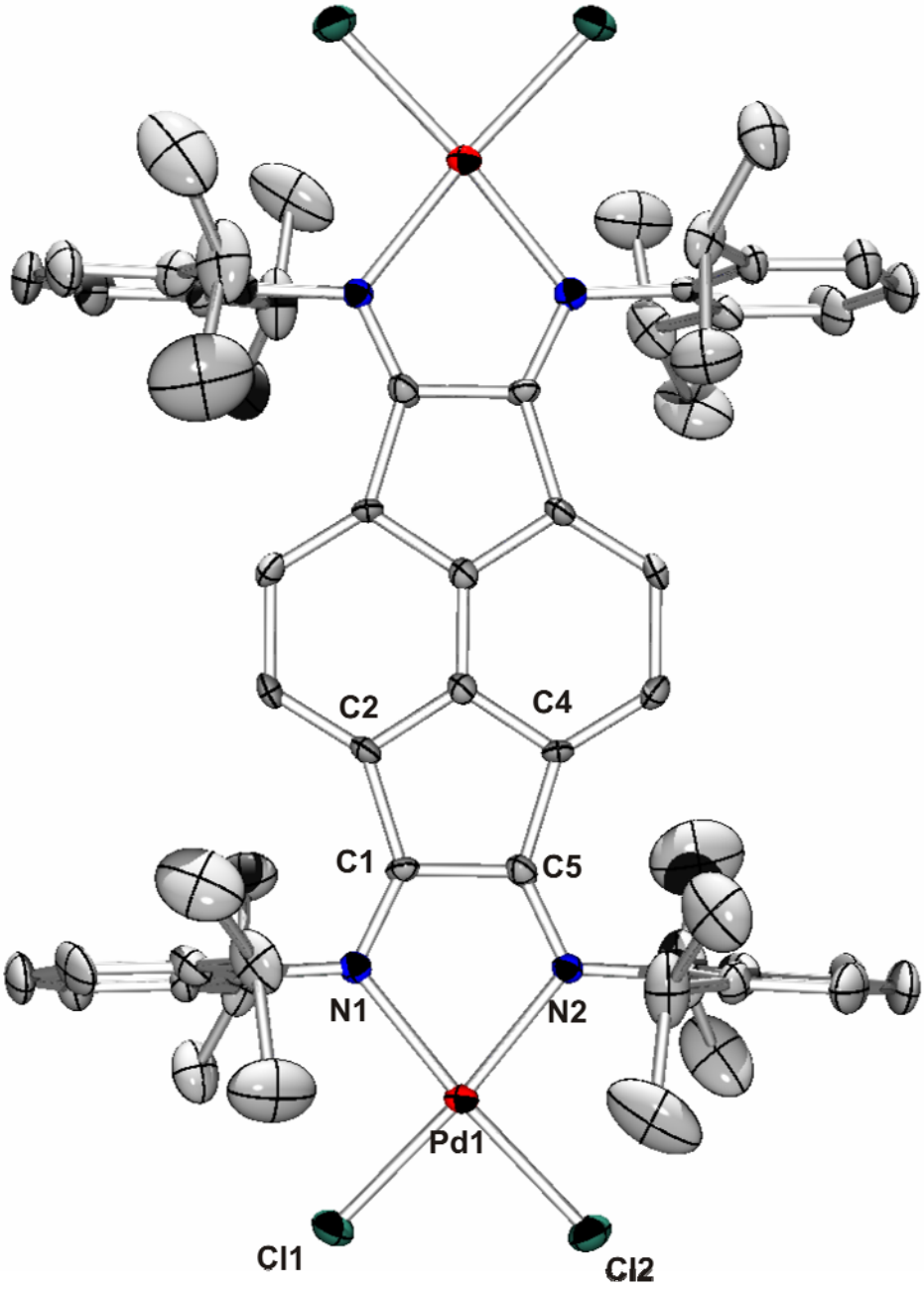

Figure 3.01. Molecular structure of 30 showing a partial numbering scheme. The thermal ellipsoids are shown at the 40% probability level. All hydrogen atoms and two molecules of dichloromethane have been omitted for clarity.

Table 3.01. Crystal data and structure refinement for 30.

Identification code	kvkv083a	
Empirical formula	C62 H72 Cl4 N4 Pd2	
Formula weight	1397.69	
Temperature	153(2) K	
Wavelength	0.71073 Å	
Crystal system	Orthorhombic	
Space group	Pbca	
Unit cell dimensions	a = 19.460(4) Å	α= 90°.
	b = 15.257(3) Å	β= 90°.
	c = 23.428(5) Å	γ = 90°.
Volume	6956(2) $Å^3$	
Z	4	
Density (calculated)	1.335 Mg/m^3	
Absorption coefficient	0.863 mm^{-1}	
F(000)	2864	
Crystal size	0.22 x 0.15 x 0.13 mm^3	
Theta range for data collection	1.74 to 27.49°.	
Index ranges	-25<=h<=25, -18<=k<=19, -30<=l<=30	
Reflections collected	25747	
Independent reflections	7963 [R(int) = 0.1078]	
Completeness to theta = 27.49°	99.8 %	
Absorption correction	None	
Refinement method	Full-matrix least-squares on F^2	
Data / restraints / parameters	7963 / 0 / 360	
Goodness-of-fit on F^2	1.087	
Final R indices [I>2sigma(I)]	R1 = 0.0830, wR2 = 0.2341	
R indices (all data)	R1 = 0.1575, wR2 = 0.2817	
Largest diff. peak and hole	3.063 and -1.726 $e.Å^{-3}$	

Table 3.02. Selected Bond Lengths (Å) for $(PdCl_2)_2$(Dipp-TIP) (30)

C1-C2	1.483(10)
C1-C5	1.484(10)
C1-N1	1.297(9)
C4-C5	1.480(10)
C5-N2	1.281(9)
N1-Pd1	2.051(6)
N2-Pd1	2.048(6)
Cl1-Pd1	2.270(2)
Cl2-Pd2	2.268(2)

Table 3.03. Selected Bond Angles (°) for $(PdCl_2)_2$(Dipp-TIP) (30)

C1-C5-C4	107.3(6)
C1-C5-N2	117.4(6)
C1-N1-Pd1	112.3(5)
C2-C1-C5	108.8(6)
C2-C1-N1	134.4(7)
C4-C5-N2	135.2(7)
C5-N1-C1	116.7(6)
C5-N2-Pd1	112.6(5)
N1-Pd1-N2	80.8(2)
N1-Pd1-Cl1	93.96(18)
N1-Pd1-Cl2	174.82(18)
N2-Pd1-Cl1	173.57(18)
N2-Pd1-Cl2	94.17(17)

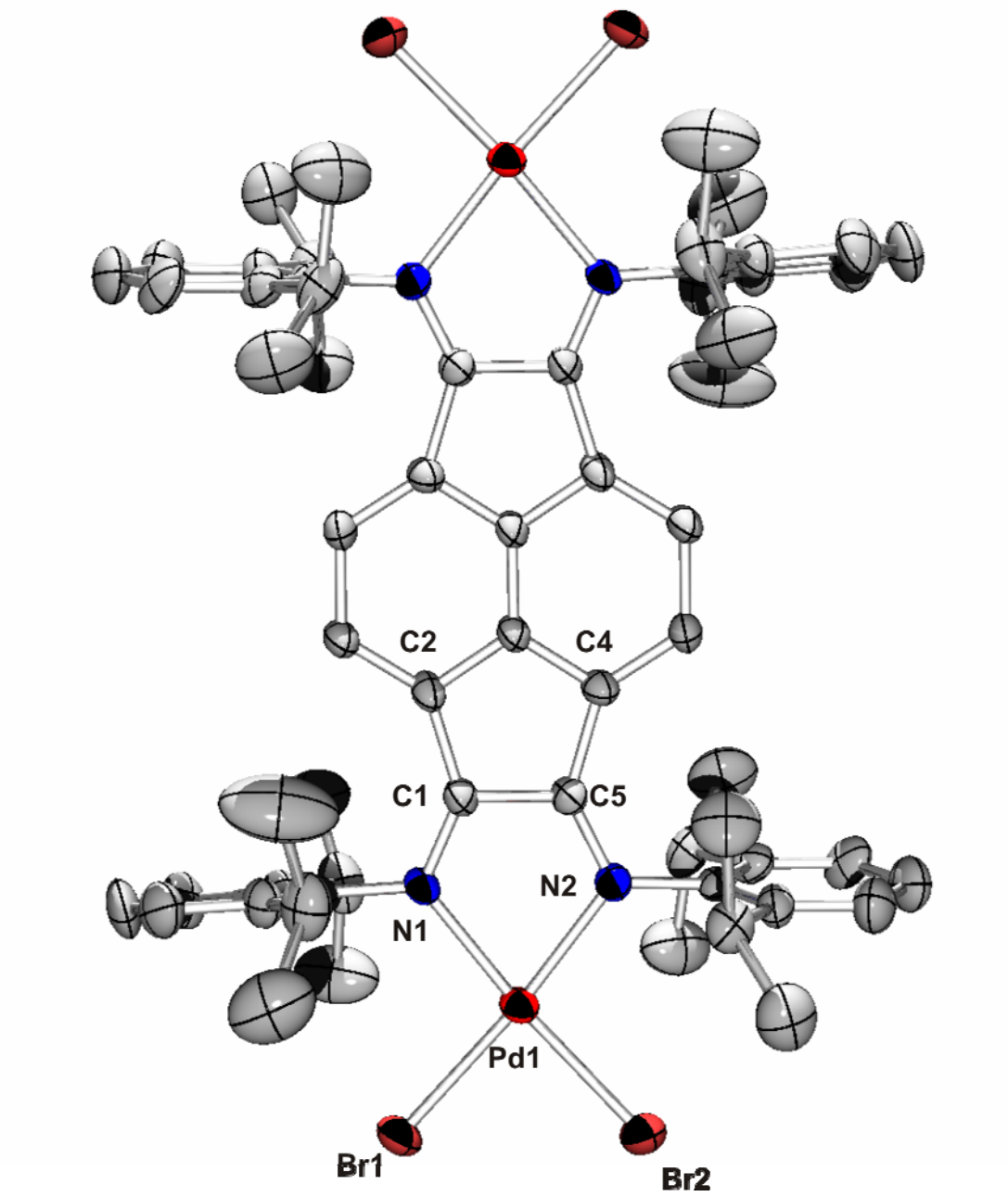

Figure 3.02. Molecular structure of 31 showing a partial numbering scheme. The thermal ellipsoids are shown at the 40% probability level. All hydrogen atoms have been omitted for clarity.

Table 3.04. Crystal data and structure refinement for 31.

Identification code	kv076b	
Empirical formula	C62 H72 Br4 N4 Pd2	
Formula weight	1405.68	
Temperature	153(2) K	
Wavelength	0.71073 Å	
Crystal system	Orthorhombic	
Space group	Pbca	
Unit cell dimensions	a = 19.605(5) Å	α= 90.000(5)°.
	b = 15.173(5) Å	β= 90.000(5)°.
	c = 23.927(5) Å	γ = 90.000(5)°.
Volume	7117(3) $Å^3$	
Z	4	
Density (calculated)	1.312 Mg/m^3	
Absorption coefficient	2.785 mm^{-1}	
F(000)	2816	
Crystal size	0.15 x 0.12 x 0.10 mm^3	
Theta range for data collection	1.90 to 27.55°.	
Index ranges	-24<=h<=25, -19<=k<=19, -31<=l<=31	
Reflections collected	26799	
Independent reflections	8177 [R(int) = 0.0623]	
Completeness to theta = 27.55°	99.5 %	
Absorption correction	None	
Refinement method	Full-matrix least-squares on F^2	
Data / restraints / parameters	8177 / 0 / 333	
Goodness-of-fit on F^2	1.062	
Final R indices [I>2sigma(I)]	R1 = 0.0672, wR2 = 0.1729	
R indices (all data)	R1 = 0.1095, wR2 = 0.1906	
Largest diff. peak and hole	2.508 and -1.527 $e.Å^{-3}$	

Table 3.05. Selected Bond Lengths (Å) for $(PdBr_2)_2$(Dipp-TIP) (31)

C1-C2	1.454(8)
C1-C5	1.503(7)
C1-N1	1.288(7)
C4-C5	1.482(7)
C5-N2	1.289(7)
N1-Pd1	2.061(4)
N2-Pd1	2.068(4)
Br1-Pd1	2.3889(8)
Br2-Pd2	2.3949(9)

Table 3.06. Selected Bond Angles (°) for $(PdBr_2)_2$(Dipp-TIP) (31)

C1-C5-C4	107.8(5)
C1-C5-N2	117.9(5)
C1-N1-Pd1	113.7(3)
C2-C1-C5	107.6(4)
C2-C1-N1	136.7(5)
C4-C5-N2	134.4(5)
C5-N1-C1	115.7(5)
C5-N2-Pd1	112.3(3)
N1-Pd1-N2	80.32(17)
N1-Pd1-Br1	94.48(11)
N1-Pd1-Br2	174.02(12)
N2-Pd1-Br1	174.41(13)
N2-Pd1-Br2	94.89(13)

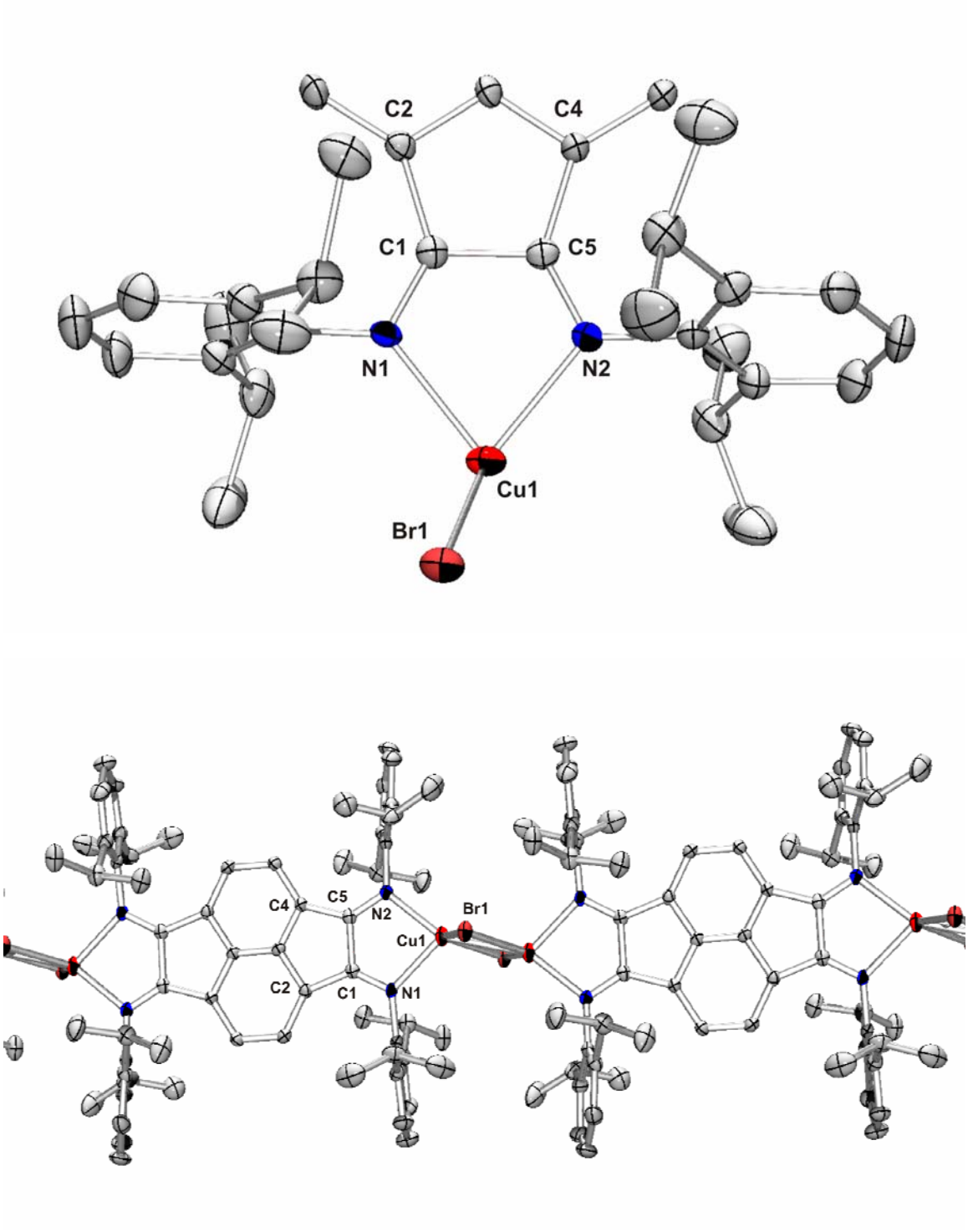

Figure 3.03. Molecular structure of 32 showing a partial numbering scheme. The thermal ellipsoids are shown at the 40% probability level. All hydrogen atoms and one molecule of THF have been omitted for clarity.

Table 3.07. Crystal data and structure refinement for 32.

Identification code	ccdkvkv059a	
Empirical formula	C35 H44 Br Cu N2 O	
Formula weight	652.17	
Temperature	153(2) K	
Wavelength	0.71073 Å	
Crystal system	Monoclinic	
Space group	P21/c	
Unit cell dimensions	a = 13.719(3) Å	α= 90°.
	b = 13.400(3) Å	β= 106.77(3)°.
	c = 19.628(4) Å	γ = 90°.
Volume	3454.9(12) $Å^3$	
Z	4	
Density (calculated)	1.254 Mg/m^3	
Absorption coefficient	1.816 mm^{-1}	
F(000)	1360	
Crystal size	0.20 x 0.20 x 0.15 mm^3	
Theta range for data collection	1.87 to 27.41°.	
Index ranges	-17<=h<=17, -14<=k<=17, -23<=l<=25	
Reflections collected	22151	
Independent reflections	7850 [R(int) = 0.0683]	
Completeness to theta = 27.41°	99.9 %	
Absorption correction	None	
Refinement method	Full-matrix least-squares on F^2	
Data / restraints / parameters	7850 / 0 / 369	
Goodness-of-fit on F^2	1.068	
Final R indices [I>2sigma(I)]	R1 = 0.0678, wR2 = 0.2037	
R indices (all data)	R1 = 0.1318, wR2 = 0.2403	
Largest diff. peak and hole	3.207 and -0.736 $e.Å^{-3}$	

Table 3.08. Selected Bond Lengths (Å) for $[(CuBr)_2(Dipp\text{-}TIP)]_n$ (32)

C1-C2	1.495(7)
C1-C5	1.504(8)
C1-N1	1.276(7)
C4-C5	1.493(7)
C5-N2	1.274(7)
Br1-Cu1	2.4132(11)

Table 3.09. Selected Bond Angles (°) for $[(CuBr)_2(Dipp\text{-}TIP)]_n$ (32)

C1-C5-C4	107.8(4)
C1-C5-N2	118.5(2)
C1-N1-Cu1	110.4(4)
C2-C1-C5	107.0(4)
C2-C1-N1	134.0(5)
C4-C5-N2	133.3(5)
C5-C1-N1	118.6(5)
C5-N2-Cu1	110.0(4)
N1-Cu1-N2	80.52(16)
N1-Cu1-Br1	126.90(13)

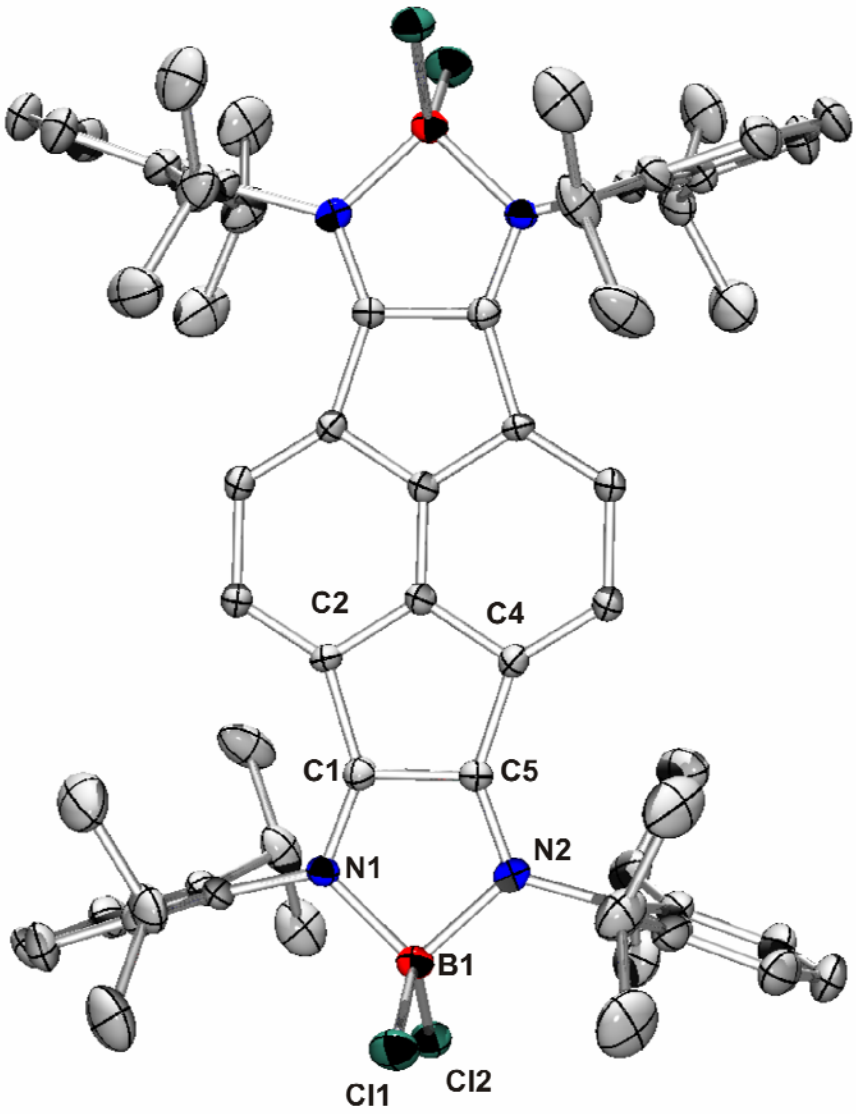

Figure 3.04. Molecular structure of the cation of 33 showing a partial numbering scheme. The thermal ellipsoids are shown at the 40% probability level. All hydrogen atoms and three dichloromethane molecules have been omitted for clarity.

Table 3.10. Crystal data and structure refinement for 33.

Identification code	borondicat	
Empirical formula	C65 H78 B4 Cl14 N4	
Formula weight	1454.55	
Temperature	153(2) K	
Wavelength	0.71073 Å	
Crystal system	Monoclinic	
Space group	P21/n	
Unit cell dimensions	a = 16.075(3) Å	α= 90°.
	b = 16.312(3) Å	β= 106.66(3)°.
	c = 17.424(4) Å	γ = 90°.
Volume	4377.2(15) $Å^3$	
Z	4	
Density (calculated)	1.405 Mg/m^3	
Absorption coefficient	0.786 mm^{-1}	
F(000)	1896	
Crystal size	0.20 x 0.11 x 0.10 mm^3	
Theta range for data collection	1.52 to 27.20°.	
Index ranges	-20<=h<=20, -20<=k<=20, -22<=l<=22	
Reflections collected	9562	
Independent reflections	9562 [R(int) = 0.0000]	
Completeness to theta = 27.20°	98.0 %	
Absorption correction	None	
Refinement method	Full-matrix least-squares on F^2	
Data / restraints / parameters	9562 / 0 / 461	
Goodness-of-fit on F^2	1.028	
Final R indices [I>2sigma(I)]	R1 = 0.1189, wR2 = 0.3085	
R indices (all data)	R1 = 0.1873, wR2 = 0.3692	
Extinction coefficient	0.0021(7)	
Largest diff. peak and hole	1.187 and -1.165 $e.Å^{-3}$	

Table 3.11. Selected Bond Lengths (Å) for $[(BCl_2)_2(Dipp\text{-}TIP)][BCl_4]_2$ (33)

C1-C2	1.459(9)
C1-C5	1.503(9)
C1-N1	1.281(8)
C4-C5	1.461(9)
C5-N2	1.277(8)
N1-B1	1.620(9)
N2-B1	1.663(9)
Cl1-B1	1.786(8)
Cl2-B2	1.789(8)

Table 3.12. Selected Bond Angles (°) for $[(BCl_2)_2(Dipp\text{-}TIP)][BCl_4]_2$ (33)

C1-C5-C4	108.3(5)
C1-C5-N2	111.7(6)
C1-N1-B1	109.6(5)
C2-C1-C5	108.8(5)
C2-C1-N1	139.4(6)
C4-C5-N2	139.7(6)
C5-N1-C1	111.6(6)
C5-N2-B1	109.3(5)
N1-B1-N2	97.5(5)
N1-B1-Cl1	111.0(5)
N1-B1-Cl2	111.5(5)
N2-B1-Cl1	111.6(5)
N2-B1-Cl2	111.0(5)

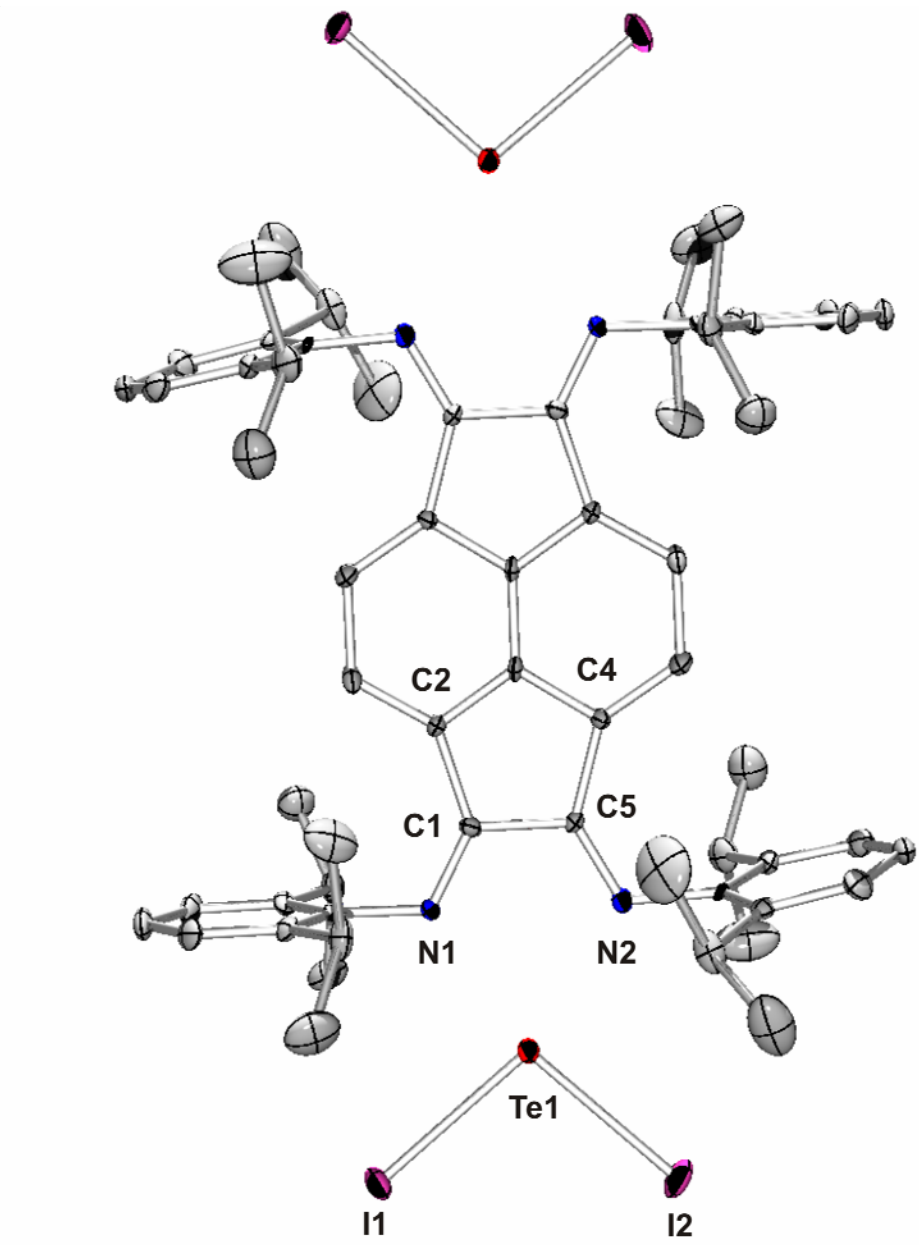

Figure 3.05. Molecular structure of 34 showing a partial numbering scheme. The thermal ellipsoids are shown at the 40% probability level. All hydrogen atoms and two molecules of dichloromethane have been omitted for clarity.

Table 3.13. Crystal data and structure refinement for 34.

Identification code	kvkv128a	
Empirical formula	C64 H76 Cl4 I4 N4 Te2	
Formula weight	1805.89	
Temperature	153(2) K	
Wavelength	0.71073 Å	
Crystal system	Monoclinic	
Space group	P21/n	
Unit cell dimensions	a = 12.794(3) Å	α= 90°.
	b = 16.144(3) Å	β= 94.13(3)°.
	c = 17.155(3) Å	γ = 90°.
Volume	3534.0(12) $Å^3$	
Z	2	
Density (calculated)	1.697 Mg/m^3	
Absorption coefficient	2.762 mm^{-1}	
F(000)	1744	
Crystal size	0.08 x 0.06 x 0.05 mm^3	
Theta range for data collection	2.06 to 27.50°.	
Index ranges	-16<=h<=16, -19<=k<=20, -22<=l<=22	
Reflections collected	13388	
Independent reflections	8080 [R(int) = 0.0687]	
Completeness to theta = 27.50°	99.5 %	
Absorption correction	None	
Refinement method	Full-matrix least-squares on F^2	
Data / restraints / parameters	8080 / 3 / 360	
Goodness-of-fit on F^2	0.940	
Final R indices [I>2sigma(I)]	R1 = 0.0469, wR2 = 0.0624	
R indices (all data)	R1 = 0.1213, wR2 = 0.0770	
Largest diff. peak and hole	1.008 and -0.814 $e.Å^{-3}$	

Table 3.14. Selected Bond Lengths (Å) for $(TeI_2)_2$(Dipp-TIP) (34)

C1-C2	1.482(6)
C1-C5	1.509(6)
C1-N1	1.281(5)
C4-C5	1.474(6)
C5-N2	1.288(5)
N1-Te1	2.426(4)
N2-Te1	2.494(4)
I1-Te1	2.8493(6)
I2-Te2	2.8428(9)

Table 3.15. Selected Bond Angles (°) for $(TeI_2)_2$(Dipp-TIP) (34)

C1-C5-C4	107.3(4)
C1-C5-N2	120.3(4)
C1-N1-Te1	116.4(3)
C2-C1-C5	107.1(4)
C2-C1-N1	132.8(4)
C4-C5-N2	132.3(4)
C5-C1-N1	120.0(4)
C5-N2-Te1	113.7(3)
N1-Te1-N2	69.40(12)
N1-Te1-I1	93.24(9)
N1-Te1-I2	165.15(9)
N2-Te1-I1	162.09(9)
N2-Te1-I2	95.79(8)

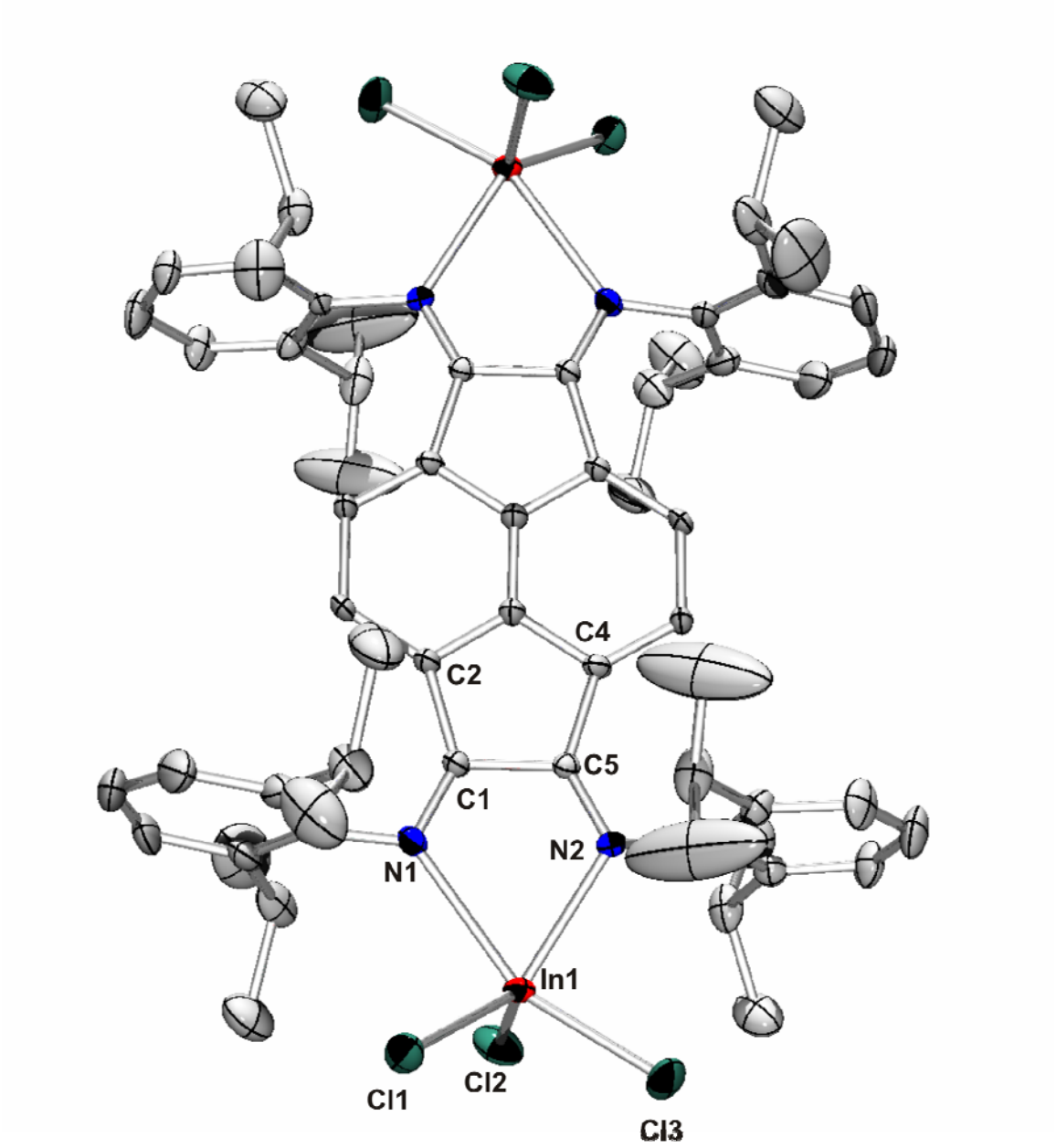

Figure 3.06. Molecular structure of 35 showing a partial numbering scheme. The thermal ellipsoids are shown at the 40% probability level. All hydrogen atoms have been omitted for clarity.

Table 3.16. Crystal data and structure refinement for 35.

Identification code	kvkv130sqa	
Empirical formula	C62 H72 Cl6 In2 N4	
Formula weight	1315.58	
Temperature	153(2) K	
Wavelength	0.71073 Å	
Crystal system	Monoclinic	
Space group	P21/n	
Unit cell dimensions	a = 11.676(5) Å	α= 90.000(5)°.
	b = 17.250(5) Å	β= 91.994(5)°.
	c = 18.117(5) Å	γ = 90.000(5)°.
Volume	3647(2) $Å^3$	
Z	2	
Density (calculated)	1.198 Mg/m^3	
Absorption coefficient	0.887 mm^{-1}	
F(000)	1344	
Crystal size	0.18 x 0.12 x 0.08 mm^3	
Theta range for data collection	1.63 to 27.47°.	
Index ranges	-15<=h<=15, -20<=k<=22, -23<=l<=23	
Reflections collected	14716	
Independent reflections	8319 [R(int) = 0.0443]	
Completeness to theta = 27.47°	99.5 %	
Absorption correction	None	
Refinement method	Full-matrix least-squares on F^2	
Data / restraints / parameters	8319 / 0 / 342	
Goodness-of-fit on F^2	0.974	
Final R indices [I>2sigma(I)]	R1 = 0.0481, wR2 = 0.1311	
R indices (all data)	R1 = 0.0797, wR2 = 0.1424	
Largest diff. peak and hole	0.825 and -0.853 $e.Å^{-3}$	

Table 3.17. Selected Bond Lengths (Å) for $(InCl_3)_2$(Dipp-TIP) (35)

C1-C2	1.463(5)
C1-C5	1.544(5)
C1-N1	1.278(4)
C4-C5	1.484(5)
C5-N2	1.261(4)
N1-In1	2.309(3)
N2-In1	2.439(3)
Cl1-In1	2.3466(13)
Cl2-In1	2.3866(15)
Cl3-In1	2.3579(12)

Table 3.18. Selected Bond Angles (°) for $(InCl_3)_2$(Dipp-TIP) (35)

C1-C5-C4	106.3(3)
C1-C5-N2	119.3(3)
C1-N1-In1	116.8(2)
C2-C1-C5	108.1(3)
C2-C1-N1	133.4(3)
C4-C5-N2	134.2(3)
C5-C1-N1	118.0(3)
C5-N2-In1	112.7(2)
N1-In1-N2	71.09(10)
N1-In1-Cl1	100.11(8)
N1-In1-Cl2	88.50(8)
N1-In1-Cl3	137.57(8)
N2-In1-Cl1	94.14(8)
N2-In1-Cl2	154.39(8)
N2-In1-Cl3	86.37(7)

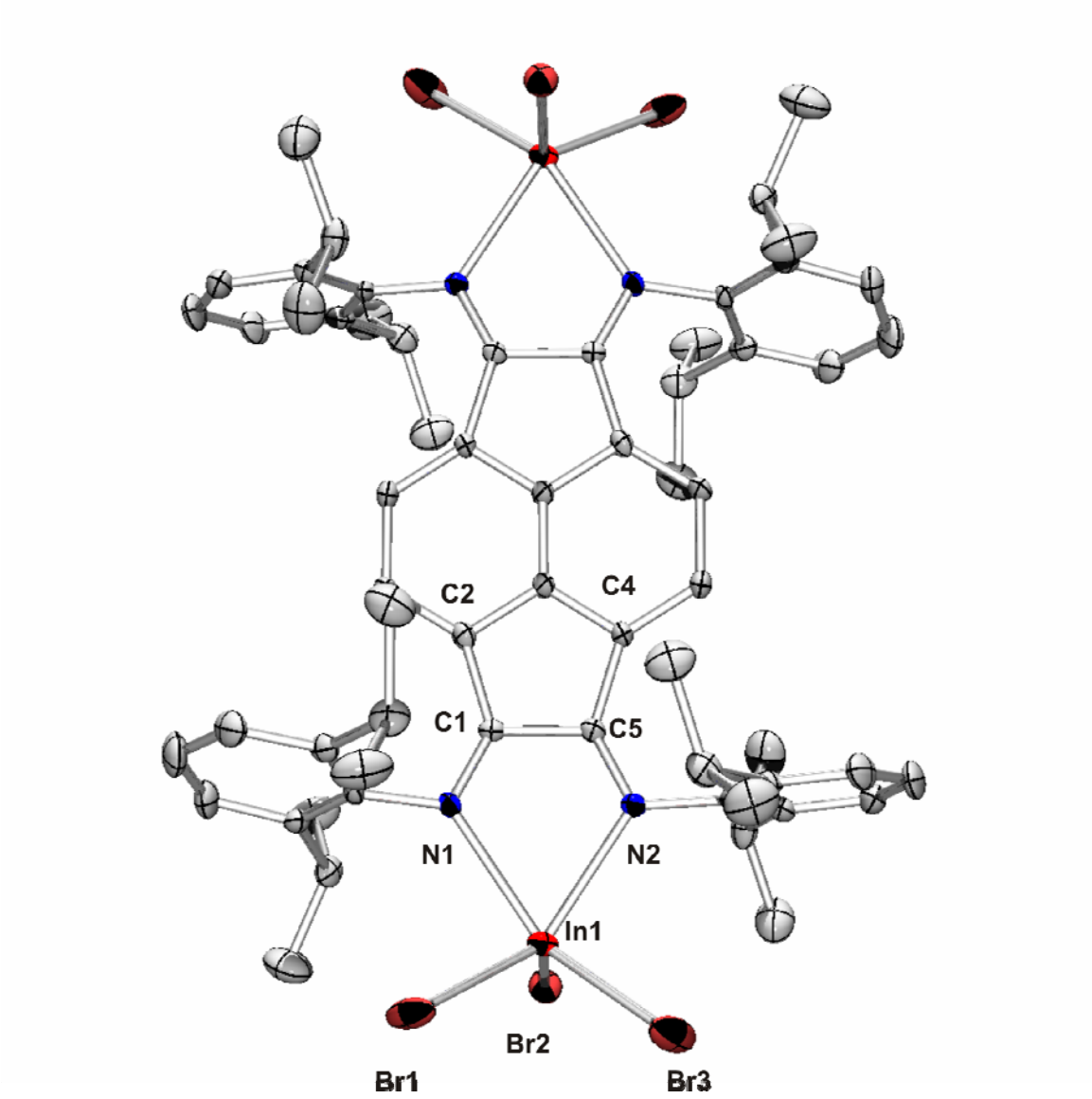

Figure 3.07. Molecular structure of 36 showing a partial numbering scheme. The thermal ellipsoids are shown at the 40% probability level. All hydrogen atoms have been omitted for clarity.

Table 3.19. Crystal data and structure refinement for 36.

Identification code	kvkv136sqa	
Empirical formula	C62 H72 Br6 In2 N4	
Formula weight	1582.34	
Temperature	153(2) K	
Wavelength	0.71073 Å	
Crystal system	Monoclinic	
Space group	P21/n	
Unit cell dimensions	a = 10.178(5) Å	α= 90.000(5)°.
	b = 21.687(5) Å	β= 92.761(5)°.
	c = 15.394(5) Å	γ = 90.000(5)°.
Volume	3394(2) $Å^3$	
Z	2	
Density (calculated)	1.548 Mg/m^3	
Absorption coefficient	4.248 mm^{-1}	
F(000)	1560	
Crystal size	0.21 x 0.15 x 0.10 mm^3	
Theta range for data collection	1.62 to 27.49°.	
Index ranges	-13<=h<=13, -28<=k<=25, -19<=l<=19	
Reflections collected	12779	
Independent reflections	7767 [R(int) = 0.0461]	
Completeness to theta = 27.49°	99.7 %	
Absorption correction	None	
Refinement method	Full-matrix least-squares on F^2	
Data / restraints / parameters	7767 / 0 / 342	
Goodness-of-fit on F^2	0.990	
Final R indices [I>2sigma(I)]	R1 = 0.0510, wR2 = 0.0948	
R indices (all data)	R1 = 0.0954, wR2 = 0.1043	
Largest diff. peak and hole	1.316 and -1.096 e.$Å^{-3}$	

Table 3.20. Selected Bond Lengths (Å) for $(InBr_3)_2$(Dipp-TIP) (36)

C1-C2	1.466(5)
C1-C5	1.529(5)
C1-N1	1.276(4)
C4-C5	1.474(5)
C5-N2	1.272(4)
N1-In1	2.410(3)
N2-In1	2.381(3)
Br1-In1	2.5047(12)
Br2-In1	2.5057(8)
Br3-In1	2.5042(9)

Table 3.21. Selected Bond Angles (°) for $(InBr_3)_2$(Dipp-TIP) (36)

C1-C5-C4	107.2(3)
C1-C5-N2	119.1(3)
C1-N1-In1	114.6(2)
C2-C1-C5	107.8(3)
C2-C1-N1	133.3(4)
C4-C5-N2	133.2(4)
C5-C1-N1	118.6(3)
C5-N2-In1	115.5(2)
N1-In1-N2	70.33(11)
N1-In1-Br1	96.61(8)
N1-In1-Br2	151.43(8)
N1-In1-Br3	85.08(7)
N2-In1-Br1	97.51(8)
N2-In1-Br2	89.92(8)
N2-In1-Br3	141.43(8)

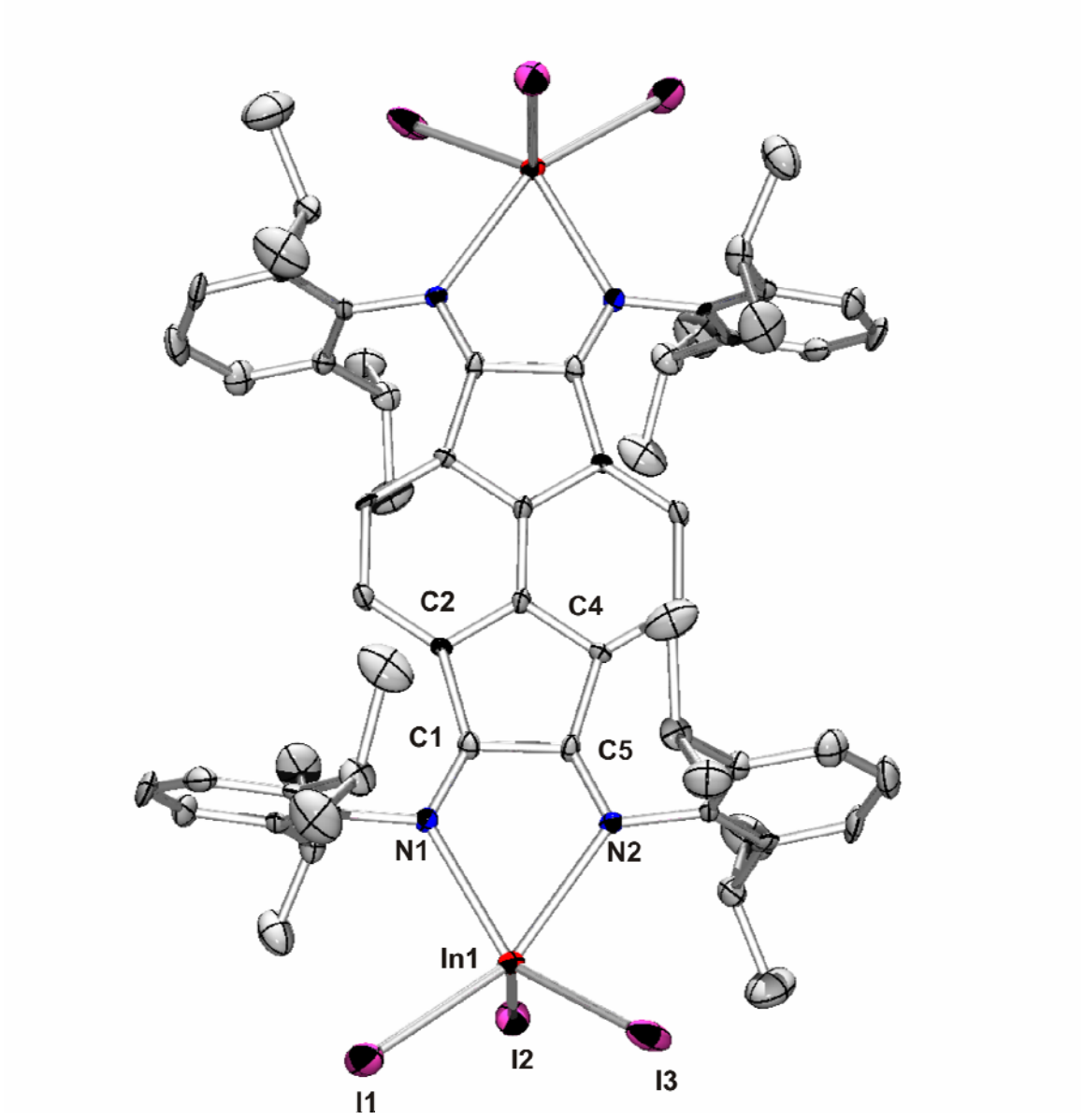

Figure 3.08. Molecular structure of 37 showing a partial numbering scheme. The thermal ellipsoids are shown at the 40% probability level. All hydrogen atoms have been omitted for clarity.

Table 3.22. Crystal data and structure refinement for 37.

Identification code	kvkv129sqa	
Empirical formula	C62 H72 I6 In2 N4	
Formula weight	1864.28	
Temperature	153(2) K	
Wavelength	0.71073 Å	
Crystal system	Monoclinic	
Space group	P21/n	
Unit cell dimensions	a = 10.370(5) Å	α= 90.000(5)°.
	b = 22.405(5) Å	β= 95.681(5)°.
	c = 15.448(5) Å	γ = 90.000(5)°.
Volume	3572(2) $Å^3$	
Z	2	
Density (calculated)	1.734 Mg/m^3	
Absorption coefficient	3.275 mm^{-1}	
F(000)	1776	
Crystal size	0.21 x 0.14 x 0.12 mm^3	
Theta range for data collection	1.61 to 27.45°.	
Index ranges	-13<=h<=13, -26<=k<=29, -20<=l<=20	
Reflections collected	13657	
Independent reflections	8139 [R(int) = 0.0558]	
Completeness to theta = 27.45°	99.7 %	
Absorption correction	None	
Refinement method	Full-matrix least-squares on F^2	
Data / restraints / parameters	8139 / 0 / 342	
Goodness-of-fit on F^2	0.944	
Final R indices [I>2sigma(I)]	R1 = 0.0535, wR2 = 0.1114	
R indices (all data)	R1 = 0.1158, wR2 = 0.1243	
Largest diff. peak and hole	1.214 and -1.082 $e.Å^{-3}$	

Table 3.23. Selected Bond Lengths (Å) for $(InI_3)_2$(Dipp-TIP) (37)

C1-C2	1.489(8)
C1-C5	1.517(8)
C1-N1	1.266(7)
C4-C5	1.523(8)
C5-N2	1.271(8)
N1-In1	2.482(5)
N2-In1	2.367(5)
I1-In1	2.7117(10)
I2-In1	2.7061(14)
I3-In1	2.7302(9)

Table 3.24. Selected Bond Angles (°) for $(InI_3)_2$(Dipp-TIP) (37)

C1-C5-C4	107.0(5)
C1-C5-N2	119.7(6)
C1-N1-In1	113.6(4)
C2-C1-C5	107.9(5)
C2-C1-N1	132.7(5)
C4-C5-N2	132.7(6)
C5-C1-N1	118.9(5)
C5-N2-In1	117.0(4)
N1-In1-N2	69.34(16)
N1-In1-I1	84.80(12)
N1-In1-I2	96.84(12)
N1-In1-I3	153.70(11)
N2-In1-I1	139.12(12)
N2-In1-I2	98.84(12)
N2-In1-I3	91.78(12)

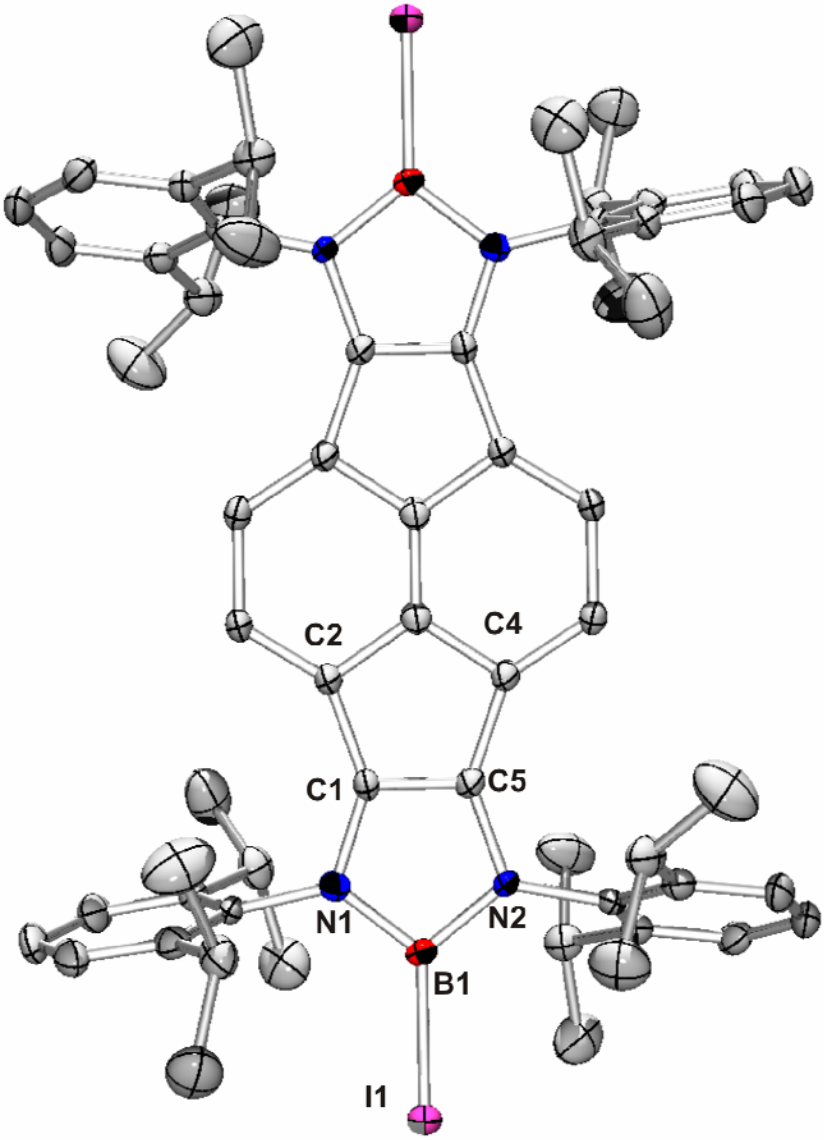

Figure 3.09. Molecular structure of the cation of 38 showing a partial numbering scheme. The thermal ellipsoids are shown at the 40% probability level. All hydrogen atoms and three molecules of dichloromethane have been omitted for clarity.

Table 3.25. Crystal data and structure refinement for 38.

Identification code	mfmf105	
Empirical formula	C65 H78 B2 Cl6 I7 N4	
Formula weight	2037.93	
Temperature	153(2) K	
Wavelength	0.71073 Å	
Crystal system	Triclinic	
Space group	P-1	
Unit cell dimensions	a = 12.626(3) Å	α= 100.25(3)°.
	b = 14.448(3) Å	β= 95.94(3)°.
	c = 23.312(5) Å	γ = 109.23(3)°.
Volume	3890.4(13) $Å^3$	
Z	2	
Density (calculated)	1.740 Mg/m^3	
Absorption coefficient	3.037 mm^{-1}	
F(000)	1958	
Crystal size	0.15 x 0.15 x 0.20 mm^3	
Theta range for data collection	1.59 to 27.48°.	
Index ranges	-16<=h<=16, -18<=k<=18, -30<=l<=30	
Reflections collected	24731	
Independent reflections	17495 [R(int) = 0.0305]	
Completeness to theta = 27.48°	98.0 %	
Absorption correction	None	
Refinement method	Full-matrix least-squares on F^2	
Data / restraints / parameters	17495 / 0 / 773	
Goodness-of-fit on F^2	0.837	
Final R indices [I>2sigma(I)]	R1 = 0.0593, wR2 = 0.1684	
R indices (all data)	R1 = 0.0942, wR2 = 0.2085	
Largest diff. peak and hole	2.264 and -1.605 $e.Å^{-3}$	

Table 3.26. Selected Bond Lengths (Å) for $[(BI)_2(Dipp\text{-}TIP)][I_5]$ (38)

C1-C2	1.450(9)
C1-C5	1.401(8)
C1-N2	1.375(8)
C4-C5	1.438(9)
C5-N1	1.368(8)
N1-B1	1.450(8)
N2-B1	1.442(8)
I1-B1	2.116(7)

Table 3.27. Selected Bond Angles (°) for $[(BI)_2(Dipp\text{-}TIP)][I_5]$ (38)

C1-C5-C4	110.5(5)
C1-C5-N1	109.3(5)
C1-N2-B1	106.3(5)
C2-C1-C5	110.5(5)
C2-C1-N2	139.3(5)
C4-C5-N1	140.2(5)
C5-C1-N2	110.2(5)
C5-N1-B1	106.9(5)
N1-B1-N2	107.2(5)
N1-B1-I1	126.3(5)
N2-B1-I1	126.5(5)

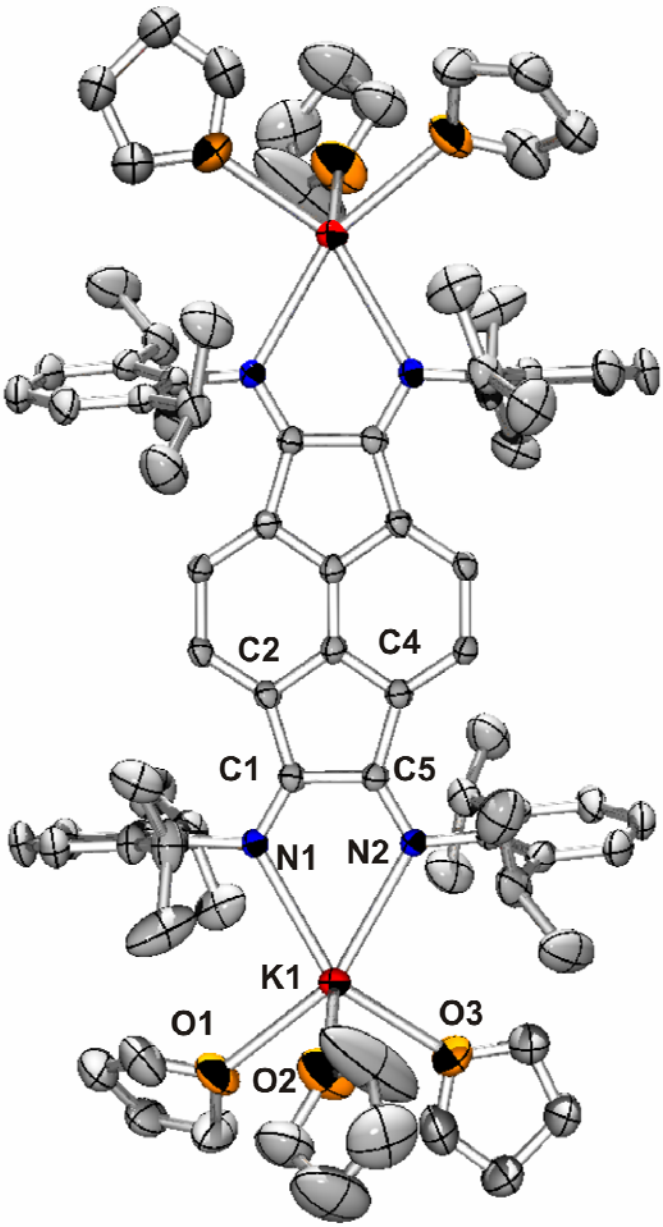

Figure 3.10. Molecular structure of 39 showing a partial numbering scheme. The thermal ellipsoids are shown at the 40% probability level. All hydrogen atoms have been omitted for clarity.

Table 3.28. Crystal data and structure refinement for 39.

Identification code	squeezeda	
Empirical formula	C86 H120 K2 N4 O6	
Formula weight	1384.06	
Temperature	153(2) K	
Wavelength	0.71073 Å	
Crystal system	Monoclinic	
Space group	P21/n	
Unit cell dimensions	a = 13.581(5) Å	α= 90.000(5)°.
	b = 17.668(5) Å	β= 107.043(5)°.
	c = 18.964(5) Å	γ = 90.000(5)°.
Volume	4351(2) $Å^3$	
Z	2	
Density (calculated)	1.057 Mg/m^3	
Absorption coefficient	0.158 mm^{-1}	
F(000)	1500	
Crystal size	0.13 x 0.08 x 0.05 mm^3	
Theta range for data collection	1.61 to 27.50°.	
Index ranges	-17<=h<=17, -22<=k<=21, -24<=l<=24	
Reflections collected	16516	
Independent reflections	9963 [R(int) = 0.0435]	
Completeness to theta = 27.50°	99.7 %	
Absorption correction	None	
Refinement method	Full-matrix least-squares on F^2	
Data / restraints / parameters	9963 / 0 / 450	
Goodness-of-fit on F^2	0.999	
Final R indices [I>2sigma(I)]	R1 = 0.0821, wR2 = 0.2351	
R indices (all data)	R1 = 0.1561, wR2 = 0.2698	
Extinction coefficient	0.0105(16)	
Largest diff. peak and hole	0.499 and -0.396 $e.Å^{-3}$	

Table 3.29. Selected Bond Lengths (Å) for $(K(THF)_3)_2$(Dipp-TIP) (39)

C1-C2	1.470(4)
C1-C5	1.485(4)
C1-N1	1.311(3)
C4-C5	1.476(4)
C5-N2	1.314(3)
N1-K1	2.744(2)
N2-K1	2.753(2)
O1-K1	2.743(3)
O2-K1	2.699(3)
O3-K1	2.667(3)

Table 3.30. Selected Bond Angles (°) for $(K(THF)_3)_2$(Dipp-TIP) (39)

C1-C5-C4	107.2(2)
C1-C5-N2	121.8(2)
C1-N1-K1	117.11(17)
C2-C1-C5	107.8(2)
C2-C1-N1	131.0(2)
C4-C5-N2	131.0(2)
C5-C1-N1	121.2(2)
C5-N2-K1	116.45(17)
N1-K1-N2	62.62(7)
N1-K1-O1	94.85(8)
N1-K1-O2	116.13(11)
N1-K1-O3	145.30(10)
N2-K1-O1	152.64(8)
N2-K1-O2	120.07(10)
N2-K1-O3	89.28(9)

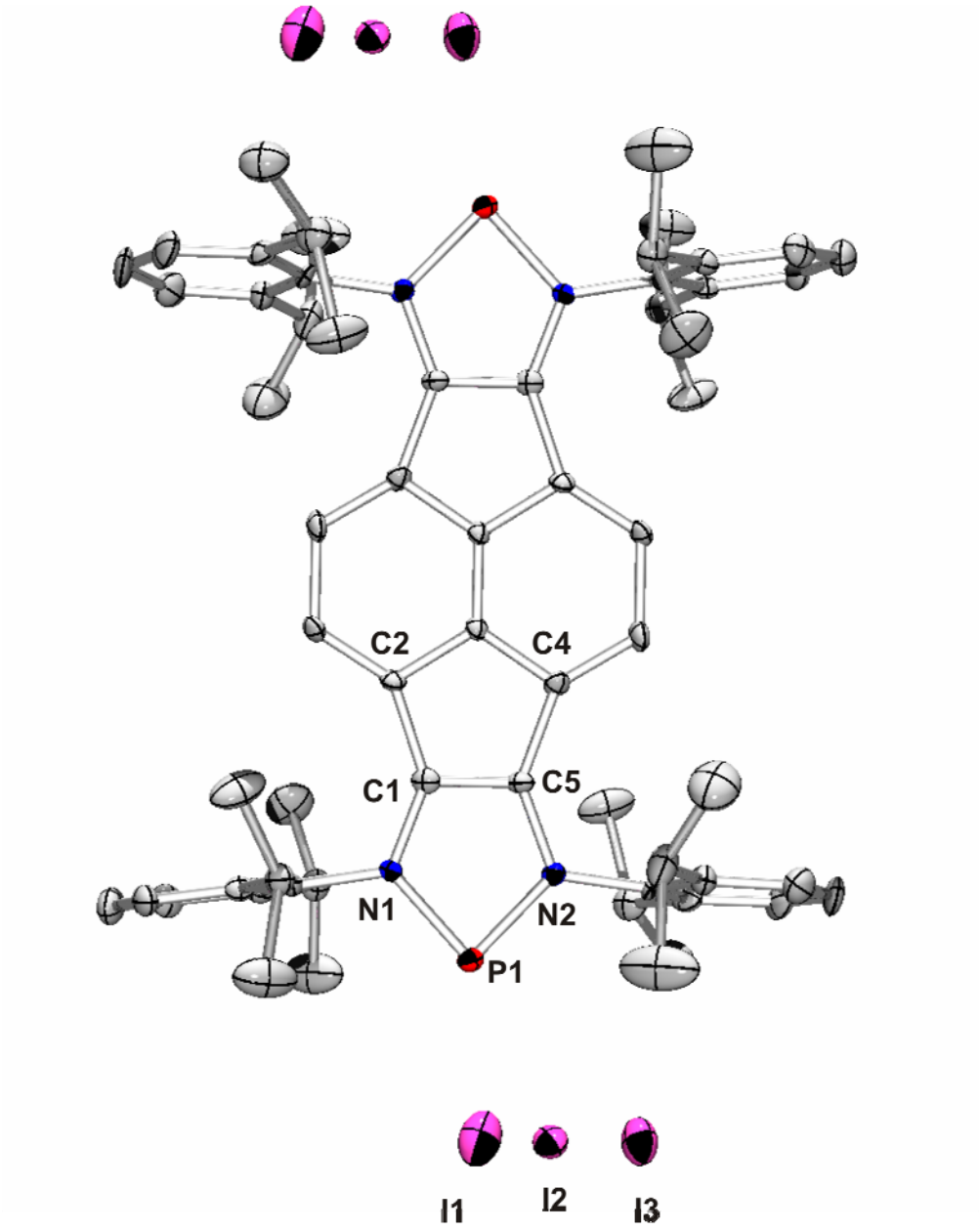

Figure 3.11. Molecular structure of 40 showing a partial numbering scheme. The thermal ellipsoids are shown at the 40% probability level. All hydrogen atoms and two molecules of dichloromethane have been omitted for clarity.

Table 3.31. Crystal data and structure refinement for 40.

Identification code	kvkv155a	
Empirical formula	C62 H72 I6 N4 P2	
Formula weight	1696.58	
Temperature	153(2) K	
Wavelength	0.71069 Å	
Crystal system	Monoclinic	
Space group	P21/c	
Unit cell dimensions	a = 11.825(5) Å	α= 90.000(5)°.
	b = 15.010(5) Å	β= 95.079(5)°.
	c = 20.439(5) Å	γ = 90.000(5)°.
Volume	3614(2) $Å^3$	
Z	2	
Density (calculated)	1.559 Mg/m^3	
Absorption coefficient	2.659 mm^{-1}	
F(000)	1640	
Crystal size	0.18 x 0.13 x 0.08 mm^3	
Theta range for data collection	1.73 to 27.45°.	
Index ranges	-15<=h<=15, -18<=k<=19, -26<=l<=26	
Reflections collected	14085	
Independent reflections	8253 [R(int) = 0.0622]	
Completeness to theta = 27.45°	99.7 %	
Absorption correction	None	
Refinement method	Full-matrix least-squares on F^2	
Data / restraints / parameters	8253 / 0 / 369	
Goodness-of-fit on F^2	1.082	
Final R indices [I>2sigma(I)]	R1 = 0.0487, wR2 = 0.0869	
R indices (all data)	R1 = 0.1586, wR2 = 0.1267	
Largest diff. peak and hole	1.267 and -1.195 $e.Å^{-3}$	

Table 3.32. Selected Bond Lengths (Å) for $[(P)_2(Dipp\text{-}TIP)][I_3]_2$ (40)

C1-C2	1.472(8)
C1-C5	1.395(9)
C1-N1	1.358(7)
C4-C5	1.481(9)
C5-N2	1.348(7)
N1-P1	1.707(5)
N2-P1	1.701(5)

Table 3.33. Selected Bond Angles (°) for $[(P)_2(Dipp\text{-}TIP)][I_3]_2$ (40)

C1-C5-C4	110.2(5)
C1-C5-N2	111.4(6)
C1-N1-P1	112.9(4)
C2-C1-C5	110.6(6)
C2-C1-N1	137.2(6)
C4-C5-N2	138.3(6)
C5-C1-N1	112.1(5)
C5-N2-P1	114.0(4)
N1-P1-N2	89.5(2)

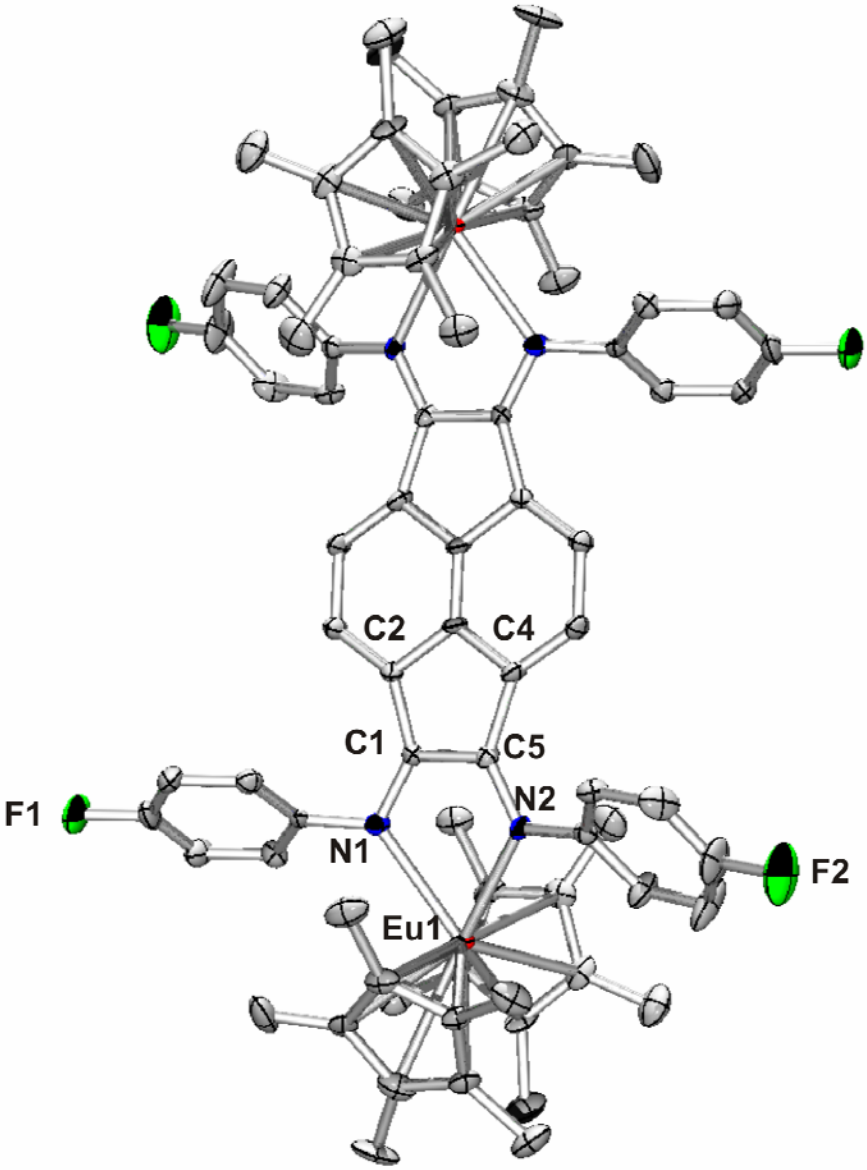

Figure 3.12. Molecular structure of 41 showing a partial numbering scheme. The thermal ellipsoids are shown at the 40% probability level. All hydrogen atoms and two molecules of toluene have been omitted for clarity.

Table 3.34. Crystal data and structure refinement for 41.

Identification code	kvkv149a	
Empirical formula	C106 H112 Eu2 F4 N4	
Formula weight	1821.92	
Temperature	153(2) K	
Wavelength	0.71073 Å	
Crystal system	Triclinic	
Space group	P-1	
Unit cell dimensions	a = 13.648(3) Å	α= 82.45(3)°.
	b = 13.792(3) Å	β= 66.98(3)°.
	c = 14.410(3) Å	γ = 70.30(3)°.
Volume	2350.5(8) $Å^3$	
Z	1	
Density (calculated)	1.287 Mg/m^3	
Absorption coefficient	1.377 mm^{-1}	
F(000)	938	
Crystal size	0.08 x 0.06 x 0.04 mm^3	
Theta range for data collection	1.54 to 27.46°.	
Index ranges	-17<=h<=17, -17<=k<=14, -18<=l<=18	
Reflections collected	15893	
Independent reflections	10647 [R(int) = 0.0596]	
Completeness to theta = 27.46°	99.0 %	
Absorption correction	None	
Refinement method	Full-matrix least-squares on F^2	
Data / restraints / parameters	10647 / 0 / 534	
Goodness-of-fit on F^2	1.050	
Final R indices [I>2sigma(I)]	R1 = 0.0782, wR2 = 0.1835	
R indices (all data)	R1 = 0.1384, wR2 = 0.2111	
Largest diff. peak and hole	2.463 and -0.748 e.$Å^{-3}$	

Table 3.35. Selected Bond Lengths (Å) for $[(C_5Me_5)_2Eu]_2$(p-F-TIP) (41)

C1-C2	1.477(11)
C1-C5	1.480(10)
C1-N1	1.323(9)
C4-C5	1.447(10)
C5-N2	1.331(9)
N1-Eu1	2.448(6)
N2-Eu1	2.460(6)
Eu-cent1	2.764(5)
Eu-cent2	2.437(5)

Table 3.36. Selected Bond Angles (°) for $[(C_5Me_5)_2Eu]_2$(p-F-TIP) (41)

C1-C5-C4	108.7(6)
C1-C5-N2	119.4(7)
C1-N1-Eu1	114.1(4)
C2-C1-C5	107.6(6)
C2-C1-N1	132.6(7)
C4-C5-N2	131.9(6)
C5-C1-N1	119.7(6)
C5-N2-Eu1	113.3(5)
N1-Eu1-N2	69.23(19)
N1-Eu1-cent1	107.11(9)
N1-Eu1-cent2	108.33(8)
N2-Eu1-cent1	107.90(9)
N2-Eu1-cent2	106.57(8)

References

1. Liu, H. R.; Gomes, P. T.; Costa, S. I.; Duarte, M. T.; Branquinho, R.; Fernandes, A. C.; Chien, J. C. W.; Singh, R. P.; Marques, M. M., *J. Organomet. Chem.* **2005,** 690, 1314-1323.
2. Dvolaitzky, M., *C. R. Acad. Sci., Ser. C* **1969,** 268, 1811-1813.
3. Matei, I.; Lixandru, T.; Comanita, E., *Bul. Inst. Politeh. Iasi.* **1960,** 6, 171-176.
4. Rose, J. M.; Mourey, T. H.; Slater, L. A.; Keresztes, I.; Fetters, L. J.; Coates, G. W., *Macromolecules* **2008,** 41, 559-567 and references therein.
5. Scarel, A.; Axet, M. R.; Amoroso, F.; Ragaini, F.; Elsevier, C. J.; Holuigue, A.; Carfagna, C.; Mosca, L.; Milani, B., *Organometallics* **2008,** 27, 1486-1494.
6. Shiotsuki, M.; White, P. S.; Brookhart, M.; Templeton, J. L., *J. Am. Chem. Soc.* **2007,** 129, 4058-4067 and references therein.
7. Ragaini, F.; Gasperini, M.; Gallo, E.; Macchi, P., *Chem. Commun.* **2005**, 1031-1033.
8. Liu, F.-Q.; Herzog, A.; Roesky, H. W.; Uson, I., *Inorg. Chem.* **1996,** 35, 741-744.
9. Gordon, J. C.; Shukla, P.; Cowley, A. H.; Jones, J. N.; Keogh, D. W.; Scott, B. L., *Chem. Commun.* **2002**, 2710-2711.
10. Schmiege, B. M.; Carney, M. J.; Small, B. L.; Gerlach, D. L.; Halfen, J. A., *Dalton Trans.* **2007**, 2547.
11. Sprengers, J. W.; de Greef, M.; Duin, M. A.; Elsevier, C. J., *Eur. J. Inorg. Chem.* **2003**, 3811-3819.
12. Fedushkin, I. L.; Chudakova, V. A.; Skatova, A. A.; Khvoinova, N. M.; Kurshkii, Y. A.; Glukhova, T. A.; Fukin, G. K.; Dechert, S.; Hummert, M.; Schumann, H., *Z. Anorg. Allg. Chem.* **2004,** 630, 501.
13. Gasperini, M.; Ragaini, F.; Gazzola, E.; Caselli, A.; Macchi, P., *Dalton Trans.* **2004**, 3376-3382.
14. Moore, J. A.; Vasudevan, K.; Hill, N. J.; Reeske, G.; Cowley, A. H., *Chem. Commun.* **2006**, 2913-2915.
15. Cucinella, S.; Salvatori, T.; Busetto, C.; Perego, G.; Mazzai, A., *J. Organomet. Chem.* **1974,** 78, 185.
16. Trost, B. M., *J. Am. Chem. Soc.* **1969,** 91, 918-923.
17. Fedushkin, I. L.; Khvoinova, N. M.; Baurin, A. Y.; Fukin, G. K.; Cherkasov, V. K.; Bubnov, M. P., *Inorg. Chem.* **2004,** 43, 7807-7815.
18. Fedushkin, I. L.; Skatova, A. A.; Chudakova, V. A.; Cherkasov, V. K.; Fukin, G. K.; Lopatin, M. A., *Eur. J. Inorg. Chem.* **2004**, 388-393.
19. Fedushkin, I. L.; Skatova, A. A.; Chudakova, V. A.; Fukin, G. K., *Angew. Chem. Int. Ed.* **2003,** 42, 3294-3298.
20. Reeske, G.; Hoberg, C. R.; Hill, N. J.; Cowley, A. H., *J. Am. Chem. Soc.* **2006,** 128, 2800-2801.
21. Schultz, M.; Boncella, J. M.; Berg, D. J.; Tilley, T. D.; Andersen, R. A., *Organometallics* **2002,** 21, 460-472.

22. Carlson, C. N.; Kuehl, C. J.; Ogallo, L.; Shultz, D. A.; Thompson, J. D.; Kirk, M. L.; Martin, R. L.; John, K. D.; Morris, D. E., *Organometallics* **2006**.
23. Trifonov, A. A.; Kirillov, E. N.; Bochkarev, M. N.; Schumann, H.; Meuhle, S., *Russ. Chem. Bull.* **1999**, 384.
24. Walter, M. D.; Berg, D. J.; Andersen, R. A., *Organometallics* **2007,** 26, 2296.
25. Sobota, P.; Utko, J.; Szafert, S., *Inorg. Chem.* **1994,** 33, 5203.
26. El-Ayaan, U.; Murata, F.; El-Derby, S.; Fukuda, Y., *J. Molec. Struct.* **2004,** 692, 209-216.
27. Evans, W. J.; Shreeve, J. L.; Ziller, J. W., *Organometallics* **1994,** 13, 731.
28. Coventry, D. N.; Batsanov, A. S.; Goeta, A. E.; Howard, J. A. K.; Marder, T. B., *Polyhedron* **2004,** 23, 2789-2795.
29. Evans, W. J.; Brady, J.; Ziller, J., *J. Am. Chem. Soc.* **2001,** 123, 7711.
30. El-Ayaan, U.; Paulovicova, A.; Yamada, S.; Fukuda, Y., *J. Coord. Chem.* **2003,** 56, (5), 373-381.
31. Evans, W. J.; Davis, B. L., *Chem. Rev.* **2002,** 102, 2119.
32. Carlson, C. N.; Kuehl, C. J.; Da Re, R. E.; Veauthier, J. M.; Schelter, E. J.; Milligan, A. E.; Scott, B. L.; Bauer, E. D.; Thompson, J. D.; Morris, D. E.; John, K. D., *J. Am. Chem. Soc.* **2006,** 128, 7230-7241.
33. Carlson, C. N.; Scott, B. L.; Martin, R. L.; Thompson, J. D.; Morris, D. E.; John, K. D., *Inorg. Chem.* **2007,** 46, (12), 5013-5022.
34. Jacoby, M., *C. & E. News* **2009**, 14-20.
35. Khusniyarov, M. M.; Harms, K.; Burghaus, O.; Sundermeyer, J., Molecular and *Eur. J. Inorg. Chem.* **2006**, 2985-2996.
36. Reeske, G.; Cowley, A. H., *Chem. Commun.* **2006**, 4856-4858.
37. Jenkins, H. A.; Dumaresque, C. L.; Vidovic, D.; Clyburne, J. A. C., *Can. J. Chem.* **2002,** 80, 1398-1403.
38. Vasudevan, K. V.; Findlater, M.; Cowley, A. H., *Chem. Commun.* **2008**, 1918-1919.
39. Fedushkin, I. L.; Skatova, A. A.; Chudakova, V. A.; Khvomova, N. M.; Baurin, A. Y.; Dechert, S.; Hummert, M.; Schumann, H., *Organometallics* **2004,** 23, 3714-3718.

Vita

Kalyan Vikram Vasudevan was born in Rockledge, Florida on December 21, 1982, the son of Sampath and Prathiba Vasudevan. After graduating from Garinger High School, Charlotte, North Carolina in May, 2000, he attended Duke University in Durham, North Carolina. He received the degrees of Bachelor of Science in Chemistry and Bachelor of Arts in Religion in May, 2004. In August, 2004 he entered the Graduate School of the University of Texas at Austin.

Permanent Address: 2004 Tom Miller St.

Austin, TX 78723

This dissertation was typed by the author.